

https://dspace.org/

Analysis of endemic South African HIV-1 isolates using anti-GP 120 aptamer(s)

Mufhandu, Hazel Tumelo

2014-02-17
http://hdl.handle.net10539/13784

Downloaded from a DSpace repository. https://dspace.org/

ANALYSIS OF ENDEMIC SOUTH AFRICAN HIV-1 ISOLATES USING ANTI-GP120 APTAMER(S)

Hazel Tumelo Mufhandu

A thesis submitted to the Faculty of Health Sciences, University of the Witwatersrand, in fulfilment of the requirements for the degree of Doctor of Philosophy

February, 2013

DECLARATION

I, Hazel Tumelo Mufhandu declare that this thesis is my own work. It is being submitted for the degree of Doctor of Philosophy at the University of the Witwatersrand, Johannesburg. It has not been submitted before for any degree or examination at this or any other University.

.....

(Signature of candidate)

..... Day of..... (Month), 2013

ABSTRACT

The HIV-1 epidemic in South Africa remains the highest worldwide with subtype C as the major circulating virus. An HIV vaccine is still elusive, and with only half of the infected population receiving antiretroviral treatment, the demand for comprehensive interventions such as the development of new therapeutic agents is indispensable. It was previously shown that a parental anti-gp120 RNA aptamer, called B40, neutralized a broad range of HIV-1 subtypes and suppressed viral replication in cultured human peripheral blood mononuclear cells by up to 10,000-fold. Therefore, in this study I explored the use of its modified synthetic derivative, called UCLA1, to neutralize HIV-1 subtype C clinical isolates. UCLA1 was shown to have high affinity for the consensus HIV-1 subtype C gp120 and neutralized subtype C isolates with IC_{50} values in the nanomolar range. There was no neutralization preference noted between viruses isolated from acute and chronic infections or between isolates from adult and paediatric patients in TZM-bl cells, PBMC or macrophage assays. The aptamer was not strain or tropism restricted since it neutralized both R5 and X4 viruses. It was also non-cytotoxic when tested in different cell lines. Mapping of UCLA1 binding sites on gp120 revealed eight amino acid residues that modulated neutralization resistance. These included residues within the co-receptor binding site, at the base of the V3 loop, and in the bridging sheet within the conserved V1/V2 stem-loop of gp120. The aptamer was also shown to have synergistic effects with T20, a gp41 fusion inhibitor and IgG1b12, an anti-CD4 binding site monoclonal antibody. Two primary viruses were tested for their ability to become resistant by culturing them under escalating concentrations of the aptamer for a maximum of 84 days. Only one of the two

viruses mutated to escape neutralization by UCLA1 at 7-fold of the IC_{50}. Six escape mutations were identified within the V3 loop and in the CD4 and co-receptor binding complex at the base of the β15 sheet and the α3 helix, confirming and extending UCLA1 binding sites mapping data. Taken together, these data show that UCLA1 has broad spectrum potency as an entry inhibitor against HIV-1 subtype C isolates suggesting it might be a suitable candidate for human clinical testing with a low propensity for developing resistance.

PUBLICATIONS FROM THIS THESIS

Hazel T Mufhandu, Elin S Gray, Maphuti C Madiga, Nancy Tumba, Kabamba B Alexandre, Thandeka Khoza, Constantinos Kurt Wibmer, Penny L Moore, Lynn Morris and Makobetsa Khati. UCLA1, a synthetic derivative of a gp120 RNA aptamer, inhibits entry of human immunodeficiency virus type-1 Subtype C**.** *2012. Journal of Virology 86 (9): 4989 - 4999.*

Hazel T Mufhandu, Kabamba B Alexandre, Elin S Gray, Lynn Morris and Makobetsa Khati. HIV-1 subtype C escape mutations generated by resistance to UCLA1 RNA aptamer inhibition. In preparation.

OTHER PUBLICATIONS NOT RELATED TO THESIS

Kabamba B. Alexandre, Elin S. Gray, **Hazel Mufhandu**, James B. McMahon, Ereck Chakauya, Barry R. O'Keefe, Rachel Chikwamba, Lynn Morris. The lectins griffithsin, cyanovirin-N and scytovirin inhibit HIV-1 binding to the DC-SIGN receptor and transfer to $CD4^+$ cells. *2012. Virology 423: 175-186.*

PRESENTATIONS AT MEETINGS

Hazel T Mufhandu, Elin S Gray, Kabamba B Alexandre, Lynn Morris and Makobetsa Khati. Aptamers targeting entry of HIV-1 Subtype C.
The Molecular Bioscience Research Thrust Research Day, 5 December 2012, Wits Professional Development Hub, Braamfontein, Johannesburg, South Africa (Oral).

Hazel T Mufhandu, Kabamba B Alexandre, Elin S Gray, Lynn Morris, and Makobetsa Khati. HIV-1 subtype C primary isolates exhibit high sensitivity to an anti-gp120 RNA aptamer.
AIDS Vaccine 2012 Conference, 9-12 September, Boston, Massachusetts, USA (Poster).

Hazel Mufhandu, Elin S Gray, Kabamba B Alexandre, Lynn Morris and Makobetsa Khati. Aptamers targeting HIV-1 entry.
2nd Regional Synthetic Biology Forum, July 2012, Irene Country Lodge, Centurion, South Africa (Oral).

Hazel Mufhandu, Elin S Gray, Maphuti C Madiga, Nancy Tumba, Kabamba B Alexandre, Thandeka Khoza, Constantinos Kurt Wibmer, Penny L Moore, Lynn Morris and Makobetsa Khati. An RNA aptamer that inhibits entry of HIV-1 subtype C.
The Council for Scientific and Industrial Research (CSIR), Biosciences, Emerging Health Technology Platform Seminars, February 2012, Pretoria, South Africa (Oral).

Hazel Mufhandu, Elin S Gray, Maphuti C Madiga, Nancy Tumba, Kabamba B Alexandre, Constantinos Kurt Wibmer, Penny L Moore, Lynn Morris and Makobetsa Khati. An RNA aptamer that inhibits entry of HIV-1 subtype C.
National Institute for Communicable Diseases (NICD) Research Forum, November 2011, Johannesburg, South Africa (Oral).

Hazel Tumelo Mufhandu, Elin Gray, Nancy Tumba, Constantinos Kurt Wibmer, Lynn Morris, and Makobetsa Khati. Molecular interaction of UCLA1 aptamer and consensus HIV-1 subtype C gp120.
6th IAS Conference on HIV, Pathogenesis, Treatment and Prevention, July 2011, Rome, Italy (Poster).

Makobetsa Khati, Marisa Joubert, Hazel Mufhandu**,** Walter Rangel Lopes de Campos. The utility of nano-aptamer bioconjugates against infectious diseases.
International workshop on nanomedicine for infectious diseases of poverty, March 2011, Magaliesberg, South Africa (Oral).

Makobetsa Khati, Hazel Mufhandu, Walter Rangel Lopes de Campos.
Aptamers: A new technology platform for drug discovery.
CSIR 3rd biennial conference: science real and relevant, August 2010, Pretoria, South Africa (Oral).

Khati M., Mufhandu H., Madiga M., Gray E., Khoza T., and Morris L. A synthetic derivative of gp120 binding RNA aptamer inhibits entry of human immunodeficiency virus type 1 subtype C Isolates.
1st World Congress of Virus and Infections, July-August 2010, BEXCO, Busan, South Korea (Oral).

Makobetsa Khati, Hazel Mufhandu, Marisa Joubert, Walter Rangel Lopes de Campos. Aptamers: A new technology platform for diagnostics, therapeutics and targeted drug delivery.
BIT 2nd Annual International conference of antibodies, May 2010, Beijing, China (Oral).

Laura Millroy, Hazel Mufhandu and Walter Rangel Lopes de Campos.
Entry inhibition of adult and paediatric HIV-1 subtype C isolates using a shortened synthetic derivative of a gp120 binding aptamer.
Oxford Virology Symposium, April 2010, University of Oxford, England (Oral).

H Mufhandu, M Madiga, E Gray, L Rotherham, T Khoza, L Morris, and M Khati. Neutralization of several adult and paediatric HIV-1 subtype C isolates using a shortened synthetic derivative of gp120 binding aptamer called UCLA1.
5th IAS Conference on HIV, Pathogenesis, Treatment and Prevention, July 2009, Cape Town, South Africa (Poster).

Makobetsa Khati, Hazel Mufhandu, Walter Rangel Lopes de Campos and Marisa Joubert. A new frontier in targeted drug delivery, therapeutics, diagnostics and eradicating poverty related diseases.
India Brazil South Africa (IBSA) workshop: Nanotechnology, drug delivery and poverty related diseases, May 2009, CSIR, Meraka Institute Pretoria, South Africa (Oral).

Hazel Mufhandu, Elin Gray, Maphuti Madiga, Natasha Taylor, Lynn Morris, and Makobetsa Khati. Entry inhibition of HIV-1 subtype C using anti-gp120 aptamer.
Keystone Symposia on Molecular and Cellular Biology. Pathogenesis and Control of Emerging Infections and Drug-Resistant Organisms, October 2008, Bangkok, Thailand (Poster).

OTHER PRESENTATIONS NOT RELATED TO THESIS

Kabamba B. Alexandre, Elin S. Gray, Hazel Mufhandu, Penny L. Moore, Ereck Chakauya, James McMahon, Barry O'Keefe, Rachel Chikwamba and Lynn Morris. The C-type lectins Griffithsin, Cyanovirin-N and Scytovirin inhibit HIV-1 interaction with the DC-SIGN receptor.
5th South African AIDS conference, June 2011, Durban, South Africa (Oral).

Kabamba B. Alexandre, Elin S. Gray, Hazel Mufhandu, Penny L. Moore, Ereck Chakauya, James McMahon, Barry O'Keefe, Rachel Chikwamba and Lynn Morris.
The C-type lectins Griffithsin, Cyanovirin-N and Scytovirin inhibit HIV-1 interaction with the DC-SIGN receptor.
AIDS Vaccine 2011, September 2011, Bangkok, Thailand (Poster).

DEDICATION

I dedicate this thesis to my husband Midiaifheli, my daughter O'Funa and my son Fhulufelo. A big thank you to my husband and children for bearing with me through all the late nights and weekends that I spent away from them due to my studies. A special dedication to my late father, Solomon Maila. My gratitude also goes out to my Mom Lebo Maila for all the support she gave me throughout my PhD years. Being a newlywed and bearing two children during my PhD years, she was the extra hands that I needed to help take care of my children while I focused on my studies. Finally, all thanks to the God Almighty for the help, courage, wisdom, strength and perseverance He granted me throughout this study.

ACKNOWLEDGEMENTS

I would like to thank my supervisors Dr Makobetsa Khati and Professor Lynn Morris for believing in my abilities to undertake the PhD project, for their supervision, guidance and moral support. Special thanks to Prof Morris for ensuring that I receive the appropriate training necessary for HIV assays, and for hosting me in her laboratories while I needed a P3 facility for my project.

I would like to specifically thank Dr Elin Gray for being a perfect mentor. Thanks for carrying me as one of your students, for your dedication in my project and for your valuable and insightful inputs towards my assays planning, data analyses and publication contributions.

Special thanks to Dr Kabamba Alexandre for offering the necessary training to work with live HI viruses, for being a supportive fellow student in times of academic need and for the help with escape mutation assay and the corresponding analysis.

I would like to thank my co-authors for their team-work dedication in attaining the publication. My gratitude also goes to Maphuti Madiga for the training in pseudovirus neutralization assay, and Tandile Hermanus for making sure that the viruses are available for use at all times. To Mary Phoswa for the PBMC isolation training and for providing clinical isolates for use when needed. To Sarah Cohen for maintaining the laboratories in good working conditions.

Finally I would like to thank my CSIR Aptamer laboratory colleagues for their moral support.

TABLE OF CONTENTS

DECLARATION ..... **ii**

ABSTRACT ..... **iii**

PUBLICATIONS FROM THIS THESIS ..... **v**

OTHER PUBLICATIONS NOT RELATED TO THESIS ..... **vi**

PRESENTATIONS AT MEETINGS ..... **vii**

OTHER PRESENTATIONS NOT RELATED TO THESIS ..... **x**

DEDICATION ..... **xi**

ACKNOWLEDGEMENTS ..... **xii**

TABLE OF CONTENTS ..... **xiv**

LIST OF FIGURES ..... **xxii**

LIST OF TABLES ..... **xxv**

ABBREVIATIONS ..... **xxvi**

AMINO ACID ABBREVIATIONS ..... **xxvii**

CHAPTER 1 ..... **1**

Introduction **1**

1. Background **2**

1.1 Global epidemiology of HIV-1 2

1.2 HIV subtypes 2

1.3 Origin of the HIV-1 epidemic in South Africa 6

2. HIV-1 formation and pathogenesis 7

2.1 HIV-1 structure 7

2.2 HIV-1 life cycle 9

2.3 HIV-1 receptors and implications of cell tropism 9

3. HIV-1 envelope glycoprotein 12

3.1 HIV native structure 12

3.2 HIV-1 gp120 molecular structure 13

3.3 Viral Entry 15

3.4 Viral entry inhibitors 16

4. Aptamers: a new class of entry inhibitors 20

4.1 Isolation of aptamers 22

4.2 Properties of aptamers 26

4.3 General aptamer applications 27

4.4 Anti gp120 RNA aptamers 29

5. Study objectives 30

CHAPTER 2 33

Production of Anti-gp120 RNA Aptamers and Evaluation of their Biological Activity 33

Chapter summary 34

1. Introduction 36

2. Materials and Methods 40

2.1 Monoclonal antibodies, proteins and plasma samples 40

2.2 Anti-gp120 RNA aptamers 41

2.3 Generation of monoclonal anti-gp120 aptamers from cloned plasmids . 41
2.3.1 Amplification of anti-gp120 aptamers 41
2.3.2 In vitro transcription 43
2.3.3 Sephadex-G50 purification 43
2.3.4 Phenol:Chloroform extraction 44
2.4 Expression of recombinant HIV-1 glycoproteins 44
2.4.1 Purification of HIV-1 glycoproteins 45
2.4.2 Protein confirmation and functionality assays 45
2.4.3 Enzyme linked immunosorbent assay (ELISA) 46
2.5 The BIAcore SPR technology 48
2.5.1 Protein immobilization onto biosensor chip 48
2.5.2 Binding affinity measurements 49
2.5.3 Binding kinetics of aptamers to HIV-1 glycoproteins 50
2.6 Single-cycle neutralization assay 51
2.7 Env-pseudoviruses used 51
3. Results 52
3.1 PCR amplification and transcription of anti-gp120 aptamers 52
3.2 Expression and purification of gp120 52
3.2.1 Antigenicity of gp120 52
3.3 Binding of RNA aptamers to gp120 proteins 55
3.3.1 Screening of binding affinity 55
3.3.2 Binding kinetics of RNA aptamers to HIV-1 glycoproteins 56
3.4 Optimization of aptamer usage in TZM-bl neutralization assay 58
4. Discussion 61

CHAPTER 3 64

Inhibition of Human Immunodeficiency Virus Type-1 Subtype C Env Pseudotyped Virus Infection with UCLA1 RNA aptamer 64

Chapter summary 65

1. Introduction 66

2. Materials and Methods 69

2.1 Truncated and mutated glycoproteins 69

2.2 Binding kinetics of RNA aptamers to HIV-1 glycoproteins 69

2.3 Cytotoxicity assay 69

2.4 Production of Env-pseudovirions 71

2.4.1 Proviral DNA PCR 71

2.4.2 Transformation of TOP10 chemically competent cells 71

2.4.3 Transfection of Env plasmid DNA 72

2.4.4 Determination of pseudovirus titers 72

2.5 Maintenance of TZM-bl cells 73

2.6 Panel of Env-pseudoviruses 74

2.7 Single-cycle neutralization assay 74

2.8 Site-directed mutagenesis 75

2.8.1 Transformation of XL1-Blue supercompetent cells 75

2.8.2 HIV-1 envelope DNA sequencing 76

2.8.3 Mutated Env-pseudotyped virus stocks 77

2.9 Synergy of UCLA1 with other entry inhibitors 77

3. Results 79

3.1 Neutralization of Env-pseudotyped viruses by UCLA1 79

3.2 UCLA1 is not cytotoxic and has a wide therapeutic index 81

3.3 Mapping UCLA1 neutralization sites using the ConC Env-pseudovirus 83

3.3.1 Mapping aptamer binding sites using ConC gp120 proteins 84

3.3.2 Sequence analysis of neutralization resistant viruses 85

3.4 Synergy of UCLA1 with other entry inhibitors 92

4. Discussion 95

CHAPTER 4 99

UCLA1 Inhibition of HIV-1 Subtype C Primary Isolates in PBMCs and Monocyte-Derived Macrophages and Evaluation of Escape Mutations 99

Chapter summary 100

1. Introduction 101

2. Materials and Methods 105

2.1 PBMC assays 105

2.1.1 PBMC Isolation 105

2.1.2 CD8 depletion of PBMCs 106

2.1.3 PBMC infection with HIV-1 and expansion of infected cultures 106

2.1.4 Virus titration in PBMCs 107

2.1.5 HIV-1 primary viruses used in PBMCs 108

2.1.6 Cytotoxicity assay in PBMCs 108

2.1.7 Neutralization of primary infectious viruses in PBMCs 108

2.1.8 Detection of viral titers in PBMCs 109

2.2 MDM assays 110

2.2.1 MDM isolation 110

2.2.2 MDM phenotyping 111

2.2.3 HIV-1 infection of MDMs 112
2.2.4 Screening of macrophage-tropic viruses 113
2.2.5 HIV-1 neutralization assay in MDMs 114
2.2.6 HIV-1 primary viruses used in MDM neutralization assay 115
2.3 HIV-1 p24-antigen immunoassay 115
2.3.1 Plate coating 116
2.3.2 ELISA 116
2.4 Evaluation of UCLA1 resistance 117
2.4.1 Generation of UCLA1 resistant viruses 117
2.4.2 HIV-1 Envelope amplification and purification 118
2.4.2.1 RT-PCR 118
2.4.2.2 PCR 118
2.4.3 HIV-1 envelope sequencing 119
3. Results 120
3.1 UCLA1 is not cytotoxic to PBMCs 120
3.2 Neutralization of HIV-1 primary isolates in PBMCs 121
3.3 MDM assay results 124
3.3.1 MDM phenotyping 124
3.3.2 Screening macrophage-tropic viruses 127
3.3.3 Neutralization of HIV-1 primary isolates in MDMs 127
3.4 Generation of UCLA1 resistant isolates 129
3.4.1 Pattern of viral growth in increasing concentrations of UCLA1 130
3.4.2 Amplification and sequencing of primary viruses selected for UCLA1 resistance 131

4. Discussion **136**

CHAPTER 5 ..... **141**

General Discussion and Conclusions **141**

APPENDICES **151**

APPENDIX A **152**

Ethics Clearance 152

APPENDIX B **153**

General suppliers 153

APPENDIX C **155**

General Materials and Methods 155

1.1 Agarose gel electrophoresis 155

1.2 Ethanol precipitation 155

1.3 Quantification of DNA and RNA 155

1.4 Denaturing polyacrylamide gel electrophoresis 156

1.5 Plasmid DNA purification 156

1.6 Purification of DNA in sequencing reaction 157

1.7 Isolation of HIV-1 RNA 157

1.8 DNA purification 158

1.8.1 PCR purification 158

1.8.2 Gel purification 158

APPENDIX D **160**

Supplementary Figures 160

Supplementary Tables 163

APPENDIX E 166

Publication 166

REFERENCES..... 167

LIST OF FIGURES

Figure 1-1: A global view of HIV infection in 2009. 4

Figure 1-2: The global distribution and genetic diversity of HIV-1. 5

Figure 1-3: HIV virion structure. 8

Figure 1-4: HIV life cycle. 11

Figure 1-5: A tomogram showing the 3D structure of the trimeric glycoprotein spike on native HIV-1. 14

Figure 1-6: Structure of the core of gp 120 envelope glycoprotein. 14

Figure 1-7: HIV-1 gp120 antigenic structure. 15

Figure 1-8: A model of Env-mediated, CD4 dependent HIV-1 entry. 16

Figure 1-9: Localization of the broadly neutralizing MAb epitopes on the HIV-1 envelope trimer. 20

Figure 1-10: Anti-gp120 aptamer. 22

Figure 1-11: In vitro selection of target-specific aptamers using SELEX technology. 23

Figure 2-1: Proposed secondary structure of aptamer B40t77 and B40. 39

Figure 2-2: Surface plasmon resonance (SPR) detects changes in the refractive index in the immediate vicinity of the surface layer of a sensor chip. 49

Figure 2-3: Gels showing PCR products of aptamers. 53

Figure 2-4: A 6% SDS-PAGE showing the purity and size of the expressed Du151 gp120 protein. 54

Figure 2-5: The antigenicity of Du151 gp120 protein. 54

Figure 2-6: BIAcore sensorgrams showing immobilization of gp120 protein and binding of aptamers to gp120. 57

Figure 2-7: Affinity of derivatives of B40 aptamer to subtype C gp120. 58
Figure 2-8: Effects of FBS on aptamer activity. 59
Figure 2-9: UCLA1 activity unaltered by different FBS concentrations. 59
Figure 2-10: Differing efficacy for different aptamers. 60
Figure 3-1: Representative dose-dependent neutralization graphs of Env-pseudotyped viruses with UCLA1. 82
Figure 3-2: Percentage viability of TZM-bl cells in the presence of varying concentrations of UCLA1. 83
Figure 3-3: Neutralization of ConC gp120 single-point mutants with UCLA1. 87
Figure 3-4: Binding kinetics of UCLA1 to truncated and mutated HIV-1 ConC gp120. 88
Figure 3-5: Amino acid sequence alignment of HIV-1 gp120 of Env-pseudotyped viruses that were tested for neutralization with UCLA1. 91
Figure 3-6: Representative dose-dependent neutralization graphs of HIV-1 subtype C Env-pseudotyped viruses showing synergism of UCLA1 with T20 and b12. 93
Figure 4-1: Percentage viability of PBMCs in the presence of varying concentrations of UCLA1. 120
Figure 4-2: Representative dose-dependent neutralization graphs of HIV-1 subtype C primary isolates in PBMCs. 122
Figure 4-3: Amino acid sequence alignment of HIV-1 gp120 of primary isolates that were tested for neutralization with UCLA1 in the PBMC assay. 123
Figure 4-4: FACS dot plots showing pure isolated macrophages. 126
Figure 4-5: Infectivity of HIV-1 primary viruses in monocyte-derived macrophages. 128

Figure 4-6: Representative dose-dependent neutralization graphs of HIV-1 subtype C primary isolates in MDM. 129
Figure 4-7: In vitro selection for UCLA1 resistant viruses..... 133
Figure 4-8: 2% agarose gel showing PCR amplified env genome of RP1..... 134
Figure 4-9: Structural representation of UCLA1 escape mutations generated under increasing concentrations of the aptamer..... 134
Figure 4-10: Amino acid sequence alignment of RP1 isolate propagated under increasing concentrations of UCLA1 (RP1 UCLA1). 135

LIST OF TABLES

Table 2-1: The binding affinity of in-house aptamers against HIV-1_{BaL} and Du151 gp120 proteins. 56

Table 3-1: Inhibition of HIV-1 subtype C envelope pseudotype viruses by UCLA1 RNA aptamer. 80

Table 3-2: Effect of single point mutations on the neutralization of the ConC virus by UCLA1..... 86

Table 3-3: Combination therapy using UCLA1, T20 and b12 against subtype C Env pseudotype viruses. 94

Table 4-1: Antibodies used for MDMs phenotyping..... 112

Table 4-2: Pre- and post-selection IC_{50} values of UCLA1 against HIV-1 primary isolates. 130

ABBREVIATIONS

µg	microgram
AIDS	Acquired Immunodeficiency Syndrome
ARV	Antiretroviral
CCR5	Chemokine (C-C motif) receptor 5
CD4	Cluster of Differentiation 4
CD4bs	Cluster of Differentiation 4 binding site
ConC	Consensus C
CoR, CoRbs	Co-receptor, Co-receptor binding site
CRF	Circulating Recombinant Forms
CXCR4	Chemokine (C-X-C motif) receptor 4
DNA	Deoxyribonucleic acid
dNTP	deoxyribonucleotidetriphosphate
D-tropic (R5X4)	Dual-tropic (CCR5, CXCR4)
ELISA	Enzyme-Linked ImmunoSorbent Assay
env	Envelope gene
Env	envelope glycoprotein
gp120, gp41	Glycoprotein 120 kDa, 41 kDa
HIV-1, HIV-2	Human Immunodeficiency Virus type-1, -2
HR1, HR2	Heptad repeat domains 1 and 2
IAVI	International AIDS Vaccine Initiative
IC_{50}	50% inhibitory concentration
ID_{50}	50% inhibitory dilution
IgG	Immunoglobulin G
kbp	kilo base pairs
kDa	Kilodalton
K_D	Equilibrium dissociation constant
MAbs	Monoclonal antibodies
MDM	Monocyte-derived macrophages
MPER	Membrane proximal external region
mRNA	messenger RNA

M-tropic	Macrophage tropic
nM	Nanomolar
NSI	Non-syncytium-inducing
PBMCs	Peripheral blood mononuclear cells
PCR	Polymerase chain reaction
RNA	Ribonucleic acid
RT	Reverse transcriptase
RT-PCR	Reverse transcriptase polymerase chain reaction
SELEX	Systematic evolution of ligands by exponential enrichment
SDS-PAGE	Sodium dodecyl sulfate-polyacrylamide gel electrophoresis
SI	Syncytium inducing
siRNA	Small interfering RNA
SPR	Surface Plasmon Resonance
$TCID_{50}$	50% Tissue culture infective dose
TMB	Tetramethylbenzidine
UCLA	University of California, Los Angeles
URF	Unique Recombinant Forms

AMINO ACID ABBREVIATIONS

Amino Acid	Three Letter Code	One Letter Code
Alanine	Ala	A
Arginine	Arg	R
Asparagine	Asn	N
Aspartic acid	Asp	D
Glutamic acid	Glu	E
Glutamine	Gln	Q
Glycine	Gly	G
Histidine	His	H
Isoleucine	Ile	I
Leucine	Leu	L

Lysine	Lys	K
Methionine	Met	M
Phenylalanine	Phe	F
Proline	Pro	P
Serine	Ser	S
Threonine	Thr	T
Tyrosine	Tyr	Y
Valine	Val	V

CHAPTER 1

Introduction

1. Background

1.1 Global epidemiology of HIV-1

Since the beginning of the AIDS epidemic, more than 60 million people have been infected with the human immunodeficiency virus (HIV) and nearly 30 million people have died (UNAIDS, 2010). An estimated 34 million people worldwide were living with HIV at the end of 2010 with 2.7 million new HIV infections and an estimated 1.8 million AIDS-related deaths (WHO/UNAIDS, 2011) (Figure 1-1). Sub-Saharan Africa remains the global epicentre of the AIDS pandemic where 22.9 million (67%) people were living with HIV at the end of 2010, representing 70% of new infections globally (WHO/UNAIDS, 2011). South Africa's epidemic remains the largest in the world with an estimated 5.6 million people living with HIV in 2009 (UNAIDS, 2010). With the high rate of new infections and only an estimated 55% of people receiving antiretroviral (ARV) treatment in 2010, the HIV/AIDS burden remains a challenge in South Africa.

1.2 HIV subtypes

HIV is among the most genetically variable human pathogens. Identification of new variants, including circulating recombinant forms (CRF) and unique recombinant forms (URF), proves the diversity and the increasing complexity (Arien et al., 2007, Pandit & Sinha, 2010, Thomson & Najera, 2005) (Figure 1-2). HIV-1 sequences are classified into three phylogenetically distinct groups - M (*Major*), O (*Outlier*), and N (*non-M/non-O*) - based upon their sequence diversity (Pandit & Sinha, 2010). The M group is globally prevalent and responsible for most of the pandemic. Group M is further stratified into eight genetically discrete subtypes - A to D, F to H, and J -

showing up to 25% to 35% sequence level variations between the genomes in different subtypes (McCutchan, 2006, Pandit & Sinha, 2010, Takebe et al., 2008, Tebit et al., 2007). In the Americas and Western Europe, subtype B predominates except in the eastern South America, where there is a substantial mix of other subtypes and recombinants in addition to subtype B (Figure 1-2). In Eastern Europe, subtype A3, B, and a mixture of recombinant strains dominate the epidemic. Two different patterns have been observed in Asia: subtype C and AB recombinants dominate central Asia whereas central Asia is dominated by AE recombinants. The Australian epidemic is predominantly driven by subtype B (Figure 1-2). Africa shows the greatest diversity. Subtype C dominates in Southern and East Africa, respectively (Hemelaar et al., 2006) and is regarded as the fastest spreading subtype as observed in Southern Africa as a whole (Essex, 1999, Thomson & Fernandez-Garcia, 2011). However, there is a significant presence of subtypes A and D (Figure 1-2) (Arien et al., 2007). By use of coalescent methods, it has been inferred that subtype C in sub-Saharan Africa is growing exponentially, with a doubling time of 2.4 years (Walker et al., 2005). Subtype C variants of monophyletic origin have been reported in India, Ethiopia, China and South America (de Oliveira et al., 2010, Hemelaar et al., 2006, Ryan et al., 2007, Salminen et al., 1996, Thomson & Najera, 2005). In Cuba, a subtype C variant related to the Ethiopian cluster is circulating in a minority of homosexual men (Thomson & Najera, 2005). West and West Central Africa harbour mainly AG recombinants in addition to subtypes A1, G and other recombinants each present at a low frequency (Arien et al., 2007). The most complex epidemic is in Central Africa, where rare subtypes and a wide variety of recombinant forms circulate (Figure 1-2) (Arien et al., 2007).

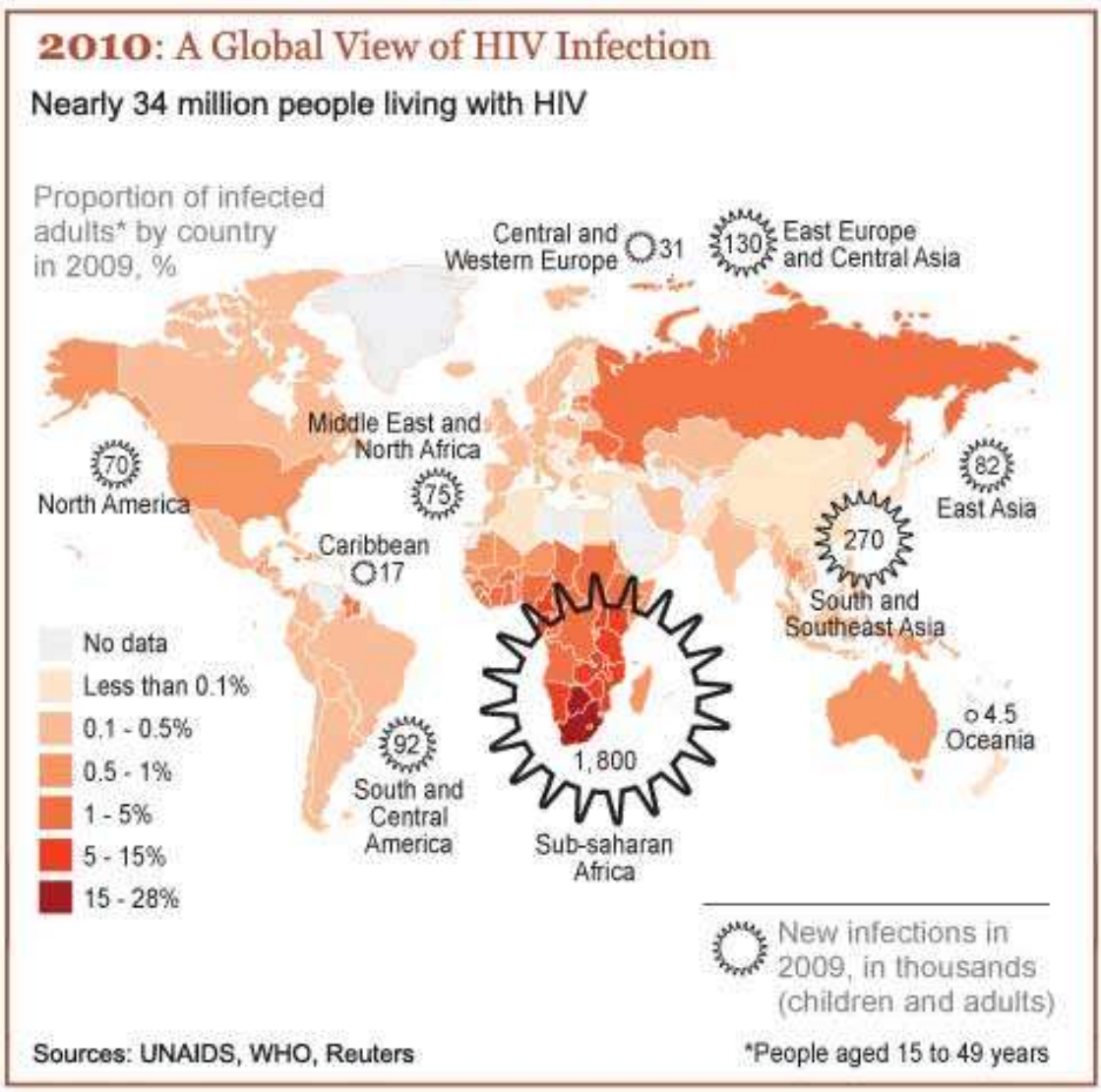

Figure 1-1: A global view of HIV infection in 2009.
WHO/UNAIDS global AIDS epidemic report, 2010. Sub-saharan Africa harbours the largest HIV infected population followed by South and Southeast Asia and East Europe and central Asia.

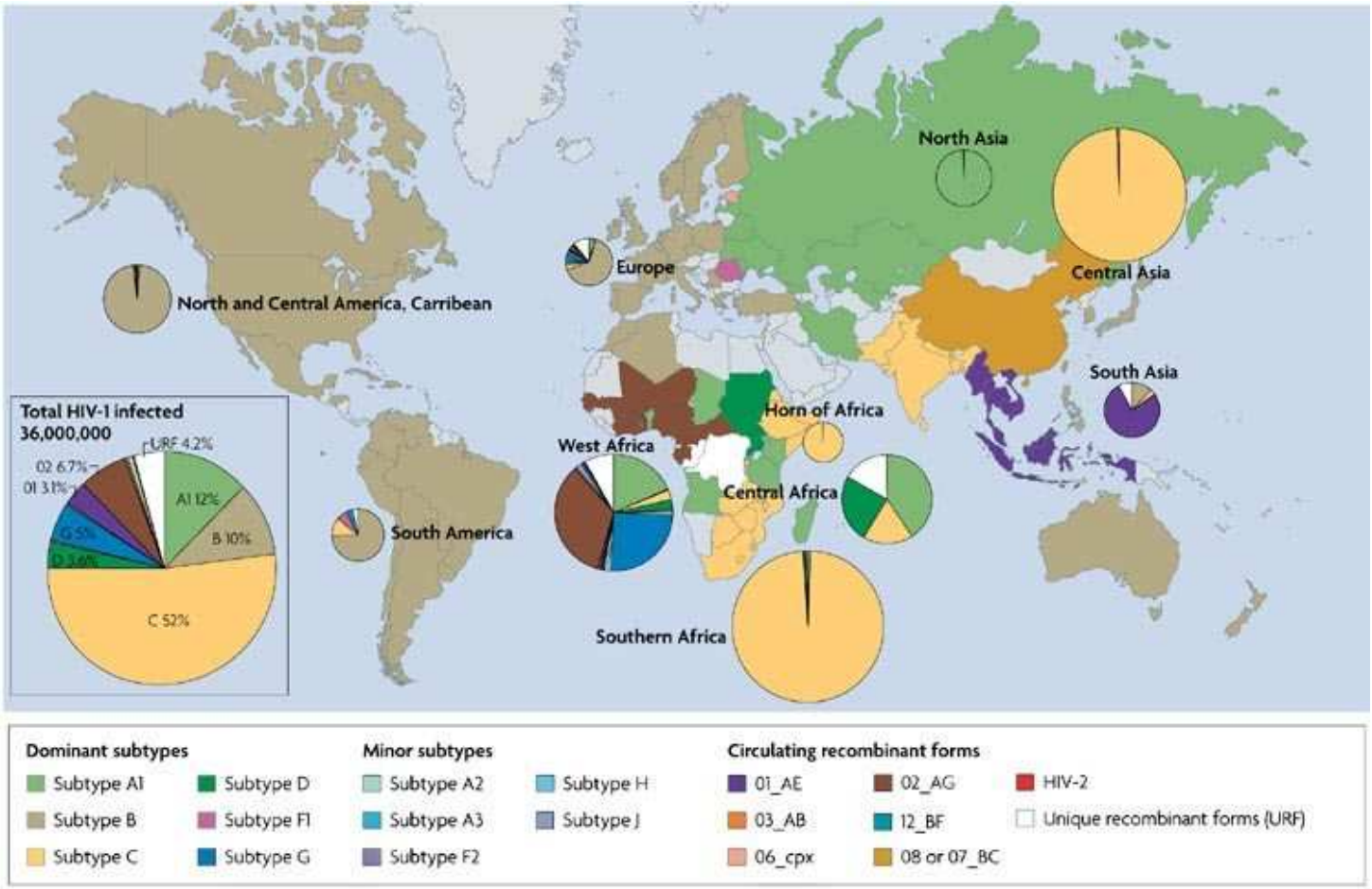

Figure 1-2: The global distribution and genetic diversity of HIV-1.
Eleven different HIV-1 epidemic patterns have been observed, as indicated by the eleven major subtypes and recombinants shown in different colors. Subtype C is shown as the most prevalent subtype mostly in Africa and Asia and to a lesser extent in South America. Map acquired from Arien *et al*., 2007.

1.3 Origin of the HIV-1 epidemic in South Africa

The initial report of HIV-1/AIDS in South Africa involved two cases published in 1983 (Ras et al., 1983). Further published data in 1985 revealed that AIDS cases were primarily confined to men who had sex with men (Klopper, 1985). Thus the initial epidemic in South Africa paralleled observations in the USA (Klopper, 1985, Puren, 2002). By 1989 the nature of the epidemic reflected a change in transmission patterns as more cases were identified in the black, primarily heterosexual group, that is, the so-called 'second' epidemic as opposed to the first that was primarily in the white, male homosexual group (Sher, 1989). This epidemic is believed to have originated from simian immunodeficiency viruses endemic in chimpanzees (SIVcpz) (Sharp et al., 2001, Sousa et al., 2012) and gorillas (SIVgor) (Van Heuverswyn et al., 2006) from sub-Saharan Africa, and it started to spread in the late 19th or early 20th century. At the time of its origin a coincidence of favourable co-factors such as intense ape hunting, social disruption, sexual promiscuity (Jennes et al.), commercial sex work, sexually transmitted diseases (STDs), colonialism, increased trading and traffic/mobility and to a lesser extent parenteral transmission for both cross-species transmission and heterosexual spread was evident (Sousa et al.). Later it was discovered that the origin of the epidemic in the USA was from Haiti in the late 1960s or early 1970s and was believed to have arrived in Haiti from central Africa through professional contacts with the Democratic Republic of Congo (Gilbert et al., 2007).

A study that examined the genetic diversity of HIV-1 in a cohort of mine workers from southern Africa countries, including Botswana, Lesotho, Swaziland and Mozambique confirmed that subtype C was predominant (Bredell et al., 1998). Another study that used both serotyping and genotyping on a selection of specimens from four

provinces, KwaZulu-Natal, Gauteng, Mpumalanga and the Western Province confirmed that the dominant subtype in each province was C (Engelbrecht et al., 1999). Moreover, there is a complex interaction between tuberculosis, hepatitis and other sexually transmitted diseases with HIV-1 that has contributed to the present disease burden (Abdool Karim et al., 2009).

2. HIV-1 formation and pathogenesis

2.1 HIV-1 structure

HIV is a member of the genus *Lentivirus* in the *Retroviridae* family (Levy, 2007). Retroviruses are so called because their RNA genome is transcribed into DNA within the cell using the viral enzyme reverse transcriptase (RT). This DNA then enters the nucleus and integrates into the cellular chromosome (Levy, 2007). Lentiviruses consist of a diverse group of animal viruses (Fauci, 1997). The human counterpart, HIV, was discovered because of its association with AIDS (Gottlieb et al., 1983). This clinical condition is characterized by a marked reduction in $CD4^+$ cells and the development of opportunistic infections as a result of the persistent replication and spread of HIV (Levy, 2007).

HIV-1 is composed of two copies of single-stranded RNA enclosed by a conical capsid comprising the viral protein p24 (Figure 1-3). The integrated form of HIV-1, also known as the provirus, is approximately 9.8 kilobases in length (Muesing et al., 1985). This in turn is surrounded by a plasma membrane of host-cell origin. The genes of HIV are located in the central region of the proviral DNA and encode at least nine proteins. The proteins are divided into 3 classes: the major structural

proteins (Gag, Pol, and Env) the regulatory proteins (Tat and Rev) and the accessory proteins (Vpu, Vpr, Vif, and Nef). The single-strand RNA is tightly bound to the nucleocapsid proteins, p6, p7 and enzymes that are indispensable for the development of the virion, such as reverse transcriptase and integrase. A matrix composed of an association of the viral protein p17 surrounds the capsid, ensuring the integrity of the virion particle (Figure 1-3). Also enclosed within the virion particle are Vif, Vpr, Nef, p7 and viral Protease. The envelope is formed when the capsid buds from the host cell, taking some of the host-cell membrane with it. The envelope includes the glycoproteins gp120 and gp41.

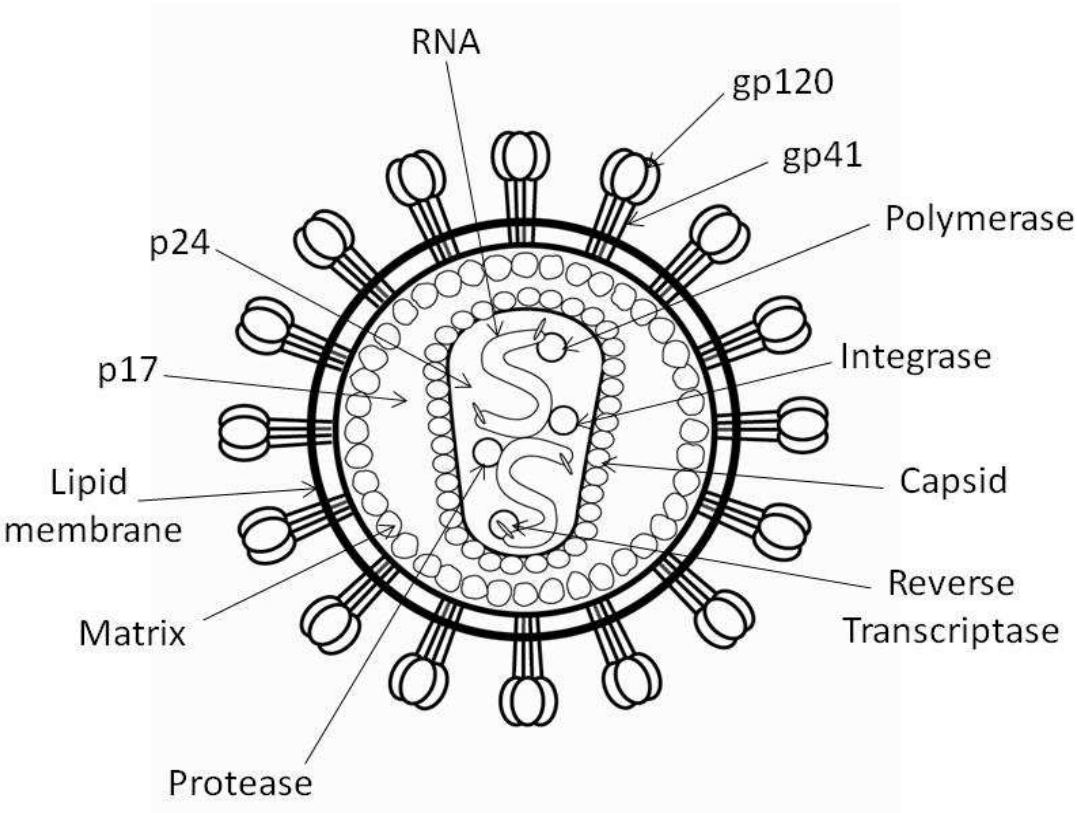

Figure 1-3: HIV virion structure.
Two copies of single stranded RNA together with the polymerase, integrase, protease and reverse transcriptase enzymes are enclosed by the capsid p24 protein. The capsid is surrounded by the matrix and p17 protein which are in turn enclosed by the lipid membrane. The membrane is composed of the envelope glycoproteins gp120 and gp41.

2.2 HIV-1 life cycle

The free virus (HIV) infects a cell by binding the envelope protein to a CD4 receptor and one of the two co-receptors (CCR5, CXCR4) on the surface of a CD4+ T lymphocytes and macrophages (Figure 1-4) (Chan et al., 1998, Wyatt et al., 1998). The virus then infects the host cell and releases its single-stranded HIV RNA into the host cell. There is growing evidence that HIV-1 entry occurs via receptor-mediated endocytosis followed by fusion with endosomes (de la Vega et al., Miyauchi et al., 2009a, Miyauchi et al., 2009b) whilst with activated macrophages it can occur by receptor-independent endocytosis (Gobeil et al., 2012). Reverse transcriptase converts the RNA to double-stranded DNA which enters the host cell's nucleus. The integrase causes integration of the viral DNA into host cell's DNA. The integrated provirus uses RNA polymerase for transcription of more single-stranded RNA and messenger RNA which are used to make HIV proteins. The proteins assemble together with copies of single-stranded RNA to form new virus particles. The newly assembled virus buds out from the host cell with its envelope consisting of glycoproteins (gp120 and gp41) that are necessary for it to bind to the CD4 and co-receptors. The protease enzyme causes maturation of the new viral copies which are then ready to infect other cells once they are matured.

2.3 HIV-1 receptors and implications of cell tropism

HIV-1 strains have previously been characterized by their ability to produce syncytia following infection of neoplastic cell lines (Fenyo et al., 1988). Syncytium inducing (SI) viruses are frequently found in progressive or late-stage HIV disease while nonsyncytium inducing (NSI) viruses are present throughout disease (Fenyo et al., 1988, Schuitemaker et al., 1992). HIV- 1 can also be classified by its ability to infect

primary macrophages and CD4+ T cell lines. All HIV-l isolates can replicate in primary T cells. However SI isolates that have adapted to transformed T cell lines, also known as T-tropic strains, cannot replicate in macrophages whereas primary NSI isolates, also known as M-tropic strains, can infect macrophages. There are also HIV-l strains that contain both SI and NSI components capable of infecting both T cell lines and primary macrophages (Michael, 1999). HIV-1 strains can also be classified by co-receptor utilization. The NSI viruses primarily utilize the C-C chemokine receptor 5 (CCR5) and are termed R5-tropic viruses whereas SI viruses primarily utilize the C-X-C chemokine receptor 4 (CXCR4) and are termed X4-tropic viruses (Berger et al., 1998). However, some primary SI isolates use CXCR4 in conjunction with CCR5 and are termed R5X4 or dual-tropic (D-tropic) viruses (Berger et al., 1998).

CCR5-tropism is characteristic of viral isolates that persist during asymptomatic disease, and are further thought to be the principal subset of virus responsible for new infections. The importance of CCR5-tropism in HIV-1 pathogenesis has been highlighted by the discovery of a subset of individuals at high risk for infection with HIV-1 that remained seronegative despite multiple opportunities for virus transmission (Samson et al., 1996). Genetic analysis of these cohorts revealed that some of these individuals were homozygous for a 32 base pair deletion in the CCR5 open reading frame (Δ32 CCR5) and their CD4 T cells were resistant to infection by R5-tropic viruses (Liu et al., 1996, Samson et al., 1996). The deletion results in a truncated receptor that is not expressed on the cell surface. The Δ32 allele is present in the white population with only a few (1%) homozygotes and approximately 20% heterozygotes (Dean et al., 1996). Although they are highly resistant to acquisition of

HIV-1, homozygous individuals can be infected by CXCR4-using viruses (Liu et al., 1996, Samson et al., 1996). Heterozygous individuals suffer a significantly slower disease course and longer time intervals before progression to AIDS, demonstrating the importance for CCR5 in HIV-1 pathogenesis. Single nucleotide polymorphisms within the promoter region of CCR5 have also been associated with differences in disease progression rates. Specifically, individuals who are *-2459A/A* have been shown to progress to AIDS more rapidly than individuals homozygous for the guanine allele (*-2459G/G)* (An et al., 2000, Martin et al., 1998, Ometto et al., 2001).

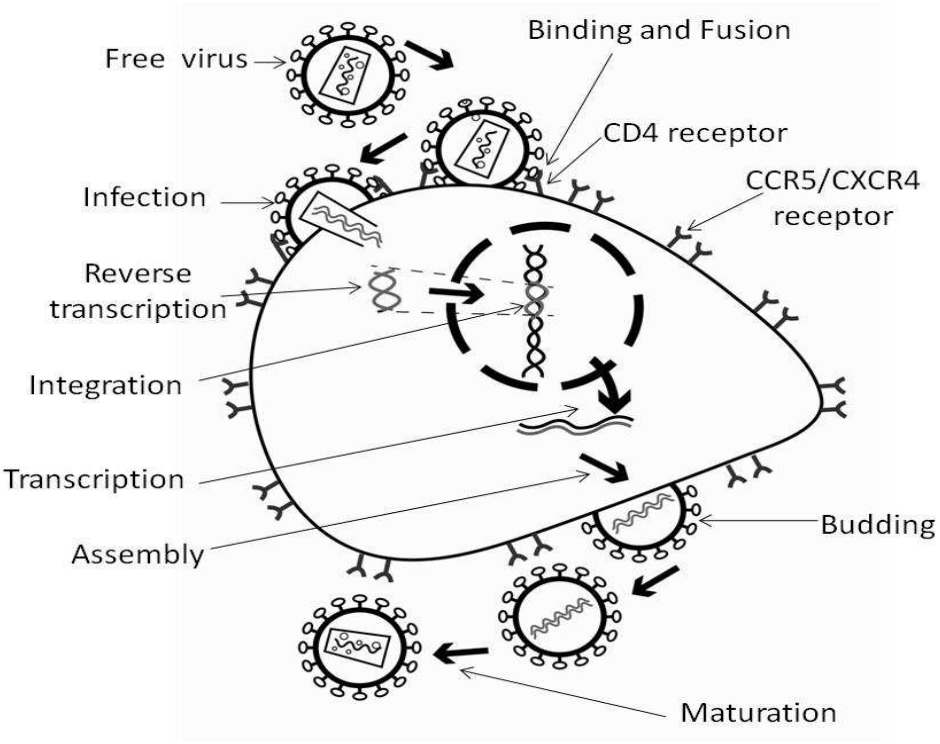

Figure 1-4: HIV life cycle.
The virus infects cells by binding and fusion of the envelope protein to a CD4 receptor and either CCR5 or CXCR4 co-receptor on the surface of host cells. Infection occurs when the virus releases its RNA into the host cell. There is increasing evidence that HIV-1 infection occurs via endocytosis. Reverse transcription of the RNA to DNA occurs by the reverse transcriptase protein. The DNA then enters the nucleus of the host cell. Integration of the viral DNA into the host cell's DNA occurs by the integrase protein. Transcription of the integrated DNAs reproduces more RNA to make HIV proteins. The proteins then assemble together with the RNA to form new virus particles. The newly assembled virus buds out from the host cell. Maturation of the new viral copies occurs by the protease enzyme.

3. HIV-1 envelope glycoprotein

3.1 HIV native structure

Entry of HIV into host cells is mediated by the viral envelopes, which are organized into trimeric spikes displayed on the surface of the virion. The Env glycoprotein is assembled from the precursor gp160 which is cleaved into three gp120 exterior subunits and three gp41 transmembrane subunits. Thus, gp120 is associated by non-covalent interactions with each subunit of the trimeric gp41 glycoprotein complex (Liu et al., 2008, Zanetti et al., 2006, Zhu et al., 2008) (Figure 1-5). A structure of a membrane bound HIV-1 Env trimer in an unliganded state was recently reported (Mao et al., 2012). Although the structure is uncleaved it revealed that the gp41-gp120 trimeric subunits form a cage-like structure with an interior void surrounding the trimer axis. The cage is believed to restrict antibody access, explaining HIV-1 persistence in the host (Mao et al., 2012). The study also shown that the unliganded gp41-gp120 trimer association is limited to gp41 transmembrane, gp41 ectodomain and the trimer association domain of gp120 including the V1, V2 and V3 variable regions. The study proposes that the variable regions restrain movement into the CD4-bound conformation by their interactions at the gp120 trimer interface. This effect has been shown when changes in the V1, V2 and V3 variable regions rendered the HIV-1 Env prone to assuming the CD4-bound conformation and allowing virus entry into cells expressing low CD4 (Kolchinsky et al., 2001, Mao et al., 2012, Musich et al., 2011, Zhang et al., 2002).

3.2 HIV-1 gp120 molecular structure

Gp120 is composed of an inner domain, an outer domain and the bridging sheet; all three structural elements contribute to CD4 and chemokine-receptor binding (Figure 1-6) (Huang et al., 2007, Mao et al., 2012, Rizzuto & Sodroski, 2000, Rizzuto et al., 1998, Zhou et al., 2007). The amino-acid sequence of human and simian immunodeficiency virus gp120 consists of five variable regions (V1-V5) interposed among more conserved regions (C1-C5) (Chen et al., 2005a, McCaffrey et al., 2004). The conserved gp120 regions form discontinuous structures important for the interaction with the gp41 ectodomain and with the viral receptors on the target cell. Antigenic and structural analyses of the most exposed components of gp120 reveal four surfaces: a non-neutralizing face, a variable surface, a neutralizing face and an immunologically silent face (Kwong et al., 2002) (Figure 1-7). The non-neutralizing face, the variable surface and the silent face are protected from the immune system by occlusion on the oligomer, by mutational variation, and by a conformational or entropic masking (Kwong et al., 2002). Gp120 is also protected by carbohydrate masking since both conserved and variable gp120 regions are extensively glycosylated (Decker et al., 2005, Kwong et al., 2002, Zhou et al., 2007). Thus most carbohydrate moieties may appear as ‘self’ to the immune system and render gp120 less visible to immune surveillance (Kwong et al., 2002, McCaffrey et al., 2004).

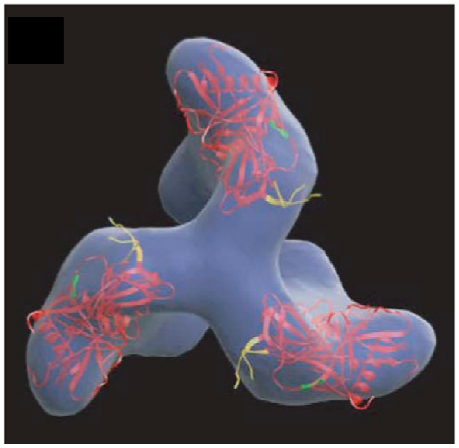

Figure 1-5: A tomogram showing the 3D structure of the trimeric glycoprotein spike on native HIV-1.
Top view of the surface of the density map with coordinates for gp120 core derived from the complex with b12. Gp120 core is shown in red and the V1/V2 and V3 loops are shown in yellow and green, respectively. Acquired from Liu *et al*., 2008.

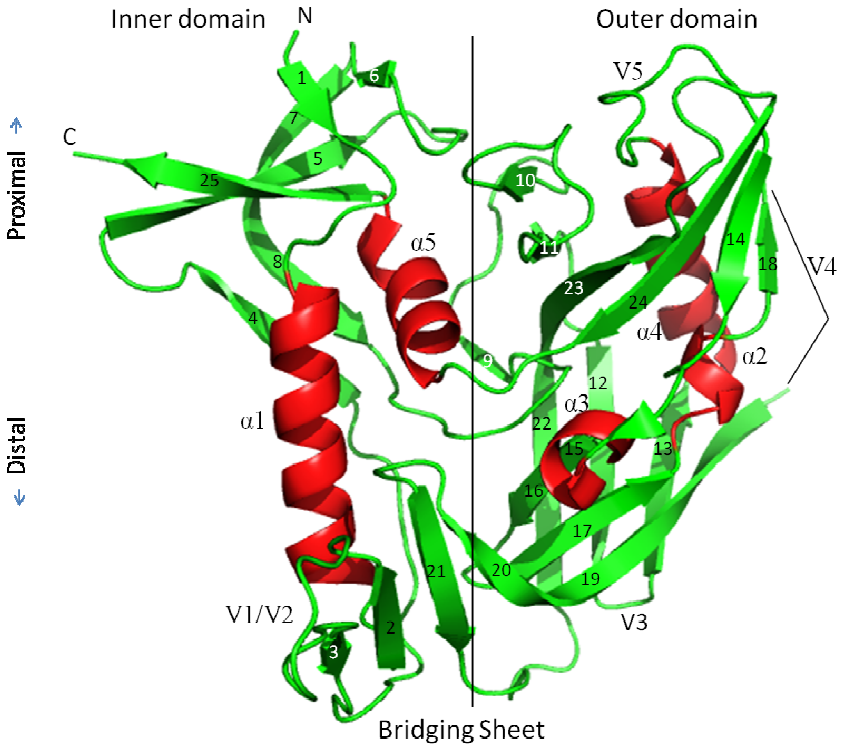

Figure 1-6: Structure of the core of gp 120 envelope glycoprotein.
Coordinates were taken from the structure of the core gp120 in complex with the CD4 receptor and 17b MAb (Protein Data Bank accession no. 1GC1). The figure was generated with PyMOL (DeLano Scientific LLC, South San Francisco, CA [http://www.pymol.org]).

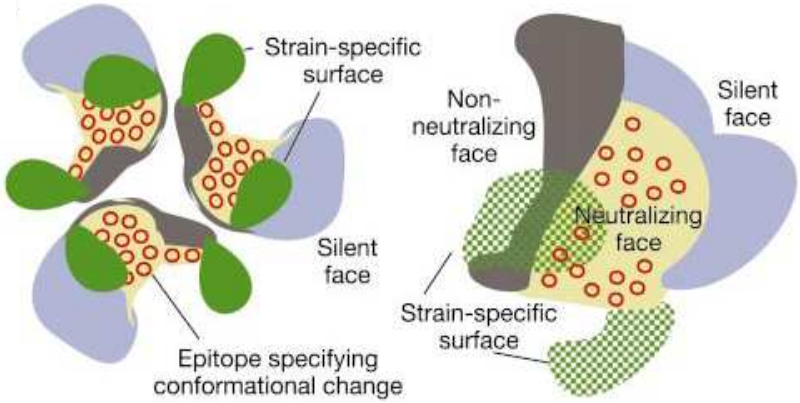

Figure 1-7: HIV-1 gp120 antigenic structure.
The antigenic structure is shown corresponding to epitopes bound by non-neutralizing antibodies (black), neutralizing antibodies that are broadly reactive (light yellow) and neutralizing antibodies that are strain specific (square pattern in forest green). The highly glycosylated gp120 surface rarely recognized by antibodies is coloured blue. Red circles designate epitopes that display unusual entropy due to conformational change. Acquired from Kwong *et al*., 2002.

3.3 Viral Entry

CD4 binding to gp120 induces conformational changes in gp120, which involve the exposure and/or formation of a binding site for CCR5 and CXCR4, which serve as obligate second receptors for virus entry (Figure 1-8) (Liu et al., 2008, Lobritz et al., 2010, Moore & Doms, 2003). Upon binding the target cell, gp120 assumes a transiently exposed conformation, which allows the exposed CD4 binding site (CD4bs) on gp120 to bind to the CD4 surface receptor. This binding exposes the V3 loop and unmasks the chemokine co-receptor binding site (Huang et al., 2007, Xiang et al., 2010). The V3 loop is the critical determinant of co-receptor tropism; a few amino acid changes can alter the co-receptor specificity from CCR5 to CXCR4. Furthermore, changes in the V3 loop have been associated with changes in susceptibility to entry inhibitors (reviewed by Hartley et al., 2005). Therefore, the CD4 and co-receptor binding induce additional conformational changes in gp41,

including exposure of the fusion peptide, which is first displaced toward the cell membrane and then inserts into it (Figure 1-8), (Doms & Moore, 2000, Liu et al., 2008). Structural rearrangements within the gp41 molecule are mediated by two triple stranded coiled-coils heptad repeat domains, N-terminal (HR1) and C-terminal (HR2) (Figure 1-8). As a result of this transition, the fusion peptide and transmembrane domain of gp41, along with their associated membranes, are brought into close proximity (Chan et al., 1997, Liu et al., 2008) and cause lipid mixing and membrane fusion (Doms & Moore, 2000, Melikyan et al., 2000, Moore & Doms, 2003) with the ultimate release of the viral core into the cytoplasm.

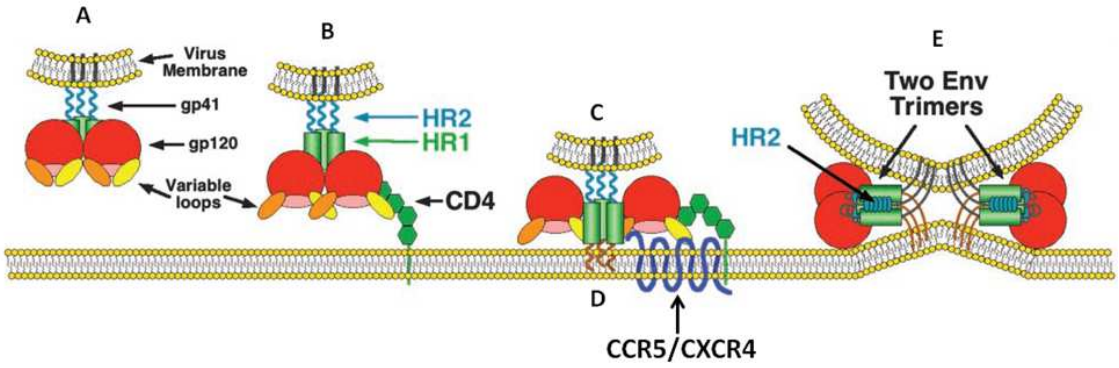

Figure 1-8: A model of Env-mediated, CD4 dependent HIV-1 entry.
(A) The functional unit of the envelope is a trimer composed of three gp41 molecules and three gp120 molecules. **(B)** Gp120 binds to host cell CD4 inducing conformational change **(C)** Binding of CD4 and gp120 with co-receptors (CCR5 or CXCR4). **(D)** Conformational change enables the fusion peptide to insert into the host cell membrane. **(E)** The heptad repeat regions pack into one another to form a stable six-helix bundle. Adapted from Moore and Doms, 2003 and Lobritz *et al*., 2010.

3.4 Viral entry inhibitors

The conserved nature of the CD4 and co-receptor binding sites of gp120 makes them attractive targets for immune intervention since they are necessary at the entry level of virus infection. Thus, various entry inhibitors have been developed due to a

better understanding of the receptor-induced conformational changes in gp120 that lead to viral infection of the cells (Berger et al., 1999, Dalgleish et al., 1984, Doms & Moore, 2000, Wyatt et al., 1998). HIV-1 entry inhibitors fall into three major classes based on the specific entry process that they target: 1) attachment inhibitors, which block the interaction between HIV-1 envelope and CD4, 2) co-receptor inhibitors, which block the interaction between HIV-1 envelope and CCR5 or CXCR4, and 3) fusion inhibitors, which prevent the virus from mixing its membrane with the host cell membrane and releasing the viral core into the cytoplasm (Figure 1-8) (reviewed by Lobritz et al., 2010).

The attachment inhibitor BMS-378806 inhibits both R5- and X4-tropic HIV-1 isolates (Lin et al., 2003). This compound binds to a pocket on gp120 important for binding CD4 and alters the conformation of the protein such that it cannot recognize CD4 (Ho et al., 2006). Peptide fusion inhibitors were designed based on the discovery that two homologous domains in the viral gp41 protein must interact with each other to promote fusion, and that mimicry of one of these domains by a heterologous protein can bind and disrupt the interactions of the virus protein. Alpha-helical peptides homologous to the leucine zipper domain of gp41 had significant antiviral activity against HIV-1, and this activity depended upon their ordered solution structure (Wild et al., 1993). Rational design ultimately produced a molecule (T-20, enfuvirtide) with potent antiviral activity in vivo (Kilby et al., 1998, Lalezari et al., 2003). The observation that the natural ligands of normal and inflammatory chemokine receptors (RANTES, MIP-1β, MIP-1α and SDF-1) possess anti-HIV-1 activity, made these chemokine receptors attractive novel targets for anti-HIV therapy (Cocchi et al., 1996). Thus the first attempt to generate a co-receptor based

entry inhibitor was modulation of the endogenous chemokine RANTES (CCL5). Deletion of two N-terminal residues of the endogenous chemokine RANTES (CCL5) residues resulted in increased potency of the chemokine (Schols et al., 1998). Addition of an aminooxypentane moiety to the N-terminus of either RANTES or MIP-1αP resulted in further increases in potency and increases in affinity for CCR5 (Townson et al., 2000).

Maraviroc, a CCR5 antagonist, manufactured by Pfizer, has been shown to inhibit virus replication in humans (Dorr et al., 2005). It has been tested in phase III efficacy trials and was approved for therapeutic use by the FDA in 2007. It is currently being used to treat patients with resistance to multiple HIV drugs but has been recently approved for first-line treatment. The CXCR4 antagonist, the bicyclam AMD3100, was shown to inhibit T-tropic HIV strains by selective antagonism of the SDF-1 chemokine receptor CXCR4 (Donzella et al., 1998, Schols et al., 1997).

The use of monoclonal antibodies (MAbs) to inhibit HIV entry by either blocking virus binding to CD4 and/or co-receptor or by post-receptor binding events have been extensively reported. One study investigated the reactivity of several known neutralizing MAbs against 90 viruses from different genetic subtypes (Binley et al., 2004). Anti-gp120 MAb IgG1b12, directed against the CD4-binding site, neutralized 50% of viruses from almost every subtype, but with lower activity against non-B viruses (39%) than B viruses (72%) (Binley et al., 2004). 4E10 MAb directed against the C terminus of the gp41 ectodomain, neutralized all viruses with moderate potency (Binley et al., 2004, Gray et al., 2006, Morris, 2007). 2G12 MAb directed against high mannose epitope of gp120 neutralized 41% of viruses, but none from

subtype C (Bures et al., 2002, Gray et al., 2006, Morris, 2007). 2F5 MAb directed against an epitope adjacent to the 4E10 epitope, neutralized 67% of viruses but non from subtype C (Binley et al., 2004, Bures et al., 2002, Gray et al., 2006, Morris, 2007). Cocktails of the abovementioned MAbs were shown to suppress viral rebound in HIV-1 infected individuals following treatment interruption (Trkola et al., 2005). They also exhibited neutralization synergy against HIV-1 primary isolates (Zwick et al., 2001).

Newly isolated broadly neutralizing MAbs represent a possibility for the eventual design of an effective antibody-based HIV vaccine (Walker et al., 2011, Walker et al., 2009, Wu et al., 2010). The VRC01 and VRC02 MAbs that bind to the CD4 binding region of gp120 broadly neutralized 91% of the tested viruses (Falkowska et al., 2012, Li et al., 2011, Wu et al., 2010, Zhou et al., 2010). VRC01 MAb was also shown to protect animals from mucosal challenge with a pathogenic chimeric SHIV (Pegu, 2011). The PGV04 (VRC-PG04) MAb, although more potent that VRC01, its activity was shown to differ from the VRC01 MAb in that it did not enhance binding of 17b or X5 CD4i MAbs to their epitopes in the CoR region on monomeric gp120 (Falkowska et al., 2012). PG9 and PG16 MAbs were shown to neutralize 70-80% of circulating HIV-1 isolates by targeting the gp120-gp41 native trimer involving the V2 and V3 loops of gp120 (Pancera et al., 2010, Walker et al., 2009). PGT MAbs 121-123 and 125-128 that binds to gp120 carbohydrates were also reported to be ten-fold more potent than PG9, PG16, VRC01 and PGV04 and 100-fold more potent than b12, 4E10 and 2G12 MAbs (Walker et al., 2011). Figure 1-9 illustrates some of the broadly neutralizing MAb epitopes on the native gp120-gp41 trimer.

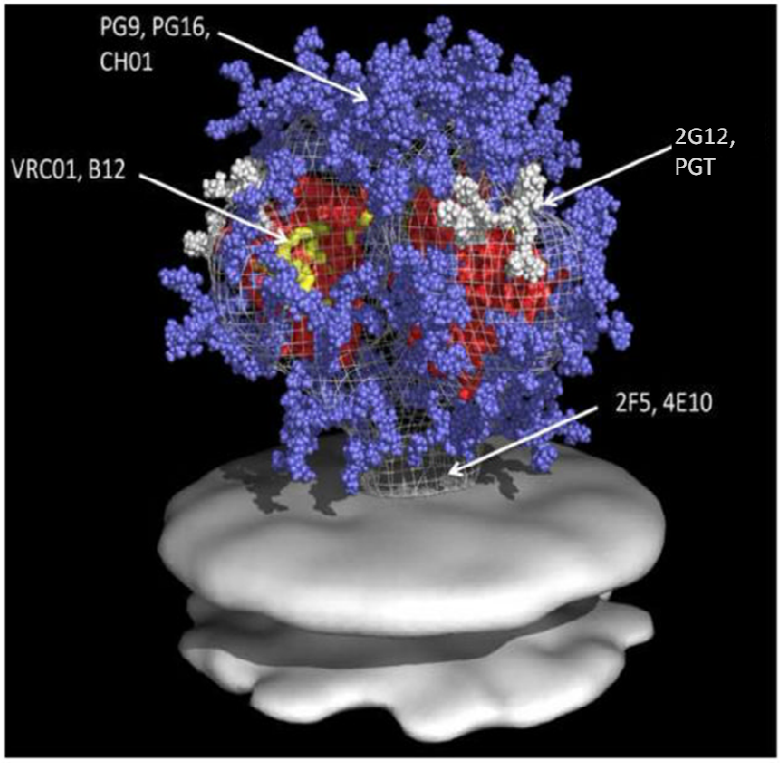

Figure 1-9: Localization of the broadly neutralizing MAb epitopes on the HIV-1 envelope trimer.
Anti-CD4 binding MAbs (VRC01, B12) are shown in yellow. Anti-V2/V3 MAbs (PG9, PG16 and CH01) are indicated in blue. The glycans, 2G12 and PGT MAbs against gp120 carbohydrates are designated in light blue and white and the core gp120 in red. Anti-gp41 MAbs are also shown at the base of the trimer. Adapted from McElrath and Hayes, 2010.

Overall, the outlined review of HIV-1 entry inhibitors shows that while there are many successful treatment options, still there is no functional cure against HIV-1. Thus, there is a need for new therapies to counter the rapid emergence of drug resistant variants, a very common aspect of HIV.

4. Aptamers: a new class of entry inhibitors

The development of the systematic evolution of ligands by exponential enrichment (SELEX) process, made possible the isolation of oligonucleotide sequences with the capacity to recognize virtually any class of target molecules with high affinity and

specificity (Bunka & Stockley, 2006, Ellington & Szostak, 1990, James, 2001, Jayasena, 1999, Proske et al., 2005, Tuerk & Gold, 1990, Zhang et al., 2004). The resulting oligonucleotide ligands are referred to as “aptamers”, derived from the latin word “aptus”, meaning “to fit” and the Greek word “meros” meaning particle (Ellington & Szostak, 1990, Jayasena, 1999, Stoltenburg et al., 2007). Aptamers are short, synthetic, single-stranded DNA or RNA molecules that fold into specific and complex 3-D structures characterized by stems, loops, bulges, hairpins, pseudoknots, triplexes, or quadruplexes (Figure 1-10), allowing them to bind specifically to other target molecules (Proske et al., 2005). Based on their 3-D structures, aptamers can well-fittingly bind to a wide variety of targets from single molecules to complex target mixtures or whole organisms (Reviewed by Stoltenburg et al., 2007). Chemical modifications of aptamers improve their binding capabilities and/or enhance their stability (Cohen et al., 2008, Khati et al., 2003, Moore et al., 2011). A number of SELEX processes have been described to select aptamers with high affinities and specificities for their targets. Many of these aptamers show affinities comparable to those observed for MAbs. In addition, aptamers are able to recognize distinct epitopes of a target molecule (Cohen et al., 2008, Mufhandu et al., 2012).

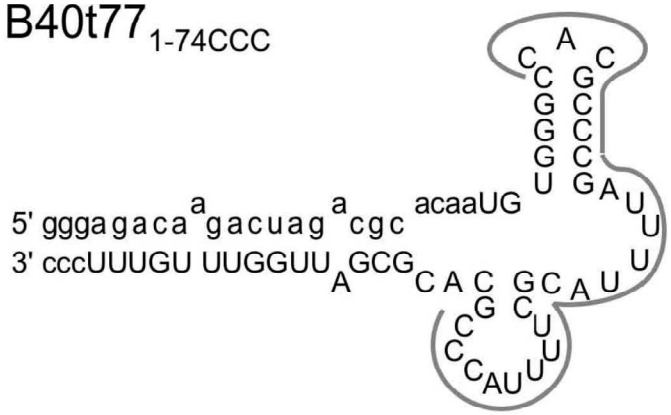

Figure 1-10: Anti-gp120 aptamer.
A nuclease-stabilized RNA aptamer targeted to gp120. All C and U residues were transcribed as 2'-fluoro analogs in original selection. Nucleotides suggested by footprinting data to be in binding core are indicated by grey line. Adapted from Dey *et al*., 2005a.

4.1 Isolation of aptamers

DNA or RNA aptamers can be routinely isolated using the systematic evolution of ligands by exponential enrichment (SELEX) process (Figure 1-10). The starting point of each SELEX process is a synthetic random DNA oligonucleotide library consisting of a multitude of ssDNA fragments with different sequences (10^{15}). This library is used directly for the selection of DNA aptamers. For the selection of RNA aptamers the library has to be transcribed into an RNA library (Ellington & Szostak, 1990, Stoltenburg et al., 2007). The SELEX procedure is characterized by the repetition of successive cycles consisting of selection (binding, partition, and elution) and amplification (Figure 1-10). In the first SELEX cycle the library and the target molecules are incubated for binding. Unbound oligonucleotides are removed by several stringent washing steps of the binding complexes. The target-bound oligonucleotides are eluted and subsequently amplified by PCR or RT-PCR. A new enriched pool of selected oligonucleotides is generated by preparation of the relevant ssDNA from the PCR products (DNA SELEX) or by in vitro transcription

(RNA SELEX). The selected oligonucleotide pool is then used for the next selection cycle (Stoltenburg et al., 2007). For each cycle, more stringent selection conditions may be used to increase the enrichment efficiency. Typically 6 to 18 iterative cycles of selection and amplification are required for the selection of high affinity, target-specific aptamers (Ellington & Szostak, 1990, Proske et al., 2005, Tuerk & Gold, 1990). The last SELEX round is finished after the amplification step and the resultant enriched aptamer pool is subjected to cloning and sequencing and further characterized on the basis of their ability to bind the target (Zhang et al., 2004). Usually, the majority of the individual sequences, >90%, in an enriched library are aptamers that bind to the target used for selection (Ellington & Szostak, 1990, James, 2001, Jayasena, 1999, Tuerk & Gold, 1990).

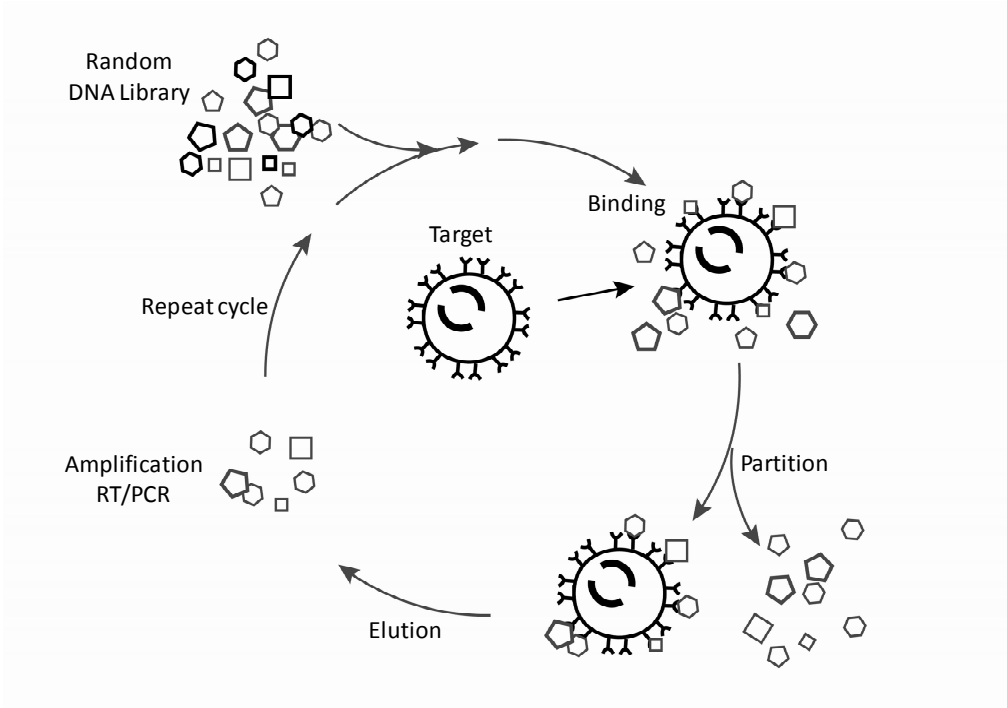

Figure 1-11: In vitro selection of target-specific aptamers using SELEX technology. The SELEX process involves the binding of a target molecule with a highly randomized DNA library. Non-binders are discarded from the process and target binders are eluted and amplified. The resulting target specific oligonucleotides are enhanced by repeating the cycle several times until a plateau is reached.

An advantage of the SELEX procedure is the possibility to adapt the conditions of further applications already during the selection process. Thus numerous variations of the procedure originally established by Tuerk and Gold, (1990) have been described during past years (Stoltenburg et al., 2007). Some of these methods were developed to increase affinity or specificity of the selecting aptamers and others to optimize the procedure. For example, the negative SELEX is a pre-selection of molecules which should not be recognized, thus removing unwanted oligonucleotides from the pool. It minimizes the co-selection of unwanted nucleic acid ligands (Rotherham et al., 2012). The counter or subtractive SELEX generates aptamers which are able to discriminate between closely related structures. It involves introduction of a selection step to the related target for elimination of aptamers which are not able to distinguish between the related structures (Shangguan et al., 2006, Stoltenburg et al., 2007). The chimeric SELEX uses two or more different libraries for production of chimerical aptamers with more than one feature or function. Each parent library will be selected first to a distinct feature followed by fusion of the selected aptamers (Neff et al., 2011, Zhou et al., 2009). The BIAcore biosensor system for selection and analyzing aptamers on biosensor chips (Khati et al., 2003). The nitrocellulose filter-based SELEX uses the nitrocellulose membrane to filter the binding oligonucleotides from the non-binders (Zhou et al., 2009).

Another advantage of the SELEX procedure is the variable ways to select for targets. That is, aptamers can be selected by aiming for a direct target, e.g., anti-HIV-1 gp120 aptamers were selected by using HIV-1 gp120 as the direct target (Khati et al., 2003). The Whole-Cell SELEX is used to aim for a target in a complex

environment that is expected to expose other native targets to the selection procedure, thus best mimicking in vivo conditions (Cerchia et al., 2005). The tissue SELEX is a method for generating aptamers capable of binding to complex tissue targets such as collections of cells in diseased tissues (Daniels et al., 2003). The Toggle-SELEX switches or toggles between targets during alternating rounds of selection (White et al., 2001). *In silico* selection of aptamers is a computational approach for designing a starting pool of RNA sequences for the selection of RNA aptamers for specific analyte binding (Chushak & Stone, 2009). First, RNA sequences are selected based on their secondary structure then a library of 3D structures of RNA molecules is generated and lastly a high-throughput virtual screening of the library is performed to select aptamers with binding affinity to a desired target (Chushak & Stone, 2009). For truncation of aptamers, secondary structural predictions are generated by computational programs such as RNAStructure 4.6 algorithm (Rockey et al., 2011) Mfold based on the Zuker algorithm (Park et al., Zuker, 1989) and Quickfold (Zhou et al., 2009).

Over the last few years, considerable efforts have focused on automating (Cox & Ellington, 2001, Eulberg et al., 2005) and technically developing the in vitro selection procedures (Bunka & Stockley, 2006). Since aptamers are derived from an in vitro process, toxins or molecules that do not elicit immune responses can serve as targets. The process also permits non-physiological selection conditions and it confers aptamers with high specificity, discriminating targets of subtle structural difference (Zhang et al., 2004).

4.2 Properties of aptamers

Aptamers are beginning to emerge as a class of molecules that rival antibodies in both therapeutic and diagnostic applications. They are different from antibodies, yet they mimic properties of antibodies in a variety of diagnostic formats (Jayasena, 1999, Keefe et al., 2010, Khati, 2010, Nimjee et al., 2005). Their advantages is that they are more stable than antibodies and can undergo denaturing and renaturing. They are smaller than antibodies (8-15 kDa versus 155 kDa for antibodies) and therefore have higher permeability and can penetrate targets more easily. They are non-immunogenic (Nimjee et al., 2005) and are produced chemically in a readily scalable process (Keefe et al., 2010). Their chemical production is not prone to viral or bacterial contamination. Conjugation chemistries for the attachment of reporter molecules such as fluorophores, biotin or radionuclides can be easily introduced during synthesis (Keefe et al., 2010). They exhibit high affinity for their targets with dissociation constant (K_D) values in the low nanomolar to picomolar range (Gopinath, 2007, Zhang et al., 2004). Nevertheless, aptamers have their own limitations. That is, their small size can render them susceptible to renal filtration thus leading to a shorter half-life (Keefe et al., 2010). Unmodified aptamers are easily degraded in serum (Moore et al., 2011). Pharmacokinetics are variable and often difficult to predict (Keefe et al., 2010). To overcome these limitations, conjugation partners such as polyethylene glycol or cholesterol can be added to increase circulating half-life (Healy et al., 2004). Chemical modifications incorporated into the sugars or internucleotide phosphodiester linkages enhance nuclease resistance (Cohen et al., 2008, Moore et al., 2011). Aptamers can be optimized for activity and persistence under physiological conditions during selection and medicinal chemistry studies conducted after discovery (Guo et al., 2008).

4.3 General aptamer applications

Since their discovery in 1990 (Ellington & Szostak, 1990, Tuerk & Gold, 1990) (Robertson and Joyce 1990), aptamers have been generated against a wide variety of targets ranging from small molecules (Mannironi et al., 1997), peptides (Nieuwlandt et al., 1995), amino acids (Geiger et al., 1996), cytokines (Kubik et al., 1997), chemokines (Santulli-Marotto et al., 2003) growth factors (Akiyama et al., 2006, Lee et al., 2009) and proteins (Lebruska & Maher, 1999), including cell membrane proteins (Lupold et al., 2002) and receptors (reviewed by Zhou & Rossi, 2010). The applications of aptamers are numerous; the versatility of this technology is reflected in the fact that there are few areas of research to which aptamers cannot be applied. The applications include: two-site binding assays (Lochrie et al., 1997), flow cytometry (Davis et al., 1998), affinity probe capillary electrophoresis (German et al., 1998), aptamers as molecular switches (Dang & Jayasena, 1996), detection of proteins immobilized on membranes (Drolet et al., 1996), polypeptide aptamers (Gourlain et al., 2001), aptamer fusion to ribozymes (aptazymes) (Hesselberth et al., 2000), aptamer microarrays (Collett et al., 2005), diagnostics and biosensors (Liu et al., 2006, Potyrailo et al., 1998, Stojanovic & Kolpashchikov, 2004), therapeutics (Vinores, 2003), biomarkers (Gold et al., 2010, Ostroff et al., 2010), combating infectious agents such as HIV (Held et al., 2006), hepatitis C virus (Fukuda et al., 2008), *Mycobacterium tuberculosis* (Chen et al., 2007, Purschke et al., 2003), and cancerous cells (Dhar et al., 2008, Liu et al., 2009, McNamara et al., 2006).

Numerous aptamers have been isolated to target therapeutic interests. For example, aptamers against HIV-1 reverse transcriptase (Li et al., 2008), Rev (Symensma et al., 1996) and integrase (Metifiot et al., 2005) inhibit viral replication. Aptamers have

been used for targeted delivery of anticancer drug inside nanoparticles to prostate cancer cells (Farokhzad et al., 2006). Aptamers have also been selected for diagnostic purposes. That is, aptamers with high affinity to HIV-1 gp120 have been used in a microarray-based HIV-1 diagnostic test (Smith et al., 2003). ssDNA aptamers with high sensitivity and specificity to CFP-10.ESAT-6 heterodimer of *Mycobaterium tuberculosis* (*M tuberculosis*) have been selected for a potential diagnostic detection of *M tuberculosis* (Rotherham et al., 2012). In addition, aptamers that detect and measure insulin activity have been selected for diagnosis of Type 1 diabetes (Yoshida et al., 2009).

One of the most studied aptamer in the therapeutic field is against the angiogenic cytokine, vascular endothelial growth factor (VEGF); anti-VEGF is a chemically modified RNA aptamer (Vinores, 2003). Clinical phase IA and phase II trials have shown that anti-VEGF therapy is a promising treatment for various forms of ocular neo-vascularization, including age-related macular degeneration (Eyetech, 2002, Eyetech, 2003). Based on the clinical trial results, the Eyetech/Pfizer aptamer (Macugen) was approved by the Food and Drug Administration in December 2004 (www.fda.gov/newsevents/newsroom/pressannouncements/2004/ucm108385.htm).
The same aptamer is being evaluated as a treatment for other diseases where VEGF may enhance the pathologies, for example, in cancer diseases where VEGF may help in the neo-vascularization of growing tumours (Lee et al., 2009). Other aptamers are currently in phase I and phase II clinical trials. NU172, a DNA aptamer currently evaluated in phase II clinical trials by ARCA Biopharma targets thrombin and is intended to be given by continuous infusion during cardiopulmonary bypass or other surgical procedures to maintain a state of anticoagulation with a rapid return to

haemostasis once the infusion ceases (Keefe et al., 2010, Nimjee et al., 2005). Another aptamer, AS1411 a G-rich DNA aptamer currently in phase II clinical trials by Antisoma targets nucleolin to inhibit proliferation of acute myeloid leukaemia (Bates et al., 2009).

4.4 Anti gp120 RNA aptamers

The toxicity associated with anti-HIV drugs, together with the appearance of strains resistant to current drugs, drives the continued search for novel strategies to fight HIV-1 (Wolkowicz & Nolan, 2005). High affinity RNA aptamers against the HIV-1 gp120 have previously been isolated (Khati et al., 2003, Sayer et al., 2002, Zhou et al., 2009). The initial gp120 aptamers were shown to have broad neutralization efficiency. They inhibited five subtypes of group M and one group O strain (Khati et al., 2003). A derivative of one of the aptamers, B40, was truncated (Dey et al., 2005a) and chemically modified further (Cohen et al., 2008) for enhanced stability. One of the stabilized aptamers, UCLA1, was shown to have broad neutralization efficiency against HIV-1 subtype C viruses even though it was selected from a subtype B HIV-1_{BaL} isolate (Mufhandu et al., 2012). Due to their target specificity, these aptamers have been identified as delivery vehicles for targeted delivery of Dicer substrate siRNA to specific cells (McNamara et al., 2006, Zhou et al., 2009). Anti-gp120 aptamer-anti-*tat/rev* siRNA chimera (Zhou et al., 2008) reduced viral replication and helper CD4+ T cell depletion in humanized mice (Neff et al., 2011). Other anti-gp120 aptamers known as photoaptamers have been selected and used for microarray-based gp120 detection (Smith et al., 2003). In contrast to anti-gp120 antibodies, these aptamers proved to have potent neutralizing activity and some of them were able to neutralize strains derived from most major subtypes of HIV,

suggesting that their target sites were conserved and functionally important to the virus (Khati et al., 2003, Mufhandu et al., 2012). It has recently been shown that some of these aptamers block gp120-CCR5 interaction on target cells. That is, the aptamer competes with the N-terminal ectodomain of CCR5 for binding to gp120 and hence the aptamer binding site must overlap with the basic, conserved, co-receptor-binding region (Dey et al., 2005b) and the V3 loop on gp120 (Cohen et al., 2008, Mufhandu et al., 2012).

Based on the previous anti-gp120 aptamer data, it was considered imperative to test these aptamers against subtype C viruses since it the most burdensome subtype worldwide. The previous cross-clade reactivity data suggested that the aptamers were likely to be efficient against subtype C viruses. Thus, a large panel of subtype C viruses was tested for neutralization with the aptamers. The binding and inhibition mechanisms were investigated in comparison to subtype B viruses. The current study also tested for aptamer resistance which was not examined in previous studies. Of note, isolation of aptamers against subtype C HIV-1 gp120 is essential and will divulge any discrepancies in efficiency against subtype C isolates when compared with aptamers isolated from a subtype B strain.

5. Study objectives

Entry of HIV-1 into cells is partly mediated by the virion surface envelope glycoprotein (gp120). This makes gp120 a desirable target for antiretroviral entry inhibitors. For this reason, a family of gp120 binding 2'-fluoro modified RNA aptamers have been isolated and shown to inhibit entry and infectivity of HIV-1

clinical isolates. Subsequently, shortened derivates of one of the aptamers called B40 were shown to bind the conserved CCR5 core and retained activity against HIV-1_{BaL}, a subtype B strain, as efficiently as the parental aptamer. Therefore, in this study, we first assessed the activity of the 2'-fluoro modified aptamers against HIV-1 subtype C clinical isolates endemic to South Africa. The cloned aptamers were amplified, transcribed and their binding affinity tested against gp120 glycoproteins. Their neutralization efficiency against subtype C isolates was also investigated. They were tested in comparison to a more stabilized, solid-phase synthesized UCLA1 aptamer. Eventually, UCLA1 was used for the remainder of study due to its improved modifications which rendered it more robust than the 2'-fluoro modified aptamers. UCLA1 was then tested against a total of 35 HIV-1 subtype C Env-pseudotyped viruses in the single-cycle, TZM-bl neutralization assay. The viruses were isolated from adult and paediatric patients at various stages of HIV-1 infection and AIDS pathogenesis. The aptamer was tested for cytotoxicity in TZM-bl cells. Its binding sites were mapped using the codon-usage optimized HIV-1 Consensus C (ConC) gp120 protein including the truncated and mutated versions of the protein. The mapping was performed by binding kinetics, single site-directed point mutations and sequencing. UCLA1 neutralization efficiency was also examined in combination with other entry inhibitors using the TZM-bl assay.

UCLA1 neutralization efficiency was further tested in the peripheral blood mononuclear cell (PBMC) and monocyte-derived macrophage cell (MDM) assays against six and four HIV-1 subtype C primary isolates, respectively. Neutralization in these assays was measured by inhibition of HIV-1 Gag p24 production. UCLA1 escape mutations were assessed by culturing primary viruses in PBMCs under

escalating concentrations of the aptamer. Lastly, selection for UCLA1 resistance was performed by culturing primary viruses in PBMCs under escalating concentrations of the aptamer. The pattern of viral growth was monitored using the HIV-1 Gag p24 assay. At selection time-point, the cultures were reverse transcribed, amplified and sequenced to assess for mutations within the *env* gene that might have occurred due to the selective pressure by UCLA1.

CHAPTER 2

Production of Anti-gp120 RNA Aptamers and Evaluation of their Biological Activity

Chapter summary

The RNA aptamers that were utilized in this study were generated from the cloned DNA aptamers (Khati et al., 2003) by *in vitro* T7 transcription and stabilized with 2'-fluoropyrimidines. The generated aptamers were tested for binding to the expressed recombinant HIV-1 subtype C Du151 and ConC glycoproteins. Binding kinetics was measured using the BIAcore® 3000 Surface Plasmon Resonance (SPR) technology. The aptamers were tested for inhibition of HIV-1 subtype C envelope pseudotyped viruses using the TZM-bl single cycle neutralization assay. Since the TZM-bl neutralization assay was developed and standardized for monoclonal antibody (MAb) HIV-1 inhibition assays (Montefiori, 2004), the aptamers had to be optimized for use in this assay. I discovered that although the RNA aptamers were stabilized with 2'-fluoropyrimidines they were inefficient when utilized in culture media supplemented with 10% fetal bovine serum (FBS) compared to 5% FBS supplemented media. The B4 aptamer succeeded in neutralizing subtype B HxB2 and subtype C Du151 pseudoviruses with 50% inhibition concentration (IC_{50}) values of 6.5 and 8 nM, respectively. No inhibition against subtype C viruses was observed with the other generated aptamers (B38, B40, B44, B84, and B40t77). The aptamers could not neutralize the subtype B HIV-1_{BaL} pseudovirus, though they were isolated against HIV-1_{BaL} gp120. From this data it was concluded that the 2-fluoropyrimidine stabilization was not sufficient for optimal efficiency of the aptamers. Thus, a solid-phase synthesized aptamer called UCLA1 was sourced and used for the remainder of the study. The more stabilized UCLA1 exhibited higher binding affinity and demonstrated high efficiency by neutralizing the HxB2 virus with an average IC_{50}

value of 0.17 nM. Its neutralization activity was not affected by the serum content in culture media.

1. Introduction

Although the production of small molecule therapeutics against HIV-1 has been growing, the increase in selection of drug-resistant viral strains and side effects accompanied with long-term use of the drugs has lead to more research on alternative anti-HIV-1 agents. Aptamers as anti-HIV-1 agents are increasing and have thus far been developed against almost each and every step of the virus' life cycle (Gold et al., 1995, Gopinath, 2007, Held et al., 2006). Only a few have been isolated against HIV-1 gp120 at the attachment entry level (Dey et al., 2005b, Khati et al., 2003, Sayer et al., 2002, Zhou et al., 2008, Zhou et al., 2009) and none have been selected against viral fusion as compared to the anti-gp41 MAb, T20.

The exploitation of the SELEX process permitted the isolation of both RNA and DNA aptamers against any target of choice (Ellington & Szostak, 1990, Stoltenburg et al., 2007). A major requirement of RNA aptamers is that they have to be chemically modified before use in order to increase their stability and acquire resistance to ribonucleases. Several modifications can be used, for example, substitution of the ribose 2'-OH group of pyrimidines at the 2'-position of ribonucleotides with 2'-amino (2'-NH2), 2'-fluoro (2'-F), or a variety of 2'-*O*-alkyl moieties. These substitutions confer resistance to nucleases that utilize the 2'-OH group for cleavage of the adjacent phosphodiester bond (Khati et al., 2003, Knudsen et al., 2002, Mayer, 2009, Stoltenburg et al., 2007, Zhou et al., 2011). The chemical modifications are also introduced to optimize binding of the aptamers to their target (Gold et al., 2010, Moore et al 2011, Cohen et al., 2008). Modifications can also be introduced at the 3'-end by capping with streptavidin and biotin and at the 5'-end with inverted thymidine,

amine, phosphate, polyethyleneglycol and cholesterol which protects the aptamer from exonucleases.

The aptamers that were utilized in this study were all isolated against subtype B HIV-1_{BaL} gp120 (Cohen et al., 2008, Dey et al., 2005a, Khati et al., 2003). The aptamers were used based on their previous neutralization data. That is, they were shown to have cross-clade neutralization efficiency (Khati et al., 2003). The parental B40 aptamer was singled out for further testing and characterization. Its truncated version, B40t77, was also characterized (Dey et al., 2005a) and confirmed to be efficient against HIV-1 subtype B gp120 (Dey et al., 2005b). UCLA1, another derivative of B40, was included in this study based on its stability and neutralization efficiency against HIV-1 subtype B gp120 (Cohen et al., 2008). Therefore, based on their robustness, the aptamers were then mainly tested against HIV-1 subtype C gp120 in the current study.

In this study, 2'-fluoro modified aptamers were used in conjunction with a solid-phase synthesized aptamer called UCLA1 (University of California, Los Angeles). Explanation of the nomenclature of the primary aptamers that were used: the B40 aptamer is the parental full length RNA aptamer with a secondary structure consisting of 117 nucleotides in length. The B40t77 aptamer (77 nucleotides in length) is a truncated derivative of the full length B40 aptamer, previously shown to have anti-HIV inhibitory activity (Dey et al., 2005a, Joubert et al., 2010). UCLA1 is a derivative of aptamer 299.2 which is a shortened derivative (54 nucleotides in length) (Cohen et al., 2008) of B40t77 (Dey et al., 2005a). The 299.2 aptamer was stabilized

by the use of six 2′-O-dimethylallylribonucleotides in the short stem 1 together with the insertion of an additional base pair in stem 2 (Cohen et al., 2008). As a result, UCLA1 (also 54 nucleotides in length) is made up of the 299.2 aptamer and chemically modified by the addition of an inverted thymidine at the 3′-end and a dimethoxyltrityloxy-$(CH_2)_6$-SS-$(CH_2)_6$-phospho linker at the 5′-end (Cohen et al., 2008). The parental B40 aptamer and its derivatives are shown (Figure 2- 1)**.**

Overall, 2'-fluoro modified anti-gp120 RNA aptamers were successfully amplified and transcribed. Gp120 glycoproteins were also efficiently expressed and purified for use with the aptamers. Their antigenicity was shown by binding to several anti-gp120 MAbs. The binding affinity of the isolated aptamers was tested against the expressed gp120s. Their binding affinity was compared with UCLA1, a more stabilized solid-phase synthesized aptamer. The aptamers were also assessed for use in the single-cycle neutralization assay against the prime targets, HIV-1 subtype C viruses. The 2'-fluoro modified aptamers were observed to exhibit low inhibition efficiency in high serum culture media compared to UCLA1 aptamer. Thus, the data shows the importance of additional aptamer modifications.

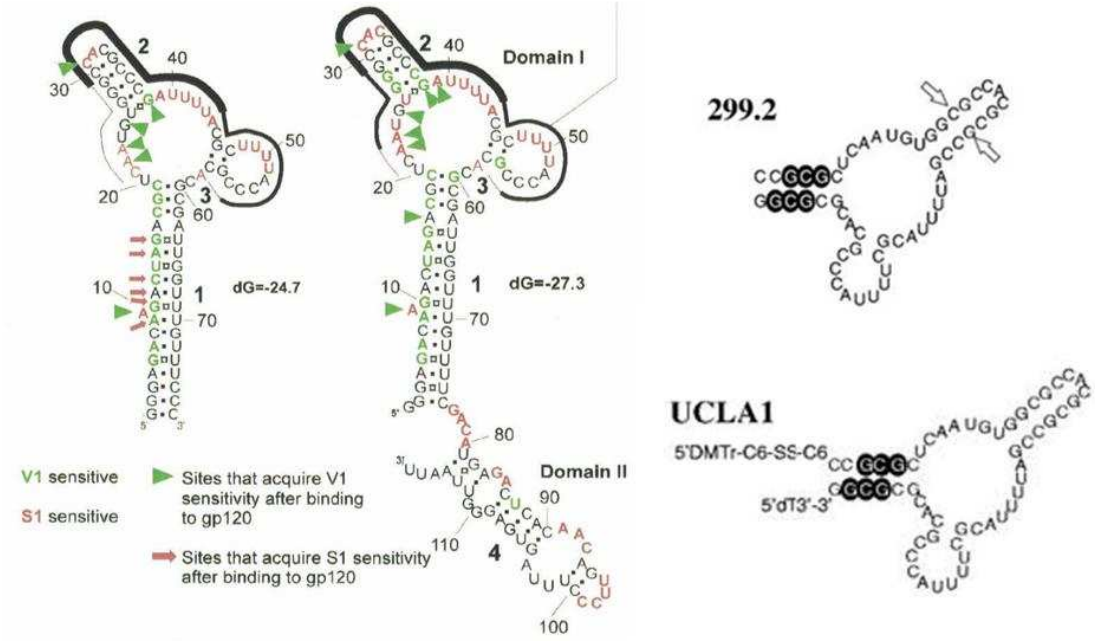

Figure 2-1: Proposed secondary structure of aptamer B40t77 and B40.
B40t77 was the first derivative of B40 from which domain II of B40 was truncated (Dey et al., 2005a). Aptamer 299.2 is another derivative of B40 whose stem has been minimized while maintaining its stabilizing effect. UCLA1 is a further derivative of B40 with the same structure as aptamer 299.2 and an inverted thymidine at the 3′-end (to block degradation by 3′-exonucleases) and a dimethoxyltrityloxy-(CH2)6-SS-(CH2)6-phospho linker at the 5′-end (Cohen et al., 2008).

2. Materials and Methods

2.1 Monoclonal antibodies, proteins and plasma samples

TZM-bl cells used for neutralization assay were obtained from the National Institutes of Health (NIH) AIDS Research and Reference Reagent Program. The TZM-bl cell line was derived from a HeLa cell clone that expresses CD4, CCR5, and CXCR4 co-receptors (Platt et al., 1998) and contains two reporter genes: firefly luciferase and Escherichia coli β-galactosidase under the control of the HIV-1 LTR promoter (Wei et al., 2002). The 293T cells used for transfection were obtained from the American Type Culture Collection (Manassas, Virginia, United States). The 293T cell line was originally derived from human embryonic kidney cells grown in tissue culture with sheared adenovirus 5 DNA (Graham et al., 1977). The Du151.2 Env expressing plasmid (Li et al., 2006) and Env-pseudotyped viruses were obtained from the NICD. The HIV genomic vector, SG3delta *env*, was used as the backbone in the production of Env-pseudotyped viruses. The codon-usage optimized HIV-1 Consensus C (ConC) envelope construct was obtained from Dr. Feng Gao (Kothe et al., 2006). The HIV-1_{BaL} gp120 was obtained from the NIH AIDS Research and Reference Reagent Program. HIV-1 positive individual plasma (IBU-21 and BB105) and plasma pool, BB Pool, prepared from individual plasma samples previously described by Li *et al*., 2006, were purchased from the South African National Blood Services in Johannesburg and used as positive controls. Specificity of these plasma samples has been shown in previous studies (Gray et al., 2006, Gray et al., 2007b, Gray et al., 2009, Li et al., 2005, Li et al., 2006). HIV-1 positive plasma serum (HIVIG), monoclonal antibodies (MAb) CD4IgG2, B6, IgG1b12 (b12), 2G12, and 447-52D, soluble CD4 (sCD4) (NIH AIDS Research and Reference Reagent Program) and

T20 fusion inhibitor (Roche, Palo Alto, California, USA) were obtained from the AIDS Virus Research Unit at the National Institute for Communicable Diseases (NICD). Ethical clearance for this study was obtained from the University of the Witwatersrand Committee for Research on Human Subjects (Appendix A). General reagents and the suppliers are listed in Appendix B.

2.2 Anti-gp120 RNA aptamers

Twelve RNA aptamer clones that were previously isolated against HIV-1_{BaL} gp120 were randomly chosen from a total of 29 available aptamers and amplified by PCR for use in this study (Dey et al., 2005a, Khati et al., 2003). The following are the 2'-fluoro modified aptamers that were utilized: B1, B3, B4, B11, B19, B28, B38, B40, B44, B65, B84 (Khati et al., 2003) and B40t77 (Dey et al., 2005a). UCLA1 was also used in the study. An initial batch of UCLA1 was donated by William James, University of Oxford for this study. Subsequent batches were custom synthesised by ATDBio Ltd, Southampton, UK. The aptamers that were isolated against HIV-1_{BaL} gp120 are referred to as in-house aptamers in this study in order to differentiate them from the solid-phase synthesized UCLA1 aptamer.

2.3 Generation of monoclonal anti-gp120 aptamers from cloned plasmids

2.3.1 Amplification of anti-gp120 aptamers

The twelve 2'-fluoro modified aptamers selected against HIV-1_{BaL} gp120, previously cloned into pCR® 3.1 vector were PCR amplified. Briefly, the plasmids were used as templates to amplify the inserted full length aptamers using the following primers: T3-

5′: AAT TAA CCC TCA CTA AAG GGA ACT GTT GTG AGT CTC ATG TCG AA, T7-3′: TAA TAC GAC TCA CTA TA GGG AGA CAA GAC TAG ACG CTC AA (Inqaba Biotec, South Africa) as previously described (Khati et al., 2003), with the T7 promoter underlined. To generate the truncated aptamer (B40t77), the truncated DNA template was PCR amplified from the full-length B40 DNA template cloned into the pCR® 3.1 cloning vector using the following primers: 5'- GGG AAA CAA ACC AAT CGC G, 3′- TAA TAC GAC TCA CTA TA GGG AGA CAA GAC TAG ACG C (Inqaba Biotec) as previously described (Dey et al., 2005b) with the T7 promoter underlined.

A typical 50 µl PCR mixture contained 1.0 µg template, Mg free PCR buffer (Promega, South Africa), 25 mM $MgCl_2$, 10 mM dNTPs, forward and reverse primers (50 µM each), and 1.25 U of *Taq* polymerase (Promega). The template was denatured at 93℃ for 3 min and amplified with 27 PCR cycles (93℃ for 30 s, 72℃ for 1 min, 72℃ for 1 min) and a final extension step at 72℃ for 8 min. The PCR product was then purified with the Wizard SV Gel and PCR Clean-Up System (Promega) according to the manufacturer's protocol. Briefly, a membrane binding solution was added to the PCR product in a binding column, centrifuged and washed twice. Thereafter, 50 µl of distilled water was added to the column and centrifuged to elute the purified DNA. The PCR products (DNA) were resolved on a 1% agarose gel by electrophoresis (Appendix C, section 1.1).

2.3.2 In vitro transcription

A 100 µl transcription reaction contained 1.5 µg template, 5 x fluoro transcription buffer (40 mM Tris-HCl, pH 8.1 and 6 mM $MgCl_2$), 1 mM 2′-F dCTP and 1 mM 2′-F dUTP (TriLink Biotechnologies, USA), 1 mM ATP, 1 mM GTP (Fermentas), 2 mM spermidine (Sigma-Aldrich), 1 mM dithiothreitol (DTT) (Merck, South Africa) and 1,000 U of T7 RNA polymerase (The Scientific Group, South Africa). The transcription reaction mixture was incubated at 37°C overnight. The transcription reaction was terminated by addition of 1 U of RNase-free DNase I (Inqaba Biotec) and incubation at 37℃ for 30 min.

2.3.3 Sephadex-G50 purification

The transcription reaction was desalted and purified with Sephadex-G50 (Sigma-Aldrich) nick spin column to remove free nucleotides. The resin was prepared with 13 g of Sephadex-G50 with 0.02% azide (Sigma-Aldrich) in 200 ml double–distilled water (ddH_20). The resin was allowed to swell for 2 h before use. A syringe was plugged with one glass bead and 10 ml of resin added to the column and left to dry. The resin was then washed with 5 ml of 150 mM $NaCl_2$. 100 µl of 0.2% phenol red (Sigma-Aldrich) in 25 mM EDTA at pH 8.0 was added to 1 ml transcription reaction and loaded onto the resin. The RNA was eluted into collection tubes by addition of 600 µl of 150 mM $NaCl_2$. The elution was repeated 10 times, thus with a total of 6 ml of 150 mM $NaCl_2$ resulting in several RNA fractions.

2.3.4 Phenol:Chloroform extraction

Proteins were removed from the transcripts (2′-F-RNA aptamers) by addition of an equal volume of phenol/chloroform (Sigma-Aldrich) (v/v 5:1, pH 4.7) followed by vigorous mixing using a vortex and centrifugation at 14 000 rpm for 1 min. The aqueous (upper) phase containing RNA was transferred to a clean Eppendorf tube, and the extraction was repeated by addition of an equal volume of chloroform (Sigma-Aldrich). The resulting aqueous layer containing RNA was transferred to a clean Eppendorf tube, and the extraction was repeated by addition of an equal volume of ddH_20. The RNA was precipitated with ethanol (Appendix C, section 1.2) and quantified with the NanoDrop spectrophotometer (Appendix C, section 1.3). The RNA transcripts were then analysed on a denaturing 11% polyacrylamide gel (Appendix C, section 1.4).

2.4 Expression of recombinant HIV-1 glycoproteins

HIV-1 ConC gp120 and Du151 gp120 were expressed in 293T cells as previously described (Gray et al., 2009). Briefly, about 6×10^7 293T cells were seeded in 560 ml DMEM (Gibco Invitrogen, South Africa) containing 10% heat-inactivated fetal bovine serum (FBS) in a Hyperflask (Corning Incorporated, South Africa) and used for transfection. Briefly, a transfection mixture of 720 µl of FuGENE 6 (Roche, South Africa) and 240 µg of consensus C Env encoding plasmid DNA in 15 ml serum-free DMEM was added to the 293T cells at 50% confluence. The transfection was incubated at 37℃ in 5% CO_2 and 95% humidity for 48 h. Culture supernatants were harvested after every 48 h and filtered through a 0.2 µm filter.

2.4.1 Purification of HIV-1 glycoproteins

The ConC and Du151 gp120s were purified by affinity chromatography using *Galantus nivalis* lectin agarose matrix (Sigma-Aldrich) and eluted with 1M methyl D manno-pyranoside (Sigma-Aldrich). The eluted gp120 was concentrated with Vivaspin 20 ultrafiltration columns (Sartorius Stedim biotech, South Africa). The concentrated gp120 was further purified by ion exchange chromatography through a resin column, FastFlow Q-Sepharose, (GE Healthcare, South Africa). The flow-through fractions were collected and concentrated as above.

2.4.2 Protein confirmation and functionality assays

The purity, size and homogeneity of the proteins were assessed using 6% sodium dodecyl sulfate-polyacrylamide gel electrophoresis (SDS-PAGE) and Western blotting as previously described (Gray et al., 2007b). Prior to loading of protein samples onto the gel, the proteins were incubated with SDS-PAGE sample buffer (0.125 M Tris-HCl, 4% (w/v) SDS 20% (v/v) glycerol, 5% (v/v) β-mercaptoethanol (Sigma-Aldrich) and 0.02% (w/v) bromophenol blue, pH 6.8), (Merck) for 5 min at 95°C. Gels were electrophoresed for 2 h at 120 V. Staining was performed using Coomassie Stain (40% methanol; 0.7% acetic acid; 0.075% Coomassie dye) (Merck). Gels were destained with Coomassie destain (40% methanol; 0.7% acetic acid) (Merck). Full Range rainbow protein molecular weight marker (AEC-Amersham, South Africa) was used as a standard with relative molecular masses of 225kDa, 150kDa, 120kDa, 76kDa and 56kDa.

Confirmation of gp120 proteins was first tested with the Western blott assay. The transfer of proteins from SDS-PAGE to polyvinylidene difluoride membranes (0.45 µm pore size, Immobilon-P (Merck Millipore, South Africa) was accomplished by soaking the gel membrane in a Blot buffer (25 mM Tris-HCl, 192 mM glycine and 20% methanol) (Sigma-Aldrich) and running the gel overnight at 90 mA. The membrane was then washed with distilled water and blocked for 1 h at room temperature in PBS/0.05% Tween20 (PBS-T) containing 2.5% non-fat milk powder (blocking solution).

Thereafter the membrane was incubated for 1 h at room temperature with a primary antibody solution consisting of polyclonal HIV Immunoglobulin (HIVIG, HIV-1 positive plasma serum) (NIH, AIDS Research and Reference Reagent Program) in blocking solution at 1:20,000. After incubation the blot was washed with PBS-T and blocked with the blocking solution for 1 h at room temperature. The blot was then incubated for 1 h at room temperature with a secondary antibody solution consisting of goat-antihuman IgG horseradish peroxidase (HRP)-conjugated antibody (Santa Cruz Biotechnology, South Africa) in blocking solution at 1:20,000. After washing the blot with PBS-T, immunoreactive bands were detected using the enhanced chemiluminescence (EZ-ECL) detection kit (Amersham Pharmacia Biotech, USA), according to the manufacturer's instructions.

2.4.3 Enzyme linked immunosorbent assay (ELISA)

The biological activity of pure Du151 and Con-C gp120 proteins was assessed by the Enzyme-Linked ImmunoSorbent Assay (ELISA) as previously described (Gray et

al., 2009). The following MAbs, obtained from NIH, were used: CD4IgG2, IgG1b12, B6 - which recognize epitopes within the CD4 binding site in the envelope glycoprotein complex (Kessler et al., 1997, Parren et al., 1996, Zwick et al., 2005), 2G12 - whose binding is dependent upon proper N-linked glycosylation (Trkola et al., 1996) and 447-52D – which binds to the V3 loop (Gorny et al., 1993). The HIV-1 subtype C positive plasma sample (BB 105) was also included in the assay. Briefly, the ELISA plate (Costar Corning Incorporated, South Africa) was coated with 100 µl of protein diluted at 4 µg/ml of in 10 ml of $NaHC0_3$ buffer (Sigma-Aldrich). The coating was performed overnight at 4℃. The plates were washed 4 times with PBS-T using the BioTek ELx50 plate washer (BioTek Instruments, USA) and blocked with 100 µl of 5% milk in PBS-T (blocking buffer) for 1 h at room temperature. MAbs and plasma were diluted in blocking buffer before use. That is, MAbs at 10 µg/ml were diluted 1:100 and the plasma sample diluted 1:5. The blocking buffer was discarded from the plates and 100 µl of the diluted MAbs and plasma were added to the plates at 4-fold serial dilutions and incubated for 1 hr at room temperature. The plates were washed 4 times as above and 100 µl of the secondary antibody (goat anti-human IgG Biotin) (Whitehead Scientific, South Africa), diluted at 1:3000, was added and incubated as above. After the second wash, 100 µl of conjugated streptavidin–HRP (Whitehead Scientific) diluted at 1:1000, was added and incubated as above. After the third wash 100 µl of 3,3',5,5'-Tetramethylbenzidine (TMB) ELISA substrate (Inqaba Biotec) was added and incubated for 2 min at room temperature. Thereafter 25 µl of sulphuric acid was added to stop the reaction and the assay was quantified by measuring OD at A_{450} on the $Versa_{max}$ turnable microplate reader (Labotec, South

Africa). The ELISA was performed as a rapid screening assay in single wells to promptly assess the antigenicity of the expressed gp120 proteins.

2.5 The BIAcore SPR technology

2.5.1 Protein immobilization onto biosensor chip

The BIAcore surface plasmon resonance (SPR) technology (GE Healthcare, Sweden) was used to determine the binding affinity and kinetics of RNA aptamers to HIV-1 gp120 proteins with the CM5 biosensor chip by direct amine coupling as described previously (Cohen et al., 2008, Dey et al., 2005a, Dey et al., 2005b, Joubert et al., 2010) (Figure 2-2). Briefly, the proteins were immobilized onto the carboxymethylated (CM5) biosensor chip by direct amine coupling. HBS-N buffer (10 mM HEPES, pH 7.4, 150 mM NaCl) (Separations Scientific, South Africa) was used as the continuous flow buffer. Samples which were injected onto the CM5 biosensor chip (Separations Scientific) were pulsed at 14 000 rpm for 1 min before use, to dislodge air bubbles. The carboxyl groups on the sensor surface of the CM5 chip were activated by injecting 70 µl of a 1:1 ratio mixture of 75 mg/ml N-ethyl-N'-(3-dimethylaminopropyl) carbodiimide (EDC) (Separations Scientific) and 11.5 mg/ml N-hydroxysuccinimide (NHS) (Separations Scientific) at a flow rate of 10 µl/min. The protein was then diluted in 10 mM NaAc, pH 5.0 to a final concentration of 50 µg/ml and 70 µl was injected onto the surface of the activated sensor chip. A 1.0 M (70 µl) ethanolamine, pH 8.0 (Separations Scientific) was injected to block excess activated carboxyl groups remaining on the surface of the sensor chip. A 10 mM (30 µl) glycine-HCl pH 2.5 was then injected to wash off unbound ligand (protein). In all experiments three adjacent flow cells were simultaneously treated as mentioned

above for a triplicate run and the last flow cell was also treated as mentioned above but omitted gp120 from the immobilization solution, and this served as a reference flow cell.

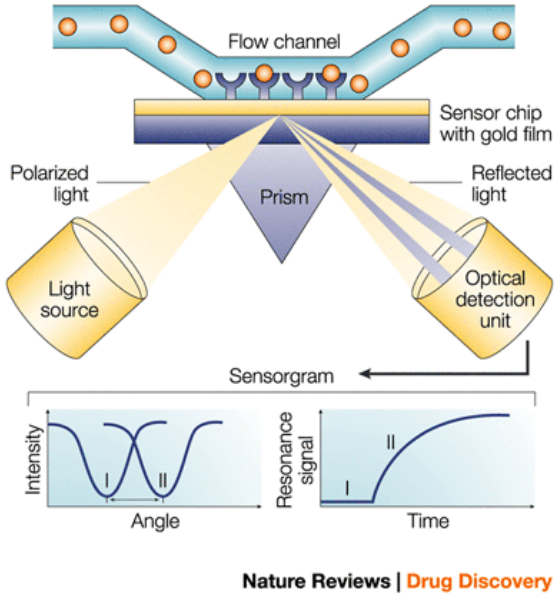

Figure 2-2: Surface plasmon resonance (SPR) detects changes in the refractive index in the immediate vicinity of the surface layer of a sensor chip.
SPR is observed as a sharp shadow in the reflected light from the surface at an angle that is dependent on the mass of material at the surface. The SPR angle shifts (from I to II in the lower left-hand diagram) when biomolecules bind to the surface and change the mass of the surface layer. This change in resonant angle can be monitored non-invasively in real time as a plot of resonance signal (proportional to mass change) versus time. The figure was acquired from Cooper, 2002.

2.5.2 Binding affinity measurements

Screening of the binding affinity of aptamers to HIV-1 gp120 proteins was performed by injecting aptamers over the covalently immobilized gp120 proteins at a flow rate of 10 µl/min. The aptamers were diluted in 5 × refolding buffer (10 mM HEPES pH 7.4, 150 mM NaCl, 1 mM $CaCl_2$, 1 mM $MgCl_2$ and 2.7 mM KCl) prior to injection as previously described (Joubert et al., 2010). The final concentration of the aptamers was 100 nM and 50 µl was injected at 5 µl/min and allowed to dissociate for at least

2 min before stopping the injection which was then replaced with the running buffer. A stringent buffer (20 µl of 20 mM NaOH) was used to regenerate the protein and dissociate the RNA that was still bound to the protein. To ascertain the biological activity of the regenerated protein, the binding affinity of 50 µg/ml of recombinant soluble CD4 (sCD4) comprising the extracellular domain of human CD4 (NIH AIDS Research and Reference Reagent Program), was assayed by binding it to the regenerated protein. The aptamer binding affinity experiments were performed in triplicate on three adjacent flow cells with the fourth flow cell serving as a negative control. Data was analysed using the BIAevaluation 4.1 software and further analyzed with GraphPad Prism 3.02 software.

2.5.3 Binding kinetics of aptamers to HIV-1 glycoproteins

Binding kinetics to measure association and dissociation constant of the aptamers from the protein were measured by kin-injecting ½ $\log_{10}$ serial dilutions of the aptamers at a flow rate of 5 µl/min with a 5 min association phase and a 10 min dissociation phase. The aptamers were diluted in 1 × refolding buffer prior to injection as previously described (Joubert et al., 2010). The stringent buffer was used as above after each dilution kinjection to dissociate the aptamer that remain bound to the protein. Each experiment was performed three times on three flow cells as described above. The association (K_a) and dissociation (K_d) constants of the resulting data curves were separately fitted to a 1:1 Langmuir binding model and analysed using the BIAevaluation 4.1 software to obtain the K_D values and further analyzed with GraphPad Prism 3.02 software. The negative control flow cell and buffer effects were subtracted as baseline.

2.6 Single-cycle neutralization assay

Neutralization was measured as a reduction in luciferase gene expression after a single-round infection of TZM-bl cells with Env-pseudotyped virus as previously described (Gray et al., 2006, Li et al., 2005, Montefiori, 2004, Montefiori, 2009). Briefly, 200 $TCID_{50}$ of pseudovirus in 50 µl of either 5% or 10% FBS DMEM complete growth medium without Dextran was incubated with 25 µl of 3-fold serially diluted aptamer and positive controls in a flat bottom 96-well plate for 1 h at 37℃ in 5% CO_2/95% air. The plasma samples (BB-pool and IBU-21) obtained from blood donors with HIV-1 subtype C infection were used as positive controls, at an initial dilution of 1:45. The assay was performed at least three times, in duplicate, for each pseudovirus tested. Infection was monitored after 48 hours of incubation at 37℃ in 5% CO_2/95% air by evaluating the Bright Glo luciferase reagent (Promega) activity. Titers were calculated as inhibition concentration (IC_{50}) or reciprocal plasma dilution (ID_{50}) values causing 50% reduction of relative light units compared to the virus control (without inhibitor) after subtracting the background (without virus).

2.7 Env-pseudoviruses used

Env-pseudotyped viruses that were used to screen for neutralization efficacy of the aptamers that were isolated against HIV-1_{BaL} gp120 included three from the subtype C reference panel (Du151.2, ZM197M.PB7 and ZM53M.PB12) (Li et al., 2006) and one clone isolated from an AIDS patient (SW7) (Cilliers et al., 2003). HIV-1 subtype B pseudoviruses (HxB2, HIV-1_{BaL} and SF162) were also used.

3. Results

3.1 PCR amplification and transcription of anti-gp120 aptamers

Twelve plasmids containing DNA for anti-gp120 aptamers (Chapter 2, section 2.2) were amplified by PCR (Chapter 2, section 2.3.1) and the PCR products analysed by gel electrophoresis (Appendix C, section 1.1). All the DNAs were 134 base pairs (bp) in length except for B65 DNA aptamer, which was shorter with only 98 bp (Figure 2-3A). To generate RNA aptamers, the PCR amplified DNAs were transcribed into RNA and the products treated with DNase-I to recover pure RNA (Figure 2-3B).

3.2 Expression and purification of gp120

Gp120 proteins were expressed for use as target proteins in functional assays for the aptamer. The purity, size and homogeneity of the Du151and ConC gp120 proteins were assessed using 6% SDS-PAGE (Figure 2-4). The protein was first purified by ion exchange chromatography purification. To recover pure protein, contaminants that persisted were removed by affinity chromatography purification.

3.2.1 Antigenicity of gp120

The antigenicity of gp120 was confirmed with ELISA by binding to anti-CD4 MAbs, CD4IgG2, B6 and IgG1b12, to 2G12 that binds to gp120 carbohydrates and to 447-52D, an anti V3 loop MAb (Figure 2-5). Binding of the Du151 gp120 was observed with the plasma and anti-CD4 MAbs compared with binding to 2G12 and 447-52D MAbs. The low antigenicity of the protein with 2G12 MAb was expected due to the absence of N295 on Du151 gp120. This was shown when an increased 2G12 binding to a mutant Du151-V295N gp120 was observed when compared to wild-type

Du151 gp120 (Chen et al., 2005b, Gray et al., 2007b). The low antigenicity observed with 447-52D MAb can be attributed to the fact that its epitope is present in only 11% of circulating viruses (Swetnam et al., 2010) and is mostly subtype B restricted (Binley et al., 2004, Hioe et al., 2010, Swetnam et al., 2010).

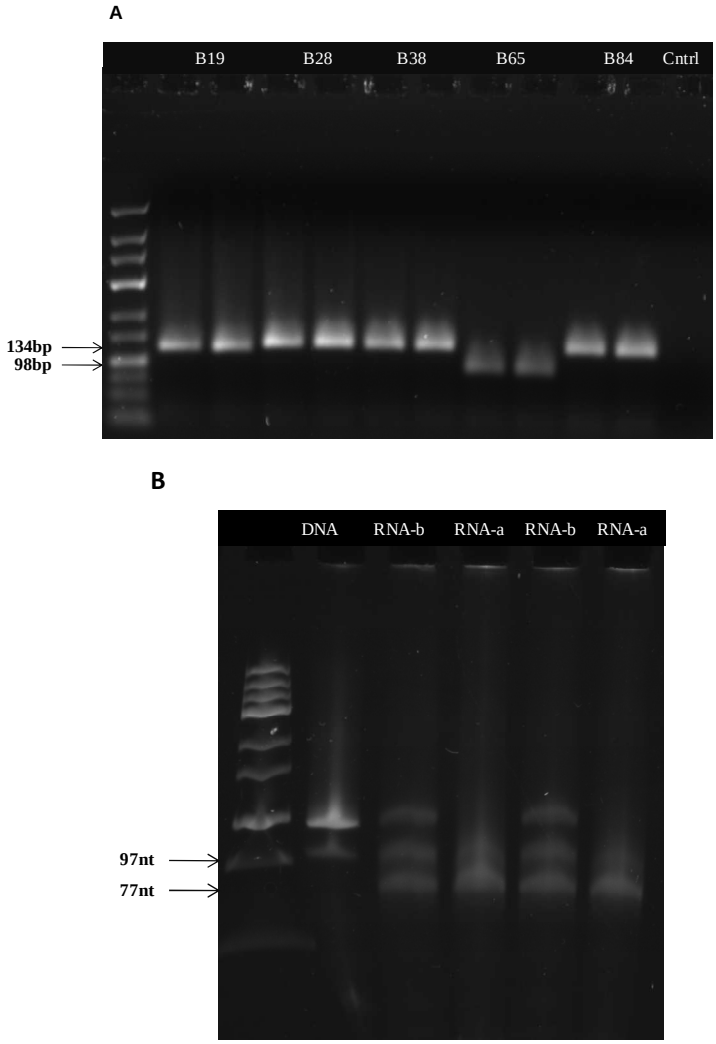

Figure 2-3: Gels showing PCR products of aptamers.
(A) A representative 2% agarose gel showing PCR products of some of the utilized 2'-fluoro modified aptamers. Lane 1 shows a 25 base pair (bp) DNA ladder, lanes 2-11 illustrate PCR products of the respective aptamers in duplicate and lane 12 a negative control. (**B)** A representative 11% denaturing polyacrylamide gel showing the truncated B40t77 RNA aptamer products. Lane 1 shows the 25 bp DNA ladder, lane 2 shows the DNA product of the truncated aptamer which is 94bp in length, lanes 3 and 5 illustrates the aptamer before Dnase-I treatment (RNA-b) and lanes 4 and 6 demonstrate the aptamer after Dnase-I treatment (RNA-a), all of which are 77bp in length.

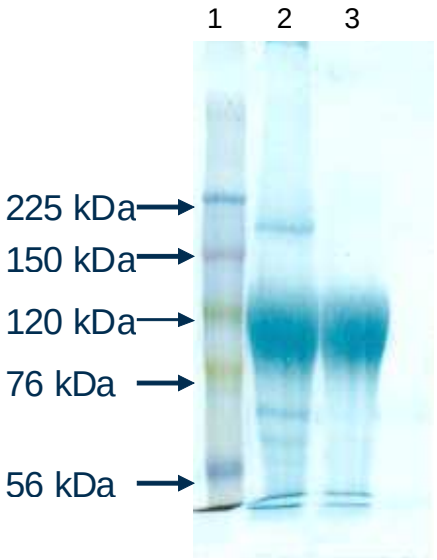

Figure 2-4: A 6% SDS-PAGE showing the purity and size of the expressed Du151 gp120 protein.
Lane 2 illustrates protein purified by affinity chromatography. Lane 3 depicts the protein purified by ion exchange chromatography. The target protein is illustrated by the thick band at 120 kDa.

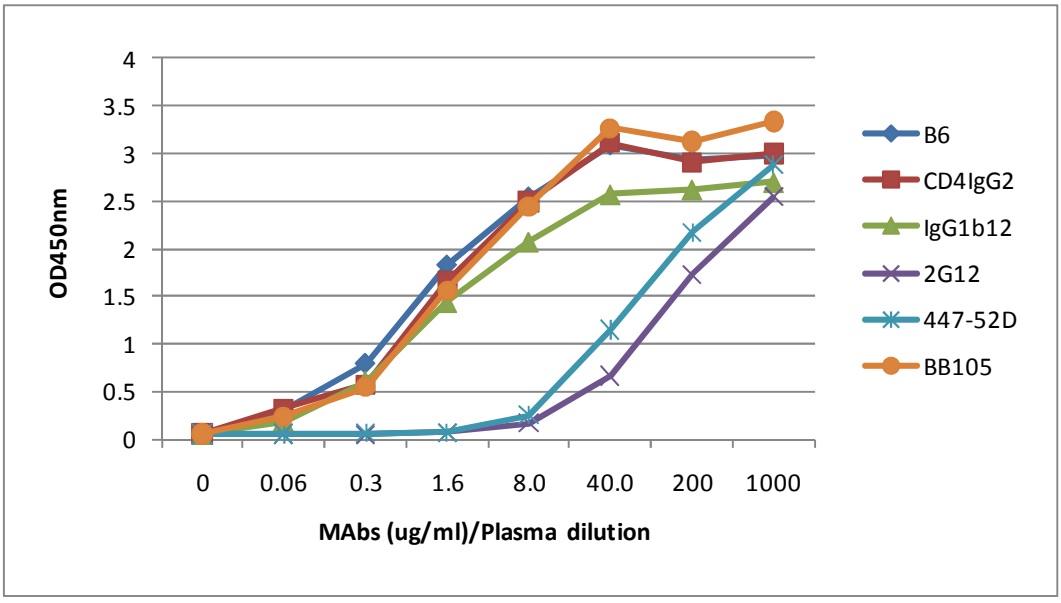

Figure 2-5: The antigenicity of Du151 gp120 protein.
The antigenicity of the protein was assessed by binding to different anti-gp120 MAbs by ELISA. The graph was plotted after subtracting the background wells without MAbs. BB105, a HIV-1 positive plasma pool was included as a positive control.

3.3 Binding of RNA aptamers to gp120 proteins

3.3.1 Screening of binding affinity

Binding of the 2'-fluoro modified RNA aptamers to gp120 was measured by the SPR technology using the BIAcore™ machine. Immobilization of the protein onto a CM5 chip is illustrated in Figure 2-6A. The EDC/NHS curve represents the activation of the carboxyl groups on surface of the sensor chip. Injection of the protein over the activated chip is represented by a gp120 curve. Ethanolamine was then injected to block excess activated carboxyl groups on the surface of the chip that could not occupied by the protein. Finally glycine was injected in order to remove excess or unbound protein. The binding affinity of in-house aptamers was measured against HIV-1_{BaL} and Du151 gp120s. On average, a high binding affinity of the aptamers was observed for the Du151 gp120 than HIV-1_{BaL} gp120 (Table 2-1). This was unexpected since the aptamers were selected against HIV-1_{BaL} gp120 (Khati et al., 2003). Sensorgrams showing the binding of aptamers to three functional gp120 glycoproteins are depicted in Figure 2-6B. UCLA1 aptamer is shown to bind to the immobilized ConC gp120 on the sensor chip with high response units compared with binding of the B40 aptamer to both Du151 and HIV-1_{BaL} gp120 proteins. The B40 aptamer is demonstrated to bind to HIV-1_{BaL} gp120 with higher response units compared with binding to Du151 protein as shown also in Table 2.1.

Table 2-1: The binding affinity of in-house aptamers against HIV-1_{BaL} and Du151 gp120 proteins.

Aptamers	Du151 gp120 binding (RU)[a]	HIV-1_{BaL} gp120 binding (RU)[a]
B40	138	184
B38	526	137
B84	152	120
B4	87	nb
B44	78	nt
B40t77	1793	nt

[a] Average binding affinity of the aptamers expressed as Response Units (RU) after subtraction of the negative control flow cell.
nb - no binding affinity observed
nt – binding affinity not tested

3.3.2 Binding kinetics of RNA aptamers to HIV-1 glycoproteins

To determine the binding kinetics of aptamers against their target gp120 proteins, the proteins were immobilized onto a CM5 chip and the aptamers injected over the proteins to obtain dissociation equilibrium constant (K_D) values. The binding kinetics of B40t77 (unmodified aptamer) and UCLA1 (modified aptamer) to ConC gp120 were measured. A tight binding of UCLA1 to ConC gp120 was observed with an average K_D of 0.15 nM and a standard deviation of the mean (± SD) of 0.01 and a Chi^2 of 1.8 ± 0.7 (Figure 2-7A). A Chi^2 of less than 2 demonstrated an acceptable fit of the data to the binding model. The B40t77 aptamer exhibited higher K_D than UCLA1 with an average K_D of 55 ± 1.9 nM and a high Chi^2 of 31 ± 5.4 (Figure 2-7B). These data showed that the modified aptamer had higher binding affinity for gp120 compared to the unmodified aptamer probably due to the higher stability of UCLA1. For this reason, only UCLA1 was consequently evaluated in all the subsequent experiments.

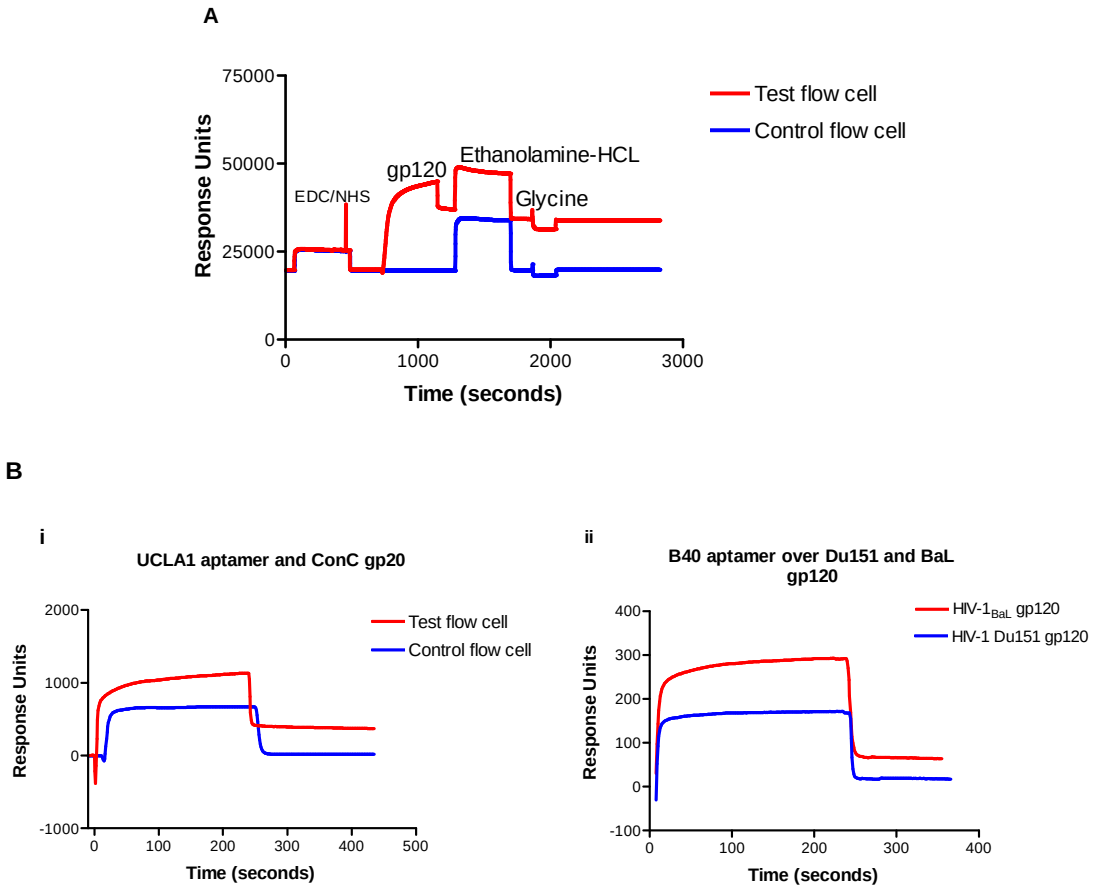

Figure 2-6: BIAcore sensorgrams showing immobilization of gp120 protein and binding of aptamers to gp120.
(A) Immobilization of gp120 protein onto the CM5 biosensor chip by direct amine coupling. The surface of the chip was activated with EDC/NHS. The protein was injected onto the surface of the activated chip. Ethanolamine was injected to block excess carboxyl groups on the surface of the chip. Unbound protein was washed off with glycine. **(B)** BIAcore sensorgrams showing binding of aptamers to gp120 proteins. **i** - Binding of UCLA1 aptamer to ConC gp120 relative to the control flow cell without protein. **ii** - Binding of B40 aptamer to a subtype C HIV-1 Du151 gp120 in comparison to a subtype B HIV-1_{BaL} gp120.

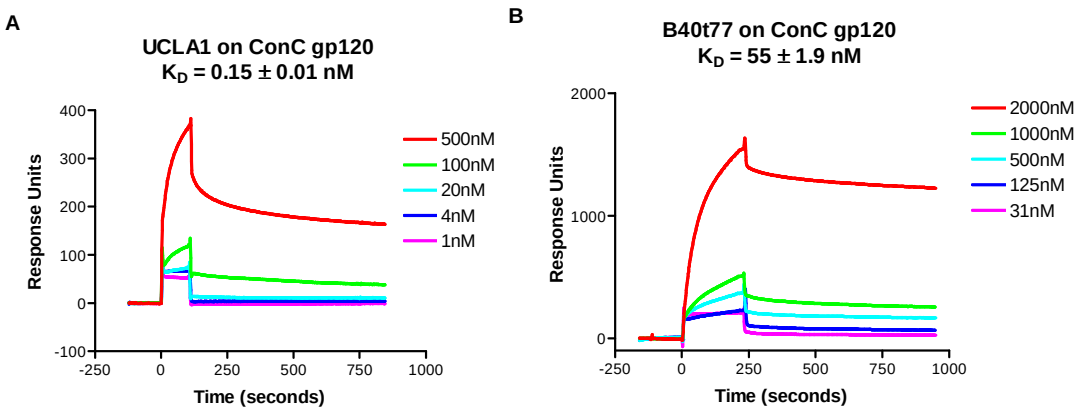

Figure 2-7: Affinity of derivatives of B40 aptamer to subtype C gp120.
(A) BIAcore® sensorgram showing the affinity constant (K_D) of UCLA1 to ConC gp120 in a concentration dependent mode. **(B)** BIAcore® sensorgram showing the K_D of B40t77 to ConC gp120 also in a concentration dependent manner.

3.4 Optimization of aptamer usage in TZM-bl neutralization assay

The in-house generated aptamers stabilized with 2'-fluoropyrimidines were observed to be affected by high FBS concentrations. Neutralization assay with culture media supplemented with 10% FBS decreased the efficiency of the aptamers when compared with 5% FBS. This is illustrated in Figure 2-8 where HxB2 pseudovirus was not neutralized by the B4 aptamer when used in 10% FBS media but was inhibited with the same aptamer in 5% FBS media. UCLA1 aptamer proved to be efficacious in both 5% and 10% FBS media. It neutralized the HxB2 and HIV-1 subtype C ZM197 pseudoviruses in 5% and 10% FBS containing media with IC_{50} values of 0.33 nM and 0.99 nM when used at an initial concentration of 100 nM, respectively (Figure 2-9). Although the B4 aptamer in 5% FBS media at 100 nM neutralized HxB2 (Figure 2-8A) and Du151 pseudoviruses (Figure 2-10A) with IC_{50} values of 6.5 and 8.0 nM, respectively, other aptamers (B40, B38, B84, B44 and

B40t77) were observed to be ineffective (Figure 2-10A). HIV-1_{BaL} pseudovirus was also not neutralized by the in-house aptamers even though the aptamers were raised against HIV-1_{BaL} gp120 (Figure 2-10B).

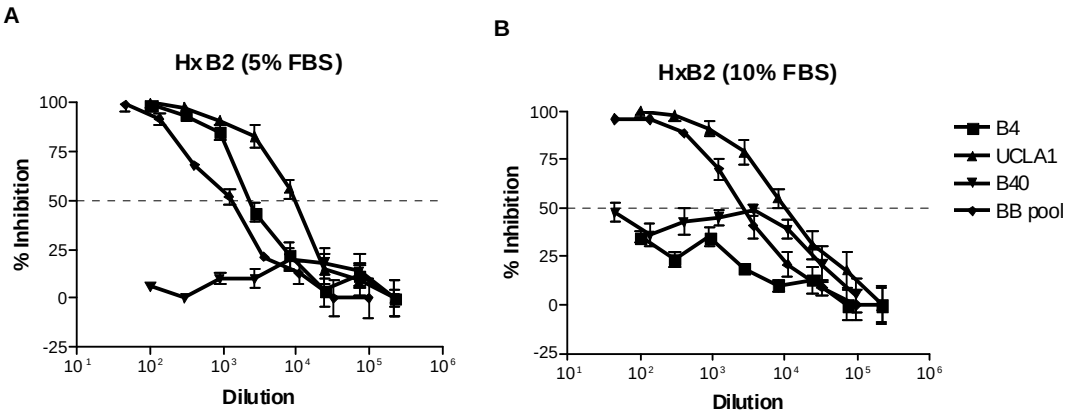

Figure 2-8: Effects of FBS on aptamer activity.
The HxB2 pseudovirus was neutralized with 100 nM of B4, B40 and UCLA1 aptamers at 3-fold serial dilutions. **(A)** The TZM-bl neutralization assay culture media was supplemented with 5% FBS. **(B)** The neutralization assay media was supplemented with 10% FBS. HIV-1 positive plasma (BB pool), was included as a positive control at an initial dilution of 1:45 and was further 3-fold serially diluted. The assay was performed in triplicate and a representative plot is shown.

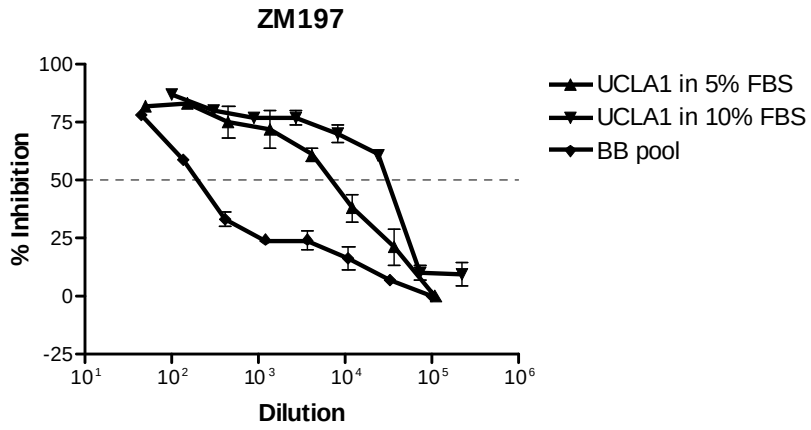

Figure 2-9: UCLA1 activity unaltered by different FBS concentrations.
A neutralization plot showing inhibition of ZM197 pseudovirus with 100 nM UCLA1 in culture media supplemented with either 5% or 10% FBS. The aptamer revealed high potency against the virus with IC_{50} values lower than 1 nM. HIV1 positive plasma, BB pool, was included as a positive control at an initial dilution of 1:45 and was further 3-fold serially diluted. The assay was performed in triplicate and a representative plot is shown.

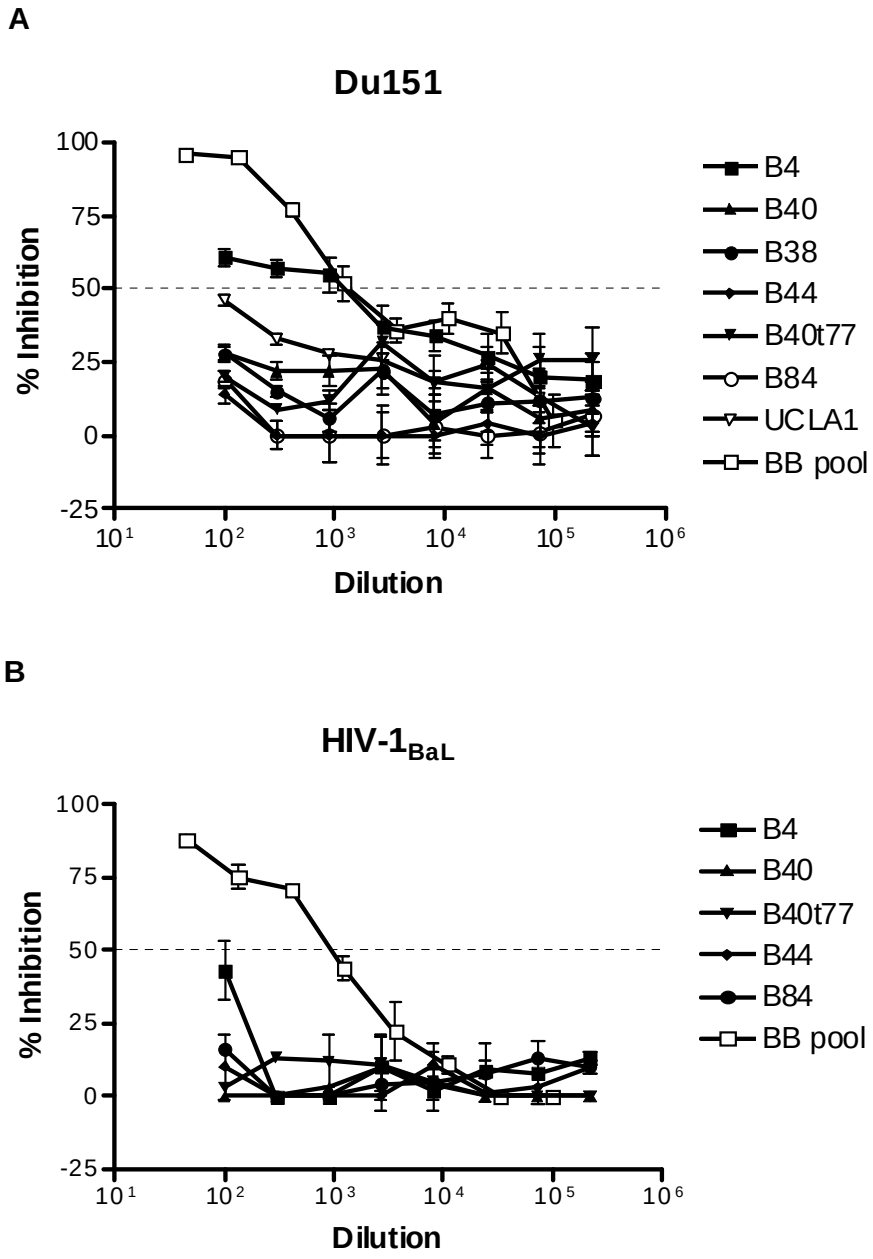

Figure 2-10: Differing efficacy for different aptamers.
Representative neutralization plots of Du151 and HIV-1_{BaL} pseudoviruses. (**A)** Du151 virus was neutralized by the B4 aptamer compared to the B40 aptamer. Both aptamers were used at an initial concentration of 100 nM, 3-fold serially diluted. UCLA1 was also ineffective against Du151. (**B)** The non-efficiency of in-house aptamers against HIV-1_{BaL} is shown. HIV-1 positive plasma, BB pool, was included as a positive control at an initial dilution of 1:45 and was further diluted in the assay at 3-fold serial dilutions. The assays were performed in triplicate.

4. Discussion

RNA aptamers were generated and purified and their binding affinity was measured by the BIAcore SPR technology. Higher binding affinity was observed for Du151 gp120 than HIV-1_{BaL} gp120. High FBS content was observed to interfere with inhibition activity of the in-house generated aptamers. Nevertheless, UCLA1 exhibited a tight association, confirmed by low K_D values, when binding with ConC gp120.

Although the in-house aptamers were isolated against HIV-1_{BaL} gp120, the high affinity for Du151 was expected since the full length B40 aptamer and its truncated derivatives has been shown to bind to conserved regions of the envelope gene (Cohen et al., 2008, Dey et al., 2005b, Joubert et al., 2010). This is also consistent with the cross-clade potency that was exhibited by these aptamers after their isolation (Khati et al., 2003). Nevertheless, it was discovered in this study that high binding affinity does not always correlate with inhibition efficiency as was observed with the Du151 virus (Table 2.1 and Figure 2.10).

Most of the in-house aptamers (B40, B38, B84, B44 and B40t77) could not inhibit the HIV-1 subtype C pseudoviruses that were tested even after decreasing the serum content in the neutralization assay. It has been previously reported that fetal calf serum contains heat-stable nucleases (von Kockritz-Blickwede et al., 2009) thus expected to degrade the RNA aptamers even though they were 2'-fluoro modified for stability. This modification has been shown to be unable to withstand nuclease attack compared to the 2'-*O*-Me modification (Ge et al., 2010, Moore et al., 2011).

Therefore, UCLA1 aptamer was used as it was observed to be highly efficacious against one subtype B and one subtype C viruses and was not affected by high serum content. Its low K_D values contributed to a stable association and better binding energy. The binding analysis model produced kinetics data with average Chi^2 values of <2 for each triplicate run, showing an adequate fit of the data to the binding model. This illustrates that the more truncated and more stabilized UCLA1 aptamer has a tight binding capacity than the other B40 aptamer derivatives thus exhibiting potent neutralizing efficacy. This effect was demonstrated in the current study by the in-house aptamers that were stabilized with only 2'-fluoropyrimidines. Although it has been shown that substitution at the 2'-position of ribonucleotides with 2'-amino (2'-NH2), 2'-fluoro (2'-F), or a variety of 2'-*O*-alkyl moieties confers resistance to ribonucleases that utilize the 2'-OH group for cleavage of the adjacent phosphodiester bond (Knudsen et al., 2002, Mayer, 2009, Stoltenburg et al., 2007), RNA aptamers require stabilization with more than a single 2' modification. This has been shown with the 299.2 aptamer which is stabilized by the use of six 2′-O-dimethylallylribonucleotides (Cohen et al., 2008) and UCLA1 aptamer which is made up of the 299.2 aptamer with an addition of an inverted thymidine at the 3′-end and a dimethoxyltrityloxy-$(CH_2)_6$-SS-$(CH_2)_6$-phospho linker at the 5′-end. UCLA1 modifications at the 3'- and 5'-ends block degradation by 3′- exonucleases and enhance correct folding and increase stability for *in vivo* usage, respectively (Cohen et al., 2008). Therefore, this confirms that a single modification is not sufficient for stability against nuclease degradation. The effect of chemical modifications was shown when UCLA1 neutralized HIV-1_{BaL} by 82% in peripheral blood mononuclear cells (PBMCs) and 84% in blood monocyte-derived macrophages compared with

aptamer 299.2 which neutralized by 77% and 56% respectively (Cohen et al., 2008). Thus, data indicate that modified aptamers have higher binding affinity and potency for their targets above levels observed with unmodified aptamers.

CHAPTER 3

Inhibition of Human Immunodeficiency Virus Type-1 Subtype C Env Pseudotyped Virus Infection with UCLA1 RNA aptamer

Published: ***Journal of Virology.*** **2012, 86(9):4989-4999**, (Appendix C).

Chapter summary

Entry of human immunodeficiency virus type 1 (HIV-1) into cells is mediated by the virion surface envelope (Env) glycoprotein gp120, making it a desirable target for antiretroviral entry inhibitors. For this reason, in this study, the activity of a shortened synthetic derivative of the B40 aptamer, called UCLA1, previously isolated against subtype B gp120, was assessed against a large panel of HIV-1 subtype C isolates. UCLA1 tightly bound to a consensus HIV-1 subtype C gp120 and neutralized isolates from this subtype with IC_{50} values in the nanomolar range. The aptamer had no apparent toxicity in the target cells with a CC_{50} value of >500 nM. Mapping of UCLA1 binding sites on gp120 revealed eight amino acid residues that modulated neutralization resistance. This included residues within the co-receptor binding site, at the base of the V3 loop, and in the bridging sheet within the conserved V1/V2 stem-loop of gp120. The aptamer was also shown to have synergistic effects with T20, a gp41 fusion inhibitor and IgG1b12, an anti-CD4 binding site monoclonal antibody. These results bode well for the future development and testing of UCLA1 in preclinical and clinical trials as HIV-1 entry inhibitor.

1. Introduction

HIV-1 binding to T lymphocytes and macrophages is mediated by gp120, which sequentially interacts with the CD4 receptor and chemokine receptors (Alkhatib et al., 1996, Atchison et al., 1996). While gp120 is a heterogeneous molecule with hypervariable loops and extensive glycosylation (Kwong et al., 2002, Kwong et al., 1998, Wyatt et al., 1998), the CD4 binding site (CD4bs) and co-receptor binding site (CoRbs) are both highly conserved (Rizzuto et al., 1998) and immunogenic (Wu et al., 2010, Zhou & Rossi, 2010). Other invariant regions on gp120 include the epitopes defined by the newly isolated broadly neutralizing monoclonal antibodies (MAbs), PG9/16 and PGT127/128 (Walker et al., 2011, Walker et al., 2009) making gp120 a desirable target for agents that block virus entry (Moore & Doms, 2003).

Entry inhibitors comprise an array of molecules that target either the virus envelope glycoprotein or host cellular receptors. This includes monoclonal antibodies (MAbs), fusion inhibitors, co-receptor antagonists and small molecule inhibitors (Binley et al., 2004, Jacobson et al., 2000, Lalezari et al., 2003, Moore & Doms, 2003, Schols, 2006). Aptamers which generally bind functional sites on their respective targets (Ellington & Szostak, 1990) have been isolated against gp120 and are being developed as potential HIV-1 entry inhibitors (Cohen et al., 2008, Dey et al., 2005a, Dey et al., 2005b, Khati et al., 2003, Moore et al., 2011, Zhou et al., 2008, Zhou & Rossi, 2010, Zhou et al., 2011, Zhou et al., 2009). RNA aptamers isolated against gp120 derived from HIV-1_{BaL}, a subtype B laboratory-adapted strain were shown to neutralize infectivity of group M (subtypes A, C, D, E and F) and group O HIV-1 clinical isolates in cell-based assays (Khati et al., 2003). One extensively studied

aptamer called B40 was truncated to a 77 nucleotides derivative called B40t77 (Dey et al., 2005a). Subsequently, a synthetic capped derivative of B40t77 called UCLA1 was manufactured by solid-phase synthesis and further shortened and modified to help folding and stability without compromising its activity (Cohen et al., 2008). UCLA1 was shown to retain *in vitro* activity against HIV-1_{BaL} (Cohen et al., 2008). The B40 aptamer and its shortened derivatives (B40t77 and UCLA1) have been shown to contact the highly variable exterior surfaces of monomeric and trimeric gp120 and bind conserved core residues in the CCR5-binding site (Cohen et al., 2008, Dey et al., 2005a, Dey et al., 2005b, Joubert et al., 2010). In one study, using an aptamer related to UCLA1 (aptamer 299.5), mutations within the V3 loop and the bridging sheet (β20) were identified using JR-CSF gp120 monomers (Cohen et al., 2008). In another study, using HIV-1_{BaL} gp120 from viral supernatants, mutations in the α1 helix, C2 domain, V3 loop, bridging sheet (β21) and F loop within the C4 domain, affected the binding of the B40t77 aptamer (Joubert et al., 2010). While some sites were common, discrepancies between these two studies were likely related to the use of different sources of gp120 and different aptamers. In general, both studies suggest that an epitope of gp120 RNA aptamers overlaps the base of the α1 helix, the CD4-induced binding sites in the bridging sheet (β21 and β20) and the variable loops (F and V3).

Since HIV-1 subtype C dominates the global HIV/AIDS epidemic and is endemic in countries with high HIV-1 prevalence rates such as South Africa (Van Harmelen et al., 1999) where this study was conducted, we assessed the sensitivity of a large panel of subtype C isolates derived from adult and paediatric patients at different

stages of HIV-1 infection to UCLA1. We examined its neutralization efficacy and identified the potential binding sites. Furthermore, we evaluated cell viability in the presence of the aptamer and its synergism with other entry inhibitors. Overall, these studies support future development and testing of UCLA1 against a large panel of clinical isolates in primary cells and preclinical studies.

2. Materials and Methods

2.1 Truncated and mutated glycoproteins

ConC truncated and mutated gp120s were also expressed and purified as outlined in Chapter 2 and used in the study to determine the binding kinetics of UCLA1. The truncated gp120s were the core, ΔV1/V2 and ΔV3 gp120. The core gp120 is a mutant that lacks amino acid residues 128-194 (V1/V2 loop) and 298-329 (V3 loop), ΔV1/V2 gp120 lacks amino acid residues 128-194 and ΔV3 gp120 lacks amino acid residues 298-329 (Decker et al., 2005, Kwong et al., 1998). The residues are numbered according to HxB2 (Kwong et al., 1998). The mutated gp120s contained single mutations in the CD4bs (D368R) or CoRbs (I420R) (Li et al., 2007, Pantophlet et al., 2003).

2.2 Binding kinetics of RNA aptamers to HIV-1 glycoproteins

The BIAcore® was used to determine the binding kinetics of UCLA1 to truncated and mutated HIV-1 ConC gp120. These were compared with the binding kinetics of the wild type ConC gp120. Each experiment was performed in triplicate by kin-injecting ½ $\log_{10}$ serial dilutions of the aptamers as described in Chapter 2 (section 2.5.3). The association (K_a) and dissociation (K_d) constants of the resulting data curves were separately fitted to a 1:1 Langmuir binding model and analysed as described in Chapter 2 (section 2.5.3). The negative control flow cell was subtracted as baseline.

2.3 Cytotoxicity assay

The cytotoxicity of UCLA1 RNA aptamer was determined in TZM-bl cells by using two cell viability assays. The ATP-based CellTiter-Glo® Luminescent Cell Viability

Assay (Promega) was used as previously described (Lopes de Campos et al., 2009). Briefly, 2 × 10^5 of TZM-bl cells in 100 µl of Dulbecco's modified eagle medium (DMEM) (Gibco Invitrogen), supplemented with 5% fetal bovine serum (FBS) (Gibco Invitrogen), 25 mM of HEPES (Gibco Invitrogen) and 50 µg/ml of Gentamicin (Sigma-Aldrich) were incubated with 50 µl of serially diluted (3-fold) UCLA-1 in triplicates for 24 h at 37℃ in 5% CO_2 and 95% humidity. Infection was monitored by evaluating the luciferase activity of ATP production by viable cells. The CellTiter 96 Aqueous Cell Proliferation Assay (Promega) was also used according to the manufacturer's protocol. The assay is composed of solutions of a novel tetrazolium compound [3-(4,5-dimethylthiazol-2-yl)-5-(3-carboxymethoxyphenyl)-2-(4-sulfophenyl)-2H-tetrazolium, inner salt; MTS] and an electron coupling reagent (phenazine methosulfate; PMS). Briefly, the dehydrogenase enzymes found in metabolically active cells converts a tetrazolium compound (MTS) into aqueous, soluble formazan which is then quantified by measuring absorbance at 490 nm. The TZM-bl cells were used at 5 × 10^5 cells/well in 50 µl D-MEM with 5% FBS. The cells were incubated with 500 nM (50 µl) of 2-fold serially diluted UCLA1 in triplicate for 72 hours at 37℃. The cells used for positive control cultures were treated with Etoposide phosphate (Sigma-Aldrich) (Osztie et al., 2001), an anti-cancer agent that inhibits topoisomerase II enzyme which aids in DNA unwinding thus causing DNA strands to break (Osztie et al., 2001). The positive control cells were incubated with 50 µl of 142 µM Etoposide phosphate in triplicate for 72 hours at 37℃ in 5% CO_2 and 95% humidity. Untreated cell cultures were used as negative controls. The MTS/PMS solution (20 µl) was then added to each well and incubated for 4 h at 37℃. To measure the amount of soluble formazan produced by cellular reduction of

the MTS, absorbance was recorded at 490 nm using the ELISA plate reader. Titers were calculated as cytotoxicity concentration values causing 50% reduction (CC_{50}) in relative light units or in absorbance compared to the aptamer control after subtracting the background (without aptamer) and expressed as percentage cell viability. Thus CC_{50} is the concentration of the aptamer that would cause cytotoxicity or inhibit cell viability by 50%.

2.4 Production of Env-pseudovirions

2.4.1 Proviral DNA PCR

The Env-pseudotyped virus stocks were generated as previously described (Gray et al., 2006, Montefiori, 2004). Briefly, the proviral DNA extracted from *in vitro* infected PBMCs was used to amplify full-length envelope genes. The 3-kilobase PCR fragments generated using EnvA: 5′-GGC TTA GGC ATC TCC TAT GGC AGG AAG AA-3′ and EnvM: 5′-TAG CCC TTC CAG TCC CCC CTT TTC TTT TA-3′ primers (Invitrogen, South Africa), (Gao et al., 1996, Gray et al., 2007a) were cloned into the pCDNA 3.1-TOPO vector (Invitrogen).

2.4.2 Transformation of TOP10 chemically competent cells

The cloned plasmid DNA (1 µl) was transformed into 50 µl of TOP10 chemically competent cells (Invitrogen) by incubating on ice for 30 min and heat shocking at 42ºC for 30 s and 2 min on ice. Thereafter 50 µl of pre-warmed SOC medium (Gibco Invitrogen) was added and incubated at 37ºC shaking for 30 min at 230 rpm. 250 µl of the transformation reaction was plated onto Luria Broth, Lennox L agar (LB agar) (Gibco Invitrogen) plates, at 0.032 g/ml supplemented with 100 µg/ml ampicillin

(Invitrogen) and the plates were inverted and incubated at 37ºC, 5% CO_2 overnight. The selected bacterial colonies were screened by PCR for insertion and correct orientation using T7 and envM primers.

2.4.3 Transfection of Env plasmid DNA

The Env-pseudotyped virus stocks were generated by co-transfecting 4 µg of the env encoding plasmid DNA with 8 µg of the HIV genomic backbone vector, SG3delta *env* into an 80% confluent monolayer of 293T cells in a 75 cm^2 cell culture flask in the presence of 48 µl of FuGENE 6 transfection reagent (Roche). The tranfection mixture was incubated for 48 hrs at 37ºC, 5% CO_2. The culture supernatant containing the pseudoviruses were then harvested, the FBS adjusted to 20% and the supernatant filtered with a 0.45 µm filter and stored at -80℃.

2.4.4 Determination of pseudovirus titers

The median tissue culture infective dose ($TCID_{50}$) of each Env-pseudotyped virus stock was determined in a single-cycle infection assay in TZM-bl cells prior to performing neutralization assays. The $TCID_{50}$ was quantified by infecting TZM-bl cells with serial 4-fold dilutions of the virus supernatant. That is, 150 µl of 10% FBS DMEM complete growth medium was added to all wells in a 96 well flat bottom culture plate (Corning Incorporated). Virus supernatant (50 µl) was transferred to the first 4 wells of a set of a dilution series (quadruplicate), mixed and serial 4-fold dilutions were performed with 50 µl for a total of 11 dilutions. The last set of wells served as negative cell control wells without virus. TZM-bl cells were added at 10,000 cells/100 µl and incubated for 48 hrs. The infection was then monitored by

evaluating the luciferase activity using the Bright Glo Reagent (Promega) following manufacturers' instructions. For this, 150 µl of culture medium was removed from each well and 100 µl of Bright Glo substrate solution (Promega) was added and incubated at room temperature for 2 min to allow complete cell lysis. The culture was then mixed and 150 µl transferred to a corresponding 96-well black plate and luminescence was measured with the Wallac 1420 Victor Multilabel Counter (Separation Scientific). A cut-off value of 2.5 times the background was considered positive for infection (Montefiori, 2004).

2.5 Maintenance of TZM-bl cells

The TZM-bl cells kept in liquid nitrogen for long term storage were thawed in a 37℃ water bath, transferred into 25 ml of 10% FBS DMEM complete growth medium and washed by centrifuging at 1 200 rpm for 10 min. The cell pellet was re-suspended in 1 ml of complete growth medium, transferred to a 75 cm^2 culture flask (Corning Incorporated) with 14 ml of the complete growth medium and incubated for 2 days at 37℃, 5% CO_2. The cells were first passaged at 1.5×10^6 total cells per 75 cm^2 cell culture flask and incubated for 2 days. After the second passage the cell monolayer was rinsed with neat PBS (Gibco Invitrogen) and disrupted at ± 50% confluence with 2.5 ml of 0.25% Trypsin in 1mM EDTA (Gibco Invitrogen) for 30 sec, the Trypsin/EDTA was then decanted and the cells incubated for 5 min 37℃, 5% CO_2 humidity. The cells were then washed and re-suspended at 5×10^6 cells/ml in chilled FBS with 10% DMSO (Sigma-Aldrich). The cells were aliquoted in 1 ml aliquots, stored at -80℃ overnight and then transferred to liquid nitrogen for long term storage (Montefiori, 2004).

2.6 Panel of Env-pseudoviruses

Env-pseudotyped viruses that were used to screen for neutralization efficacy of UCLA1 comprised those from the CAPRISA 002 Acute Infection study cohort (Gray et al., 2007a), subtype C reference panel (Li et al., 2006), clones from paediatric isolates (Gray et al., 2006), one clone isolated from an AIDS patient (SW7) (Cilliers et al., 2003), and a subtype C consensus sequence clone (ConC) (Kothe et al., 2006) (Table 1). The subtype C pseudoviruses were all R5 strains, except for RP1 and SW7, which were X4 viruses (Table 1). An X4-tropic subtype B pseudovirus, HxB2 reference strain, was also used. A pseudovirus with the Vesicular stomatitis Virus G (VSV-G) envelope gene was used as a negative control.

2.7 Single-cycle neutralization assay

Neutralization was measured as a reduction in luciferase gene expression after a single-round infection of TZM-bl cells with Env-pseudotyped virus as described in chapter 2 (section 2.8). The aptamer was tested at a maximum initial concentration of 50 nM. The plasma samples (BB-pool and IBU-21) were used as positive controls, at an initial dilution of 1:45. Vesicular Stomatitis Virus G (VSV-G) Env-pseudotyped virus with the same genomic vector backbone (SG3delta *env*) as the HIV-1 Env-pseudotyped viruses was used as the *env* negative contol. Other positive controls that were used were the T20 fusion inhibitor (Chen et al., 1995, Kilby et al., 2002, Wild et al., 1993) and the 4E10 MAb (Burton et al., 1991) whose binding sites are located in gp41. Both were tested at initial concentrations of 40 µg/ml and 20 µg/ml, respectively. The assay was performed at least three times, in duplicate, for each pseudovirus tested.

2.8 Site-directed mutagenesis

Specific amino acid changes within the ConC gp120 were introduced using the QuikChange Site-Directed Mutagenesis Kit (Stratagene, South Africa) as previously described (Alexandre et al., 2010, Gray et al., 2007b, Gray et al., 2009) according to the manufacturers' protocol. A total of 19 single point mutations were introduced in ConC gp120. That is, primers were designed for 5 mutations (Invitrogen) while 14 single point mutated ConC gp120s were obtained from the NICD. Generally, the mutations were introduced within the CD4bs and CoRbs of gp120 spanning the V3 loop and the C1 to C5 regions, excluding the C2 region. The primers were diluted at 1:1000 in ddH_20, mixed and left to dissolve for at least 1 h at room temperature. They were further diluted at 1:1000 in ddH_20 to 140 ng/µl. The ConC gp120 plasmid DNA was amplified using the QuikChange Site-Directed Mutagenesis PCR protocol. A 50 µl PCR reaction mixture consisted of 100 ng of the plasmid DNA, 5 µl of 10 × reaction buffer, 140 ng/µl (1.25 µl) of both forward and reverse primers, 1µl dNTP mix. The final volume was made up to 50 µl with ddH_20. Then 2.5 U (1µl) of *Pfu Turbo* DNA polymerase was added to the PCR mixture. The template was denatured at 95ºC for 30 s, and amplified with 18 PCR cycles (95℃ for 30 s, 55℃ for 1 min, 68℃ for 1 min). The ConC gp120 supercoiled double- stranded plasmid DNA in the amplified reaction mixture was digested with 10 U (1 µl) of *Dpn* I restriction enzyme at 37ºC for 2 h.

2.8.1 Transformation of XL1-Blue supercompetent cells

The plasmid DNA was transformed into XL1-Blue supercompetent cells (Stratagene) as follows: 4 µl of β-mercaptoethanol (Sigma-Aldrich), a reducing agent to break

down toxic metabolites produced by cells in culture to enhance transformation, was added to 250 µl of the XL1-Blue supercompetent cells and incubated on ice for 10 min. The cells were then aliquoted at 50 µl into pre-chilled Eppendorf tubes. This was followed by addition of 5 µl of the *Dpn* I treated DNA reaction, which was mixed and incubated on ice for 30 min. The transformation reactions were heat pulsed at 42ºC for 30 s and then placed on ice for 2 min. The SOC medium was warmed and 500 µl added to the transformation reactions and incubated at 37ºC shaking for 1 h at 230 rpm. 250 µl of each transformation reaction was plated onto LB agar plates prepared at 31.25 g/ml. The LB agar was supplemented with 100 µg/ml of ConC resistant antibiotic, kanamycin, (Invitrogen) and cultured overnight at 37ºC. The mutated ConC plasmid DNA single colonies that grew on the agar plates were selected and expanded overnight by incubating at 37ºC shaking at 230 rpm in liquid Ultrapure LB broth culture medium (USB Corporation, South Africa) supplemented with 100 µg/ml kanamycin. The mutated plasmid cultures were purified with the QIAprep Spin Miniprep Kit (Appendix C, section 1.5).

2.8.2 HIV-1 envelope DNA sequencing

The DNA samples from the molecular *env* clones and primary *env* isolates were confirmed by nucleotide sequencing using the ABI PRISM Big Dye Terminator Cycle Sequencing Ready Reaction kit (Applied Biosystems, South Africa) as previously described (Alexandre et al., 2010, Gray et al., 2008, Gray et al., 2007a). The 10 µl sequencing PCR reaction mixture consisted of 300 ng of purified plasmid DNA, 2.6 µl of Ready reaction mix, 5.4 µl of Bioline Buffer and 2 µl of primer. Eight primers (Inqaba Biotechnologies) were used to sequence the *env* gene (gp160) of the clone

or virus of interest (Appendix D, Supplementary Table 1). Thus a sequencing PCR reaction was performed for each of the 8 primers. The templates were amplified with 25 PCR cycles (96℃ for 10 s, 50℃ for 5 sec, 60℃ for 4 min). The resulting DNA was purified using the sodium acetate (NaOAc) purification method (Appendix C, section 1.6) prior to use for sequencing.

2.8.3 Mutated Env-pseudotyped virus stocks

After the presence of ConC gp120 mutations was confirmed by sequence analysis, co-transfection of the 293 T cells with the mutated plasmid DNAs and HIV genomic backbone vector was performed as mentioned above in order to generate mutated ConC gp120 Env-pseudotyped virus stocks. The mutated ConC gp120 pseudotyped viruses were titered in TZM-bl cells for detection of the $TCID_{50}$ of each virus stock, as mentioned above. The mutated pseudoviruses were then tested for resistance to UCLA1 using the single-cycle neutralization assay as mentioned above. This was performed to map the binding sites of UCLA1 to ConC gp120.

2.9 Synergy of UCLA1 with other entry inhibitors

UCLA1 was tested for synergism with the CD4bs MAb, b12 (McInerney et al., 1997) and the T20 fusion inhibitor which binds to the C-terminus of the ectodomain of gp41 (Kilby et al., 1998). The single-cycle neutralization assay was used to test a total of 6 Env-pseudotyped viruses with UCLA1+T20 and UCLA1+b12 combinations. The agents were mixed in a fixed ratio that reflected their relative individual potency. The aptamer was used at a maximum initial concentration of 50 nM while the b12 and T20 were used at a maximum initial concentration of 50 µg/ml equivalent to 312 µM and 11.13 mM respectively. The assay was performed at least three times in

duplicate for each virus tested. The synergy was quantified and expressed as a combination index (CI) using the IC_{50} values (Chou & Talalay, 1984). Calculation of the CI was based on the Chou-Talalay equation: $CI = (D)_1/(Dx)_1 + (D)_2/(Dx)_2$ in which $(Dx)_1$ and $(Dx)_2$ in the denominators are the concentrations of agent 1 and agent 2 alone that are required to neutralize the HIV-1 subtype C Env pseudovirus by x% respectively, and D_1 and D_2 in the numerators are the concentrations of agent 1 and agent 2 when used in combination that also neutralize the virus by x%. A CI value of less than 1, equal to 1, or more than 1, indicates synergism, additive effect and antagonism, respectively (Chou & Talalay, 1984, Zwick et al., 2001). Dose reduction index (DRI) was also determined for each combination therapy used. The DRI is a measure of how many fold the dose of each compound in a synergistic combination may be reduced at a given effect level as compared with the doses of each compound alone. The DRI was calculated using the Chou-Talalay equation, that is, DRI_1 and DRI_2 are the first and second terms of the CI equation, respectively. Therefore, $DRI_1 = (Dx)_1/(D)_1$ and $DRI_2 = (Dx)_2/(D)_2$ (Chou & Talalay, 1984, Nagashima et al., 2001, Zwick et al., 2001).

3. Results

3.1 Neutralization of Env-pseudotyped viruses by UCLA1

UCLA was tested in the TZM-bl neutralization assay against a panel of env-pseudotyped viruses isolated from adult and paediatric patients at different stages of HIV infection. The aptamer inhibited entry of 29 of 35 (83%) subtype C viruses by >50% (range 62-91%), (Table 3-1). Six viruses showed a reduced sensitivity of 30-46% neutralization and were considered to be resistant. Of the 29 subtype C viruses neutralized by UCLA1, 27 were R5 and two were X4 tropic strains. The HxB2 (IIIB) virus, which is an X4 subtype B lab-adapted reference strain and generally neutralization sensitive to antibodies, was almost completely neutralized (99%) by UCLA1 (Table 3-1).

All viruses were titered against a 3-fold serially diluted UCLA1 starting at 50 nM to calculate IC_{50} values. The IC_{50} values were less than 1.0 nM with an average of 0.8 ± 0.9 nM for all the 29 sensitive viruses (Table 3-1). Representative graphs are shown for 8 sensitive subtype C viruses, the subtype B HxB2 virus as well as 3 resistant viruses (Figure 3-1). UCLA1 neutralized the sensitive viruses in a dose-dependent manner while the curves of the 3 resistant viruses did not reach the 50% neutralization cut-off. Overall, all tested viruses were sensitive to the BB plasma pool used as a positive control, suggesting that the sensitivity of the 29 viruses was not due to a generally neutralization-sensitive phenotype. A bar chart showing representative neutralization data of other tested viruses is illustrated (Appendix D, Supplementary Figure 1). UCLA1 neutralization curves often exhibited gradual slopes that reached a plateau at less than 100% neutralization. Although

neutralization curves with similar profiles have been reported previously using MAbs, the mechanism for this is not well understood (Honnen et al., 2007, Pinter et al., 2005, Walker et al., 2009).

Table 3-1: Inhibition of HIV-1 subtype C envelope pseudotype viruses by UCLA1 RNA aptamer.

Env Clone	Subtype	Patient	Stage of infection	Tropism	Accession number	% Inhibition 50nM UCLA1[a]	IC_{50} (nM)[b]	TI[c]
HXB2.C8.3	B	Adult	Chronic	X4	AF358142	**98.5 ± 1.73**	0.17	5 882
CAP63.2.00.A9J	C	Adult	Acute	R5	EF203973	**90.8 ± 3.24**	0.14	7 143
ZM233M.PB6	C	Adult	Acute	R5	DQ388517	**87.8 ± 4.98**	0.04	25 000
CAP210.2.00.E8	C	Adult	Acute	R5	DQ435683	**87.5 ± 6.82**	0.09	11 111
Du156.12	C	Adult	Acute	R5	DQ411852	**86.0 ± 2.37**	0.63	1 587
CAP85.2.00.09J	C	Adult	Acute	R5	EF203985	**84.5 ± 8.50**	0.04	25 000
ZM197.M.PB7	C	Adult	Acute	R5	DQ388515	**83.7 ± 3.14**	0.38	2 632
Consensus C	C	Synthetic		R5	DQ401075	**82.8 ± 6.12**	0.10	10 000
RP1.12	C	Paediatric	Chronic	X4	DQ447271	**81.5 ± 8.66**	0.60	1 667
CAP256.2.00.C7	C	Adult	Acute	R5	EF203981	**78.8 ± 3.41**	0.16	6 250
CAP45.2.00.G3J	C	Adult	Acute	R5	DQ435682	**77.0 ± 10.88**	0.30	3 333
CAP228.2.00.51	C	Adult	Acute	R5	EF203968	**76.6 ± 6.06**	0.31	3 226
CAP61.2.00.E11	C	Adult	Acute	R5	EF203959	**76.5 ± 1.73**	0.38	2 632
ZM214M.PL15	C	Adult	Acute	R5	DQ388516	**76.0 ± 1.15**	0.23	4 348
SW7.14	C	Adult	Chronic	X4	AF411966	**74.5 ± 4.04**	0.73	1 370
TM3.8	C	Paediatric	Chronic	R5	DQ447268	**74.2 ± 9.71**	0.13	7 692
ZM249M.PL1	C	Adult	Acute	R5	DQ388514	**74 .0 ± 1.31**	0.55	1 818
CAP88.2.00.B5J	C	Adult	Acute	R5	EF203972	**73.8 ± 4.37**	0.95	1 053
Du172.17	C	Adult	Acute	R5	DQ411853	**72.3 ± 8.12**	0.60	1 667
CAP239.2.00.F5	C	Adult	Acute	R5	EF203984	**72.0 ± 8.35**	0.19	5 263
CAP255.2.00.16	C	Adult	Acute	R5	EF203982	**70.0 ± 0.89**	0.28	3 571
Du422.1	C	Adult	Acute	R5	DQ411854	**69.8 ± 4.96**	0.33	3 030
CAP08.2.00.F6J	C	Adult	Acute	R5	EF203976	**69.7 ± 1.37**	0.95	1 053
CAP206.2.00.8J	C	Adult	Acute	R5	EF203967	**68.2 ± 11.06**	0.66	1 515
CAP248.2.00	C	Adult	Acute	R5	FJ229824	**68.0 ± 3.30**	0.62	1 613
RP6.6	C	Paediatric	Chronic	R5	DQ447269	**67.5 ± 2.78**	0.44	2 273
CAP244.2.00.D3	C	Adult	Acute	R5	DQ435684	**67.0 ± 1.15**	0.44	2 273
RP4.3	C	Paediatric	Chronic	R5	DQ447270	**66.3 ± 6.71**	0.48	2 083
TM7.9	C	Paediatric	Chronic	R5	DQ447267	**63.8 ± 1.58**	0.16	6 250
ZM53M.PB12	C	Adult	Acute	R5	AY423984	**62.0 ± 4.65**	0.75	1 333
COT9.6	C	Paediatric	Chronic	R5	DQ447272	46.3 ± 2.25	NT	ND
CAP84.2.00.32J	C	Adult	Acute	R5	EF203963	46.0 ± 3.78	NT	ND
ZM109F.PB4	C	Adult	Acute	R5	AY424138	39.7 ± 9.48	NT	ND
Du151.2	C	Adult	Acute	R5	DQ411851	33.0 ± 10.50	NT	ND
Du123.6	C	Adult	Acute	R5	DQ411850	32.3 ± 13.69	NT	ND
COT6.15	C	Paediatric	Chronic	R5	DQ447266	30.0 ± 8.08	NT	ND

[a]Average percentage inhibition of the respective Env-pseudotyped viruses by UCLA1 used at a concentration of 50 nM. Viruses that exhibited more than 50% inhibition (bold) were considered sensitive to neutralization. The percentage inhibition average ± SD is for triplicate data.
[b]IC_{50} is the concentration of UCLA1 that inhibited entry of the respective viruses by 50%. Viruses that were not titred (NT) and exhibited less than 50% inhibition were considered not neutralized.
[c]TI values were obtained by the general formula CC_{50}/IC_{50}. TIs could not be determined (ND) for viruses that were not titred.

3.2 UCLA1 is not cytotoxic and has a wide therapeutic index

The cytotoxicity of UCLA1 in TZM-bl cells was first examined with the ATP-based CellTiter-Glo® Luminescent Cell Viability Assay. The cells remained 90-100% viable after 24 hours incubation with UCLA1 (Figure 3-2). The aptamer was further tested for cytotoxicity in TZM-bl cells with the MTS-based CellTiter 96 Aqueous Cell Proliferation Assay. The cells had an average viability of 95% ± 0.11, after 72 hours incubation (Figure 3-2). The positive control cells with Etoposide phosphate exhibited 3% ± 1% viability. Both assays were performed using a maximum concentration of 500 nM of UCLA1.

The estimated therapeutic index (TI) of the aptamer was calculated using the general formula, TI = CC_{50}/IC_{50}, for all the tested viruses. Since 90-100% of the cells remained viable after incubation with a maximum concentration of 500 nM of UCLA1, we estimated the CC_{50} to be more than twice the maximum concentration of the aptamer (1000 nM) that resulted in 90-100% cell viability. Thus the TI was calculated at a standard CC_{50} of 1000 nM. The average estimated TI of the UCLA aptamer was therefore 5,096 ± 2,285 for the 83% neutralized subtype C Env-pseudotype viruses (Table 3-1).

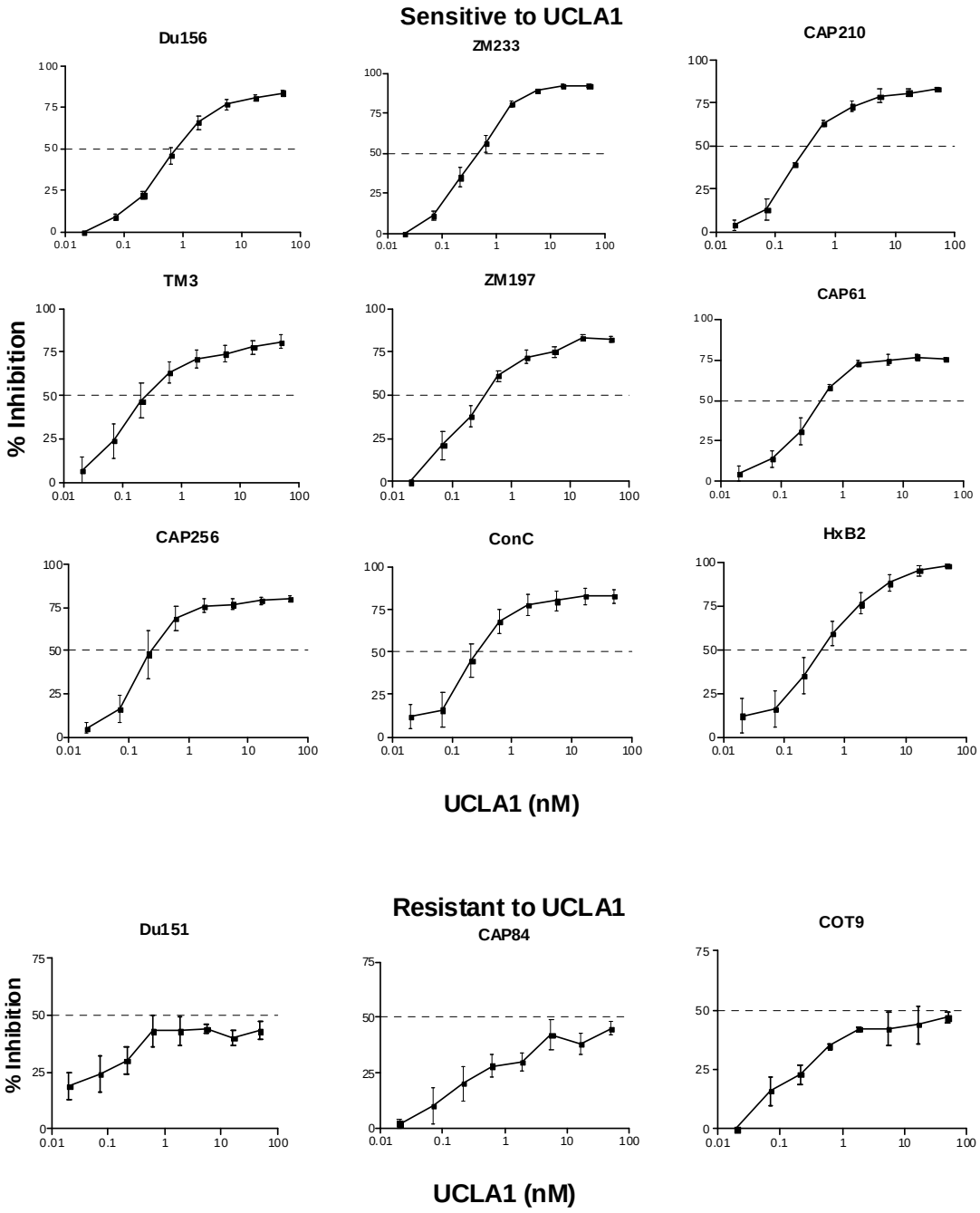

Figure 3-1: Representative dose-dependent neutralization graphs of Env-pseudotyped viruses with UCLA1.

Infection of HIV-1 subtype C viruses and a subtype B HxB2 reference strain was inhibited with UCLA1 in TZM-bl cells. The aptamer was used at a starting concentration of 50 nM. The IC_{50} of UCLA1 is indicated with the dotted line. Nine viruses sensitive to UCLA1 neutralization are shown in the top panel and three resistant viruses are depicted in the lower panel.

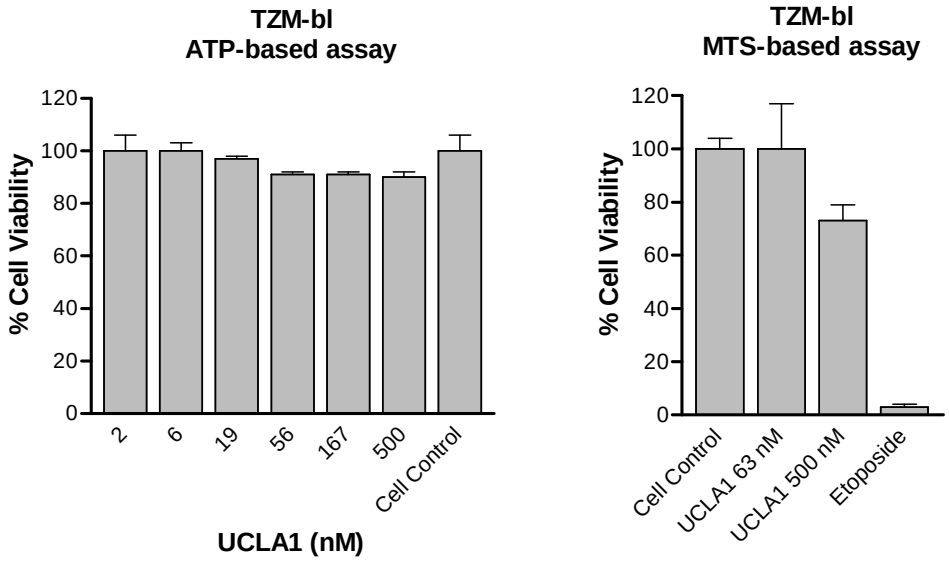

Figure 3-2: Percentage viability of TZM-bl cells in the presence of varying concentrations of UCLA1.
Two different assays were used to assess the cytotoxicity of the aptamer, the ATP-based assay and the MTS-based assay. Etoposide phosphate was used in the positive control cultures of the MTS-based assay. Untreated cell cultures were used as negative controls. The assays were done three times in triplicate.

3.3 Mapping UCLA1 neutralization sites using the ConC Env-pseudovirus

The amino acid residues involved in sensitivity to neutralization were determined using a panel of 19 single site-directed point mutations made in the ConC Env-pseudotyped virus (Table 3-2). Six of these (K121A, I307A, R419A, K421A, I423A and A440E) were selected based on published data that implicated these sites in aptamer binding (Cohen et al., 2008, Joubert et al., 2010). Two additional residues (R298 and P299) could not be tested due to low virus yields. Five mutations (S365I, S375M, V430A, F468V and G471E) were included based on sequence alignment of the tested Env-pseudoviruses that were neutralized by the aptamer compared to those that were not neutralized. The remaining 8 mutations (L125A, K305A, R308A,

H330Y, N332A, L369P, D474A and R476A) were selected from available constructs since they were within the CD4bs and CoRbs of gp120. Of the 19 single point mutants, 8 conferred resistance to the aptamer in a single-cycle neutralization assay, with all exhibiting IC_{50} values of ≥ 10 nM and a range of 10-30 fold effect compared to wild-type virus (Figure 3-3A and Table 3-2). The L369P mutation exhibited the strongest resistance to the aptamer with a 30-fold increase in the IC_{50} value compared with the IC_{50} of the wild-type ConC virus. Similar high resistance was observed with L125A, K305A and R419A with IC_{50} values that were 24-, 25- and 20-fold increased compared with wild-type IC_{50}. A schematic representation of the location of these residues on gp120 is shown (Figure 3-3B) with reference to JRF-L gp120 structure 2B4C (Huang et al., 2005) using PyMol (2008, DeLano Scientific LLC). Overall, the mutations were found within the CoRbs, at the base of the V3 loop (K305A, I307A, R308A, and H330Y), in the bridging sheet within the conserved V1/V2 stem-loop of gp120 (K121A and L125A) and within the C4 region (R419A). An overlap with one amino acid in the CD4-induced epitope within the C3 region (L369P) was also observed.

3.3.1 Mapping aptamer binding sites using ConC gp120 proteins

To further explore the dependence of UCLA1 on regions of gp120, we examined the binding kinetics to core gp120 (lacking V1/V2 and V3) as well as ΔV1/V2 gp120 and ΔV3 gp120. In addition, gp120 proteins containing a single mutation in the CD4bs (D368R) or the CoRbs (I420R) were also tested. The average K_D of the aptamer with the core gp120 was 0.7 ± 0.9 nM which was 5-fold higher than the K_D of wild-type ConC gp120 (Figure 3-4A and B). These data confirmed the role of variable loops in aptamer binding. Contributions from both V1/V2 and V3 were indeed evident based

on the average K_D values for ΔV1/V2 (0.4 ± 0.1 nM) and ΔV3 (0.5 ± 0.1 nM) gp120s. Similar levels were obtained for the I420R and D368R gp120s, sites which could not be tested by neutralization as these viruses were non-infectious, but nevertheless confirmed the CoRbs and the CD4bs as modulating sites for aptamer binding. While these binding data generally support the neutralization data, it is important to note that assessing epitopes on monomeric gp120 is inherently different to those found on the trimeric complex on the viral membrane, as observed in this study and others (Pantophlet et al., 2003). This was evident with Du151 whose pseudotyped virus was not sensitive to UCLA1 (Table 3-1 and Figure 3-1), despite its gp120 with a K_D value of 5.8 ± 2.2 nM and a Chi^2 value of 3.1 ± 1.2 (Figure 3-4C).

3.3.2 Sequence analysis of neutralization resistant viruses

The amino acid sequences of the Env-pseudotype viruses that were not neutralized by UCLA1 were aligned with ConC gp120 and examined for residues shown to confer resistance (Figure 3-5). The ZM109 virus that was not neutralized in the TZM-bl assay contained a Tyrosine at residue 330 (H330Y) which was one of the point mutations that conferred neutralization resistance to UCLA1 (Figure 3-5). COT6, COT9 and Du151 viruses contained K305R/Q, and Du151 also had R419K. Overall, 4 of the 6 viruses that were resistant in the TZM-bl assay had substitutions at residues that were identified as resistance mutations by ConC epitope mapping. Although K305R/Q, H330Y and R419K had effects on UCLA1 binding to these resistant viruses, other viruses that contained the same mutations were sensitive to UCLA1 suggesting a strain-dependent effect (Figure 3-5). Reasons for the resistance of the other 2 viruses (CAP84 and Du123) could not be deduced from the amino acid alignment.

Table 3-2: Effect of single point mutations on the neutralization of the ConC virus by UCLA1.

Gp120 Region	Binding Site	ConC gp120 mutations[a]	Mutants IC_{50} (nM)[b]	Mutant fold effect to wt[c]
C1	CoR	K121A	**28**	**17x**
	CD4	L125A	**40**	**24x**
V3		K305A	**41**	**25x**
		I307A	**36**	**22x**
		R308A	**35**	**21x**
	CoR	H330Y	**17**	**10x**
		N332A	0.11	0.06x
C3	CD4	S365I	6	4x
	CD4	L369P	**50**	**30x**
		S375M	4	2x
C4	CoR	R419A	**34**	**20x**
	CoR	K421A	1	0.6x
	CoR	I423A	0.43	0.3x
	CD4	V430A	1	0.6x
	CoR	A440E	3	1.8x
C5		F468V	9	5.4x
	CD4	G471E	2	1.2x
	CD4	D474A	0.46	0.3x
	CD4	R476A	1	0.6x

[a]Amino acids were labelled based on HxB2 numbering. The residues are defined according to the designation by Kwong (1998), Zhou (2007) and colleagues.
[b]Mutant IC_{50} - concentration of UCLA1 that inhibited 50% of infection of the respective mutant
[c]Fold decrease in neutralization sensitivity to the aptamer calculated as mutant IC_{50}/wild-type IC_{50}. Wild-type (wt) IC_{50} was calculated at an average of 1.67 nM.
Values representing a significant neutralization resistance were shown in bold. Values represent the average of at least three independent experiments.

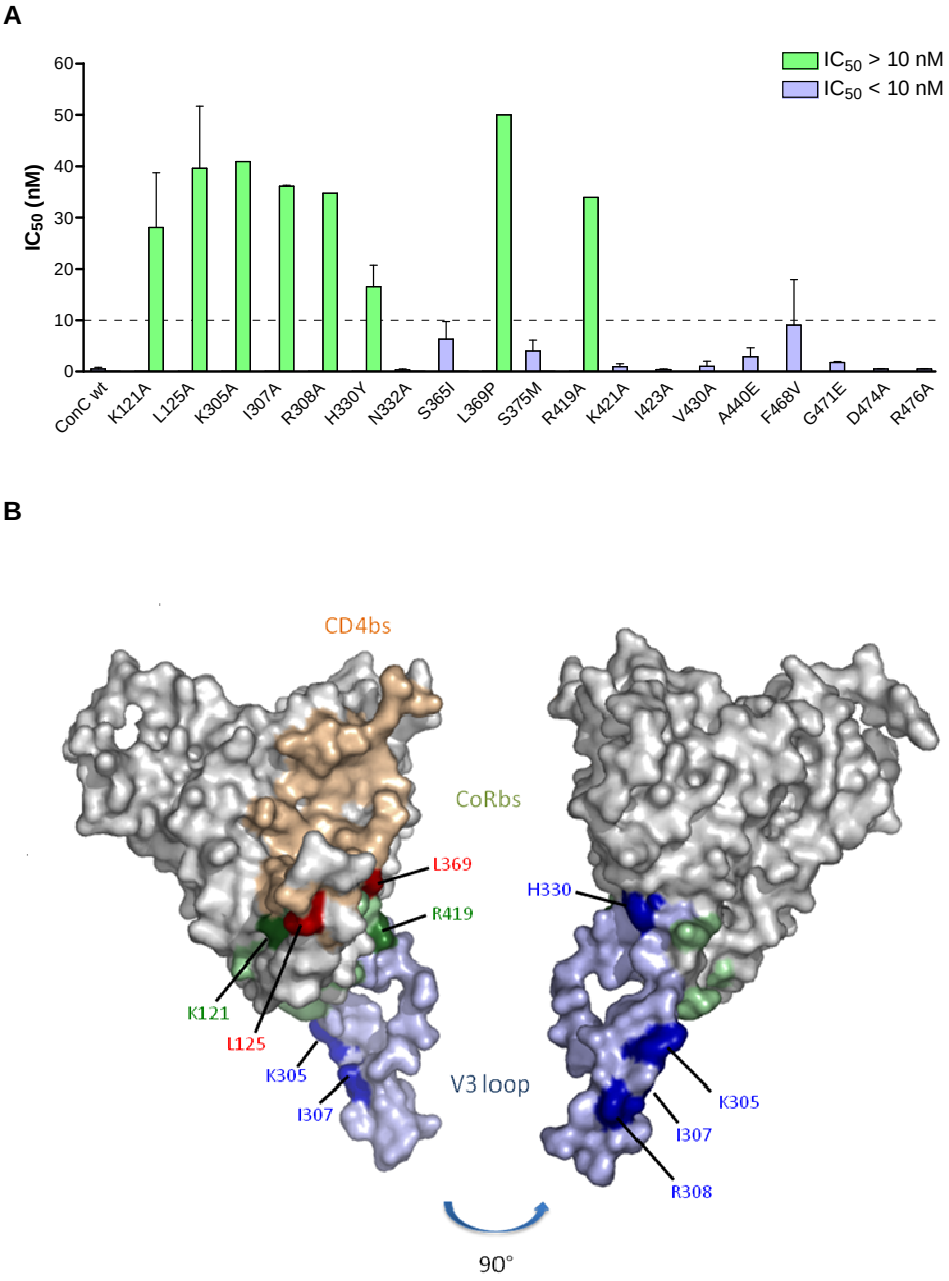

Figure 3-3: Neutralization of ConC gp120 single-point mutants with UCLA1.
(A) Graph depicts the IC_{50} values of the mutants, that is, the concentration of UCLA1 that inhibited entry of the respective mutated viruses by 50%. The dotted line indicates an IC_{50} of 10 nM used as cut-off to determine neutralization escape mutations (≥6 fold increase from wild-type virus IC_{50}). **(B)** Structural representation of the amino acid residues involved in UCLA1 neutralization resistance. Blue depicts the V3 loop, green depicts the CoRbs and tan depicts the CD4bs. Residues causing neutralization escape are marked in dark shades of the corresponding region. The picture was rotated at 90º for a clear view of the H330 and R308 residues. Coordinates were taken from the structure of gp120JRFL core with V3 ligated with CD4 and X5 (Protein Data Bank accession no. 2B4C). The figure was generated with PyMOL (DeLano Scientific LLC, South San Francisco, CA [http://www.pymol.org]).

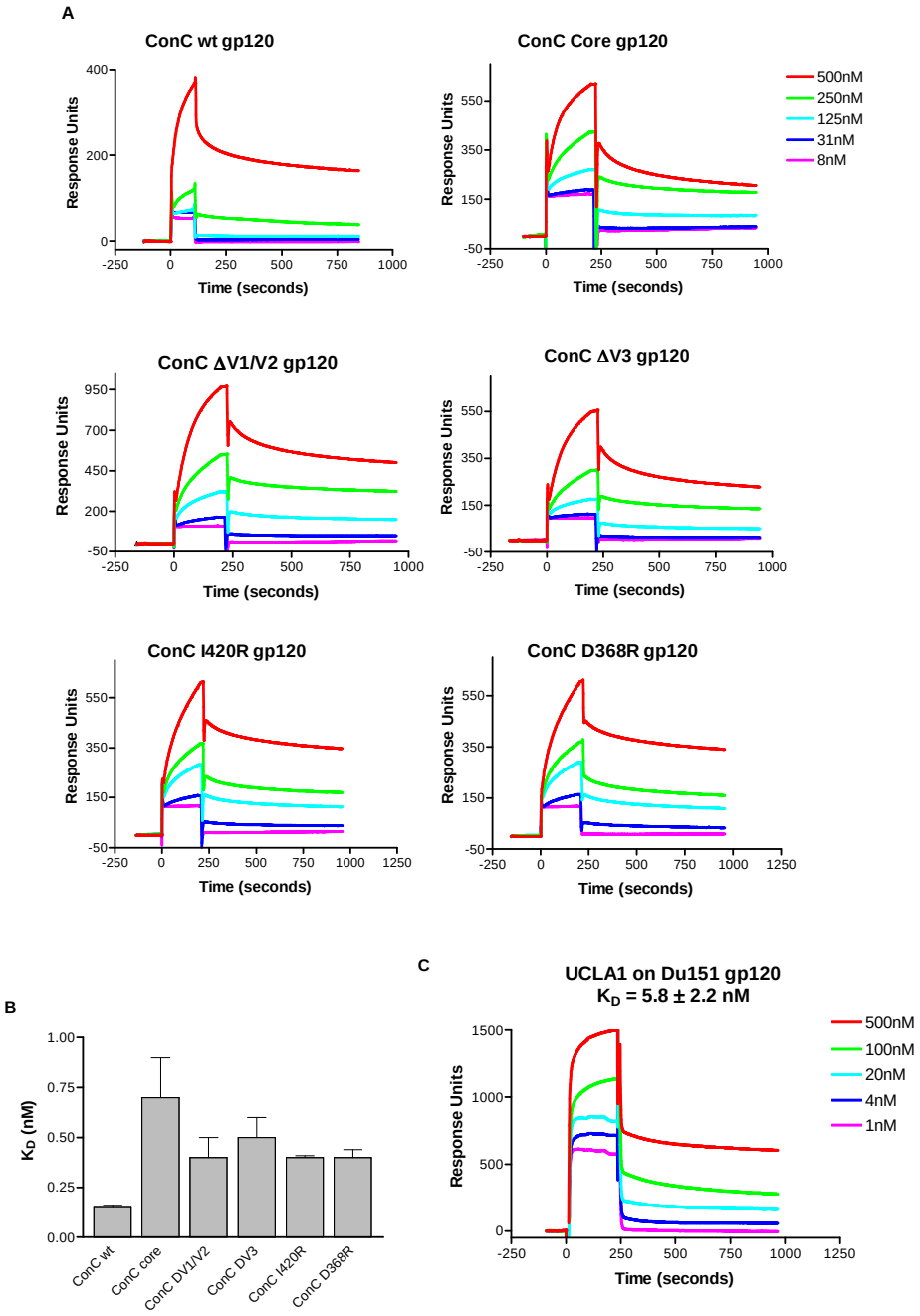

Figure 3-4: Binding kinetics of UCLA1 to truncated and mutated HIV-1 ConC gp120. **(A)** BIAcore® sensorgrams showing association and dissociation of UCLA1 from the core, ΔV1/V2 and ΔV3 truncated HIV-1 Con-C gp120, and from I420R (CoRbs) and D368R (CD4bs) mutated HIV-1 Con-C gp120. The truncated and mutated ConC glycoproteins were compared with the wild-type ConC gp120. UCLA1 was simultaneously injected over the immobilized gp120 at 2-fold dilutions (500 nM to 8 nM). **(B)** Bar chart representation of the K_D values of the truncated and mutated glycoproteins compared with the K_D of the wild-type gp120. **(C)** The binding profile of ½ log dilutions (500 nM to 1.0 nM) of UCLA1 over the immobilized HIV-1 Du151 gp120. The binding kinetics was generated in triplicate.

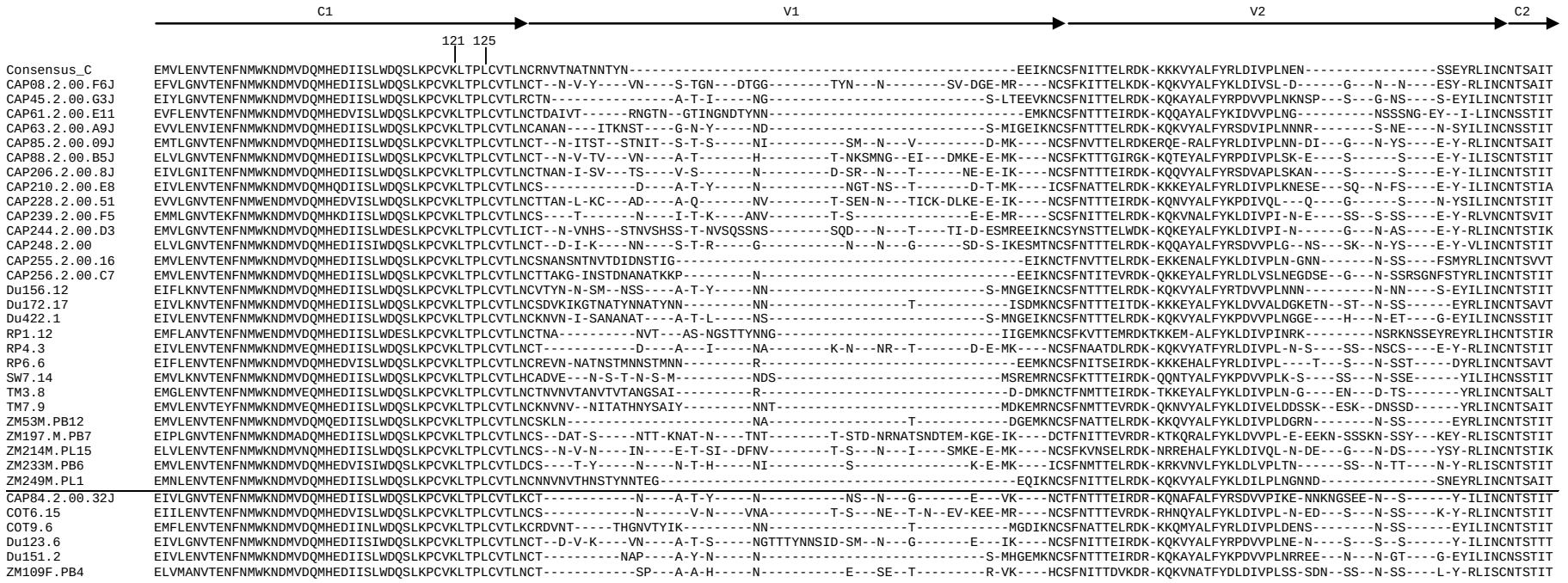
C1
V1
V2
C2
121 125
Consensus_C
CAP08.2.00.F6J
CAP45.2.00.G3J
CAP61.2.00.E11
CAP63.2.00.A9J
CAP85.2.00.09J
CAP88.2.00.B5J
CAP206.2.00.8J
CAP210.2.00.E8
CAP228.2.00.51
CAP239.2.00.F5
CAP244.2.00.D3
CAP248.2.00
CAP255.2.00.16
CAP256.2.00.C7
Du156.12
Du172.17
Du422.1
RP1.12
RP4.3
RP6.6
SW7.14
TM3.8
TM7.9
ZM53M.PB12
ZM197.M.PB7
ZM214M.PL15
ZM233M.PB6
ZM249M.PL1
CAP84.2.00.32J
COT6.15
COT9.6
Du123.6
Du151.2
ZM109F.PB4

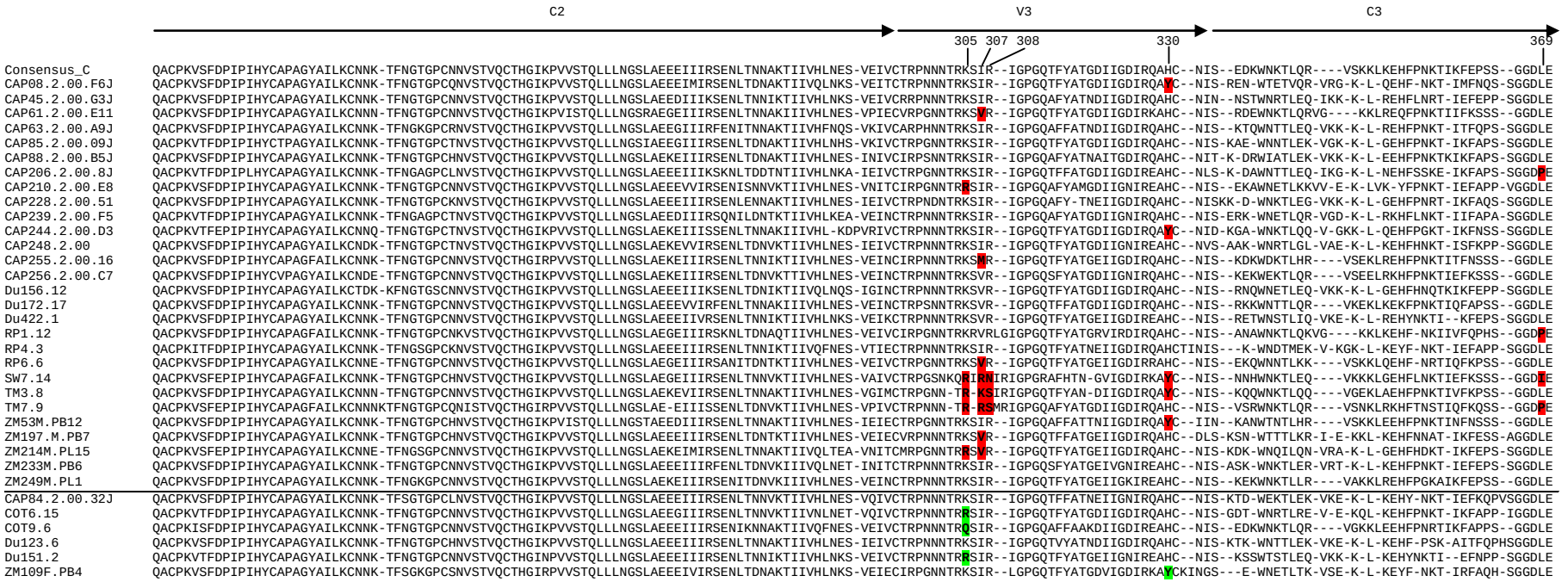
C2
V3
C3
305 307 308
330
369
Consensus_C QACPKVSFDPIPIHYCAPAGYAILKCNNK-TFNGTGPCNNVSTVQCTHGIKPVVSTQLLLNGSLAEEEIIIRSENLTNNAKTIIVHLNES-VEIVCTRPNNNTRKSIR--IGPGQTFYATGDIIGDIRQAHC--NIS--EDKWNKTLQR----VSKKLKEHFPNKTIKFEPSS--GGDLE
CAP08.2.00.F6J QACPKVSFDPIPIHYCAPAGYAILKCNNK-TFNGTGPCQNVSTVQCTHGIKPVVSTQLLLNGSLAEEEIMIRSENLTDNAKTIIVQLNKS-VEITCTRPNNNTRKSIR--IGPGQTFYATGDIIGDIRQAYC--NIS-REN-WTETVQR-VRG-K-L-QEHF-NKT-IMFNQS-SGGDLE
CAP45.2.00.G3J QACPKVSFDPIPIHYCAPAGYAILKCNNK-TFNGTGPCNNVSTVQCTHGIKPVVSTQLLLNGSLAEEDIIIKSENLTNNIKTIIVHLNKS-VEIVCRRPNNNTRKSIR--IGPGQAFYATNDIIGDIRQAHC--NIN--NSTWNRTLEQ-IKK-K-L-REHFLNRT-IEFEPP-SGGDLE
CAP61.2.00.E11 QACPKVSFDPIPIHYCAPAGYAILKCNNN-TFNGTGPCNNVSTVQCTHGIKPVISTQLLLNGSRAEGEIIIRSENLTNNAKIIIVHLNES-VPIECVRPGNNTRKSVR--IGPGQTFYATGDIIGDIRKAHC--NIS--RDEWNKTLQRVG----KKLREQFPNKTIIFKSSS--GGDLE
CAP63.2.00.A9J QACPKVSFDPIPIHYCAPAGYAILKCNNK-TFNGKGPCRNVSTVQCTHGIKPVVSTQLLLNGSLAEEGIIIRFENITNNAKTIIVHFNQS-VKIVCARPHNNTRKSIR--IGPGQAFFATNDIIGDIRQAHC--NIS--KTQWNTTLEQ-VKK-K-L-REHFPNKT-ITFQPS-SGGDLE
CAP85.2.00.09J QACPKVTFDPIPIHYCTPAGYAILKCNNK-TFNGTGPCTNVSTVQCTHGIKPVVSTQLLLNGSIAEEGIIIRSENLTDNAKTIIVHLNHS-VKIVCTRPGNNTRKSIR--IGPGQTFYATGDIIGDIRQAHC--NIS-KAE-WNNTLEK-VGK-K-L-GEHFPNKT-IKFAPS-SGGDLE
CAP88.2.00.B5J QACPKVSFDPIPIHYCAPAGYAILKCNNK-TFNGTGPCHNVSTVQCTHGIKPVVSTQLLLNGSLAEKEIIIRSENLTDNAKTIIVHLNES-INIVCIRPSNNTRKSIR--IGPGQAFYATNAITGDIRQAHC--NIT-K-DRWIATLEK-VKK-K-L-EEHFPNKTKIKFAPS-SGGDLE
CAP206.2.00.8J QACPKVTFDPIPLHYCAPAGYAILKCNNK-TFNGAGPCLNVSTVQCTHGIKPVVSTQLLLNGSLAEEEIIIKSKNLTDDTNTIIVHLNKA-IEIVCTRPGNNTRKSIR--IGPGQTFFATGDIIGDIREAHC--NLS-K-DAWNTTLEQ-IKG-K-L-NEHFSSKE-IKFAPS-SGGDPE
CAP210.2.00.E8 QACPKVSFDPIPIHYCAPAGYAILKCNNK-TFNGTGPCNNVSTVQCTHGIKPVVSTQLLLNGSLAEEEVVIRSENISNNVKTIIVHLNES-VNITCIRPGNNTRRSIR--IGPGQAFYAMGDIIGNIREAHC--NIS--EKAWNETLKKVV-E-K-LVK-YFPNKT-IEFAPP-VGGDLE
CAP228.2.00.51 QACPKVSFDPIPIHYCAPAGYAILKCNNK-TFNGTGPCKNVSTVQCTHGIKPVVSTQLLLNGSLAEEEIIIRSENLENNAKTIIVHLNES-IEIVCTRPNDNTRKSIR--IGPGQAFY-TNEIIGDIRQAHC--NISKK-D-WNKTLEG-VKK-K-L-GEHFPNRT-IKFAQS-SGGDLE
CAP239.2.00.F5 QACPKVTFDPIPIHYCAPAGYAILKCNNK-TFNGAGPCTNVSTVQCTHGIKPVVSTQLLLNGSLAEDIIIRSQNILDNTKTIIVHLKEA-VEINCTRPNNNTRKSIR--IGPGQAFYATGDIIGNIRQAHC--NIS-ERK-WNETLQR-VGD-K-L-RKHFLNKT-IIFAPA-SGGDLE
CAP244.2.00.D3 QACPKVTFEPIPIHYCAPAGYAILKCNNQ-TFNGTGPCTNVSTVQCTHGIKPVVSTQLLLNGSLAEKEIIISSENLTNNAKIIIVHL-KDPVRIVCTRPNNNTRKSIR--IGPGQTFYATGDIIGDIRQAYC--NID-KGA-WNKTLQQ-V-GKK-L-QEHFPGKT-IKFNSS-SGGDLE
CAP248.2.00 QACPKVSFDPIPIHYCAPAGYAILKCNDK-TFNGTGPCTNVSTVQCTHGIKPVVSTQLLLNGSLAEKEVVIRSENLTDNVKTIIVHLNES-IEIVCTRPNNNTRKSIR--IGPGQTFYATGDIIGNIREAHC--NVS-AAK-WNRTLGL-VAE-K-L-KEHFHNKT-ISFKPP-SGGDLE
CAP255.2.00.16 QACPKVSFDPIPIHYCAPAGFAILKCNNK-TFNGTGPCNNVSTVQCTHGIRPVVSTQLLLNGSLAEKEIIIRSENLTNNIKTIIVHLNES-VEINCIRPNNNTRKSMR--IGPGQTFYATGEIIGDIRQAHC--NIS--KDKWDKTLHR----VSEKLREHFPNKTITFNSSS--GGDLE
CAP256.2.00.C7 QACPKVSFDPIPIHYCVPAGYAILKCNDE-TFNGTGPCNNVSTVQCTHGIKPVVSTQLLLNGSLAEKEIIIRSENLTDNVKTTIVHLNES-VEINCTRPNNNTRKSVR--IGPGQSFYATGDIIGNIRQAHC--NIS--KEKWEKTLQR----VSEELRKHFPNKTIEFKSSS--GGDLE
Du156.12 QACPKVSFDPIPIHYCAPAGYAILKCTDK-KFNGTGSCNNVSTVQCTHGIKPVVSTQLLLNGSLAEEEIIIKSENLTDNIKTIIVQLNQS-IGINCTRPNNNTRKSVR--IGPGQTFYATGDIIGDIRQAHC--NIS--RNQWNETLEQ-VKK-K-L-GEHFHNQTKIKFEPP-SGGDLE
Du172.17 QACPKVSFDPIPIHYCAPAGYAILKCNNK-TFNGTGPCNNVSTVQCTHGIKPVVSTQLLLNGSLAEEEVVIRFENLTNNAKIIIVHLNES-VEINCTRPSNNTRKSVR--IGPGQTFFATGDIIGDIRQAHC--NIS--RKKWNTTLQR----VKEKLKEKFPNKTIQFAPSS--GGDLE
Du422.1 QACPKVSFDPIPIHYCAPAGYAILKCNNK-TFNGTGPCNNVSTVQCTHGIKPVVSTQLLLNGSLAEEEIIVRSENLTNNIKTIIVHLNKS-VEIKCTRPNNNTRKSVR--IGPGQTFYATGEIIGDIREAHC--NIS--RETWNSTLIQ-VKE-K-L-REHYNKTI--KFEPS-SGGDLE
RP1.12 QACPKVSFDPIPIHYCAPAGFAILKCNNK-TFNGTGPCNKVSTVQCTHGIKPVVSTQLLLNGSLAEGEIIIRSKNLTDNAQTIIVHLNES-VEIVCIRPGNNTRKRVRLGIGPGQTFYATGRVIRDIRQAHC--NIS--ANAWNKTLQKVG----KKLKEHF-NKIIVFQPHS--GGDPE
RP4.3 QACPKITFDPIPIHYCAPAGYAILKCNNK-TFNGSGPCKNVSTVQCTHGIKPVVSTQLLLNGSLAEEEIIIRSENLTNNIKTIIVQFNES-VTIECTRPNNNTRKSIR--IGPGQTFYATNEIIGDIRQAHCTINIS---K-WNDTMEK-V-KGK-L-KEYF-NKT-IEFAPP-SGGDLE
RP6.6 QACPKVSFDPIPIHYCAPAGYAILKCNNE-TFNGTGPCNNVSTVQCTHGIKPVVSTQLLLNGSLAEGEIIIRSANITDNTKTIIVHLNES-VEIVCTRPGNNTRKSVR--IGPGQTFYATGEIIGDIRRAHC--NIS--EKQWNNTLKK----VSKKLQEHF-NRTIQFKPSS--GGDLE
SW7.14 QACPKVSFEPIPIHYCAPAGFAILKCNNK-TFNGTGPCHNVSTVQCTHGIKPVVSTQLLLNGSLAEGEIIIRSENLTNNVKTIIVHLNES-VAIVCTRPGSNKQRIRNIRIGPGRAFHTN-GVIGDIRKAYC--NIS--NNHWNKTLEQ----VKKKLGEHFLNKTIEFKSSS--GGDIE
TM3.8 QACPKVSFDPIPIHYCAPAGYAILKCNNN-TFNGTGPCNNVSTVQCTHGIKPVVSTQLLLNGSLAEKEVIIRSENLTNNAKTIIVHLNES-VGIMCTRPGNN-TR-KSIRIGPGQTFYAN-DIIGDIRQAYC--NIS--KQQWNKTLQQ----VGEKLAEHFPNKTIVFKPSS--GGDLE
TM7.9 QACPKVSFEPIPIHYCAPAGFAILKCNNNKTFNGTGPCQNISTVQCTHGIRPVVSTQLLLNGSLAE-EIIISSENLTDNVKTIIVHLNES-VPIVCTRPNNN-TR-RSMRIGPGQAFYATGDIIGDIRQAHC--NIS--VSRWNKTLQR----VSNKLRKHFTNSTIQFKQSS--GGDPE
ZM53M.PB12 QACPKVSFDPIPIHYCAPAGYAILKCNNK-TFNGTGPCHNVSTVQCTHGIKPVISTQLLLNGSTAEEDIIIRSENLTNNAKTIIVHLNES-IEIECTRPGNNTRKSIR--IGPGQAFFATTNIIGDIRQAYC--IIN--KANWTNTLHR----VSKKLEEHFPNKTINFNSSS--GGDLE
ZM197.M.PB7 QACPKVSFDPIPIHYCAPAGYAILKCNNK-TFNGTGPCHNVSTVQCTHGIKPVVSTQLLLNGSLAEEEIIIRSENLTDNTKTIIVHLNES-VEIECVRPNNNTRKSVR--IGPGQTFFATGEIIGDIRQAHC--DLS-KSN-WTTTLKR-I-E-KKL-KEHFNNAT-IKFESS-AGGDLE
ZM214M.PL15 QACPKVSFEPIPIHYCAPAGYAILKCNNE-TFNGSGPCNNVSTVQCTHGIKPVVSTQLLLNGSLAEKEIMIRSENLTNNAKTIIVQLTEA-VNITCMRPGNNTRRSVR--IGPGQTFYATGEIIGDIRQAHC--NIS-KDK-WNQILQN-VRA-K-L-GEHFHDKT-IKFEPS-SGGDLE
ZM233M.PB6 QACPKVSFDPIPIHYCAPAGYAILKCNNK-TFNGTGPCNNVSTVQCTHGIKPVVSTQLLLNGSLAEEEIIIRFENLTDNVKIIIVQLNET-INITCTRPNNNTRKSIR--IGPGQSFYATGEIVGNIREAHC--NIS-ASK-WNKTLER-VRT-K-L-KEHFPNKT-IEFEPS-SGGDLE
ZM249M.PL1 QACPKVSFDPIPIHYCAPAGYAILKCNNK-TFNGKGPCNNVSTVQCTHGIKPVVSTQLLLNGSLAEKEIIIRSENITDNVKIIIVHLNES-VEINCTRPNNNTRKSIR--IGPGQTFYATGEIIGKIREAHC--NIS--KEKWNKTLLR----VAKKLREHFPGKAIKFEPSS--GGDLE
CAP84.2.00.32J QACPKVSFDPIPIHYCAPAGYAILKCNNK-TFSGTGPCLNVSTVQCTHGIKPVVSTQLLLNGSLAEEEIIIRSENLTNNVKTIIVHLNES-VQIVCTRPNNNTRKSIR--IGPGQTFFATNEIIGNIRQAHC--NIS-KTD-WEKTLEK-VKE-K-L-KEHY-NKT-IEFKQPVSGGDLE
COT6.15 QACPKVTFDPIPIHYCAPAGYAILKCNNK-TFNGTGPCNNVSTVQCTHGIKPVVSTQLLLNGSLAEEGIIIRSENLTNNVKTIIVNLNET-VQIVCTRPNNNTRRSIR--IGPGQTFYATGDIIGDIRQAHC--NIS-GDT-WNRTLRE-V-E-KQL-KEHFPNKT-IKFAPP-IGGDLE
COT9.6 QACPKISFDPIPIHYCAPAGYAILKCNNK-TFNGTGPCNNVSTVQCTHGIKPVVSTQLLLNGSLAEEEIIIRSENIKNNAKTIIVQFNES-VEIVCTRPNNNTRQSIR--IGPGQAFFAAKDIIGDIREAHC--NIS--EDKWNKTLQR----VGKKLEEHFPNRTIKFAPPS--GGDLE
Du123.6 QACPKVSFDPIPIHYCAPAGYAILKCNNK-TFNGTGPCHNVSTVQCTHGIKPVVSTQLLLNGSLAEEEIIIRSENLTNNAKTIIVHLNES-IEIVCTRPNNNTRKSIR--IGPGQTVYATNDIIGDIRQAHC--NIS-KTK-WNTTLEK-VKE-K-L-KEHF-PSK-AITFQPHSGGDLE
Du151.2 QACPKVTFDPIPIHYCAPAGYAILKCNNK-TFNGTGPCNNVSTVQCTHGINPVVSTQLLLNGSLAEEEIIIRSENLTNNIKTIIVHLNKS-VEIVCTRPNNNTRRSIR--IGPGQTFYATGEIIGNIREAHC--NIS--KSSWTSTLEQ-VKK-K-L-KEHYNKTI--EFNPP-SGGDLE
ZM109F.PB4 QACPKVSFDPIPIHYCAPAGYAILKCNNK-TFSGKGPCSNVSTVQCTHGIRPVVSTQLLLNGSLAEEEIVIRSENLTDNAKTIIVHLNKS-VEIECIRPGNNTRKSIR--LGPGQTFYATGDVIGDIRKAYCKINGS---E-WNETLTK-VSE-K-L-KEYF-NKT-IRFAQH-SGGDLE

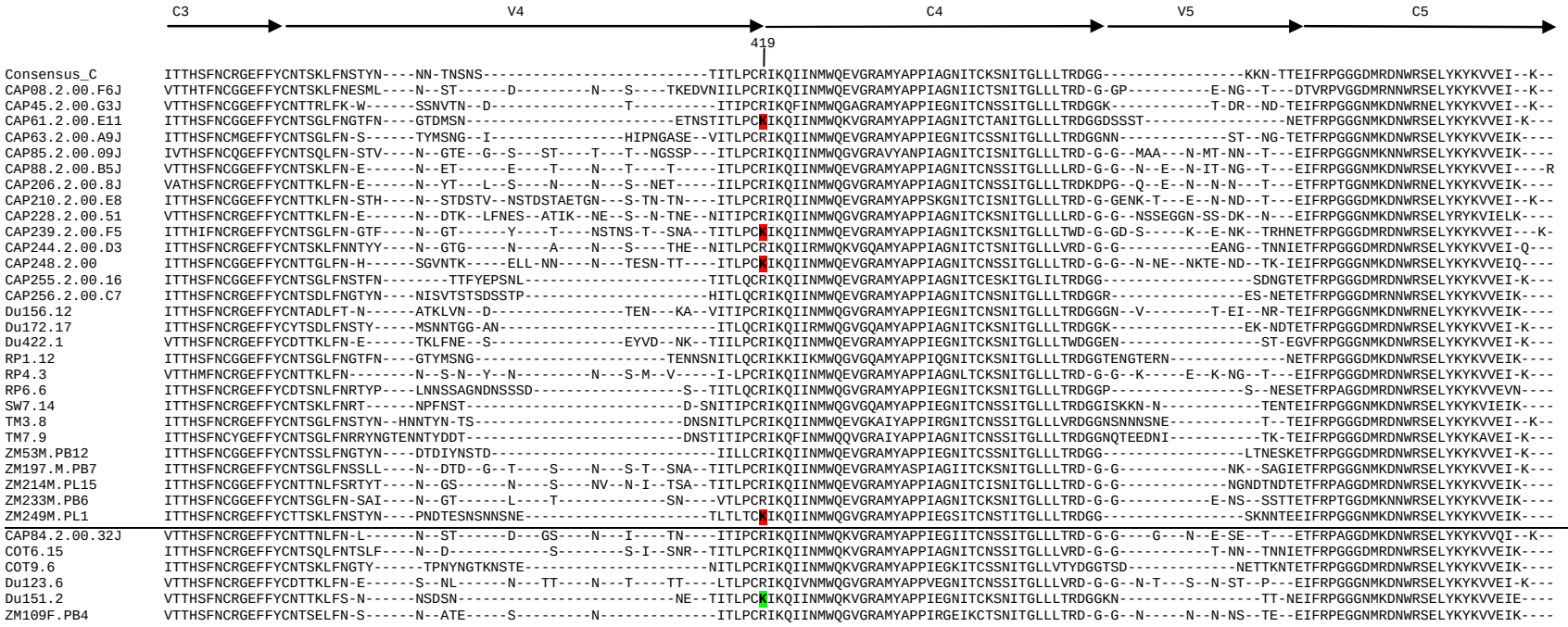

Figure 3-5: Amino acid sequence alignment of HIV-1 gp120 of Env-pseudotyped viruses that were tested for neutralization with UCLA1.

The resistant viruses, listed below the horizontal line in the alignment, were compared with viruses that were sensitive to UCLA1 including the ConC virus that was used for mapping of UCLA1 binding sites. The amino acid residues that were shown to modulate binding of UCLA1 are numbered and their respective regions exhibited within the *env* genome. The numbering is according to the HxB2 sequence. The residues highlighted in red are different from those that were shown to modulate UCLA1 binding however the viruses remained sensitive. Resistant viruses that naturally possess the introduced mutations are highlighted in green.

3.4 Synergy of UCLA1 with other entry inhibitors

Both T20 and b12 have been previously shown to act synergistically with other HIV-1 entry inhibitors (Alexandre et al., 2011, Nagashima et al., 2001, Tremblay et al., 2000, Zwick et al., 2005). Thus, we next evaluated any possible synergistic effects of UCLA1 with T20 and b12, respectively. Synergism was examined using the single cycle neutralization assay with Env-pseudotyped viruses. The aptamer showed synergism with T20 for 5 of 6 (83%) viruses tested (Figure 3-6) with CI values ranging from 0.13 - 0.46 (Table 3-3). Slight synergism was observed for ZM249 with UCLA1+T20 combination with a CI value of 0.84. There was also synergism between the aptamer and b12 MAb for 4 of 6 (67%) viruses tested (Figure 3-6), with CI values ranging from 0.5 - 0.7 (Table 3-3). The combination of UCLA1 and b12 resulted in an additive effect (CI = 0.93) for the neutralization of Du156. Although b12 neutralization of ZM53 was relatively moderate (IC_{50} value = 46.14 nM), the antibody combination with UCLA1 resulted in 2-fold decrease of the $IC_{50,}$ from 6.22 nM (UCLA1) to 2.8 nM (UCLA1+b12) (Table 3-3). There was no synergism between UCLA1 and b12 for the neutralization of SW7. This is probably due to the fact that this virus is resistant to b12 as shown previously for other subtype C viruses (Dr E Gray, unpublished data). The dose reduction indices for T20, b12 and UCLA1 were determined to be in the range of 3.7 – 27.0, 1.5 – 16.4 and 1.8 – 11.2, respectively, clearly indicating that lower concentrations of these compounds were required to neutralize the viruses. The data revealed that less T20, b12 and UCLA1 were required to inhibit the tested viruses, when used in combination. Thus, on average, 11-fold less T20, 5-fold less b12 and 5-fold less UCLA1 were required to neutralize virus infection when in combination.

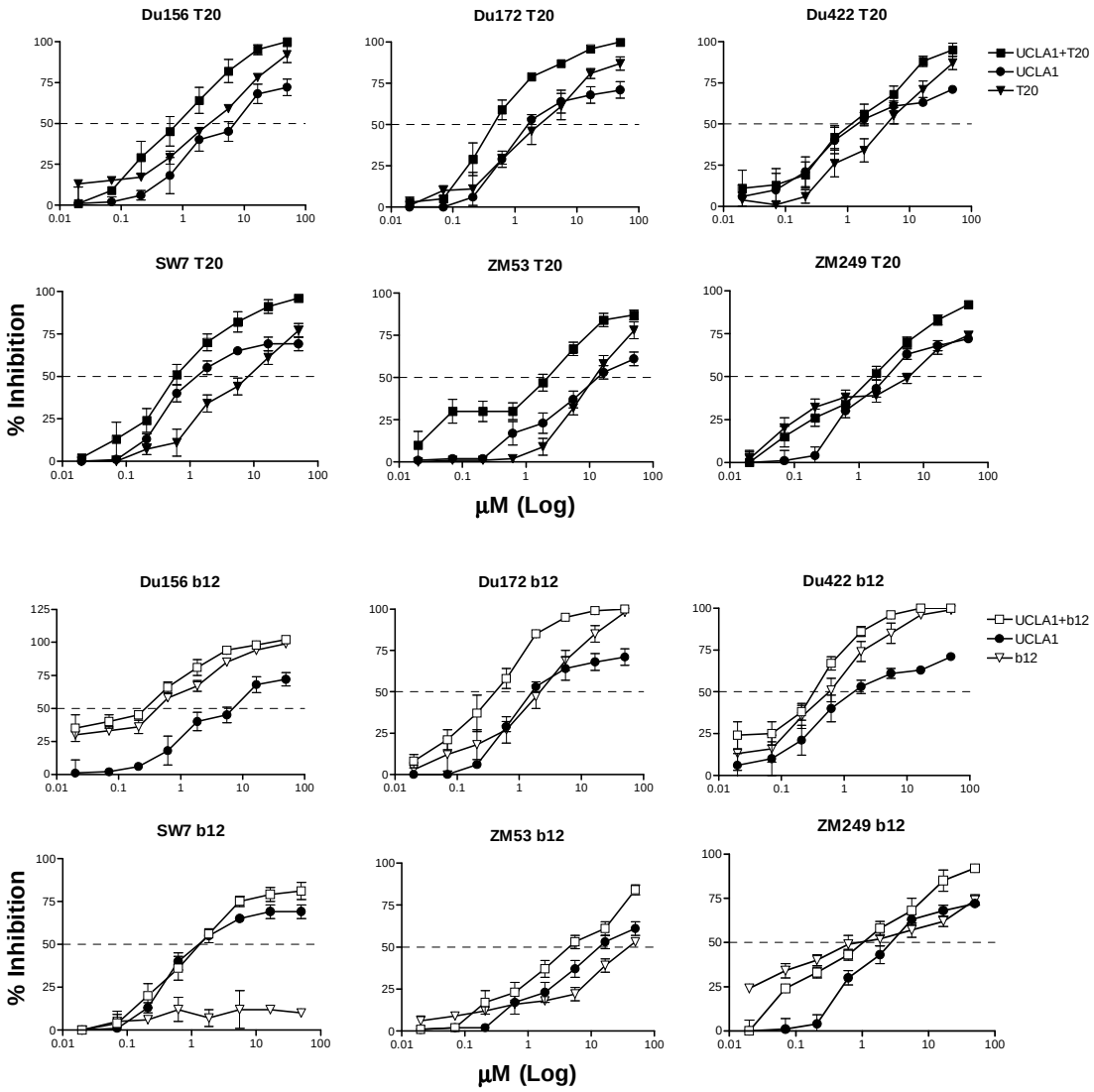

Figure 3-6: Representative dose-dependent neutralization graphs of HIV-1 subtype C Env-pseudotyped viruses showing synergism of UCLA1 with T20 and b12.
The aptamer was used at a maximum starting concentration of 50 nM when used alone and in combination. b12 and T20 were used at a maximum initial concentration of 50 µg/ml each and in combination with UCLA1. The 50 µg/ml concentration used for b12 and T20 is equivalent to 312 µM and 11.13 mM respectively.

Table 3-3: Combination therapy using UCLA1, T20 and b12 against subtype C Env pseudotype viruses.

		UCLA1			T20		
	Combination Index[a]	UCLA1 (nM)[b]	UCLA1+T20 (μM)	Dose reduction index[c]	T20 (μg/ml)[d]	UCLA1+T20 (μM)	Dose reduction index[c]
Du156.12	**0.37**	1.20	0.31	3.9	2.87	0.31	9.3
Du172.17	**0.43**	1.83	0.34	5.4	1.39	0.34	4.1
Du422.1	**0.13**	3.69	0.33	11.2	8.90	0.33	27.0
SW7.14	**0.43**	0.74	0.27	2.7	3.98	0.27	14.7
ZM53M.PB12	**0.46**	6.22	1.73	3.6	9.72	1.73	5.6
ZM249M.PL1	0.84	2.80	1.60	1.8	5.85	1.60	3.7

		UCLA1			b12		
	Combination Index[a]	UCLA1 (nM)[b]	UCLA1+b12 (μM)	Dose reduction index[c]	b12 (μg/ml)[d]	UCLA1+b12 (μM)	Dose reduction index[c]
Du156.12	0.93	1.20	0.30	4.0	0.44	0.30	1.5
Du172.17	**0.56**	1.83	0.22	8.3	0.50	0.22	2.3
Du422.1	**0.65**	3.69	0.53	7.0	1.04	0.53	2.0
SW7.14	1.62	0.74	1.19	0.6	50.00	1.19	42.0
ZM53M.PB12	**0.5**	6.22	2.82	2.2	46.14	2.82	16.4
ZM249M.PL1	**0.7**	2.80	0.87	3.2	2.26	0.87	2.6

[a]Combination Index (CI) was calculated using the Chou and Talalay equation (7). CI values of 0.3 to 0.7, 0.7 to 0.85, 0.85 to 0.9, 0.9 to 1.1 and >1.1 represent synergism, moderate synergism, slight synergism, additive effect and antagonism, respectively. CI values representing synergism are in bold.
[b]UCLA1 was used at an initial concentration of 50 nM alone and in combination with T20 and with b12
[c]Dose reduction index is calculated as the ratio of drug concentration required for inhibition when the drug is used alone or in combination
[d]T20 and b12 were used at an initial concentration of 50 μg/ml (equivalent to 312 μM and 11.13 mM, respectively) alone and in combination with UCLA1.

4. Discussion

UCLA1 RNA aptamer was used to inhibit entry of HIV-1 subtype C Env-pseudotyped viruses into TZM-bl cells. Its potential efficacy was suggested by its broad spectrum potency against the globally diverse subtype C viruses. The lack of toxicity in TZM-bl cells confirmed that its action was due to its efficacy and not cell toxicity. Mapping of UCLA1 binding to HIV-1 subtype C gp120 revealed more contact sites than observed with the subtype B glycoprotein (Cohen et al., 2008).

UCLA1 neutralized a large panel of Env-pseudotyped viruses isolated from both acute and chronically infected adult and paediatric patients, suggesting broad spectrum potency against subtype C viruses. There was no neutralization preference noted between viruses isolated from acute and chronic infections or between isolates from adult and paediatric patients. The data also suggest that the efficacy of UCLA1 is not strain or tropism restricted since it was able to neutralize R5 and X4 viruses. This neutralization data concur with other studies that have utilized parental, first generation derivatives or exactly the same aptamer for inhibition of HIV-1 subtype B R5 tropic viruses (Cohen et al., 2008, Dey et al., 2005b, Khati et al., 2003, Moore et al., 2011).

Mutagenesis was performed to define in more detail the residues on gp120 influencing UCLA1 anti-HIV activity. Eight mutated residues were found to confer UCLA1 neutralization resistance. Six of these were involved in CCR5 binding and were localized at the base of the V3 loop (K305A, I307A, R308A, H330Y), the bridging sheet within the conserved V1/V2 stem-loop that makes up the CD4-

induced epitope (K121A) and the C4 domain (R419A) (Kwong et al., 1998, Pantophlet et al., 2003, Rizzuto et al., 1998, Zhou et al., 2007). Two residues in the CD4bs, K125A residue within the bridging sheet region and the L369P residue lying in the C3 region adjacent to the Phe43 cavity were also implicated (Kwong et al., 1998, Pantophlet et al., 2003, Rizzuto & Sodroski, 2000). Residues, K121, H330, L369 and R419 have been previously shown to modulate binding of other HIV-1 inhibitors within the conserved core residues (Cormier et al., 2001, Pantophlet et al., 2003, Rizzuto & Sodroski, 2000, Rizzuto et al., 1998) including aptamers 299.5 (Cohen et al., 2008) and B40t77 (Joubert et al., 2010). Overall, 4 of the 8 residues were located within the V3 loop and 2 within the V1/V2 bridging sheet confirming the SPR data using V-loop deleted gp120 proteins, also shown by others (Cohen et al., 2008, Dey et al., 2005b, Joubert et al., 2010, Khati et al., 2003). Differences in the K_D values between wild-type and V-loop deleted proteins were more subtle than the effect of single point mutations in gp120 on neutralization. The effect of I420R and D368R in reducing binding is likely due to their close proximity to identified residues rather than a direct effect; although this could not be tested. Interestingly, two residues that were tested against both HIV-1 subtype B and C were shown to act differently for the different viruses. That is, K421 and I423 residues were identified as aptamer binding sites for a subtype B virus but not for subtype C. Although K421 is conserved in all primate immunodeficiency viruses (Kwong et al., 1998), it was not observed as an aptamer binding site for subtype C viruses. The I423 residue is moderately conserved amongst HIV-1 viruses (Kwong et al., 1998) thus the binding difference in this residue can be expected between the two different subtypes. Similar effects with the K421 site have been observed with MAbs such as b6, b12

and CD4. That is, mutation of this residue did not affect binding of the MAbs to subtype B HIV-1 gp120 (Pantophlet et al., 2003) on page 92.

UCLA1 exhibited synergism with T20 fusion inhibitor and IgG1b12 MAb with dose reduction indices showing that lower T20 and b12 concentrations are required to inhibit HIV-1 when used in combination with UCLA1. The aptamer exhibited synergism with T20 fusion inhibitor likely because these compounds target different regions of the viral envelope, that is, gp120 and gp41, respectively. It has been shown that the stem and tip of the V3 loop are important in maintaining the interaction between gp120 and gp41 for viral entry (Cormier et al., 2001, Huang et al., 2007, Huang et al., 2005, Xiang et al., 2010). Thus, since the V3 loop was shown to be involved in UCLA1 binding, this is in support of the observed UCLA1 and T20 synergism. Since b12 epitope includes the L369 and R419 (Pantophlet et al., 2003), which were both shown in this study to affect UCLA1 neutralization, it was interesting to discover synergism between these two agents. This finding suggests that L369 and R419 might not be direct contact residues for UCLA1 but peripheral sites that modulate the aptamers' reactivity accounting for the lack of competition when used in combination with the b12 MAb. Alternatively these agents might be transmitting an allosteric effect to the neighbouring protomers, thus increasing binding affinity or site accessibility. The b12 MAb was previously shown to effectively neutralize most of the currently tested viruses (Li et al., 2006) however ZM53 virus required a higher concentration of b12 to be effectively neutralized while SW7 was resistant to this MAb (Dunfee et al., 2009, Gray et al., 2005). Thus, synergism between b12 and UCLA1 for ZM53 neutralization suggests that UCLA1 can increase the sensitivity of

viruses that are partially resistant to the MAb. On the other hand, the lack of synergism for SW7 implies that this increase in sensitivity cannot be achieved if the virus is completely resistant to the antibody.

Taken together, the results indicate that UCLA1 RNA aptamer has broad spectrum potency against several subtype C viruses at low nanomolar concentrations. The non-cytotoxic nature, high therapeutic index, neutralization potency and synergistic effect of the aptamer suggest that UCLA1 can be further tested against HIV-1 subtype C primary isolates to determine its efficacy in *ex vivo* conditions that mimic the natural course of infection.

CHAPTER 4

UCLA1 Inhibition of HIV-1 Subtype C Primary Isolates in PBMCs and Monocyte-Derived Macrophages and Evaluation of Escape Mutations

Chapter summary

In the previous chapter the activity of UCLA1 was tested against a large panel of HIV-1 subtype C Env-pseudotype viruses. In this chapter the efficacy of UCLA1 was evaluated against HIV-1 subtype C clinical isolates in freshly isolated peripheral mononuclear cells (PBMCs) and monocyte-derived macrophage cells (MDMs). UCLA1 neutralized primary isolates in PBMCs and MDMs with IC_{50} values in the nanomolar range similar to TZM-bl cells. The aptamer was also shown to be non-toxic to PBMCs. Two primary viruses were cultured in PBMCs with increasing concentrations of UCLA1 over 12 weeks in order to select for escape mutations. The Du422 isolate showed only a 3-fold increase in IC_{50} while the RP1 isolate revealed a 7-fold increase thus showing evidence of genetic changes of the latter isolate. These changes were located within the V3 and V4 loops, in the bridging sheet next to the V1/V2 loop, in the C2 region between β4 and β5 sheets and within the CD4 and CoR binding complexes in the α3 and α5 helices. Some of these mutations, notably the ones within the V3 loop, the bridging sheet and the α3 helix were previously shown by point mutation analysis to confer UCLA1 escape.

1. Introduction

HIV infects different target cells in addition to the $CD4^+$ T lymphocytes in PBMCs (Cameron et al., 1987, Collin et al., 1991), in particular, macrophages which are long-lived, terminally-differentiated tissue-resident cells that are phenotypically and functionally heterogeneous (Gordon & Martinez, 2010, Murray & Wynn, 2011). As innate immune sentinel phagocytes, their role involves clearance of pathogens, apoptotic cells and debris, and antigen presentation to T cells (Gordon & Martinez, 2010, Murray & Wynn, 2011). The blood monocytes and tissue macrophages remain productively infected by HIV-1, often without obvious cytopathic effects, forming long-lived virus reservoirs (Coiras et al., 2009, Khati et al., 2001) with the potential to transmit HIV-1 to activated $CD4^+$ T cells during cell-to-cell interactions (Gousset et al., 2008, Groot et al., 2008, Waki & Freed, 2010) and the eventual spread to organs such as the brain and bone marrow (Aquaro et al., 2000, Duncan & Sattentau, 2011, Gartner et al., 1986, Gendelman et al., 1985, Gendelman et al., 1989, Gras & Kaul, 2010, Levy, 2007, Meltzer et al., 1990, Phillips et al., 1998). Ongoing viral replication and dissemination has also been noted during highly active anti-retroviral therapy (HAART), especially in macrophages compared with resting T cells (Crowe & Sonza, 2000, Perelson et al., 1997, Zhu, 2000). Thus HIV harboured in macrophages may escape immune surveillance and anti-viral therapy and can therefore play a key role in regulating the intensity and progression of disease in HIV infection even during therapy. This finding has led to some suggestions that HIV-1 induced pathogenesis is a macrophage-centered immunopathology (Meyaard et al., 1993, Mosier & Sieburg, 1994). Thus, the significantly low activity of reverse transcriptase and protease inhibitors against chronically infected macrophages (Aquaro et al., 2002,

Perno et al., 1998) warrants testing of other inhibitors against HIV infection of macrophages to reduce the source of viral particles from the reservoirs (Brodie, 2000).

Aptamer-based neutralization assays have been previously reported targeting the HIV-1 gp120 extracellular protein in PBMCs and MDMs. In a recent review, these RNA aptamers were reported to have the most potent *in vitro* antiviral efficacy of all HIV-1 entry inhibitors described to date (Held et al., 2006). The aptamers were shown to bind their target protein with high affinity and high specificity, and neutralise a broad range of R5 HIV-1 clinical isolates (Khati et al., 2003). These aptamers prevented entry and suppressed viral replication in cultured PBMCs by up to 10 000-fold (Khati et al., 2003) and MDMs by up to 84% (Cohen et al., 2008).

Thus far, neutralizing antibody assays quantify a reduction in HIV-1 infection in mitogen-stimulated PBMCs by the ELISA-based p24 antigen detection. Although this system is difficult to standardize because of substantial genetic and phenotypic variations in uncloned virus stocks and wide donor–donor variability, it should be performed in parallel with the highly standardized Env-pseudotype virus neutralization assay (Li et al., 2005, Mascola et al., 2005, Montefiori, 2004, Montefiori, 2009, Montefiori & Mascola, 2009) to facilitate data correlation between the two assays (Binley et al., 2004, Brown et al., 2007, Choudhry et al., 2007, Mann et al., 2009, Polonis et al., 2008). The assay is also indispensable in order to determine the effect of any inhibitor under *ex vivo* conditions compared to *in vitro* conditions. Moreover, the use of primary target cells is still considered “gold

standard" since it emulates *in vivo* conditions (Mann et al., 2009, Polonis et al., 2008).

The human host's immune system and the antiviral drugs used in treatment regimens trigger viral evolution. Nearly 25 antiretroviral (ARV) drugs have been licensed for the treatment of HIV-1 (Shafer & Schapiro, 2008). In proportion with the increase in new ARV and ARV classes, there has been an increase in knowledge about drug resistance and the effects that different amino acid substitutions have on HIV drug susceptibility (Shafer & Schapiro, 2008). The *in vitro* generation of escape mutations is used to decipher the magnitude of their potency in addition to their neutralization efficiency particularly against primary isolates. Although anti-HIV-1 gp120 aptamers have been characterized in more detail in terms of stability (Moore et al., 2011), as targeted delivery vehicles (McNamara et al., 2006, Zhou et al., 2009) and for delivery of nanoparticles (Dhar et al., 2008), there are not a lot of studies on aptamer escape mutations. Only one recent publication that used an aptamer siRNA chimera (an anti-gp120 and anti-tat/rev siRNA chimera) to reduce viral replication and $CD4^+$ T cells in humanized mice reported point mutations in HIV *env* unique to treated animals, with more mutations in gp120. However, no dominant mutations were observed in gp120 (Neff et al., 2011).

Therefore, based on UCLA1 activity against Env-pseudotype viruses, we examined its neutralization efficacy against HIV-1 subtype C clinical isolates cultured in PBMCs and monocyte-derived macrophages (MDMs). Furthermore, clinical isolates were cultured under increasing UCLA1 concentrations for the evaluation of generation of

escape mutations. My data suggest that UCLA1 can efficiently block infection in primary cells but that escape mutation can arise in some isolates after prolonged exposure at high concentrations.

2. Materials and Methods

2.1 PBMC assays

2.1.1 PBMC Isolation

PBMCs were freshly isolated by the Ficoll-Hypaque method (Bures et al., 2000, Trkola et al., 1998) from HIV-seronegative buffy coats purchased from the South African Blood Transfusion Services (SABTS) in Johannesburg, South Africa. A buffy coat is anticoagulated blood that is centrifuged after collection from blood donor units. These were centrifuged at 2 000 rpm for 10 min at 4ºC. Residual plasma was removed and the leukocytes and platelets (cell layer on top of red cells) collected and diluted 1:1 with phosphate-buffered saline (PBS) (Gibco Invitrogen, South Africa) mixed and carefully layered onto 20 ml Ficoll-Paque (GE Healthcare, South Africa). The cells were then centrifuged at 2 000 rpm for 30 min at room temperature to separate lymphocytes from granulocytes. The top layer which consists of PBS was discarded and mononuclear cells were collected at the interface between Ficoll and PBS layers. The cells were washed twice with PBS by centrifuging at 2 000 rpm for 10 min at 4ºC in order to dilute out the Ficoll and remove platelets. Red blood cells were lysed for 10 min at room temperature with 10 ml of red blood cell (RBC) Lysis Buffer (Biocom biotech, South Africa). The cells were washed twice as above and the cell pellet was re-suspended in Rosewell Park Memorial Institute Medium (RPMI) 1640 with glutamine and HEPES medium (Gibco Invitrogen) supplemented with 20% heat-inactivated fetal bovine serum (FBS) and 50 µg/ml gentamicin (Sigma-Aldrich, South Africa). The medium was then referred to as growth medium. Phytohemagglutinin (PHA) (Sigma-Aldrich) was added to the media for activation of

the lymphocyte cells. The cells were then seeded at 2×10^6 cells/ml in 150 cm^2 cell culture flasks (Corning Incorporated, South Africa) and incubated for 2-3 days at 37^oC, 5% CO_2 prior to use.

2.1.2 CD8 depletion of PBMCs

Since CD4 T cells are the main targets of HIV-1 and given that CD8 T cells can be inhibitory, PBMCs were depleted of CD8 T cells by adding RosetteSep human CD8 depletion cocktail (Separation Scientific, South Africa) into 50 µl/ml of whole blood. The blood was mixed thoroughly for 30 sec, incubated for 20 min at room temperature and mixed with an equal volume of PBS. The mixture was carefully layered onto 15 ml Ficoll-Paque and centrifuged at 2 000 rpm for 30 min at room temperature to separate the enriched lymphocytes from granulocytes. The enriched cells were collected at the interface between Ficoll and PBS layers. The CD8 depleted lymphocytes were then washed three times with PBS by centrifugation at 2 000 rpm, 4ºC for 10 min. The cell pellet was re-suspended in 50 ml of 20% RPMI growth medium supplemented with PHA. The cells were then seeded at 2×10^6 cells/ml in 150 cm^2 cell culture flasks and incubated for 2-3 days at 37ºC, 5% CO2 prior to use.

2.1.3 PBMC infection with HIV-1 and expansion of infected cultures

The PHA activated CD8 depleted PBMCs were infected with 500 - 2500 $TCID_{50}$ of virus containing supernatants and incubated overnight at 37ºC, 5% CO_2. The

infected cells were washed twice with 20 ml of 20% RPMI growth medium to remove excess virus by centrifugation at 1 200 rpm for 10 min. The supernatant was discarded and the cell pellet re-suspended in 30 ml of fresh 20% RPMI growth medium supplemented with 5% interleukin-2 (IL-2) (Roche, South Africa) (complete growth medium) and incubated for 10 days at 37ºC, 5% CO_2 for virus expansion. The virus-containing supernatants were harvested on days 7 and 10 and clarified by filtration through 0.45 µm filters. FBS at 1:10 dilution and 10% DMSO were added and the supernatants distributed in 1 ml aliquots and frozen at -80℃ for later use.

2.1.4 Virus titration in PBMCs

To determine the median tissue culture infective dose ($TCID_{50}$) in PBMCs, the virus was titrated by adding 100 µl of IL-2 complete growth medium to the first 3 wells of a set of a dilution series (triplicate) in a round bottom 96-well culture plate (Costar Corning Incorporated, South Africa) with 25 µl of virus. Five-fold serial dilutions were then performed with 25 µl for a total of 7 dilutions. The 8th set of wells served as negative cell control without virus. 100 µl of PBMCs at 5×10^6 cells/ml were added to each well and incubated overnight at 37ºC, 5% CO_2. The cultures were washed to remove excess virus by centrifugation at 1 200 rpm for 10 min. The supernatant was discarded and the cultures were replenished with IL-2 complete growth medium. The cultures were then incubated at 37ºC, 5% CO_2 for 7 days, changing the media on days 2 and 4 of the incubation period. Virus-containing supernatants were harvested on day 7 into 96-well culture plates (Costar Corning Incorporated) and diluted at 1:10 (25 µl virus in 225 µl 0.5% Triton-X-100) with 0.5% Triton-X-100 (Sigma-Aldrich) to inactivate the virus. The cultures were replenished with fresh IL-2 growth medium on

each harvesting day. The 96-well culture plates with harvested supernatants were stored at 4ºC in zip-lock plastic bags until further use.

2.1.5 HIV-1 primary viruses used in PBMCs

Infectious HIV-1 subtype C primary isolates that were used included two isolates from the Durban female sex workers cohort (Bures et al., 2002, Van Damme et al., 2000), two paediatric isolates (Choge et al., 2006), one isolate from an AIDS patient with TB co-infection (Cilliers et al., 2003) and one isolate from the CAPRISA 002 Acute Infection study cohort (van Loggerenberg et al., 2008). Four of these were R5, one was R5X4 (RP1) (Choge et al., 2006) and another was an X4 virus (SW7) (Cilliers et al., 2003).

2.1.6 Cytotoxicity assay in PBMCs

The cytotoxicity of UCLA1 was determined in PBMCs by using the MTS-based CellTiter 96 Aqueous Cell Proliferation Assay (Promega, South Africa) as outlined in Chapter 3, section 2.3. The CD8 depleted PHA/IL-2 stimulated PBMCs were used at 5×10^4 cells/well in 50 µl RPMI 1640 with 5% FBS. The assay was performed in triplicate including control cultures.

2.1.7 Neutralization of primary infectious viruses in PBMCs

The neutralization of the HIV-1 subtype C primary isolates was measured as a reduction of p24 antigen production in CD8 depleted PHA/IL-2 stimulated PBMCs as described previously (Alexandre et al., 2010, Bures et al., 2000). The neutralization assay was performed with RPMI 1640 medium supplemented with 5% FBS, 5% IL-2

and 50 µg/ml gentamicin (growth medium). The assay was carried out with 15 µl of 500 $TCID_{50}$ of HIV-1 primary isolates and a 3-fold serially diluted UCLA1 at an initial concentration of 100 nM in 40 µl of growth medium. The culture supernatant was harvested on days 3, 5 and 7 and replaced with an equal amount of fresh growth medium. For each harvest the p24 antigen concentration was measured by ELISA using the Vironostika HIV-1 Antigen Microelisa System (Biomerieux, South Africa), according to the manufacturer's instructions. The assay was performed at least three times, in triplicate, for each primary isolate tested. The IC_{50} values were calculated as p24 antigen titers causing 50% reduction of p24 antigen production compared to the virus control (without inhibitor).

2.1.8 Detection of viral titers in PBMCs

The viral titer in PBMC cultures was detected by measuring p24 production using the Vironostika ELISA System as mentioned above. The measurement of viral titers was performed for evaluation of $TCID_{50}$, for detection of neutralization titers and for measurement of primary isolate expanded stocks. The standard curve was generated with 4-fold serial dilutions of supernatant from H9 cells infected with HIV-1 IIIB at an initial concentration of 1 ng/ml. The p24 assay was measured with 100 µl of the Triton-X-100 lysates that were further lysed by incubating with 25 µl of Disrupt-Buffer at 37ºC, 5% CO_2 for 1 hour, using the micro-ELISA plate coated with p24 antibody. The plate was washed 4 times with the 25 × wash buffer (40 ml buffer in 960 ml dH_20) using the PW40 plate washer (Sanofi Diagnostics Pasteur, France). The bound lysates were conjugated to the p24 antibody on the ELISA plate with 100 µl of conjug-1ER secondary antibody, incubated at 37ºC, 5% CO_2 for 1 hour and

washed as above. The ELISA plate was developed by adding 100 µl of 1:1 mixture of TMB and UP substrates. The plate was read immediately after addition of the substrate mix using the $Versa_{max}$ turnable microplate reader (Molecular Devices, CA, USA) on the kinetics mode at a wavelength of 650 nm. The data was captured using the Softmax Pro software 4.8 version. The $TCID_{50}$ titers were calculated according to the method of Reed and Muench (Johnson, 1990, WHO-UNAIDS, 2002). The wells with <0.2 ng/ml of p24 were considered negative. The p24 assay for detection of neutralization titers was performed as described above except that harvests from the negative control cultures (virus without inhibitor) were first tested for p24 in order to identify the harvests that had viral growth. The activity of the aptamer was then measured at the time-point that corresponded to the early part of the linear growth period of the virus control (Zhou & Montefiori, 1997). The neutralization titers were determined at the 80% level of the reduction in p24 antigen production of the test cultures compared with the negative control cultures (without inhibitor).

2.2 MDM assays

2.2.1 MDM isolation

Differentiated macrophages were isolated from PBMCs by adherence of monocytes to tissue culture flasks as described (Crowe, 2004). The isolated PBMCs pellet (section 2.1.1 above) was re-suspended in 25 ml of Lonza X-VIVO-10 culture media (Whitehead Scientific, South Africa) supplemented with 10% FBS (growth media). The cells were seeded in 150 cm^2 tissue culture flasks and incubated for 90 min @ 37℃, 5% CO_2. Non-adherent floating T cells were decanted and the adherent monocytes were washed 2-3 times with 10 ml of neat X-VIVO-10 media to remove

the residual floating T cells. The monocytes were then incubated overnight in 25 ml of growth media at 37℃, 5% CO_2. Culture media was decanted and the monocytes monolayer was rinsed 2-3 times with 10 ml of PBS. The adherent cell monolayer was disrupted by incubating the culture flasks at 4℃ for 1 hr in 20 ml chilled PBS (Collin et al., 1991). The monolayer was detached by gentle scraping and the cells were added to 2.5 ml FBS and centrifuged at 2 000 rpm for 10 min at room temperature. The cells were re-suspended at 0.5 – 1.0 × 10^6 cells/ml in 10% FBS RPMI growth medium supplemented with 5 ng/ml of human granulocyte macrophage colony stimulating factor (GM-CSF). The monocytes were cultured for 5-7 days in either 75 cm^2 tissue culture flasks, 96- or 24-well plates, depending on the assay to be performed, for differentiation into macrophages.

2.2.2 MDM phenotyping

To confirm the phenotype of the differentiated macrophages the cells in tissue culture flasks were detached as described above and prepared for fluorescence activated cell sorter (FACS) analysis (Collin et al., 1991, Crowe, 2004). Briefly, the differentiated cells were re-suspended in 700 µl of fixing solution (PBS with 1.5% formaldehyde and 2% BSA), aliquoted at 100 µl into FACS staining tubes (Becton Dickinson Labware, South Africa) and incubated for 20 min at room temperature. The cells were washed by centrifugation at 1 000 rpm for 10 min with PBS in 10% BSA (wash solution) and re-suspended in 100 µl of wash solution. Indirect cell surface staining was performed, that is, the cells were first stained with mouse primary MAbs followed by fluorescent goat anti-mouse secondary MAbs. The mouse primary MAbs that were used were CD14, CD68, MHC II (Santa Cruz Biotechnology,

South Africa) and CD3 (R&D Systems, South Africa) (Table 4-1). The CD14 MAb was used to stain undifferentiated monocytes and CD68 and MHC II MAbs stained differentiated monocytes (macrophages). They were used at titrated concentrations of 10 µg/ml (5 µl), 20 µg/ml (10 µl) and 40 µg/ml (20 µl) each. The cells were incubated at room temperature for 30 min, washed twice and stained for a second time with fluorescent goat anti-mouse secondary MAbs, Alexa Flour 514, Alexa Flour 488 (Invitrogen) and PE Cy5.5 (Caltag Laboratories, Thailand), (Table 4-1). The secondary MAbs were also titrated at the same concentrations as the primary MAbs. The cells were incubated in the dark at room temperature for 30 min, washed and re-suspended in 500 µl wash solution. The cells were then acquired on the BD FACSCalibur flow cytometer (Immunocytometry Systems, USA).

Table 4-1: Antibodies used for MDMs phenotyping.

Mouse Primary MAbs	Goat anti-mouse Secondary MAbs
CD68 or MHC II	**Alexa Flour (AF) 488** (FITC-Blue laser)[a]
CD14	**AF 514** (Red laser)[b]
CD3	**PECy5.5** (Red laser)[b]

[a,b]The two excitation laser beams that were used in the acquisition of the stained cells to reflect different flourescence for the different acquired cell populations. Cell acquisition was performed with the FACSCalibur flow cytometer.

2.2.3 HIV-1 infection of MDMs

HIV-1 subtype C primary isolates were used to infect the differentiated macrophages. The virus-containing supernatants were added to the macrophages ($0.5 – 1.0 \times 10^6$ cells/ml) in 24-well tissue culture plates at 1:1 dilution and incubated

overnight at 37℃, 5% CO_2 (Crowe, 2004). Control wells contained cells with media only. Virus inoculum was removed after overnight incubation by aspirating the supernatants. The cells were washed twice with 1 ml of warm PBS supplemented with 1% FBS. An additional wash was performed with 1 ml of RPMI supplemented with 10% FBS (RPMI growth media). The washes were performed manually by the addition and aspiration of media. The cells were then incubated for a further 6 days in 1 ml RPMI growth media at 37℃, 5% CO_2. On day 7 half of the virus supernatants were harvested from each well and the cultures were replenished with an equal volume of fresh RPMI growth media and incubated at 37℃, 5% CO_2 for a further 7 days. To inactivate the virus, the harvests were diluted 1:5 with 1.25% Empigen BB detergent (Sigma-Aldrich) buffer (50 µl virus supernatant in 200 µl 1.25% Empigen) to a final concentration of 1% Empigen. The harvest plates were stored at 4ºC in zip-lock plastic bags until further use (Patience, 1991). The supernatants were harvested every 7th day for a total of 4 weeks.

2.2.4 Screening of macrophage-tropic viruses

A panel of 25 HIV-1 subtype C primary viruses were screened for macrophage (R5)-tropism for the selection of those to be used in MDM neutralization assay. The panel included four viruses from the CAPRISA 002 Acute Infection study cohort (van Loggerenberg et al., 2008), five from the Durban female sex workers cohort (Bures et al., 2002, Van Damme et al., 2000), eight paediatric isolates (Choge et al., 2006), five from AIDS/TB co-infected patients and three AIDS patients co-infected with cryotococcus meningitis (Cilliers et al., 2003). Twenty of the viruses were R5, four were R5X4 (CM9, RP1, SW20 and SW30) (Choge et al., 2006, Cilliers et al., 2003)

and one X4 virus, SW7 (Cilliers et al., 2003). The dual tropic and X4 viruses were included to determine whether they will be able to switch receptor usage and infect the macrophages. The infection screening was performed by infecting MDMs with the viruses as outlined in the paragraph above. The screening was performed as a rapid assay tested in single wells. The cultures were maintained for 42 days and harvested on every 7th day.

2.2.5 HIV-1 neutralization assay in MDMs

UCLA1 was tested for neutralization of HIV-1 subtype C infected MDM according to a previously described protocol (Crowe, 2004). The aptamer was used at a starting concentration of 100 nM with 3-fold serial dilutions in RPMI supplemented with 5% FBS (growth media). Virus supernatants of the primary isolates were added to the serially diluted aptamer at 1:1 dilution and incubated for 1 hr at 37℃, 5% CO_2. Differentiated macrophages cultured at 0.5 – 1.0 × 10^6 cells/ml in 96-well culture plates were used for the neutralization assay. Half of the volume of the cell supernatants was aspirated and the aptamer/virus mix added to the cells and incubated overnight at 37℃, 5% CO_2. The assay was performed in triplicate and included control wells without aptamer. The cells were washed 3 times by aspirating the virus inoculum from each well and adding 250 µl of RPMI growth media. The cells were then incubated for a further 6 days in RPMI growth media at 37℃, 5% CO_2. On day 7, 50 µl of virus supernatants were harvested from each well and the cultures replenished with an equal volume of RPMI growth media and incubated at 37℃, 5% CO_2 for a further 7 days. The supernatants were harvested every 7th day for a maximum of 21 days. The harvested viral supernatants were inactivated with

1.25% Empigen BB detergent and stored as mentioned above until further use (McKeating et al., 1991, Moore et al., 1990).

2.2.6 HIV-1 primary viruses used in MDM neutralization assay

HIV-1 subtype C primary isolates that were used in the MDM neutralization assay included the same infectious virus isolated from the Durban cohort mentioned in Chapter 4, section 2.1.5, another paediatric isolate (Choge et al., 2006), two additional HIV-1 isolates from co-infected patients, one with tuberculosis and another with cryptococcal meningngitis (Choge et al., 2006, Cilliers et al., 2003) and one more isolate from the CAPRISA cohort mentioned in Chapter 4, section 2.1.5. The subtype C primary viruses were all R5 strains. An R5-tropic subtype B primary virus, ADA reference strain, was also used.

2.3 HIV-1 p24-antigen immunoassay

The macrophages were evaluated for infection with viruses and neutralization with UCLA1 using the HIV-1 p24 antigen detection assay, a twin-site sandwich ELISA, based on a previously published method (McKeating et al., 1991, Moore et al., 1990). Briefly, p24 antigen is captured from a detergent lysate of virions by a polyclonal antibody adsorbed to a solid phase. Bound p24 is detected with an alkaline phosphatase-conjugated anti-p24 monoclonal antibody and a luminescent detection system. This p24 assay replaced the Vironostika kit that was used in the PBMC neutralization assay due to its termination in the marketplace.

2.3.1 Plate coating

The sheep anti-HIV p24 Gag coating antibody D7320 (Aalto Bio Reagents Ltd., Ireland) was reconstituted to 4 µg/ml in 10 ml of $NaHCO_3$ buffer (Sigma-Aldrich). White 96-well plates (Costar Corning Incorporated) were coated with 100 µl of the reconstituted D7320 coating antibody and incubated overnight at room temperature. The plates were washed 3 times with 1 × Tris Buffered Saline (TBS) (Bio-Rad, South Africa) using the BioTek ELx50 plate washer (BioTek Instruments, USA). 150 ul of 2% BSA (Roche) in 1 × TBS (blocking buffer) was added to each well and the plates incubated at room temperature for 1 hr.

2.3.2 ELISA

The standard curve was generated with 6 times 4-fold dilutions of 1 µg/ml of recombinant HIV-1 p24 (Aalto BioReagents, Ireland) in 1% EMPIGEN buffer and incubated at room temperature for 1 hr. The blocking buffer was discarded from the plates. The plates were washed and 100 µl of the harvested viral supernatants was added in triplicate including the standard curve dilutions and incubated for 3 hr at room temperature. After the second wash 100 ul of anti HIV-1 p24 Alkaline Phospatase monoclonal conjugate (EH12AP) (Aalto Bioreagents) was added to the plates at 1:8000 in 2% BSA, 0.05% tween/TBS. The plates were incubated for 1 hr at room temperature and washed 4 times with 0.1% Tween (Sigma-Aldrich) in TBS and twice with 1× TROPIX buffer (Applied Biosystems, South Africa). The plates were developed by adding 50 ul of TROPIX CDPS Saphire II (Applied Biosystems) diluted 1:4 in 1× TROPIX buffer and incubated for 45 min at room temperature. The reduction in p24 antigen production was measured on the Wallac 1420 Victor

Multilabel luminometer (Separation Scientific, South Africa). The neutralization titers were determined at the 80% level of the reduction in p24 antigen production of the test cultures compared with the negative control cultures (without inhibitor).

2.4 Evaluation of UCLA1 resistance

2.4.1 Generation of UCLA1 resistant viruses

To generate UCLA1 resistant viruses 1000 $TCID_{50}$ of HIV-1 subtype C primary isolates were cultured in the presence of increasing concentrations of UCLA1. The Du422 (R5-tropic) and RP1 (R5X4-tropic) primary viruses were selected for this study due to their different tropisms. The viruses were cultured in 2 ml of 1×10^6 CD8 depleted PBMCs. The starting concentration of the aptamer was the IC_{50} of each virus that was tested. Virus cultures without UCLA1 were used as negative controls. All cultures were maintained in RPMI 1640 containing 5% FBS and IL-2 (0.05 µg/ml). Viruses were passaged every 7 days by transferring 200 µl of the previous culture into 1.8 ml of freshly isolated CD8 depleted PBMCs. After every passage 1.8 ml of the culture supernatant was centrifuged at 2000 rpm for 10 min. The supernatant was aliquoted at 300 µl and stored at -80ºC for later use with neutralization assays. The cell pellet was re-suspended in 1 ml PBS, split into 2 aliquots and washed by centrifugation as above and the pellet stored at -80 ºC for later genotyping. UCLA1 concentration was increased whenever the viral growth, measured by p24 antigen ELISA, in the aptamer-containing culture was similar or more than the negative control culture. When there was no viral growth the cultures were passaged in the same UCLA1 concentration as used in the preceding 7 days. When viral growth declined, UCLA1 was used at a lower concentration. When the

viral titre could not be detected, frozen supernatants were thawed and used for continuation of the experiment. The aliquot used to restart the experiment was taken from the period when the viral growth was in the log phase. Isolation of viral RNA from the frozen aliquots was performed using the QIAamp mini spin viral isolation kit (Appendix C, section 1.7).

2.4.2 HIV-1 Envelope amplification and purification

2.4.2.1 RT-PCR

The extracted RNA was reverse transcribed into cDNA using the OFM19 primer: 5'-GCA CTC AAG GCA AGC TTT ATT GAG GCT TA-3'. The RT-PCR mixture consisted of 0.5 µM primer, 0.5 mM dNTP mix (10 mM each) and ddH_20 to a final volume of 13 µl. The RT-PCR mixture was heated at 65℃ for 5 min. The mixture was added to a final volume of 20 µl which consisted of 0.2 mM DTT, 2 U/µl RNase Inhibitor, 10 U/µl Superscript III reverse transcriptase with a corresponding 1× buffer (Invitrogen). The RT-PCR cycling conditions were: 50℃ for 60 min, 55℃ for 60 min, 70℃ for 15 min, 37℃ for 20 min.

2.4.2.2 PCR

The envelope gene was amplified by nested PCR as described previously (Salazar-Gonzalez et al., 2008). The following primers were used for the first round PCR: OFM19 (Chapter 4, section 2.4.2.1) and VIF1: 5′- GGG TTT ATT ACA GGG ACA GCA GAG-3′. The first round PCR reaction mixture consisted of 0.2 µM primers, 2 mM $MgSO_4$, 1.25 mM dNTP (10 mM each), and High Fidelity Platinum Taq DNA polymerase with the corresponding 1 × buffer (Invitrogen), 1 µl cDNA input and

ddH_20 to a final volume of 20 µl. The PCR cycling conditions were: 94℃ for 5 min, 35 cycles of 94℃ for 30 sec, 55℃ for 30 sec and 6 8℃ for 4 min, followed by a final extension step at 68℃ for 10 min. EnvA and EnvM pr imers (Chapter 3, section 2.4.1) were used for the second round PCR (Gao et al., 1996, Gray et al., 2007a) . The 50 µl second round PCR mixture consisted of the same reagents and concentrations as the first round PCR reaction mixture and 1 µl of the first round PCR reaction product. The amplified products were detected by agarose gel electrophoresis (Appendix C, section 1.1). The amplified DNA was purified with QIAquick PCR purification Kit (Appendix C, section 1.8.1). The DNA was gel purified with QIAquick gel purification kit when multiple bands were detected after PCR purification (Appendix, C section 1.8.2).

2.4.3 HIV-1 envelope sequencing

The DNA samples from the primary isolates were confirmed by nucleotide sequencing using the ABI PRISM Big Dye Terminator Cycle Sequencing Ready Reaction kit (Applied Biosystems) as described earlier (chapter 3, section 2.8.2) except that the 20 µl sequencing PCR reaction mixture consisted of 100 µg of purified DNA, 4 µl of Ready reaction mix, 2 µl of 5 × Big Dye Terminator sequencing buffer and 1 µl of primer. The DNA sequencing reactions were purified using the sodium acetate (NaOAc) purification method as described (Appendix C, section 1.6). The sequences were resolved on an automated genetic analyzer and changes in the sequenced envelopes were identified using Sequencher v.4.5 (Genecodes, Ann Arbor, MI), Clustal X (v 1.83) and Bioedit (v 5.0.9).

3. Results

3.1 UCLA1 is not cytotoxic to PBMCs

In order to determine whether UCLA1 was cytotoxic to the PBMCs, its effect in these cells was examined with the MTS-based CellTiter 96 Aqueous Cell Proliferation Assay. The PBMCs exhibited an average viability of 99% ± 0.11 after 72 hours incubation (Figure 4-1). The cells were used with a maximum concentration of 500 nM of UCLA1. The Etoposide phosphate positive control exhibited an average of 36 ± 1% viability (Figure 4-1).

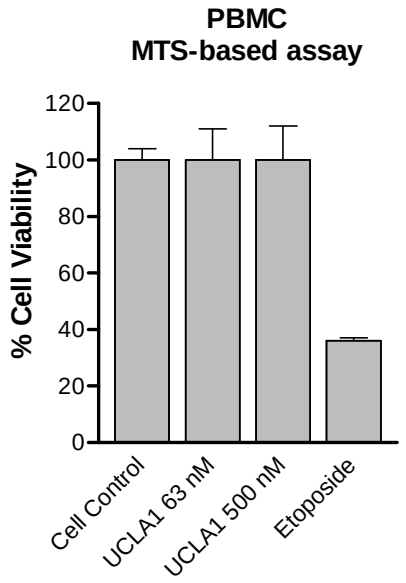

Figure 4-1: Percentage viability of PBMCs in the presence of varying concentrations of UCLA1.
The MTS-based assay was used to test the viability of the PBMCs. Etoposide phosphate was used as a positive control. Untreated cell cultures were used as negative controls. The assay was performed three times in triplicate. The error bars indicate the standard deviation of the mean.

3.2 Neutralization of HIV-1 primary isolates in PBMCs

To determine the ability of UCLA1 to inhibit HIV-1 subtype C infection of primary cells, neutralization assays were performed using 6 infectious subtype C clinical isolates in PBMCs. Viral infection was measured by p24 ELISA at the time-point that corresponded to the early part of the linear growth period of the virus control. Thus, p24 was usually measured using the day 5 cultures. Four of the 6 (67%) primary isolates were neutralized by UCLA1 in a dose-dependent manner (Figure 4-2). The concentration of the aptamer that inhibited 50% of virus infection (IC_{50}) was within a range of 7-35 nM. The 4 included primary viruses isolated from acutely infected adults (Du422 and CAP63) and chronically infected infants (RP1 and TM3), all of which used CCR5 except RP1 which was dual-tropic (R5X4). Two isolates, SW7 (X4-tropic) and Du156 (R5-tropic), were not neutralized by UCLA1 in the PBMC assay despite their corresponding cloned envelopes being neutralized in the TZM-bl assay (Table 3-1). Indeed there was no correlation between the degrees of inhibition for each of the 4 sensitive viruses when the 2 assays were compared (Chapter 3, Table 3-1 and Figure 4-2).

3.2.1 Sequence analysis of resistant viruses

The amino acid sequences of the primary isolates that were not neutralized by UCLA1 were aligned with those that were sensitive to the aptamer and examined for residues associated with resistance. Neutralization resistance could not be explained from the amino acid sequence alignment. That is, the SW7 primary isolate which was resistant in the PBMC assay had mutations K305R, H330Y and L369I (Figure 4-3). Since the SW7 pseudovirus contained the same changes but was sensitive in the

TZM-bl assay, these residues were unlikely to be resistance-conferring in the PBMC assay. This was also noted with the TM3 isolate which had the H330Y mutation but was sensitive to UCLA1 in PBMCs. Similarly, an I307V change was observed in both Du156 and Du422 which differed in their sensitivity to UCLA1 in PBMCs, suggesting that this residue might not be involved in conferring resistance in the PBMC assay (Figure 4-3).

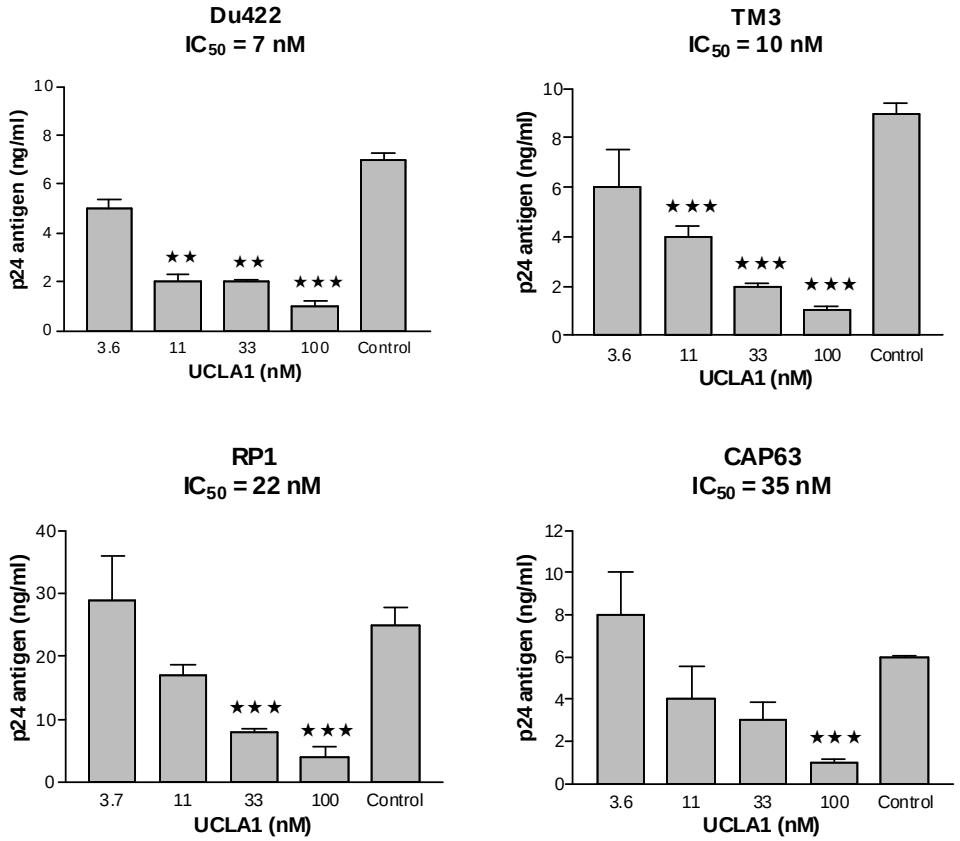

Figure 4-2: Representative dose-dependent neutralization graphs of HIV-1 subtype C primary isolates in PBMCs.
UCLA1 was used at a starting concentration of 100 nM. Neutralization was measured as a reduction in p24 production compared to the control without aptamer. The bars represent a dose-dependent inhibition of the p24 antigen by UCLA1. The IC_{50} values were calculated as p24 antigen titers causing 50% reduction of p24 antigen production compared with the virus control (without UCLA1). The assay was performed at least three times, in triplicate, for each primary isolate tested. UCLA1 inhibition that showed statistically significant difference compared to the virus control as determined by a t-test are indicated by asterisks where ** and *** indicate *p* values of less than 0.01 and 0.005, respectively.

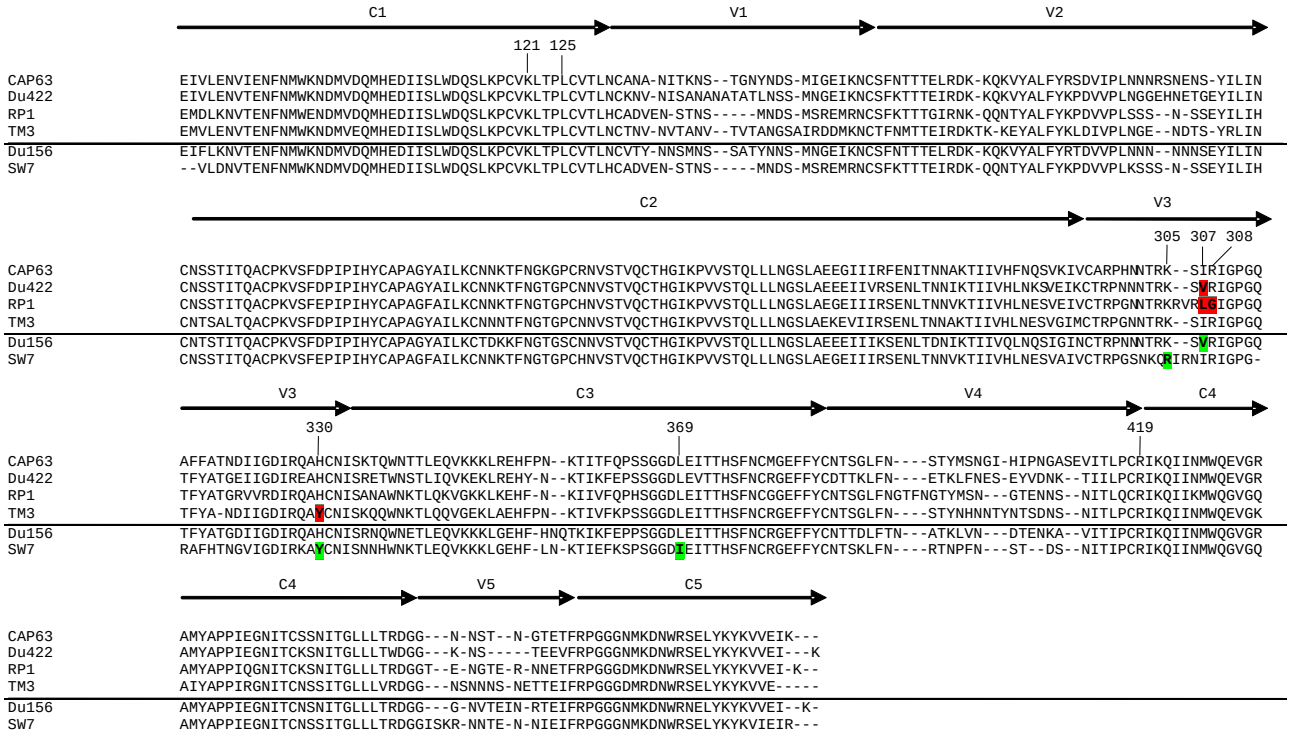

Figure 4-3: Amino acid sequence alignment of HIV-1 gp120 of primary isolates that were tested for neutralization with UCLA1 in the PBMC assay.

The viruses that were not neutralized by the aptamer are listed below the horizontal line in the sequence alignment. The amino acid residues that were changed by site-directed mutagenesis of ConC gp120 are numbered and their respective regions exhibited within the env genome. The numbering is according to the sequence of the HxB2 gp120. The amino acid residues that were shown to modulate binding of UCLA1 are highlighted in red. Residues that supposedly confer UCLA1 resistance are highlighted in green.

3.3 MDM assay results

3.3.1 MDM phenotyping

The purity of the isolated MDMs was confirmed by FACS cell surface staining. The macrophages were identified in region 2 (R2) (MHC II^+/AF 488^+) at a purity of 99.98% (Figure 4-4A) and at a purity of 99.96% ($CD68^+$/AF 488^+) (Figure 4-4B). The R1 regions represent the total population of acquired cells. All regions (R2, R3, R4, R5 and R6) were gated from the R1 regions (Figure 4-4A and B). Similarly pure isolated macrophage cells were identified with different MAb titrations. That is, staining of MHC II and CD68 both with AF 488 at 20 µg/ml and 40 µg/ml titrations resulted in >97% and >99% pure isolated macrophages, respectively (Appendix D – Supplementary Figure 2 - A and B). The T lymphocytes were negatively selected with CD3 labelled with PE Cy5.5 MAb and classified as a negative cell population gated in regions 4 and 6 (R4 and R6) (Figure 4-4A and B). The undifferentiated monocytes were also negatively selected by staining with CD14 labelled with Alexa Flour 514 (AF 514) MAb and regarded as an additional negative cell population gated in regions 3 and 5 (R3 and R5) (Figure 4-4A and B). Each of the negative cell populations (R3, R4, R5 and R6) contained <2.3% of cells thus confirming the >99% purity of the isolated macrophages with both MHC II and CD68 staining. The MAb titrations revealed that 10 µg/ml of the antibodies was sufficient for macrophage phenotype staining since it exhibited similar staining patterns to the 20 µg/ml and 40 µg/ml titrations.

A

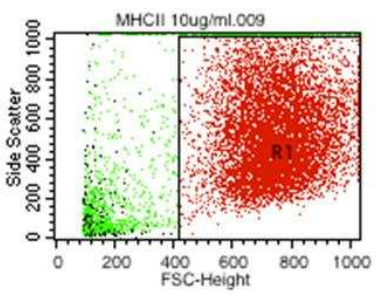

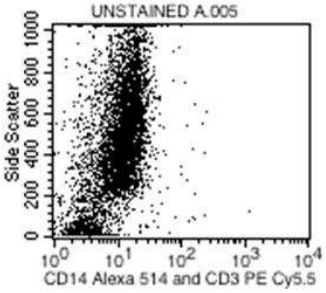

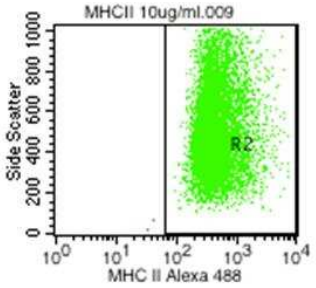

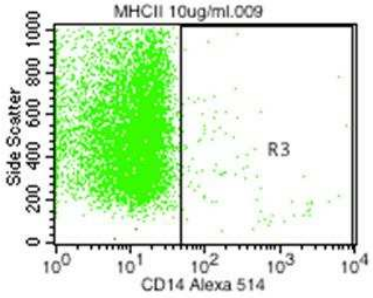

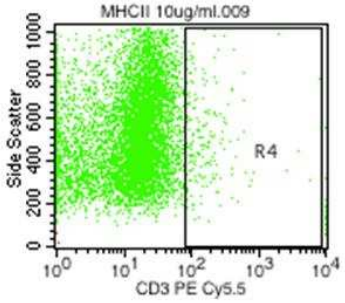

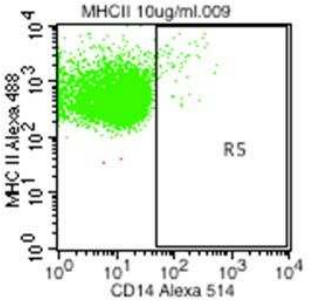

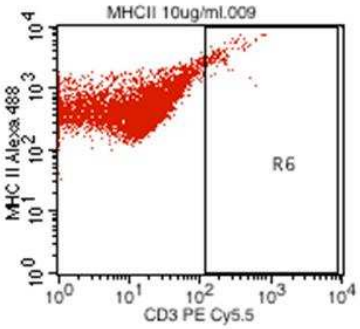

Region Statistics

Sample ID: MHCII 10ug/ml
Acquisition Date: 20-Nov-09
Gate: G1
Gated Events: 8508
Total Events: 10000

Region	Events	% Gated	% Total
R1	8508	100.00	85.08
R2	8506	99.98	85.06
R3	93	1.09	0.93
R4	188	2.21	1.88
R5	88	1.03	0.88
R6	115	1.35	1.15

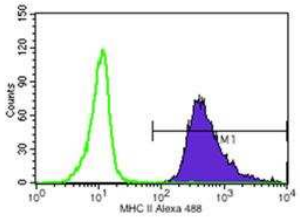

Sample ID: MHCII 10ug/ml
Acquisition Date: 20-Nov-09
Gate: G1
Gated Events: 8595
Total Events: 10000

Marker	Events	% Gated	% Total
All	8595	100.00	85.95
M1	8594	99.99	85.94

B

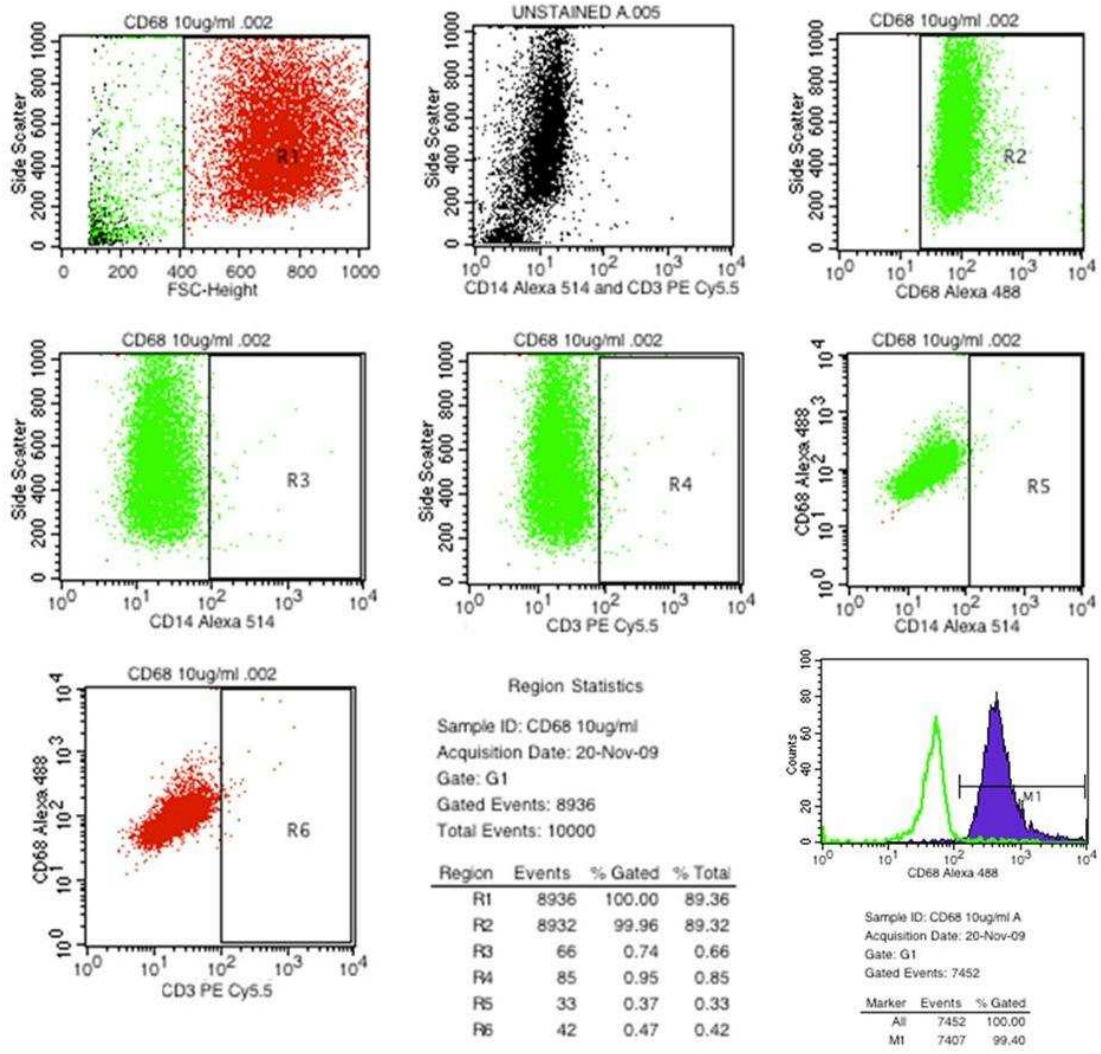

Figure 4-4: FACS dot plots showing pure isolated macrophages.
(A) FACS dot plots showing the phenotype of pure differentiated macrophages by staining with MHCII and AF 488 MAbs at 10 µg/ml. The macrophages were gated in R2 at 99.98%. A histogram with the M1 region of MHCII/AF 488 positive macrophage population is shown. **(B)** FACS dot plots showing the phenotype of pure differentiated macrophages after staining with CD68 and AF 488 MAbs at 10 µg/ml. The macrophages were gated in R2 at 99.96%. Also included is a histogram with the M1 region showing the CD68/AF 488 positive macrophage population.

3.3.2 Screening macrophage-tropic viruses

Infectivity of the viruses was evaluated by measuring HIV-1 Gag p24 antigen. Of the 25 primary viruses that were tested for macrophage infection only 5 showed an increasing trend of p24 production over the 42 days of culture (Figure 4-5). Du156 had a lower infectivity rate with the highest p24 reading of 3.7 ng/ml on day 35. Thus, 4 subtype C isolates (CM1, COT9, Du422 and SW14) were used to evaluate UCLA1 neutralization in MDMs. A subtype B isolate (ADA) was also included as a macrophage-tropic reference strain.

3.3.3 Neutralization of HIV-1 primary isolates in MDMs

To determine the ability of UCLA1 to inhibit HIV-1 subtype C infection of macrophages, neutralization assays were performed using 4 infectious subtype C macrophage-tropic isolates in MDM. Viral infection was measured by p24 ELISA every seventh day for a maximum of 21 days of culture. Three of the 4 (75%) primary isolates were neutralized by UCLA1 in a dose-dependent manner with IC_{50} values in a range of 3.6-13.6 nM (Figure 4-6) compared with the virus control (without UCLA1). The p24 readings shown in Figure 4-6 were measured on day 7 for ADA and day 14 for Du422, COT9 and SW14 viruses. The assays were performed on different days and thus with different donor samples. The neutralized viruses were all R5-tropic and included an acutely infected adult isolate (Du422) and chronically infected adult and paediatric isolates (SW14 and COT9). Although the CM1 infectivity rate was higher than the other tested isolates (Figure 4-6), it was observed to be resistant to UCLA1. CM1 was regarded resistant due to its low inhibition rate (< 50%) with 100 nM UCLA1. An additional HIV-1 subtype B

macrophage-tropic isolate (ADA) was also tested and it was neutralized in a dose-dependent manner with an IC_{50} of 5.8 nM (Figure 4-6). It was noted that the p24 levels in the control cultures were reduced compared to the levels obtained during screening (Figure 4-5). This was due to PBMC donor variability given that the assays were performed on different days with new donor samples each day.

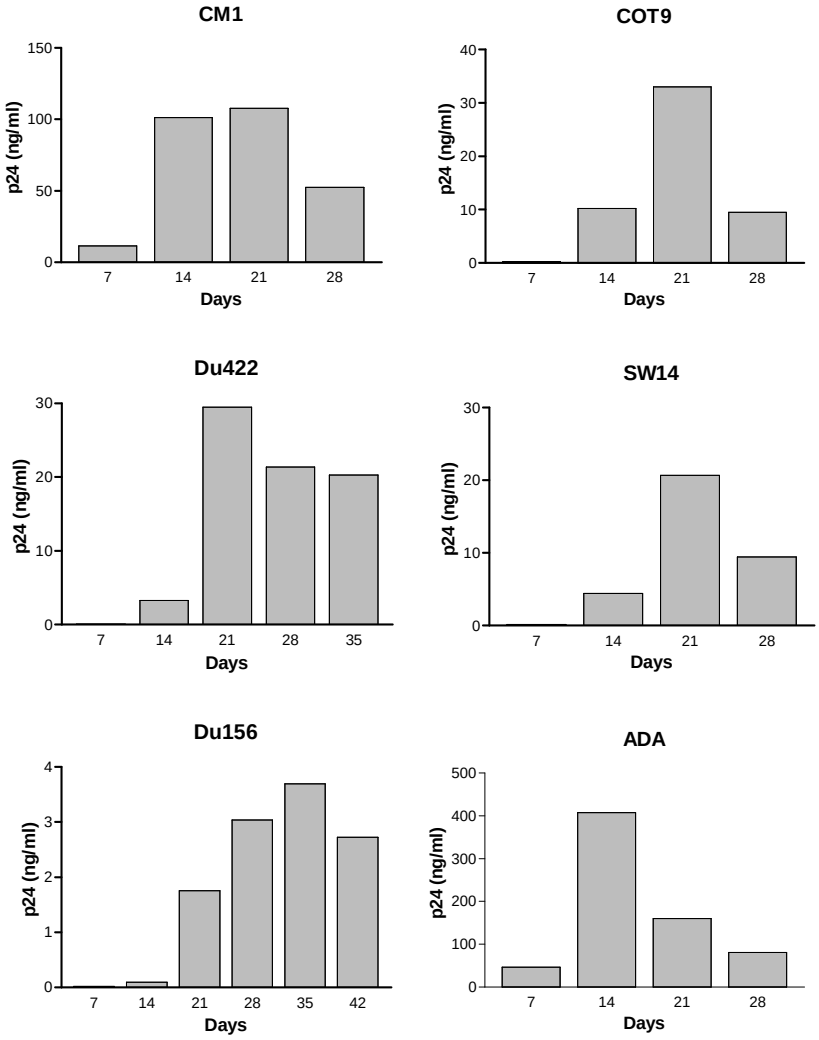

Figure 4-5: Infectivity of HIV-1 primary viruses in monocyte-derived macrophages. The viruses were cultured for 42 days to evaluate their infectivity in MDMs. Infectivity was measured as HIV-1 Gag p24 production. p24 was evaluated using supernatants that were harvested once per week.

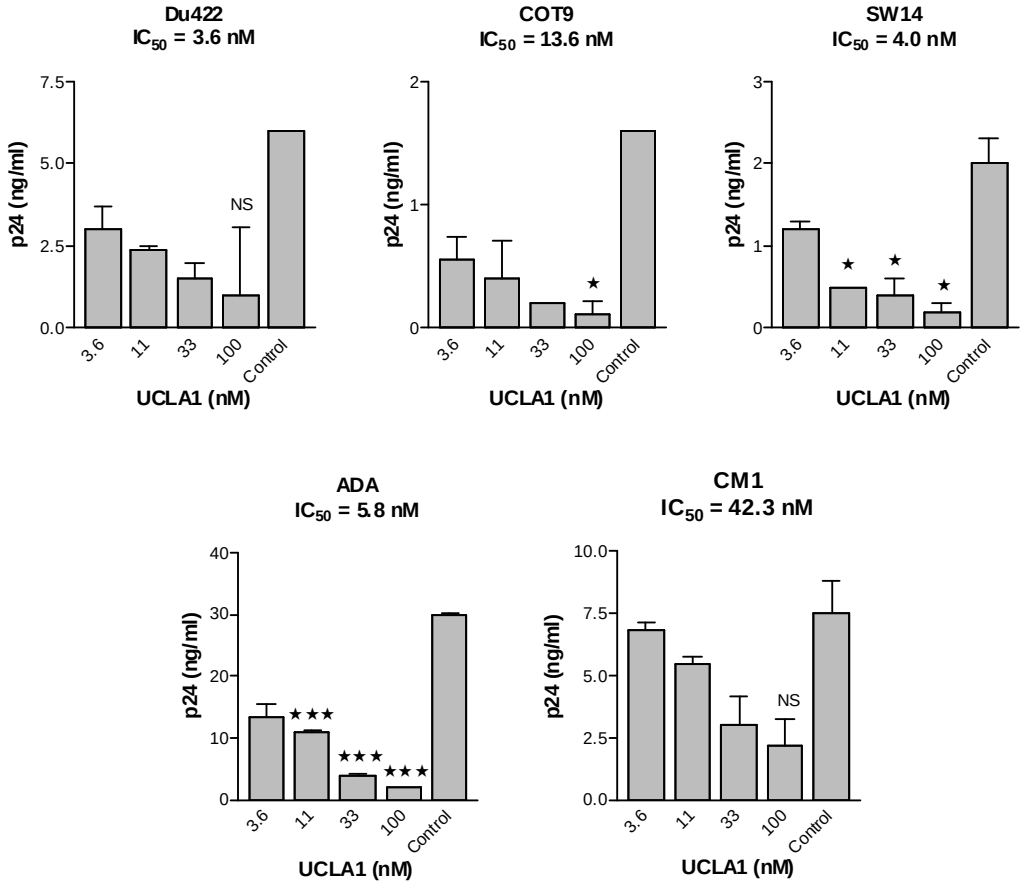

Figure 4-6: Representative dose-dependent neutralization graphs of HIV-1 subtype C primary isolates in MDM.
UCLA1 was used at a starting concentration of 100 nM. Neutralization was measured as a reduction in p24 production compared to the control without aptamer. The IC_{50} values were calculated as p24 antigen titers causing 50% reduction of p24 antigen production compared with the virus control (without UCLA1). The assay was performed at least three times, in triplicate, for each primary isolate tested. Statistical significant difference of UCLA1 inhibition compared to the virus control was determined by *t-test* and indicated by asterisks where * and *** indicate *p* values of less than 0.05 and 0.001, respectively. Absence of statistical significant difference is represented as NS.

3.4 Generation of UCLA1 resistant isolates

In order to select for UCLA1 resistance, two HIV-1 subtype C primary isolates were cultured in CD8 depleted PBMCs with escalating concentrations of UCLA1. The

concentration of the aptamer was increased depending on the viral growth, starting with the concentration equal to IC_{50} of each virus (Table 4-2). Negative control cultures consisting of wild type viruses without UCLA1 were included for comparison. Viral growth of the cultures was measured weekly by p24 antigen ELISA. The RP1 isolate was cultured for 84 days (12 weeks) and the Du422 isolate for 77 days (11 weeks). The viruses were isolated after completion of their propagation under increasing concentrations of UCLA1 (Appendix D – Supplementary Tables 2 and 3). The IC_{50} values for RP1 and Du422 at isolation time-point were 219.6 nM and 73.6 nM, that is, 7-fold and 3-fold respectively compared to the initial p24 values before selection (Table 4-2). Thus, UCLA1 was observed to be more potent against Du422 requiring lower concentrations to inhibit 50% of virus.

Table 4-2: Pre- and post-selection IC_{50} values of UCLA1 against HIV-1 primary isolates.

Virus	Pre-selection IC_{50} (nM)	Post-selection IC_{50} (nM)	IC_{50} fold increase	Selection weeks
RP1.12	33.0	219.6	7	12
Du422	23.6	73.6	3	11

IC_{50} is the concentration of UCLA1 causing 50% inhibition of virus infection.

3.4.1 Pattern of viral growth in increasing concentrations of UCLA1

The viral growth, measured by p24 antigen production, varied during the resistance selection and in some instances was markedly reduced when compared with the control cultures (without UCLA1) thus confirming UCLA1 anti-HIV activity in the test

cultures. This was observed for Du422 at week 6 where the p24 for the culture with UCLA1 was 10-fold (38.56 ng/ml) less than the control culture (387.77 ng/ml) (Figure 4-7 and Appendix D, Supplementary Table 3). Similarly, the p24 for RP1 culture with UCLA1 at week 5 was 6-fold (3.85 ng/ml) less than the control culture (25.17 ng/ml) (Figure 4-7 and Appendix D, Supplementary Table 2).

3.4.2 Amplification and sequencing of primary viruses selected for UCLA1 resistance

The virus supernatants of the cultures used for the generation of resistant isolates were frozen every 7 days, in conjunction with the p24 assay. At selection time-point, the supernatants were reverse transcribed and amplified by PCR (Figure 4-8). An agarose gel was performed to confirm the presence and size of the envelope DNA in the viral supernatants after selection. The amplified gp160 genome was sequenced to assess for mutations within the *env* gene that might have occurred due to the selective pressure by UCLA1 (Figure 4-9). No mutations were generated by the Du422 isolate even at increased UCLA1 concentrations. Six RP1 mutations were detected at the base of the V3 loop (R322Q), within the V4 loop (N410S), in β3 of the bridging sheet next to the V1/V2 loop (R202T), in the C2 region between β4 and β5 sheets (F223Y), within the CD4 and CoR binding complex in the α3 helix (P369L) and in the α5 helix next to the CD4 and CoR binding complex within the β24 sheet (K476R) (Figure 4-9 and 4-10). The RP1 control viral quasispecies also exhibited amino acid changes at isolation time point when compared with the wild-type isolate (Figure 4-10). The changes were identified within the V1/V2 (N148K, K152N) and V3 (I324V) loops together with the amino acid change that was identified in the UCLA1

sequence (P369L). Although the identified changes were not confirmed (due to time constrains) to cause UCLA1 resistance, it is assumed that the RP1 control virus was also subjected to some selective pressure due to the continuous propagation in culture. Nevertheless, the pressure was not related to UCLA1 since its IC_{50} was 3-fold less compared to UCLA1 virus. This was not observed with the Du422 control virus thus suggesting a virus-dependent effect. The identification of the P369L change in the control sequence might be an indication that this residue is highly unstable and that the virus can undergo random mutations with or without pressure from an inhibitor. Therefore, the changes that were inferred to confer resistance were the V1/V2 (R202T) and V3 (R322Q) loop mutations. The inference is based on published data which showed the following residue positions to be involved in UCLA1 binding: 121 and 125 (C1 region), 297, 298, 305, 307, 308 and 330 (V3 loop), 369 (C3 region) and 419, 421 and 423 (C4 region) (Cohen et al., 2008, Mufhandu et al., 2012).

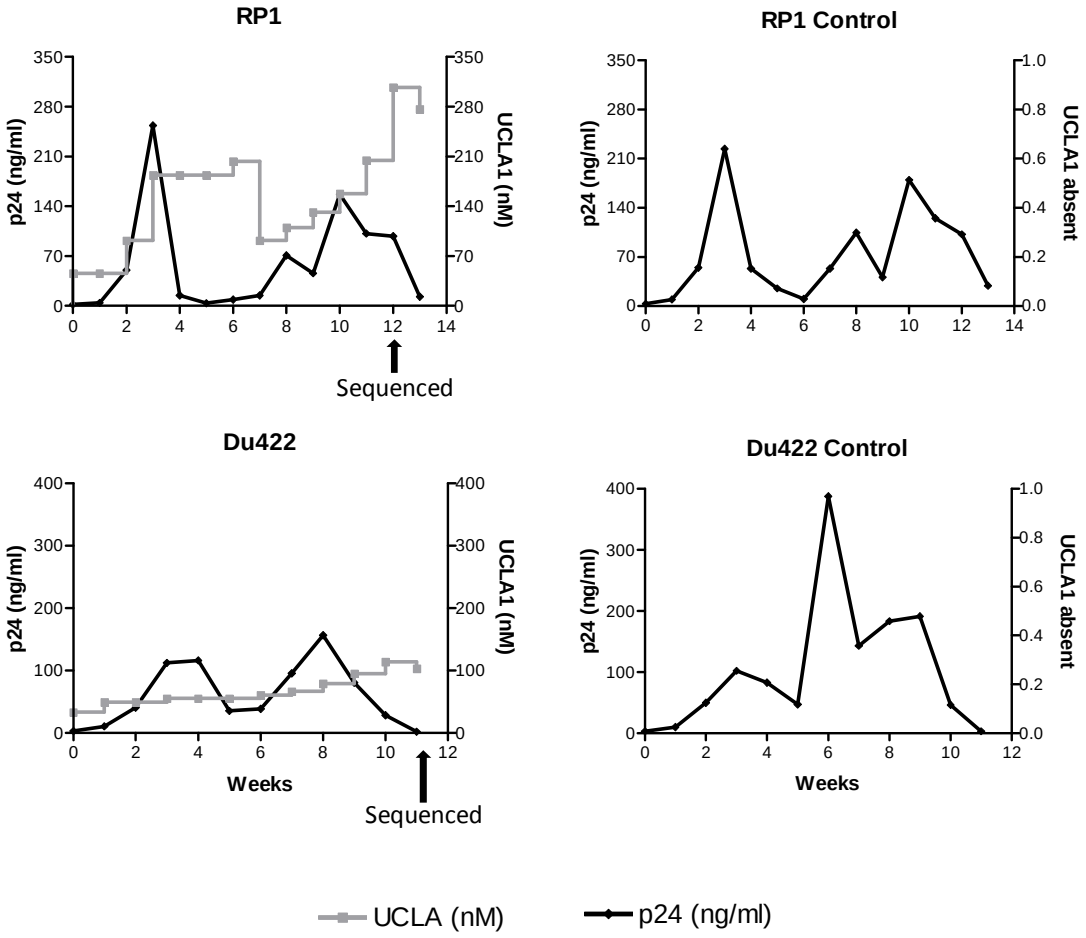

Figure 4-7: In vitro selection for UCLA1 resistant viruses.
HIV-1 subtype C primary isolates (RP1 and Du422) were cultured in PBMCs with increasing concentrations of UCLA1 for a maximum of 12 weeks. The concentration of the aptamer was increased only when p24 production in the culture with UCLA1 was similar or higher than the control culture. RP1 and Du422 were isolated and sequenced at week 12 and 11, respectively.

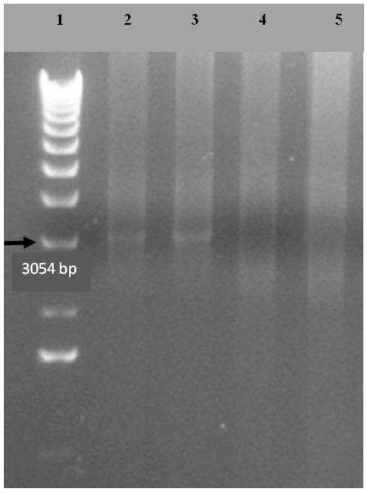

Figure 4-8: 2% agarose gel showing PCR amplified env genome of RP1.
The RP1 isolate was cultured with UCLA1 (lanes 2 and 3) and without (lane 4). Lanes 1 and 5 show a molecular weight marker and a negative control PCR, respectively.

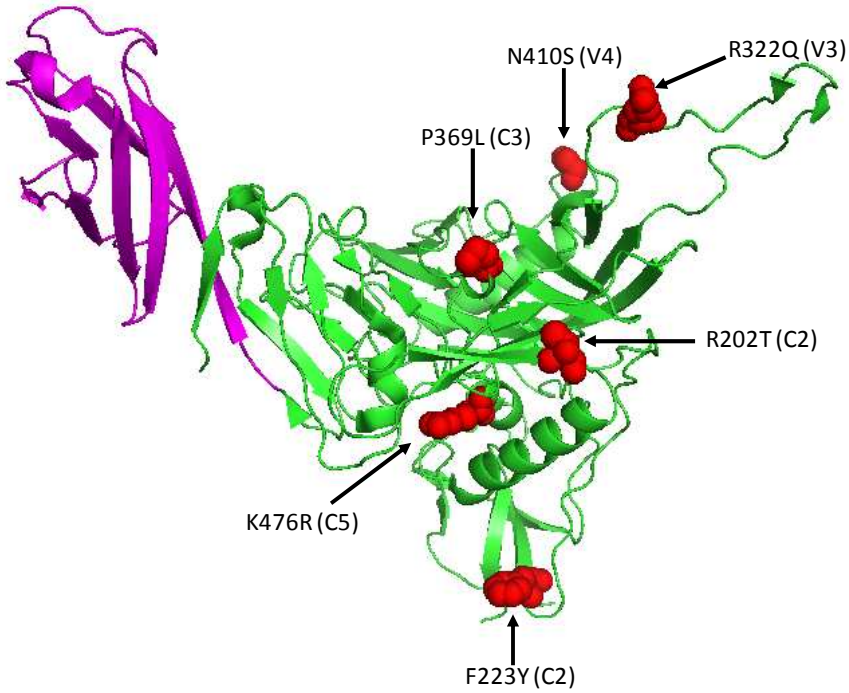

Figure 4-9: Structural representation of UCLA1 escape mutations generated under increasing concentrations of the aptamer.
Residues implicated in UCLA1 escape are in red spheres and their locations within gp120 are mentioned in parenthesis. The numbering is according to the HxB2 sequence. Coordinates were taken from the structure of gp120JRFL core with V3 ligated with CD4 and X5 (Protein Data Bank accession no. 2B4C). The X5 antibody is removed from the depicted structure. Gp120 is represented in green and CD4 in magenta. The structure was generated with PyMOL (DeLano Scientific LLC, South San Francisco, CA [http://www.pymol.org]).

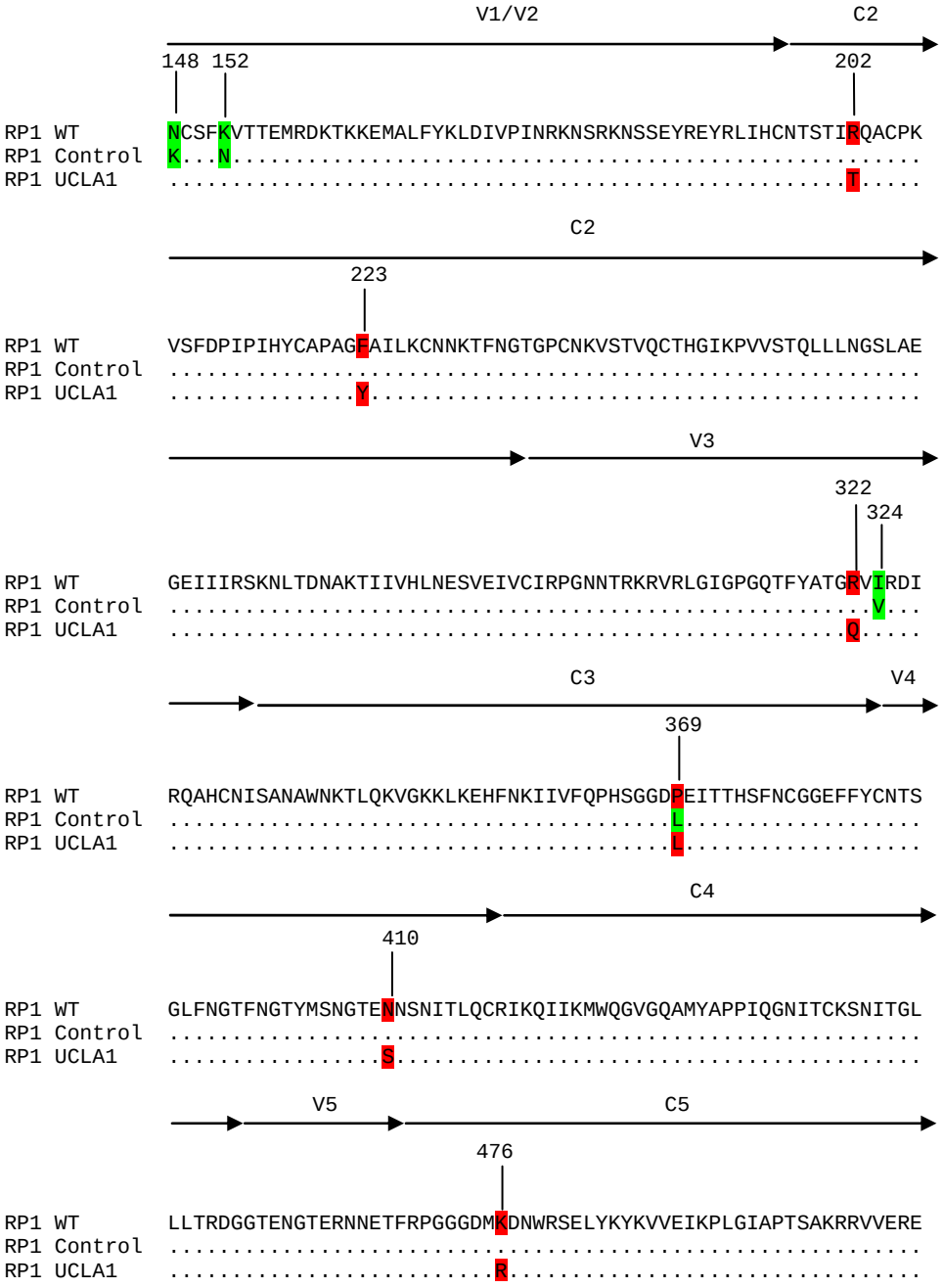

Figure 4-10: Amino acid sequence alignment of RP1 isolate propagated under increasing concentrations of UCLA1 (RP1 UCLA1).
The sequence from UCLA1 selected culture was compared with the wild-type RP1 sequence (RP1) and the sequence of the RP1 virus that was propagated without aptamer (RP1 Control). The amino acid changes that were observed after propagation, at 12 weeks, are highlighted in red for RP1 UCLA1 sequence and in green for the RP1 Control sequence. The numbering is according to the HxB2 sequence.

4. Discussion

UCLA1 RNA aptamer was used to inhibit entry of HIV-1 subtype C primary isolates into PBMC and macrophages. As observed with the Env-pseudotype viruses, there was no neutralization preference noted between viruses isolated from acute and chronic infections or between isolates from adult and paediatric patients. Thus, the data suggest that the efficacy of UCLA1 in PBMCs is not strain or tropism restricted since it was able to neutralize CCR5 and CXCR4 primary isolates. The aptamer was also non-toxic in PBMCs which confirmed that its neutralization efficiency was as a result of its activity as opposed to cell damage. UCLA1 escape mutations were observed at high concentrations of the aptamer, more than 5-fold of the IC_{50} values.

It was noted that UCLA1 showed higher efficiency against Env-pseudotyped viruses compared to primary isolates, as previously noted by others (Alexandre et al., 2010, Binley et al., 2004, Fenyo et al., 2009, Li et al., 2005). The reasons why UCLA1 was less potent in the PBMC and MDM assays are unknown but may be related to viral quasispecies, longer culture periods and inactivation of the aptamer. UCLA1 neutralized clinical isolates in MDMs with IC_{50} values in the nanomolar range (<14 nM) lower than PBMC values. It was interesting to note the higher efficiency of UCLA1 against macrophages. Blood monocytes and tissue macrophages are known to function as virus reservoirs *in vivo* and thus serve as obstacles to HIV clearance due to their contribution to persistence of HIV infection (Collin et al., 1991, Crowe et al., 2003, Meltzer et al., 1990). Therefore, with the enhanced potency against macrophages, UCLA1 can help to reduce infection of the reservoirs cells. Low p24 levels were observed in the MDM neutralization assays compared to macrophage-

tropic screening results. This was due to PBMC donor variability since the assays were performed on different days with new donor samples each day. Our PBMC and MDMs neutralization data concur with other studies that have utilized similar aptamers to inhibit HIV-1 subtype B R5-tropic viruses (Collin et al., 1991, Dey et al., 2005a, Khati et al., 2003, Moore et al., 2011). In this study, only R5-tropic primary viruses were competent to grow and get neutralized in MDMs. This might be due to viral entry determinants, that is, CD4 binding and co-receptor binding mechanisms. A previous study identified V3 loop determinants of macrophage-tropic viruses suggesting that a conformational change in the V3 loop increased exposure of the CD4bs (Duenas-Decamp et al., 2009). This was observed with the mapping of UCLA1 binding which revealed the V3 loop and the CD4 complex to be involved in modulating aptamer binding.

The study also demonstrated that the continuous propagation of HIV-1 subtype C primary isolates under increasing concentrations of UCLA1 resulted in escape mutations of the RP1 isolate whereas no mutations were generated by the Du422 isolate. The escape mutations that were inferred to confer resistance were those in the bridging sheet next to the V1/V2 loop (R202T) and within the V3 loop (R322Q) (Cohen et al., 2008, Mufhandu et al., 2012). The other detected mutations within the C2 region (R202T and F223Y) were not unexpected since a mutation within this region has been shown to decrease binding of the B40t77 aptamer to HIV-1_{BaL} gp120 (Joubert et al., 2010). This might be due to the fact that some of the B40t77 binding sites to gp120 are common to UCLA1 binding sites (Cohen et al., 2008, Joubert et al., 2010, Mufhandu et al., 2012). Nevertheless, the R202T mutation has

been shown not to have drastic effects on the binding of broadly neutralizing MAbs (Pantophlet et al., 2003, Walker et al., 2011, Walker et al., 2009). The observed P369L mutation within the CD4 and co-receptor binding complexes in the C3 region was observed earlier in this study by site-directed mutagenesis which suggested this residue as a peripheral site contributing in the modulation of the aptamers' reactivity. However, it was discovered in this study that the residue is highly unstable and that primary viruses can undergo random mutations with or without pressure from an inhibitor. The V3 loop mutation was also not unusual since we have shown the loop to be involved in UCLA1 binding by site-directed mutagenesis and ΔV3 and core gp120 truncations (Mufhandu et al., 2012). The V4 loop mutation (N410S) was observed for the first time in this study as an escape mutation with a potential to have an effect on aptamer binding to gp120. However, mutations within the V4 loop have been shown to decrease binding of b6, b12 (Pantophlet et al., 2003), PG16 (Walker et al., 2009) and PG135 MAbs to gp120 (Walker et al., 2011). Thus, a probable similar effect of the N410S mutation against to gp120 was observed. The mutated residue observed in the α5-helix (K476R) has been identified as one of the essential sites in anti-core antibody binding and for optimal viral infectivity (Pietzsch et al., 2010, Scheid et al., 2009). The site is highly conserved across different clades of HIV-1 and is predominantly represented as R476. The high degree of conservation correlates to viral fitness, as mutating the epitope results in loss of infectivity (Pietzsch et al., 2010). Therefore, the RP1 isolate probably generated the K476R mutation in order to gain fitness and survive the high concentrations of UCLA1. Ideally, all the observed mutations were supposed to be cloned to make mutated Env pseudoviruses for further testing to confirm their role in UCLA1

resistance. Regrettably, due to time constrains, the mutations could not be tested further.

On the contrary, it cannot be ruled out that the inferred resistance might be due to the mutations that enhance other aspects of virus replication. For example, the HIV-1 Nef and Vpu accessory genes have been shown to be involved in HIV-1 replication and pathogenesis. Nef enhances HIV-1 cytoplasmic entry by fusion at the plasma membrane (Kawano et al., 1997, Schaeffer et al., 2001). It has also been suggested that the entry of HIV-1 through endocytosis is facilitated by Nef (Jere et al., 2010, Pizzato et al., 2008). The Vpu gene has been shown to down-regulate the CD4 receptor in the rough endoplasmic reticulum to prevent its continuous interaction with the HIV-1 envelope glycoprotein which may be detrimental to efficient viral replication and spread (Dube et al., 2010). Another function of the Vpu protein is to facilitate release of virus from infected cells (Hout et al., 2004). This transmembrane protein interacts with the CD4 molecule in the rough endoplasmic reticulum (RER), resulting in its degradation via the proteasome pathway. Vpu also has been shown to enhance virion release from infected cells.

It was interesting to note that the resistant virus was isolated from a chronic paediatric dual-tropic patient whereas the Du422 R5 virus isolated from an acutely infected adult patient was unable to produce mutations. This might suggest that the fitness level and stage of infection play significant roles in HIV-1 infection. The resistant virus isolated from a rapid progressor patient (Choge et al., 2006) suggests that the virus has a high fitness level. However, there's a need to test more isolates

to examine the stage of infection and tropism required to generate UCLA1 resistance.

Accordingly, the results indicate that UCLA1 has broad spectrum potency against HIV-1 subtype C primary isolates at low nanomolar concentrations, in different primary cell lines, suggesting probable *in vivo* efficiency although advanced assessment on bioavailability, stability and dose response analysis are required. The low rate of amino acid sequence changes associated with UCLA1 resistance suggests that the aptamer is not exerting excessive pressure on the virus probably due to the very low concentrations that are utilized. Since the study has shown that the aptamer is robust even at low nanomolar quantities, it might be an indication that UCLA1 can remain efficacious over longer periods of time provided that it is maintained at low concentrations.

CHAPTER 5

General Discussion and Conclusions

The innovation of the SELEX process to generate aptamers has created an opportunity to discover new ways to target HIV. Despite the fact that HIV-1 has evolved many strategies to avoid antibody recognition, the conserved regions in the envelope glycoprotein renders it an attractive target for alternative treatment options. The existence of anti-HIV-1 gp120 RNA aptamers demonstrates the efficiency of these oligonucleotides against HIV-1. These aptamers were isolated against a subtype B virus (HIV-1_{BaL}), and given that subtype C viruses are responsible for the majority of HIV-1 infections worldwide and more specifically in the sub-Saharan Africa, this work focused on using the aptamers to neutralize infection of subtype C viruses. Since the aptamers are RNA-based and require to be modified for stability, one solid-phase synthesised, highly modified aptamer (UCLA1) was mainly used during the course of the study.

A panel of subtype C viruses were characterized for their sensitivity to neutralization by UCLA1 aptamer. Overall, 83% of subtype C envelope clones and an average of 71% primary isolates exhibited sensitivity to UCLA1, with IC_{50} values of <1 nM and <35 nM, respectively. It was noted that the neutralization assay in TZM-bl cells is more sensitive than the primary isolate-based assays although UCLA1 was used at a higher concentration for both PBMC and MDM than for the TZM-bl assay. This has been observed previously with neutralizing MAbs where Env-pseudotyped viruses were more sensitive to neutralization by a wide spectrum of antibody specificities than were their PBMC parental viruses (Binley et al., 2004, Fenyo et al., 2009, Li et al., 2005). It has been suggested that this effect is due to the cells used to generate the pseudoviruses (Mascola et al., 2005) and not the nature of the target cells or the

clonal nature of the envelope (Li et al., 2005, Reeves et al., 2002). The presence of viral quasispecies, longer culture periods, nonspecific uptake by other cells, multiple replication cycles in the PBMC assay (Alexandre et al., 2010) or inactivation of the aptamer in the culture probably account for the differences. Other factors that could account for the discrepancy are differences in CCR5 density (Choudhry et al., 2006), the CD4:CCR5 ratio (Polonis et al., 2008), effects of cellular proteins incorporated into the viral membrane (Beausejour & Tremblay, 2004, Louder et al., 2005, Rizzuto & Sodroski, 1997) and viral entry mechanisms of the two cell types (Miyauchi et al., 2009a). Nevertheless, the extra sensitivity of the Env-pseudotyped virus-based neutralization assay might be expected to generate false-positive and not false-negative outcomes (Gray et al., 2006).

UCLA1 lack of toxicity in both TZM-bl cells and PBMCs confirmed that its action was due to its efficacy and not cell toxicity The non cytotoxic nature of the aptamer extends recent findings which showed that the parental B40 aptamer was not toxic to PBMCs and human cardiomyocytes (Lopes de Campos et al., 2009). Both cell types remained 100% viable and metabolically functional even when exposed to up to 2 μM of the B40 aptamer (Lopes de Campos et al., 2009).

It was interesting to note the higher potency of UCLA1 against HIV-1 in macrophages (IC_{50}s $\leq$14 nM) compared with PBMCs (IC_{50}s <35 nM). Macrophage cells can be an obstacle to HIV-1 clearance within the body since they can be latently infected and thus serve as virus reservoirs. Only R5-tropic primary viruses thrived in MDM cultures. This is attributed to viral entry mechanisms, that is, the CD4 and CoR binding mechanisms. R5 or macrophage-tropism has been shown to

correlate with sensitivity to inhibitors of CD4-gp120 interactions (Brown et al., 2011, Duenas-Decamp et al., 2009, Gray et al., 2005, Peters et al., 2008) indicating that the macrophage tropic phenotype is strongly dependent on Env-CD4 binding affinity and/or exposure of the CD4bs. This is also confirmed by the high number of R5-tropic envelope clones that were neutralized in the TZM-bl assay, although the number of X4-tropic tested viruses was low. Similarly, variable sensitivity to CCR5 inhibitors has also been observed for macrophage-tropic viruses (Peters et al., 2008). A recent study employing a panel of R5 *env* sequences identified a correlation between entry efficiency and stable CD4 expression in $CCR5^{low}$ cell lines, suggesting that macrophage-tropic viruses could efficiently use low levels of co-receptor (Sterjovski et al., 2010). Inhibition by the CCR5 entry inhibitor maraviroc was also shown to be reduced in the R5-tropic viruses, implying that conformational changes that enhanced R5 binding also impaired small molecule inhibition (Sterjovski et al., 2010).

The breadth of UCLA1 neutralization against HIV-1 subtype C was observed at 83% for Env pseudoviruses, 75% for primary viruses in MDM assay and 67% for primary viruses in PBMC assay. Furthermore, the potency of UCLA1 was exhibited by IC_{50} range of 0.04-0.95 nM for Env pseudoviruses, 3.6-13.6 nM for the MDM assay and 7-35 nM for the PBMC assay. Thus, overall the breath and potency of UCLA1 was comparable to other HIV-1 entry inhibitors such as the lectins, Griffithsin (median IC_{50} 0.4 nM) and Cyanovirin-N (median IC_{50} 1.8 nM) (Alexandre et al., 2010); original prototype broadly neutralizing MAbs, IgG1b12 (median IC_{50} 6.9 µg/ml) and 4E10 (median IC_{50} 6.7 µM) (Li et al., 2006); CCR5 antagonists, Maraviroc median IC_{50} 0.69

nM (95% CI, 0.37–1.28 nM) (Dorr et al., 2005), TAK-220 (median IC_{50} 1.1 nM) (Takashima et al., 2005), CXCR4 antagonist, AMD3100 (median IC_{50} 4.0 nM) (Bridger et al., 1999, Schols, 2006); the recently published PGV04 (median IC_{50} 0.25 µg/ml) (Falkowska et al., 2012) and PGT MAbs (median IC_{50} 1.1 µg/ml) (Falkowska et al., 2012, Walker et al., 2011), VRC01 MAb (geometric mean IC_{50} 0.33 µg/ml) (Wu et al., 2010, Zhou et al., 2010), and PG9 (median IC_{50} 0.22 µg/ml) and PG16 MAb (median IC_{50} 0.25 µg/ml) MAbs (Walker et al., 2009).

In Chapter 2 it was comprehended that RNA aptamers require intense chemical modifications in order to remain stable against serum degradation and nucleases. The stability of UCLA1 was tested even further in another study (Moore et al., 2011). That is, another UCLA1 derivative (UCLA005) comprising of a terminal Cy5 dye at the 5'- end followed by three locked nucleic acid thymidines instead of the 5'-DMTr-C6-SS-C6 moiety of UCLA1 was generated and its stability tested in biological fluids (Moore et al., 2011). The aptamer was exposed to rectal or vaginal lavages for increasing lengths of time and analyzed by PAGE. Quantification of the residual full-length aptamer over time provided a measurement of the half-life of the aptamer in the lavages. The calculated half-lives demonstrated a large variability between the rectal samples (from <1 min to >24 h), and no statistically significant difference between rectal or vaginal samples was revealed (mean 100 *versus* 187 min). When the aptamer was further chemically modified for protection from degradation on all four of the most susceptible cleavage sites for vaginal nucleases, UCLA005v11, protection of all nucleotides resulted in a 4-fold increase in aptamer stability with a

half-life of 242 min (Moore et al., 2011). This data further confirmed the need for the intense modification of RNA aptamers for their increased stability.

UCLA1 binding mapped by site-directed mutagenesis revealed mutated residues that conferred resistance to be located within the CoRbs at the base of the V3 loop, in the CD4-induced epitope within the bridging sheet and the C4 domain (Kwong et al., 1998, Pantophlet et al., 2003, Rizzuto et al., 1998, Zhou et al., 2007). The data correlated with mapping by SPR using mutated and truncated gp120s which revealed less affinity for UCLA1 and the V-loop deleted gp120s as previously shown with related aptamers (Cohen et al., 2008, Dey et al., 2005b). The reduced UCLA1 affinity observed with I420R and D368R can be related to the decreased neutralization potency that was observed with these mutations using broadly neutralizing MAbs such as PGV04 (Falkowska et al., 2012) and PG16 (Walker et al., 2009). This data also substantiate the involvement of sites within the CD4-induced epitope (C3) and C4 domain of gp120. The implicated sites within the V3 loop, the bridging sheet next to the V1/V2 loop and the CD4-induced epitope were furthermore validated by UCLA1 escape mutations data. These sites were generated by one primary isolate under the selective pressure of increasing aptamer concentrations over time. The other tested isolate remained sensitive to UCLA1 over 11 weeks under increasing UCLA1 concentrations. Other implicated sites were within the V4 loop, between β4 and β5 sheets and next to the receptor binding complex in the α5 helix. These sites are reported for the first time in this study to modulate aptamer binding although mutations within the V4 loop have been shown to decrease binding of the b12 MAb (Pantophlet et al., 2003). Given that we have observed by site-

directed mutagenesis that UCLA1 has common binding sites to gp120 as b12, this infers that the newly identified V4 loop site might actually be involved in UCLA1 binding. However, site-directed mutagenesis is needed to confirm this.

The observed UCLA1 and b12 MAb synergy was interesting since both were shown to target the same epitopes (L369 and R419) (Pantophlet et al., 2003). This finding suggests that L369 and R419 might not be direct contact residues for UCLA1 but peripheral sites that modulate the aptamers' reactivity. Alternatively these agents might be transmitting an allosteric effect to the neighbouring protomers, thus increasing binding affinity or site accessibility. This confirms the finding that aptamer binding causes conformational changes on gp120 thus exposing distal sites that the aptamer can access and increase binding to gp120 as previously shown with the B40t77 aptamer against HIV-1_{BaL} gp120 (Joubert et al., 2010). Furthermore, an association between R5-tropic viruses and sensitivity to b12 has been demonstrated (Dunfee et al., 2009, Gray et al., 2005) thus substantiating the observed UCLA1 and b12 synergy.

Previous studies have also shown that the 299.5 aptamer and B40t77 aptamer epitopes overlap the base of the α1 helix next to the bridging sheet (β2 and β3), the CD4bs in the bridging sheet (β21 and β20) and the V3 loop (Cohen et al., 2008, Joubert et al., 2010). This is not surprising given that UCLA1, B40t77 and 299.5 are modified derivatives, possessing the same core structure which is suggested to be their binding core (Cohen et al., 2008, Dey et al., 2005a). Mapping data in this study also correlated with a previous competition study of B40t77 and various MAbs

(Joubert et al., 2010). That is, competition between B40t77 and b12 or b6 suggested shared binding sites possibly including L369 and R419 identified in this study. Competition between B40t77 and 17b or CD4 confirmed the L125 and L369 UCLA1 sites within the CD4 complex. Inhibition enhancement was observed when B40t77 was used together with the anti-V3 MAb, 19b, suggesting that the aptamer and the MAb have non-overlapping binding sites within the V3 loop (Joubert et al., 2010), thus confirming the identified V3 loop residues as part of the sites modulating UCLA1 binding. It was interesting to note that two of the V3 loop sites that were identified were shown to confer resistance to the CCR5 small molecule inhibitor, Vicriviroc, (Kuhmann et al., 2004, Marozsan et al., 2005, Ogert et al., 2008, Tsibris et al., 2008). The mutations were detected across three different subtypes (subtypes B and G), (Kuhmann et al., 2004, Ogert et al., 2008) and subtype C (Tsibris et al., 2008). This suggests that the residues form part of the specific sites that are exposed in the V3 loop when gp120 binds to the CD4 receptor (Huang et al., 2005, Xiang et al., 2010).

UCLA1 resistance could not be fully explained from the amino acid sequence alignments probably because other residues within gp120 modulate aptamer neutralization efficacy. In addition, the presence of resistance-associated mutations in some sensitive viruses in both the TZM-bl and PBMC sequence alignments attests to the complex nature of resistance and brings into question the value of these types of analyses. Furthermore, there might be distal conformational changes that reduce binding affinity of the aptamer to gp120 as previously shown with the B40t77 aptamer against HIV-1_{BaL} gp120 (Joubert et al., 2010).

The escape mutations assay revealed that the aptamer was more robust against R5-tropic, acute infection strain while the dual-tropic chronic infection isolate was able to escape the high concentrations of the aptamer. This is the first study to report the generation of escape mutations against anti-gp120 aptamers. Nonetheless, the mutations have to be confirmed as the cause of UCLA1 resistance. Regrettably due to time constrains, the escape cultures were not propagated for longer periods of time. Thus, further studies with more primary isolates and a longer assay period will contribute to a better understanding of HIV-1 escape mechanism from neutralizing aptamers. Furthermore, isolation of aptamers against subtype C HIV-1 gp120 will divulge any discrepancies in efficiency against subtype C isolates when compared with UCLA1 which was isolated from a subtype B strain. Although humanized mice have been tested for cell-type specific delivery of siRNA for the treatment of HIV-1 infection (Neff et al., 2011, Wheeler et al., 2011), more studies with humanized mice and non-human primates are essential to validate safety and efficacy of aptamers.

The overall robustness of UCLA1 observed in this study makes it an excellent candidate for therapy against HIV-1 subtype C infection. As discussed above, the stability of an aptamer plays a major role in its efficiency rate. A more stabilized version of UCLA1, named UCLA005v11, is already available for downstream applications such as a microbicide (Moore et al., 2011). Since the aptamer has been shown in this study to have synergism with other entry inhibitors, it can be tested in combination with other microbicides such as tenofovir which has been shown to be efficient against 39% of subtype C infections at a clinical trial level (Sokal et al., 2012). The aptamer can also be explored for aptamer-mediated targeted delivery

systems against HIV-1 gp120 as previously described as siRNA-aptamer chimeras (Zhou et al., 2008) and aptamer sticky bridge –siRNA conjugates (Zhou et al., 2009) against HIV *tat/rev* proteins. Thus, the aptamer warrants for further testing in clinical trials especially against HIV-1 subtype C infection.

APPENDICES

APPENDIX A

Ethics Clearance

UNIVERSITY OF THE WITWATERSRAND, JOHANNESBURG

Division of the Deputy Registrar (Research)

HUMAN RESEARCH ETHICS COMMITTEE (MEDICAL)
R14/49 Mufhandu

CLEARANCE CERTIFICATE	**PROTOCOL NUMBER M070449**
PROJECT	Human immunodeficiency virus - host interactions: Analysis of endemic SA clinical isolates of HIV-1 using anti-gp120 aptamers
INVESTIGATORS	Ms HT Mufhandu
DEPARTMENT	School of Pathology
DATE CONSIDERED	07.05.04
DECISION OF THE COMMITTEE*	APPROVED UNCONDITIONALLY

Unless otherwise specified this ethical clearance is valid for 5 years and may be renewed upon application.

DATE 07.05.31 **CHAIRPERSON** .....
(Professors PE Cleaton-Jones, A Dhai, M Vorster, C Feldman, A Woodiwiss)

*Guidelines for written 'informed consent' attached where applicable

cc: Supervisor : Morris L Prof

DECLARATION OF INVESTIGATOR(S)

To be completed in duplicate and **ONE COPY** returned to the Secretary at Room 10005, 10th Floor, Senate House, University.

I/We fully understand the conditions under which I am/we are authorized to carry out the abovementioned research and I/we guarantee to ensure compliance with these conditions. Should any departure to be contemplated from the research procedure as approved I/we undertake to resubmit the protocol to the Committee. **I agree to a completion of a yearly progress report.**

PLEASE QUOTE THE PROTOCOL NUMBER IN ALL ENQUIRIES

APPENDIX B

General suppliers

Aalto BioReagents, Ireland

AEC-Amersham, South Africa

Applied Biosystems, South Africa

Becton Dickinson Labware Falcon, South Africa

Biocom biotech, South Africa

Biomerieux, South Africa

Bio-Rad, South Africa

Caltag Laboratories, Thailand

Corning Incorporated, South Africa

Costar Corning Incorporated, South Africa

GE Healthcare, South Africa

GE Healthcare, Sweden

Gibco Invitrogen, South Africa

Inqaba Biotec, South Africa

Invitrogen, South Africa

Merck, South Africa

Merck Millipore, South Africa

Promega, South Africa

Qiagen, South Africa

R&D Systems, South Africa

Roche, South Africa

Santa Cruz Biotechnology, South Africa

Sartorius Stedim biotech, South Africa

Separations Scientific, South Africa

Sigma-Aldrich, South Africa

Stratagene, South Africa

The Scientific Group, South Africa

TriLink Biotechnologies, USA

Whitehead Scientific, South Africa

APPENDIX C

General Materials and Methods

1.1 Agarose gel electrophoresis

PCR products (DNA) were resolved on a 1% agarose gel by electrophoresis. Agarose (Sigma-Aldrich, South Africa) gels were prepared in 1 × TBE containing 5 µl of 0.5 µg/ml ethidium bromide. The DNA samples were mixed 1:1 with DNA loading buffer (Inqaba Biotec) and electrophoresed for 1 hr at 100 V in 1 × TBE buffer. A DNA molecular weight marker X (Promega) was used as a reference for the size of DNA fragments in the sample. The DNA fragments were detected by ultraviolet illumination using the Molecular Imager ChemiDoc XRS+ Imaging System (Bio-Rad, France).

1.2 Ethanol precipitation

Isolated RNA was precipitated by addition of 0.1 vol. of 3 M sodium acetate (pH 5.2) (Sigma-Aldrich) and 2.5 vol. of absolute ethanol (Sigma-Aldrich) at -80°C overnight. The RNA was then pelleted by centrifugation at 14 000 rpm (4°C) for 30 min, washed with 1 ml of 80% ethanol followed by centrifugation at 14 000 rpm (4°C) for 5 min to remove residual salt. The wash was repeated twice and the pellet was air-dried and then re-suspended in dd$H_2$0.

1.3 Quantification of DNA and RNA

The concentrations of the DNA and RNA were respectively determined by measuring UV absorbance at 260 nm using the NanoDrop ND-1000 spectrophotometer

(Thermo Fisher Scientific, South Africa). The purity of the nucleic acids was determined by the $OD_{260/280}$ ratio. Pure DNA and RNA have a value of approximately 1.5 and 2.0, respectively.

1.4 Denaturing polyacrylamide gel electrophoresis

RNA transcripts were analysed on a denaturing (8 M urea) 11% polyacrylamide gel consisting of 4.8 g urea (Merck), 2.7 ml 40% Bis-acrylamide (Sigma-Alrich) and 1 ml 10 × TBE. The mixture was made up to 10 ml with ddH_2O and polymerized by addition of 50 µl 10% APS (Sigma-Alrich) and 10 µl TEMED (Merck). The polymerized gel was pre-run for 30 min at 200 V. Before loading into the gel, the transcripts were mixed with the RNA loading dye (Inqaba Biotec) and run for 30 min at 200 V followed by ethidium bromide (Sigma-Aldrich) staining of the gel for visualization. The RNA aptamers were heat denatured at 70℃ for 5 min, cooled down at room temperature for 10 min and refolded with 5 × refolding buffer (10 mM HEPES pH 7.4, 150 mM NaCl, 1 mM $CaCl_2$, 1 mM $MgCl_2$ and 2.7 mM KCl) before use.

1.5 Plasmid DNA purification

Mutated ConC plasmid DNA cultures were purified with the QIAprep Spin Miniprep Kit (Qiagen, South Africa) following the manufacturer's protocol. Briefly, the LB-kanamycin culture medium was centrifuged at 5 000 rpm for 10 min at 4ºC to pellet the bacterial cells. The culture supernatant was discarded and the cells were then re-suspended in 250 µl proprietary buffer P1 with RNase A and LyseBlue and mixed thoroughly in order to break the cell clumps. The bacterial cells were further lysed

with 250 µl of buffer P2 and then precipitated with 350 µl of buffer N3. The cell solutions were then centrifuged at 13 000 rpm for 10 min to pellet the lysed cells and the supernatants were then centrifuged in QIAprep spin columns for 60 s. The spin columns were washed twice for 60 s with 500 µl buffer PB and 750 µl buffer PE, respectively. The DNA was then eluted with 100 µl of the elution buffer and quantified on the Nanodrop spectrophotometer (Appendix C, section 1.3).

1.6 Purification of DNA in sequencing reaction

The DNA sequencing reactions were purified using the sodium acetate (NaOAc) purification method. Briefly, 50 µl of 1:25 dilution of 100% ethanol (EtOH) and 3 M NaOAc (Sigma-Aldrich), pH 4.6 was added to the sequencing reactions, mixed and centrifuged at 2 000 g for 30 min. The supernatant was discarded and the pellets washed with 100 µl of chilled 70% EtOH by centrifugation at 2 000 g for 5 min. The supernatant was discarded and the pellets were dried at 65ºC for 3 min. The dry DNA pellet was stored at 4ºC and ready to be resolved on the ABI 3100 automated genetic analyzer. The sequences were assembled and edited using Sequencher 4.0 software (Gene Codes, United States).

1.7 Isolation of HIV-1 RNA

Isolation of viral RNA from frozen aliquots of primary viruses grown under increasing concentrations of UCLA1 was performed using the QIAamp mini spin viral isolation kit (QIAGEN, South Africa) according to the manufacturer's protocol. Briefly, 140 µl of the cultured virus supernatant was added to 560 µl of viral lysis buffer AVL with carrier RNA, mixed and incubated at room temperature for 10 min for viral lysis. The

RNA was washed by centrifugation for 1 min at 8 000 rpm with 560 µl of 100% ethanol in spin columns. The ethanol wash was repeated and the columns washed with 500 µl of lysis buffer AW1. The last wash was by centrifugation at 13 000 rpm for 3 min with 500 µl of lysis buffer AW2. The columns were further centrifuged at 8 000 rpm for 1 min and the RNA was eluted into clean collection tubes by spinning 40 µl of elution buffer AVE at 8 000 rpm for 1 min. A double elution was performed for increased RNA yields. The RNA was either stored at -70 ℃ for later use or used immediately for RT-PCR.

1.8 DNA purification

1.8.1 PCR purification

The PCR products (DNA) were purified with the QIAquick PCR purification Kit (QIAGEN) according to the manufacturer's protocol. Five volumes of buffer were added to 1 volume of the PCR product, mixed and the DNA was bound to the membrane of the in spin columns by centrifugation at 13 000 rpm for 1 min. The DNA was washed with 750 µl of buffer PE by spinning as above and the residual wash buffer removed by an additional 1 min spin. The DNA was eluted by spinning 30 µl of the elution buffer at 10 000 rpm for 2 min. The DNA was resolved on a 1% agarose gel by electrophoresis as outlined above. The purified DNA was quantified on the Nanodrop spectrophotometer as described (chapter 2, section 2.3.7).

1.8.2 Gel purification

The DNA was gel purified when multiple bands were observed after PCR purification. The QIAquick gel purification kit (QIAGEN) was used according to the

manufacturers' instructions. Briefly, the DNA fragment was excised from the agarose gel and weighed. Three volumes of solubilisation and binding buffer QG was added to 1 volume of gel (100 mg ~ 100 µl), mixed and incubated at 50ºC for 10 min or until the gel was completely dissolved. One gel volume of isopropanol was added to the sample for increased DNA yields and mixed. The DNA was bound to the spin columns by centrifugation at 13 000 rpm for 1 min. The DNA was washed by spinning as above with 500 µl of buffer QG followed by 750 µl of buffer PE. The DNA was eluted into clean collection tubes with 30 µl elution buffer and spinning as above. The purified DNA was quantified on the Nanodrop spectrophotometer.

APPENDIX D

Supplementary Figures

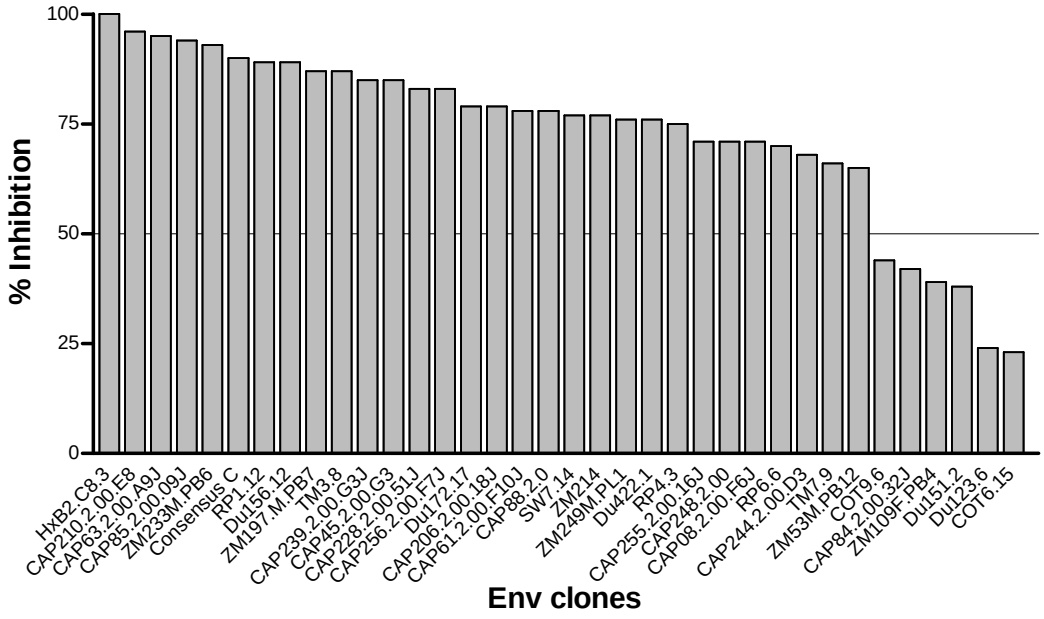

Supplementary Figure 1: Neutralization of a panel of subtype C HIV-1 Env-pseudotyped viruses with UCLA1 RNA aptamer.
Neutralization was measured as a reduction of virus infectivity relative to the virus control (without aptamer). The graph depicts representative percentage inhibition of each virus tested. The viruses were neutralized within a range of 65-100% inhibition. The IC_{50} points are indicated with the dotted line. The six resistant viruses are included at <45% inhibition.

A

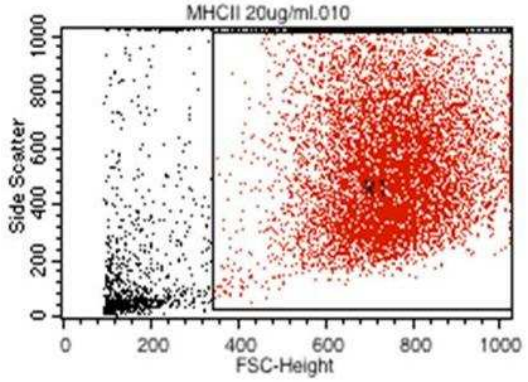

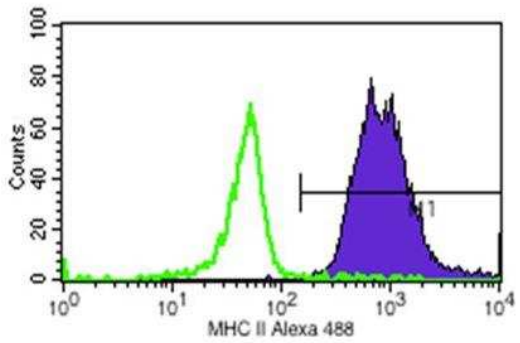

Sample ID: MHCII 20ug/ml
Acquisition Date: 20-Nov-09
Gate: G1
Gated Events: 8698
Total Events: 10000

Marker	Events	% Gated	% Total
All	8698	100.00	86.98
M1	8696	99.98	86.96

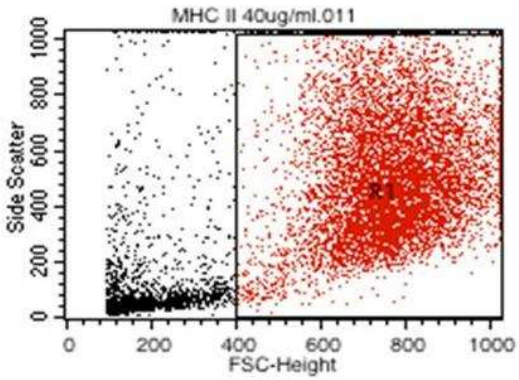

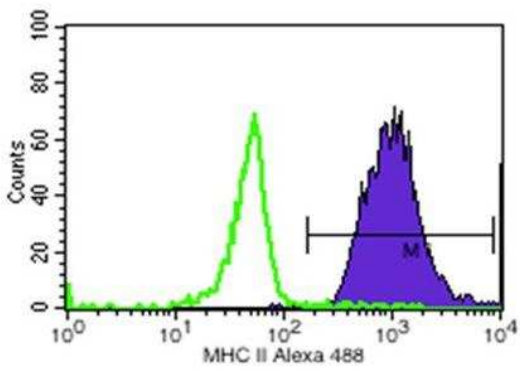

Sample ID: MHCII 40ug/ml
Acquisition Date: 20-Nov-09
Gate: G1
Gated Events: 7895

Marker	Events	% Gated
All	7895	100.00
M1	7719	97.77

B

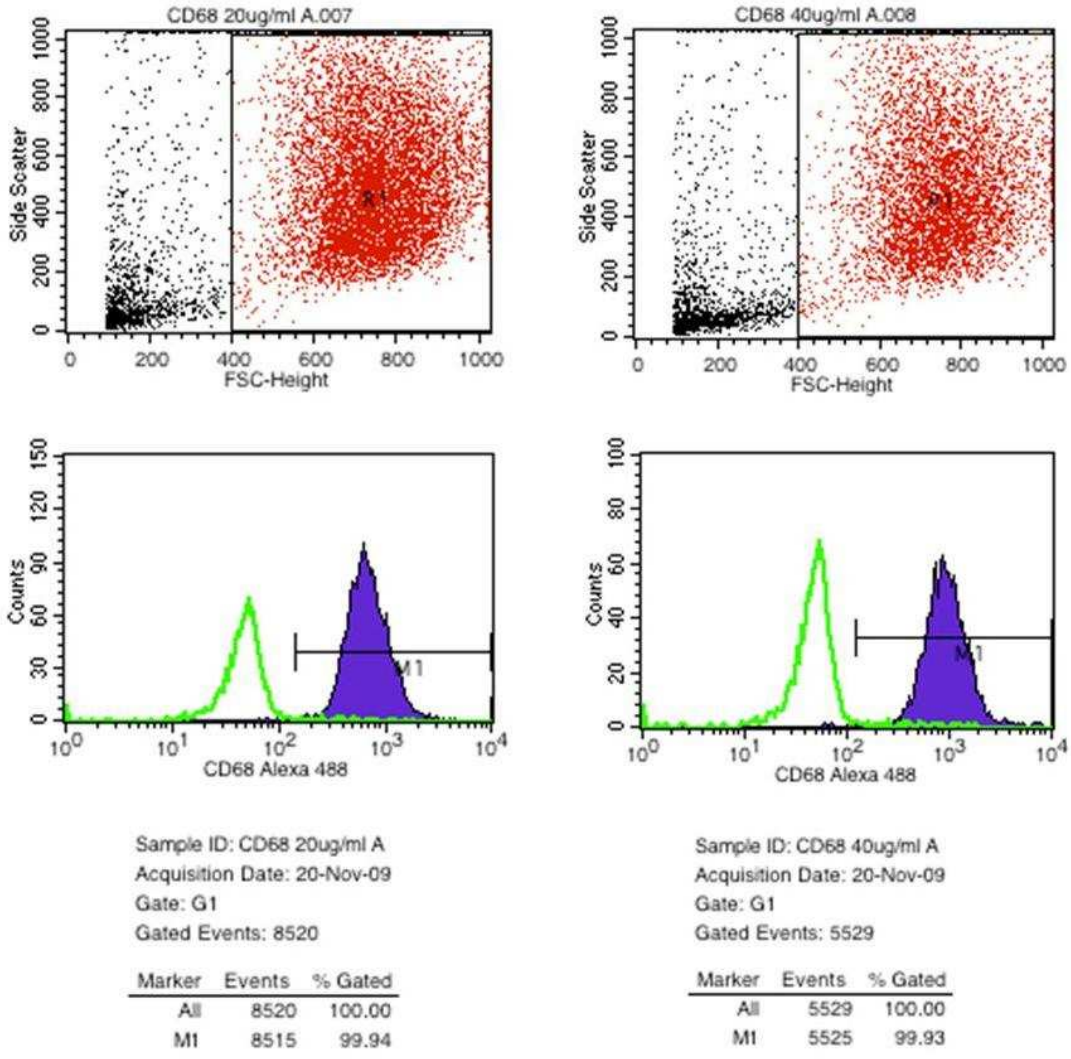

Sample ID: CD68 20ug/ml A
Acquisition Date: 20-Nov-09
Gate: G1
Gated Events: 8520

Marker	Events	% Gated
All	8520	100.00
M1	8515	99.94

Sample ID: CD68 40ug/ml A
Acquisition Date: 20-Nov-09
Gate: G1
Gated Events: 5529

Marker	Events	% Gated
All	5529	100.00
M1	5525	99.93

Supplementary Figure 2: FACS dot plots and histograms showing the phenotype of the differentiated macrophages
(A) FACS staining was performed with MHC II and AF 488 MAbs both titrated at 20 µg/ml and 40 µg/ml. The R1 region illustrates the total acquired cell population. The M1 region depicts the positively stained macrophages. (**B)** Staining performed with CD68 and AF 488 MAbs both titrated at 20 µg/ml and 40 µg/ml illustrating the phenotype of differentiated macrophages. The R1 region shows the total acquired cell population. The M1 region represents the positively stained macrophages.

Supplementary Tables

Supplementary Table 1: Primers used to sequence gp160 envelope gene.

Primer Name[a]	Primer Sequence
E175r	CTA TTT TGT GCA TCA GAT GCT AAA
EnvBf	TTA ACA CAA GCC TTG CCA AAG GT
A589r	CAG AGT GGG GTT AAC TTT ACA C
Ar	TGC TGC TCC CAA GAA CCC AA
Df	AGC ACA TTG TAA CAT TAG T
Mf	GGA GGA GAT ATG AGG GAC AAT TGG
E210f	TAA CAA ATT GGC TGT GGT ATA TAA
CTr	GAC TTC CCA GAT ACT TAA GAG CTT CCC ACC

[a]f and r in primer names denotes the forward and reverse direction of the primer sequences respectively.

Supplementary Table 2: **Replication of the RP1 isolate in PBMCs under escalating concentrations of UCLA1 over a maximum period of 84 days. The RP1 replication (p24) rate and inhibition (IC_{50}) rate in the presence of UCLA1 were monitored and compared to the control wells without aptamer over time. The percentage of UCLA1 concentration was not recorded when the aptamer concentration was unchanged.**

RP1

	UCLA1 p24 (ng/ml)	Control p24 (ng/ml)	UCLA1 IC_{50} (nM)	UCLA1 concentration % increase/decrease
Day 0	1.9	3.5	33.0	
Day 7	4.2	9.4	33.0	
Day 14	50.6	54.6	65.7	100% Increase
Day 21	253.6	223. 3	184.0	100% Increase
Day 28	45.9	83.6	131.4	100% Increase
Day 35	3.9	25.1	131.4	
Day 42	9.0	10.0	145.0	10% Increase
Day 49	14.6	53.4	65.7	
Day 56	71.0	104.5	78.6	20% Increase
Day 63	46	41.0	94.3	20% Increase
Day 70	157.2	180.0	113.0	20% Increase
Day 77	102	125.0	146.4	30% Increase
Day 84	97.8	102.3	219.6	50% Increase

Supplementary Table 3: Replication of the Du422 isolate in PBMCs under escalating concentrations of UCLA1 over a maximum period of 11 weeks. Du422 replication rate (p24) rate and inhibition (IC_{50}) rate in the presence of UCLA1 were monitored and compared to the control wells without aptamer over time. The percentage of UCLA1 concentration was not recorded when the aptamer concentration was unchanged.

Du422

	UCLA1 p24 (ng/ml)	Control p24 (ng/ml)	UCLA1 (nM)	UCLA1 concentration % increase/decrease
Day 0	2.94	3.08	23.6	
Day 7	10.58	9.85	35.4	50% Increase
Day 14	40.45	49.81	35.4	
Day 21	112	102	39.3	
Day 28	116.67	82.93	39.3	
Day 35	35	47	39.3	
Day 42	38.56	387.77	43.2	10% Decrease
Day 49	95.57	143.14	47.5	10% Increase
Day 56	156.56	183.57	56.6	20% Increase
Day 63	80.8	191.39	67.8	20% Increase
Day 70	28.08	46.18	81.4	20% Increase
Day 77	1.9	3	73.6	10% Decrease

APPENDIX E

Publication

Hazel T. Mufhandu, Elin S. Gray, Maphuti C. Madiga, Nancy Tumba, Kabamba B. Alexandre, Thandeka Khoza, Constantinos Kurt Wibmer, Penny L. Moore, Lynn Morris and Makobetsa Khati.

UCLA1, a Synthetic Derivative of a gp120 RNA Aptamer, Inhibits Entry of Human Immunodeficiency Virus Type 1 Subtype C.

Journal of Virology, 2012, **86(9)**:4989-4999.

Journal of Virology

UCLA1, a Synthetic Derivative of a gp120 RNA Aptamer, Inhibits Entry of Human Immunodeficiency Virus Type 1 Subtype C

Hazel T. Mufhandu, Elin S. Gray, Maphuti C. Madiga, Nancy Tumba, Kabamba B. Alexandre, Thandeka Khoza, Constantinos Kurt Wibmer, Penny L. Moore, Lynn Morris and Makobetsa Khati

J. Virol. **2012, 86(9):4989. DOI: 10.1128/JVI.06893-11.**
Published Ahead of Print 29 February 2012.

Updated information and services can be found at:
http://jvi.asm.org/content/86/9/4989

These include:

SUPPLEMENTAL MATERIAL http://jvi.asm.org/content/suppl/2012/04/03/86.9.4989.DC1.html

REFERENCES This article cites 58 articles, 30 of which can be accessed free at: http://jvi.asm.org/content/86/9/4989#ref-list-1

CONTENT ALERTS Receive: RSS Feeds, eTOCs, free email alerts (when new articles cite this article), more»

Information about commercial reprint orders: **http://jvi.asm.org/site/misc/reprints.xhtml**
To subscribe to to another ASM Journal go to: **http://journals.asm.org/site/subscriptions/**

Journals.ASM.org

Downloaded from http://jvi.asm.org/ on April 10, 2012 by guest

JVI Journals.ASM.org

UCLA1, a Synthetic Derivative of a gp120 RNA Aptamer, Inhibits Entry of Human Immunodeficiency Virus Type 1 Subtype C

Hazel T. Mufhandu,[a] Elin S. Gray,[b] Maphuti C. Madiga,[b] Nancy Tumba,[b] Kabamba B. Alexandre,[b] Thandeka Khoza,[a] Constantinos Kurt Wibmer,[b] Penny L. Moore,[b] Lynn Morris,[b,c] and Makobetsa Khati[a,d]

Emerging Health Technologies Platform, Biosciences Unit, CSIR, Pretoria, South Africa[a]; AIDS Virus Research Unit, National Institute for Communicable Diseases, Johannesburg, South Africa[b]; University of the Witwatersrand, Johannesburg, South Africa[c]; and Department of Medicine, Groote Schuur Hospital and University of Cape Town, Cape Town, South Africa[d]

Entry of human immunodeficiency virus type 1 (HIV-1) into cells is mediated by the virion surface envelope (Env) glycoproteins, making it a desirable target for antiretroviral entry inhibitors. We previously isolated a family of gp120 binding RNA aptamers and showed that they neutralized the infectivity of HIV-1. In this study, we assessed the activity of a shortened synthetic derivative of the B40 aptamer, called UCLA1, against a large panel of HIV-1 subtype C viruses. UCLA1 tightly bound to a consensus HIV-1 subtype C gp120 and neutralized isolates of the same subtype with 50% inhibitory concentrations (IC_{50}s) in the nanomolar range. The aptamer had little toxicity in tests with cell lines and primary cells. Furthermore, it exhibited high therapeutic indices, suggesting that it may be effective at very low doses. Mapping of UCLA1 binding sites on gp120 revealed eight amino acid residues that modulated neutralization resistance. This included residues within the coreceptor binding site, at the base of the V3 loop, and in the bridging sheet within the conserved V1/V2 stem-loop of gp120. The aptamer was also shown to have synergistic effects with T20, a gp41 fusion inhibitor, and IgG1b12 (b12), an anti-CD4 binding site monoclonal antibody. These results suggest that UCLA1 may be suitable for development as a potent HIV-1 entry inhibitor.

Human immunodeficiency virus type 1 (HIV-1) binding to T lymphocytes and macrophages is mediated by the glycoprotein gp120, which sequentially interacts with the CD4 receptor and chemokine receptors of the susceptible host cell (3, 4). While gp120 is a heterogeneous molecule with hypervariable loops and extensive glycosylation (27, 28, 52), the CD4 binding site and coreceptor binding site (CoRbs) are both highly conserved (43) and immunogenic (51, 54). Other invariant regions on gp120 include the epitopes defined by the newly isolated broadly neutralizing monoclonal antibodies (MAbs) PG9/16 and PGT127/128 (48, 49), making gp120 a desirable target for agents that block virus entry (35).

Entry inhibitors comprise an array of molecules that target either the virus envelope glycoprotein or host cellular receptors. This includes MAbs, fusion inhibitors, coreceptor antagonists, and small molecule inhibitors (5, 22, 29, 35, 45). Some of these have proven to be effective additions to the reverse transcriptase and protease inhibitors that are presently used to treat HIV-1 infection and are also being considered in prevention science. Artificial nucleic acid ligands called aptamers, which assume a defined three-dimensional structure and generally bind functional sites on their respective targets (15), have been isolated against gp120 and are being developed as potential HIV-1 entry inhibitors (10, 13, 14, 25, 36, 53–56). Aptamers are selected through several rounds of amplification, and they bind a wide range of macromolecules, including those with low immunogenicity or high toxicity (38, 50). They are able to discriminate between targets based on subtle structural changes such as the presence or absence of a methyl or hydroxyl group (38). Due to their high specificity, aptamers can be directed against very defined targets; as a result, they have been applied to a wide range of therapeutics, especially for cancer treatment (54). They can be used to transport inhibitory molecules to specific cells, reducing the off-target effects seen in current treatments (54). Studies have looked at chemically binding or cosynthesizing aptamers and small interfering RNA (siRNA) so that they can be selectively targeted to cells expressing relevant receptors (7, 54). Their small size increases bioavailability and provides access to many biological compartments (24). Furthermore, preparation is fast and simple, allowing for easy scale-up of production.

We have previously isolated 2′-fluoro-substituted RNA aptamers against HIV-1_{BaL} gp120 and shown that they neutralized infectivity of group M and group O HIV-1 clinical isolates in cell-based assays (25). One extensively studied aptamer called B40 was used to produce B40t77, a shortened derivative comprising 77 nucleotides. Subsequently a synthetic, capped derivative of B40t77 called UCLA1 (10) was manufactured by solid-phase synthesis and further shortened and modified to help folding and stability, without compromising its activity (10). The B40 aptamer and its shortened derivatives (B40t77 and UCLA1) have been shown to contact the highly variable exterior surfaces of monomeric and trimeric gp120 and to bind conserved core residues in the CCR5-binding site (10, 13, 14, 23). In one study, using an aptamer related to UCLA1 (aptamer 299.5), mutations within the V3 loop and the bridging sheet (β20) were identified using JR-CSF gp120 monomers (10). In another study, using HIV-1_{BaL} gp120 from viral supernatants (trimeric gp120), mutations in the α1 helix, C2 domain, V3 loop, bridging sheet (β21), and F loop within the C4 domain affected the binding of the B40t77 aptamer (23). While

Received 24 November 2011 **Accepted** 17 February 2012
Published ahead of print 29 February 2012
Address correspondence to Makobetsa Khati, mkhati@csir.co.za.
Supplemental material for this article may be found at http://jvi.asm.org/.
Copyright © 2012, American Society for Microbiology. All Rights Reserved.
doi:10.1128/JVI.06893-11

Downloaded from http://jvi.asm.org/ on April 10, 2012 by guest

some sites were common, discrepancies between these two studies were likely related to the use of different sources of gp120 and different aptamers. In general, both studies suggest that an epitope of the gp120 RNA aptamers overlaps the base of the α1 helix, the CD4-induced binding sites in the bridging sheet (β21 and β20), and the variable loops (F and V3).

Since HIV-1 subtype C dominates the global HIV/AIDS epidemic and is endemic in countries with high HIV-1 prevalence rates such as South Africa (47), where this study was conducted, we assessed the sensitivity of a large panel of subtype C isolates derived from adult and pediatric patients at different stages of HIV-1 infection against UCLA1. We examined its neutralization efficacy and identified the potential binding sites. Furthermore, we evaluated cell viability in the presence of the aptamer and its synergism with other entry inhibitors. Overall, these studies suggest that UCLA1 has properties that make it suitable for further development as a potential HIV-1 entry inhibitor.

MATERIALS AND METHODS

RNA aptamers. The B40t77 and UCLA1 (University of California, Los Angeles) anti-gp120 RNA aptamers were used in this study. B40t77 aptamer (77 nucleotides in length) is a truncated derivative of the full-length B40 RNA aptamer (117 nucleotides in length) previously shown to have anti-HIV inhibitory activity (13, 23, 25). UCLA1 is a derivative of aptamer 299.2, which is a shortened derivative (54 nucleotides in length) of B40t77 (10, 13). The 299.2 aptamer was stabilized by the use of six 2′-O-dimethylallyl ribonucleotides in the short stem 1 together with the insertion of an additional base pair in stem 2 (10). As a result, UCLA1 (also 54 nucleotides in length) is made up of the 299.2 aptamer and chemically modified by the addition of an inverted thymidine at the 3′ end (to block degradation by 3′-exonucleases) and a dimethoxyltrityloxy-$(CH_2)_6$-SS-$(CH_2)_6$-phospho linker at the 5′-end (10). UCLA1 is chemically modified for protection against nucleases and to enhance correct folding and increase its stability for *in vivo* usage (10, 36, 44). An initial batch of UCLA1 was donated for this study by William James, University of Oxford. Subsequent batches were custom synthesized by ATDBio, Ltd., Southampton, United Kingdom.

Cell lines, antibodies, envelope-encoding plasmids, plasma samples, and HIV-1 primary isolates. The TZM-bl cells used for neutralization assay were obtained from the National Institutes of Health (NIH) Reference and Reagent Program. The 293T cells used for transfection were obtained from the American Type Culture Collection (Manassas, VA). The Du151 Env-expressing plasmid (31), Env-pseudotyped viruses, and replication-competent viruses were obtained from the AIDS Virus Research Unit at the National Institute for Communicable Diseases (NICD). The HIV-1 consensus C (ConC) envelope construct was obtained from Feng Gao (26). An HIV-1-positive plasma pool (BB pool) prepared from individual plasma samples as previously described by Li et al. (31), was purchased from the South African National Blood Services in Johannesburg and used as a positive control. IgG1b12 MAb (b12) (NIH Reference and Reagent Program) and T20 fusion inhibitor (Roche, Palo Alto, CA) were obtained from the NICD.

Expression of recombinant HIV-1 consensus C gp120. HIV-1 ConC gp120 was expressed in 293T cells, purified by affinity chromatography using a *Galanthus nivalis* lectin agarose matrix (Sigma-Aldrich, Sweden), and eluted with 1 M methyl-α-D-mannopyranoside (Sigma), as previously described (20). The purity, size, and homogeneity of the protein were assessed using sodium dodecyl sulfate-polyacrylamide gel electrophoresis (SDS-PAGE) and Western blotting as previously described (19). The biological activity of pure proteins was assessed by enzyme-linked immunosorbent assay (ELISA) as previously described (19). Truncated and mutated ConC glycoproteins were generated at the NICD. These included the core gp120 (a mutant that lacks the V1/V2 and V3 loops) (28) and V1/V2-deleted (ΔV1/V2) and V3-deleted (ΔV3) gp120s, as well as gp120 with either the I420R mutation in the CoRbs or the D368R mutation in the CD4 binding site (CD4bs) (32, 40).

Site-directed mutagenesis. Specific amino acid changes in the ConC gp120 were introduced using the QuikChange site-directed mutagenesis kit (Stratagene, La Jolla, CA). The presence of mutations was confirmed by sequence analysis using an ABI Prism BigDye terminator cycle sequencing ready reaction kit (Applied Biosystems, Foster City, CA) and an ABI 3100 automated genetic analyzer. The sequences were assembled and edited using Sequencher (version 4.0) software (Gene Codes, Ann Arbor, MI).

Binding kinetics of RNA aptamers to recombinant HIV-1 consensus C gp120. The BIAcore 3000 surface plasmon resonance (SPR) technology (GE Healthcare) was used to determine the binding kinetics of RNA aptamers to recombinant HIV-1 ConC gp120 with the CM5 biosensor chip by direct amine coupling as described previously (10, 13, 14, 23). The RNA aptamers (UCLA1 and B40t77) were kin injected over the covalently immobilized synthetic HIV-1 ConC gp120. The aptamers were diluted in 1× refolding buffer prior to injection, as previously described (23). Binding kinetics to measure the association and dissociation constants of the aptamers from the protein were measured by kin injecting ½ $\log_{10}$ serial dilutions of the aptamers at a flow rate of 5 μl/min with a 5-min association phase and a 10-min dissociation phase. The BIAcore was also used to determine the binding kinetics of UCLA1 to truncated and mutated HIV-1 ConC gp120 compared to the binding kinetics of the wild-type ConC gp120. The truncated gp120s were the core, ΔV1/V2, and ΔV3 gp120. The core gp120 lacks amino acid residues 128 to 194 (V1/V2 loop) and 298 to 329 (V3 loop), ΔV1/V2 gp120 lacks amino acid residues 128 to 194, and ΔV3 gp120 lacks amino acid residues 298 to 329 (12, 28). The residues are numbered according to HxB2 numbering. The mutated gp120s contained single mutations in the CD4bs (D368R) or CoRbs (I420R). Each experiment was performed at least three times in triplicate using three neighboring flow cells, and the fourth flow cell served as a negative control. The association (K_a) and dissociation (K_d) constants of the resulting data curves were separately fitted to a 1:1 Langmuir binding model and analyzed using the BIAevaluation 4.1 software to obtain the equilibrium dissociation constant (K_D) values. The negative control flow cell and buffer effects were subtracted as a baseline.

Cytotoxicity assay. The cytotoxicity of UCLA1 RNA aptamer was determined by using two cell viability assays. The ATP-based CellTiter-Glo luminescent cell viability assay (Promega) was used as previously described (33). A tetrazolium compound [3-(4,5-dimethylthiazol-2-yl)-5-(3-carboxymethoxyphenyl)-2-(4-sulfophenyl)-2H-tetrazolium, inner salt; MTS]-based CellTiter 96 aqueous cell proliferation assay (Promega) was also used according to the manufacturer's protocol. That is, the dehydrogenase enzymes found in metabolically active cells converts a tetrazolium compound (MTS) into aqueous, soluble formazan which is then quantified by measuring absorbance at 490 nm. The assay was performed in both TZM-bl cells and peripheral blood mononuclear cells (PBMCs). The TZM-bl cells were used at 5×10^5 cells/well in 50 μl Dulbecco's modified Eagle's medium (DMEM) with 5% fetal bovine serum (FBS). The phytohemagglutinin/interleukin-2-stimulated (PHA/IL-2) peripheral blood mononuclear cells (PBMCs) were used at 5×10^4 cells/well in 50 μl RPMI 1640 with 5% FBS. Both cell types were incubated with 500 nM (50 μl) 2-fold serially diluted UCLA1 in triplicate for 72 h at 37°C. The cells used for positive control cultures were treated with etoposide phosphate, an anticancer agent that inhibits topoisomerase II enzyme, which aids in DNA unwinding, thus causing DNA strands to break (39). The positive control cells were incubated with 50 μl of 142 μM etoposide phosphate in triplicate for 72 h at 37°C in 5% CO_2 and 95% humidity. Untreated cell cultures were used as negative controls. The MTS-phenazine methosulafte (PMS) solution (20 μl) was then added to each well and incubated for 4 h at 37°C. To measure the amount of soluble formazan produced by cellular reduction of the MTS, absorbance was recorded at 490 nm using the ELISA plate reader. Titers were calculated as CC_{50} values indicating a 50% reduction in relative light units or in absorbance com-

Downloaded from http://jvi.asm.org/ on April 10, 2012 by guest

TABLE 1 Inhibition of HIV-1 subtype C envelope pseudotype viruses by UCLA1 RNA aptamer

Env clone	Subtype	Patient	Stage of infection	Tropism	Accession no.	% inhibition by 50 nM UCLA1[a]	IC_{50} (nM)[b]	TI[c]
HXB2.C8.3	B	Adult	Chronic	X4	AF358142	**98.5 ± 1.73**	0.17	5,882
CAP63.2.00.A9J	C	Adult	Acute	R5	EF203973	**90.8 ± 3.24**	0.14	7,143
ZM233 M.PB6	C	Adult	Acute	R5	DQ388517	**87.8 ± 4.98**	0.04	25,000
CAP210.2.00.E8	C	Adult	Acute	R5	DQ435683	**87.5 ± 6.82**	0.09	11,111
Du156.12	C	Adult	Acute	R5	DQ411852	**86.0 ± 2.37**	0.63	1,587
CAP85.2.00.09J	C	Adult	Acute	R5	EF203985	**84.5 ± 8.50**	0.04	25,000
ZM197.M.PB7	C	Adult	Acute	R5	DQ388515	**83.7 ± 3.14**	0.38	2,632
Consensus C	C	Synthetic		R5	DQ401075	**82.8 ± 6.12**	0.10	10,000
RP1.12	C	Pediatric	Chronic	X4	DQ447271	**81.5 ± 8.66**	0.60	1,667
CAP256.2.00.C7J	C	Adult	Acute	R5	EF203981	**78.8 ± 3.41**	0.16	6,250
CAP45.2.00.G3J	C	Adult	Acute	R5	DQ435682	**77.0 ± 10.88**	0.30	3,333
CAP228.2.00.51J	C	Adult	Acute	R5	EF203968	**76.6 ± 6.06**	0.31	3,226
CAP61.2.00.E11J	C	Adult	Acute	R5	EF203959	**76.5 ± 1.73**	0.38	2,632
ZM214 M.PL15	C	Adult	Acute	R5	DQ388516	**76.0 ± 1.15**	0.23	4,348
SW7.14	C	Adult	Chronic	X4	AF411966	**74.5 ± 4.04**	0.73	1,370
TM3.8	C	Pediatric	Chronic	R5	DQ447268	**74.2 ± 9.71**	0.13	7,692
ZM249 M.PL1	C	Adult	Acute	R5	DQ388514	**74 0.0 ± 1.31**	0.55	1,818
CAP88.2.00.B5J	C	Adult	Acute	R5	EF203972	**73.8 ± 4.37**	0.95	1,053
Du172.17	C	Adult	Acute	R5	DQ411853	**72.3 ± 8.12**	0.60	1,667
CAP239.2.00.F5J	C	Adult	Acute	R5	EF203984	**72.0 ± 8.35**	0.19	5,263
CAP255.2.00.16J	C	Adult	Acute	R5	EF203982	**70.0 ± 0.89**	0.28	3,571
Du422.1	C	Adult	Acute	R5	DQ411854	**69.8 ± 4.96**	0.33	3,030
CAP08.2.00.F6J	C	Adult	Acute	R5	EF203976	**69.7 ± 1.37**	0.95	1,053
CAP206.2.00.8J	C	Adult	Acute	R5	EF203967	**68.2 ± 11.06**	0.66	1,515
CAP248.2.00	C	Adult	Acute	R5	FJ229824	**68.0 ± 3.30**	0.62	1,613
RP6.6	C	Pediatric	Chronic	R5	DQ447269	**67.5 ± 2.78**	0.44	2,273
CAP244.2.00.D3	C	Adult	Acute	R5	DQ435684	**67.0 ± 1.15**	0.44	2,273
RP4.3	C	Pediatric	Chronic	R5	DQ447270	**66.3 ± 6.71**	0.48	2,083
TM7.9	C	Pediatric	Chronic	R5	DQ447267	**63.8 ± 1.58**	0.16	6,250
ZM53 M.PB12	C	Adult	Acute	R5	AY423984	**62.0 ± 4.65**	0.75	1,333
COT9.6	C	Pediatric	Chronic	R5	DQ447272	46.3 ± 2.25	NT	ND
CAP84.2.00.32J	C	Adult	Acute	R5	EF203963	46.0 ± 3.78	NT	ND
ZM109F.PB4	C	Adult	Acute	R5	AY424138	39.7 ± 9.48	NT	ND
Du151.2	C	Adult	Acute	R5	DQ411851	33.0 ± 10.50	NT	ND
Du123.6	C	Adult	Acute	R5	DQ411850	32.3 ± 13.69	NT	ND
COT6.15	C	Pediatric	Chronic	R5	DQ447266	30.0 ± 8.08	NT	ND

[a] Average percentage of inhibition of the respective Env-pseudotyped viruses by the UCLA1 aptamer used at a concentration of 50 nM. Viruses that exhibited more than 50% inhibition (values in boldface) were considered sensitive to neutralization. The average percentage of inhibition ± SD is shown for triplicate data.

[b] IC_{50} is the concentration of the UCLA1 aptamer that inhibited entry of the respective viruses by 50%. Viruses for which titers were not determined (NT) and which exhibited less than 50% inhibition were considered not neutralized.

[c] TI values were obtained by the general formula CC_{50}/IC_{50}. TIs could not be determined (ND) for viruses for which titers were not determined.

pared to the aptamer control after subtracting the background (without aptamer). Thus, CC_{50} is the concentration of the aptamer that would cause cytotoxicity or inhibit cell viability by 50%.

Production of pseudovirus stocks. Env-pseudotyped virus stocks were generated, and the 50% tissue culture infective doses ($TCID_{50}$) were quantified as previously described (17, 19, 34). These were derived from the CAPRISA 002 acute infection study cohort (18), subtype C reference panel (31), pediatric and AIDS patients' isolates (9, 17), and a subtype C consensus sequence clone (ConC) (26). The subtype C pseudoviruses were all R5 strains, except for RP1 and SW7, which were X4 viruses (Table 1). An X4-tropic subtype B pseudovirus, HxB2 reference strain, was also used. A pseudovirus with the vesicular stomatitis virus G (VSV-G) envelope gene was used as the negative control. The mutated ConC gp120 virus stocks were generated, and their $TCID_{50}$s were quantified as previously described (17, 19, 34).

Single-cycle neutralization assay. Neutralization was measured as a reduction in luciferase gene expression after a single-round infection of TZM-bl cells with Env-pseudotyped virus as previously described (17, 34). UCLA1 was tested at a maximum initial concentration of 50 nM and was 3-fold serially diluted in DMEM with 5% FBS without dextran. The positive control BB pool was used at an initial dilution of 1:45. The assay was performed at least three times, in duplicate, for each pseudovirus tested. Titers were calculated as inhibition concentration (IC_{50}) or reciprocal plasma dilution (ID_{50}) values causing 50% reduction of relative light units compared to the virus control (without inhibitor) after subtracting the background (without virus).

Neutralization of primary infectious viruses. Neutralization was measured as a reduction of p24 antigen production of HIV-1 subtype C primary isolates in PHA-stimulated PBMCs as described previously (1, 6). The neutralization assay was performed with 500 $TCID_{50}$s of HIV-1 primary isolate in 3-fold serially diluted UCLA1 at an initial concentration of 100 nM in 40 μl of RPMI 1640 medium supplemented with 5% FBS, 5% interleukin-2 (IL-2), and gentamicin (50 μg/ml) (growth medium). The culture supernatant was collected on days 3, 5, and 7 and replaced with an equal amount of fresh growth medium. For each harvest, the p24 antigen concentration was measured by ELISA using the Vironostika HIV-1 antigen Microelisa system (bioMérieux, Boseind, Netherlands), according to the manufacturer's instructions. The assay was performed at least three

Downloaded from http://jvi.asm.org/ on April 10, 2012 by guest

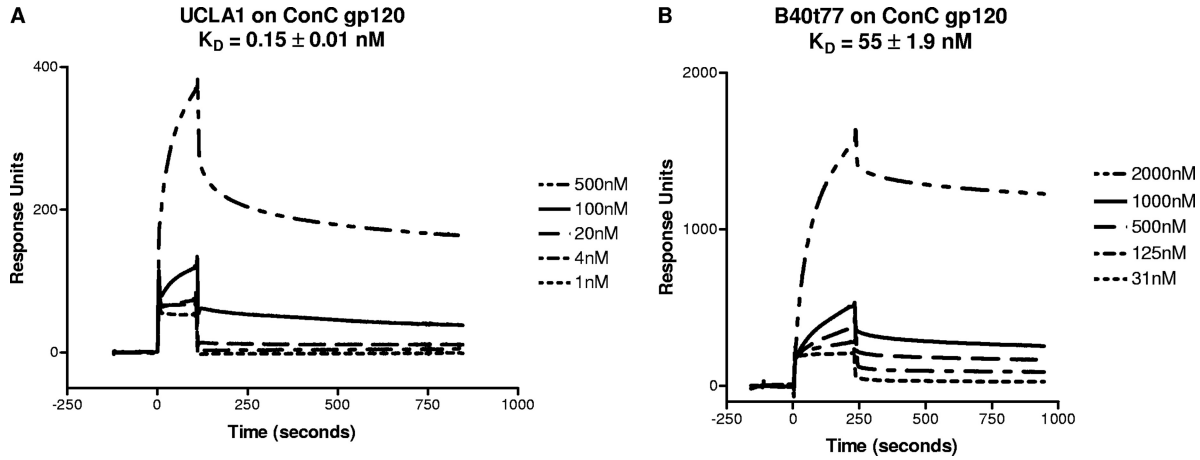

FIG 1 (A) BIAcore sensorgram showing the equilibrium dissociation constant (K_D) of UCLA1 from a synthetic HIV-1 ConC gp120. The aptamer was simultaneously injected over the immobilized gp120 at ½ $\log_{10}$ dilutions with the initial concentration at 500 nM followed by 100 nM, 20 nM, 4 nM, and 1 nM. (B) BIAcore sensorgram showing the K_D of B40t77 aptamer from HIV-1 ConC gp120. The aptamer was simultaneously injected over the immobilized gp120 at 2-fold dilutions with the initial concentration at 2,000 nM, followed by 1000 nM, 500 nM, 125 nM, and 31 nM.

times, in triplicate, for each primary isolate tested. The IC_{80} values were calculated as p24 antigen titers causing 80% reduction of p24 antigen production compared to the virus control (without inhibitor).

Synergy of UCLA1 with other entry inhibitors. UCLA1 was tested for synergism with the CD4bs MAb, b12, and the T20 fusion inhibitor. The single-cycle neutralization assay was used to test a total of 6 Env-pseudotyped viruses with UCLA1-T20 and UCLA1-b12 combinations. The agents were mixed in a fixed ratio that reflected their relative individual potency. The aptamer was used at a maximum initial concentration of 50 nM, while b12 and T20 were used at a maximum initial concentration of 50 μg/ml, equivalent to 312 μM and 11,131 μM, respectively. The assay was performed at least three times in duplicate for each virus tested. The synergy was quantified and expressed as a combination index (CI) using the IC_{50}s (8). Calculation of the CI was based on the Chou-Talalay equation: $CI = (D)_1/(Dx)_1 + (D)_2/(Dx)_2$, in which $(Dx)_1$ and $(Dx)_2$ in the denominators are the concentrations of agent 1 and agent 2 alone that are required to neutralize the HIV-1 subtype C Env pseudovirus, and D_1 and D_2 in the numerators are the concentrations of agent 1 and agent 2 when used in combination that also neutralize the virus. A CI value of less than 1, equal to 1, or more than 1, indicates synergism, an additive effect, and antagonism, respectively (8, 59). A dose reduction index (DRI) was also determined for each combination therapy used. The DRI is a measure of how many fold the dose of each compound in a synergistic combination may be reduced at a given effect level compared with the doses of each compound alone. The DRI was calculated using the Chou-Talalay equation: that is, DRI_1 and DRI_2 are the first and second terms of the CI equation, respectively. Therefore, $DRI_1 = (Dx)_1/(D)_1$ and $DRI_2 = (Dx)_2/(D)_2$ (8, 37, 59).

RESULTS

Binding of RNA aptamers to recombinant HIV-1 consensus C gp120. In order to determine the binding kinetics of B40t77 (unmodified aptamer) and UCLA1 (modified aptamer) to ConC gp120, the protein was immobilized onto a CM5 chip to obtain the dissociation equilibrium constant (K_D) values. A tight binding of the UCLA1 to ConC gp120 was observed with an average K_D of 0.15 nM, a standard deviation (SD) of the mean of 0.01, and a χ^2 value of 1.8 ± 0.7 (Fig. 1A). A χ^2 value of less than 2 demonstrates an acceptable fit of the data to the binding model exhibiting appropriate binding of the aptamer to the gp120 (23). The B40t77 aptamer exhibited higher K_D values than UCLA1, with an average K_D of 55 ± 1.9 nM and a high χ^2 value of 31 ± 5.4 (Fig. 1B). These data established that the modified aptamer had higher binding affinity for gp120 compared to the unmodified aptamer, and thus for all further experiments, we made use of the higher-affinity UCLA1 aptamer.

UCLA1 neutralization of Env-pseudotyped viruses. UCLA1 was tested in the TZM-bl neutralization assay against a panel of *env*-pseudotyped viruses isolated from adult and pediatric patients at different stages of HIV infection. The aptamer inhibited entry of 29 of 35 (83%) subtype C viruses by >50% (range, 62 to 91%), (Table 1). Six viruses showed a reduced sensitivity with <46% neutralization and were considered to be resistant. Of the 29 subtype C viruses neutralized by UCLA1, 27 were R5-tropic and two were X4-tropic strains. The HxB2 (IIIB) virus, which is an X4 subtype B lab-adapted reference strain and generally neutralization sensitive, was almost completely neutralized (99%) by UCLA1 (Table 1).

All viruses' titers were determined against a 3-fold serially diluted UCLA1 starting at 50 nM to calculate IC_{50}s. The IC_{50}s were less than 1.0 nM, with an average of 0.8 ± 0.9 nM for all of the 29 sensitive viruses (Table 1). Representative graphs are shown for 9 sensitive and 3 resistant viruses (see Fig. S1 in the supplemental material). UCLA1 neutralized the sensitive viruses in a dose-dependent manner, while the curves of the 3 resistant viruses did not reach the 50% cutoff, although they were sensitive to the positive control from HIV-infected donors (BB pool) (see Fig. S1). The UCLA1 neutralization curves often exhibited gradual slopes that reached a plateau at less than 100% neutralization, in contrast to curves for the BB pool, which exhibited sharp slopes. Although neutralization curves with similar profiles have been reported previously using MAbs, the mechanism for this is not well understood (21, 41, 49).

Neutralization of HIV-1 primary isolates. To determine the ability of UCLA1 to inhibit HIV-1 subtype C infection of primary cells, neutralization assays were performed using infectious subtype C clinical isolates in PBMCs. Viral infection was measured by p24 ELISA after 5 days of culture. Four of the 6 (67%) primary isolates were neutralized by UCLA1 in a dose-dependent manner

Downloaded from http://jvi.asm.org/ on April 10, 2012 by guest

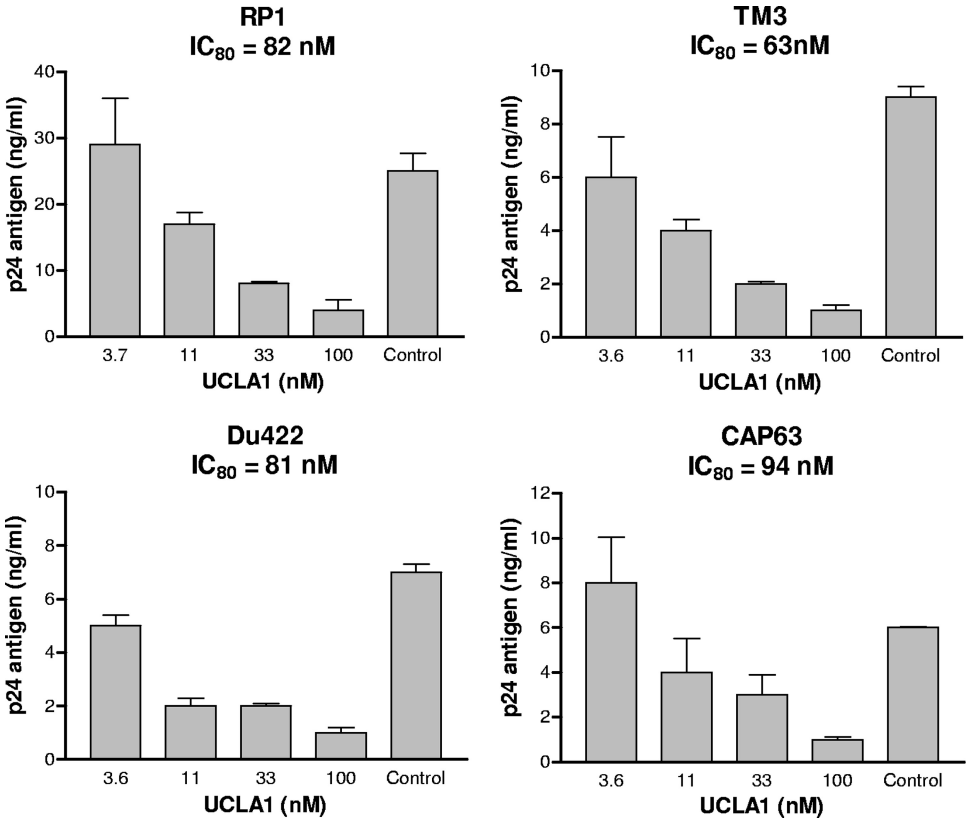

FIG 2 UCLA1 neutralization of HIV-1 subtype C primary isolates in PBMCs. UCLA1 was used at a starting concentration of 100 nM. The IC_{80} values were calculated as p24 antigen titers causing 80% reduction of p24 antigen production compared with the virus control (without UCLA1). The bars represent a dose-dependent inhibition of the p24 antigen by UCLA1. The assay was performed at least three times, in triplicate, for each primary isolate tested.

(Fig. 2). The concentration of the aptamer that inhibited 80% of virus infection (IC_{80}) was within a range of 63 to 94 nM. The 4 included primary viruses isolated from acutely infected adults (Du422 and CAP63) and chronically infected infants (RP1 and TM3), all of which used CCR5, except RP1, which was X4 (Table 1). Two isolates (SW7 and Du156) were not neutralized by UCLA1 in the PBMC assay despite their corresponding cloned envelopes being neutralized in the TZM-bl assay (Table 1). Indeed there was no correlation between the degrees of inhibition for each of the 4 sensitive viruses when the two assays were compared (Table 1 and Fig. 2).

UCLA1 is not cytotoxic and has a wide therapeutic index. The cytotoxicity of UCLA1 was first examined in TZM-bl cells with the ATP-based CellTiter-Glo luminescent cell viability assay. The cells remained 90 to 100% viable after 24 h of incubation with 500 nM UCLA1 (Fig. 3). The aptamer was further tested for cytotoxicity in both PBMCs and TZM-bl cells with the MTS-based CellTiter 96 aqueous cell proliferation assay. The PBMCs exhibited an average viability of 99% ± 0.11%, while the TZM-bl cells had an average viability of 95% ± 0.11%, after 72 h of incubation (Fig. 3). Both cell types were tested with a maximum concentration of 500 nM UCLA1. TZM-bl cells incubated with etoposide phosphate, which was used as a positive control, showed 3% ± 1% viability compared to PBMCs, which showed 36% ± 1% viability.

The estimated therapeutic index (TI) of the aptamer was calculated using the general formula TI = CC_{50}/IC_{50}, for all of the tested viruses. Since 90 to 100% of the cells remained viable after incubation with a maximum concentration of 500 nM UCLA1, we estimated the CC_{50} to be ≥twice the maximum concentration of the aptamer (i.e., 1,000 nM). Thus, the TI was calculated at a standard CC_{50} of 1,000 nM. The average estimated TI of UCLA1 was therefore 5,096 ± 2,285 (range, 25,000 to 1,053) for the 83% neutralized subtype C Env-pseudotype viruses (Table 1).

Mapping aptamer neutralization sites using the ConC Env-pseudovirus. The amino acid residues involved in sensitivity to neutralization were determined using a panel of 19 single site-directed point mutations made in the ConC Env-pseudotyped virus (Table 2). Six of these (K121A, I307A, R419A, K421A, I423A, and A440E) were selected based on published data that implicated these sites in aptamer binding (10, 23). Two additional published residues (R298 and P299) could not be tested due to low virus yields. Five mutations (S365I, S375M, V430A, F468V, and G471E) were included based on sequence alignment of the tested Env-pseudoviruses that were neutralized by the aptamer compared to those that were not neutralized. The remaining 8 mutations (L125A, K305A, R308A, H330Y, N332A, L369P, D474A, and R476A) were selected from available constructs since they were within the CD4bs and CoRbs of gp120. Of the 19 single point mutants tested, 8 conferred resistance to the aptamer in a single-cycle neutralization assay, with all exhibiting IC_{50}s of >10 nM and a range of 10- to 30-fold effect compared to wild-type virus (Fig. 4A and Table 2). A schematic representation of the location of

Downloaded from http://jvi.asm.org/ on April 10, 2012 by guest

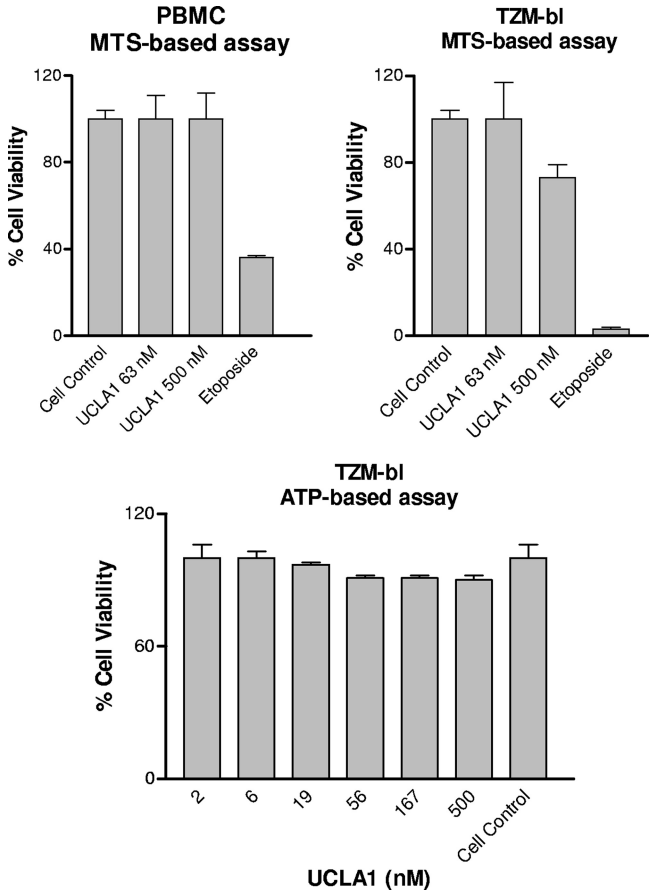

FIG 3 Percentage viability of TZM-bl cells and PBMCs in the presence of various concentrations of UCLA1. Two different assays were used to assess the cytotoxicity of the aptamer. The ATP-based assay was used to test the viability of TZM-bl cells, and the MTS-based assay was used to test the viability of both the TZM-bl cells and PBMCs. Etoposide phosphate was used in the positive control cultures of the MTS-based assay. Untreated cell cultures were used as negative controls. The assays were done three times in triplicate.

these residues on gp120 is shown in Fig. 4B. Overall, the mutations were found within the CoRbs at the base of the V3 loop (K305A, I307A, R308A, and H330Y), in the bridging sheet within the conserved V1/V2 stem-loop of gp120 (K121A and L125A), and within the C4 region (R419A) and the CD4-induced epitope in the C3 region (L369P).

Mapping aptamer binding sites using ConC gp120 proteins. To further explore the dependence of UCLA1 on regions of gp120, we examined the binding kinetics to core gp120 as well as ΔV1/V2 gp120 and ΔV3 gp120. In addition, gp120 proteins containing a single mutation in the CD4bs (D368R) or the CoRbs (I420R) were also tested. The relative K_Ds for each of these proteins are shown in Fig. 5, and the corresponding sensorgrams are shown in Fig. S2 in the supplemental material. For core gp120, the average K_D was 0.7 ± 0.9 nM, which was ~5-fold higher than the K_D of wild-type ConC gp120 (0.15 ± 0.01 nM), confirming the role of variable loops in aptamer binding. Indeed, contributions from both V1/V2 and V3 were evident based on the average K_D values for ΔV1/V2 (0.4 ± 0.1 nM) and ΔV3 (0.5 ± 0.1 nM) gp120s. Interestingly, similar levels were obtained for the I420R and D368R gp120s, sites which could not be tested by neutralization as these viruses are nonfunctional, but which nevertheless confirm the CoRbs and the CD4bs as modulating sites for aptamer binding. While these binding data generally support the neutralization data, it is important to note that assessing epitopes on monomeric gp120 is inherently different from assessing those found on the trimeric complex on the viral membrane. This was evident with Du151, whose pseudotyped virus was not sensitive to UCLA1 (Table 1; see Fig. S1 in the supplemental material), despite its gp120 having a K_D value of 5.8 ± 2.2 nM and a χ^2 value of 3.1 ± 1.2 (see Fig. S3 in the supplemental material).

Sequence analysis of neutralization-resistant viruses. The amino acid sequences of the Env-pseudotype viruses that were not neutralized by UCLA1 were aligned with ConC gp120 and examined for residues shown to confer resistance (see Fig. S4A in the supplemental material). The ZM109 virus that was not neutralized in the TZM-bl assay contained H330Y, which was identified as conferring resistance by ConC point mutational analysis (Fig. 4). COT6, COT9, and Du151 viruses contained K305R/Q, and Du151 also had R419K. Overall, 4 of the 6 viruses that were resistant in the TZM-bl assay had substitutions at residues that were identified as resistance mutations by ConC epitope mapping. Although K305R/Q, H330Y, and R419K had an effect on aptamer binding in these resistant viruses, other viruses that contained the same mutations were sensitive to UCLA1, suggesting context dependence (see Fig. S4A). Reasons for the resistance of the other 2

TABLE 2 Effect of single point mutations on the neutralization of the ConC virus by the UCLA1 aptamer

gp120 region	Binding site	ConC gp120 mutation(s)[a]	Mutant IC_{50} (nM)[b,c]	Fold effect for mutant vs wild type[c,d]
C1	CoR	K121A	**28**	**17**
	CD4	L125A	**40**	**24**
V3		K305A	**41**	**25**
		I307A	**36**	**22**
		R308A	**35**	**21**
	CoR	H330Y	**17**	**10**
		N332A	0.11	0.06
C3	CD4	S365I	6	4
	CD4	L369P	**50**	**30**
		S375M	4	2
C4	CoR	R419A	**34**	**20**
	CoR	K421A	1	0.6
	CoR	I423A	0.43	0.3
	CD4	V430A	1	0.6
	CoR	A440E	3	1.8
C5		F468V	9	5.4
	CD4	G471E	2	1.2
	CD4	D474A	0.46	0.3
	CD4	R476A	1	0.6

[a] Amino acids were labeled based on HxB2 numbering. The residues are defined according to the designations by Kwong, Zhou, and colleagues (28, 57).
[b] The mutant IC_{50} is the concentration of the UCLA1 aptamer that inhibited 50% of infection of the respective mutant.
[c] Values representing a significant neutralization resistance are shown in bold. Values represent the average of at least three independent experiments.
[d] The fold decrease in neutralization sensitivity to the aptamer was calculated as mutant IC_{50}/wild-type IC_{50}. The wild-type IC_{50} was calculated as an average of 1.67 nM.

Downloaded from http://jvi.asm.org/ on April 10, 2012 by guest

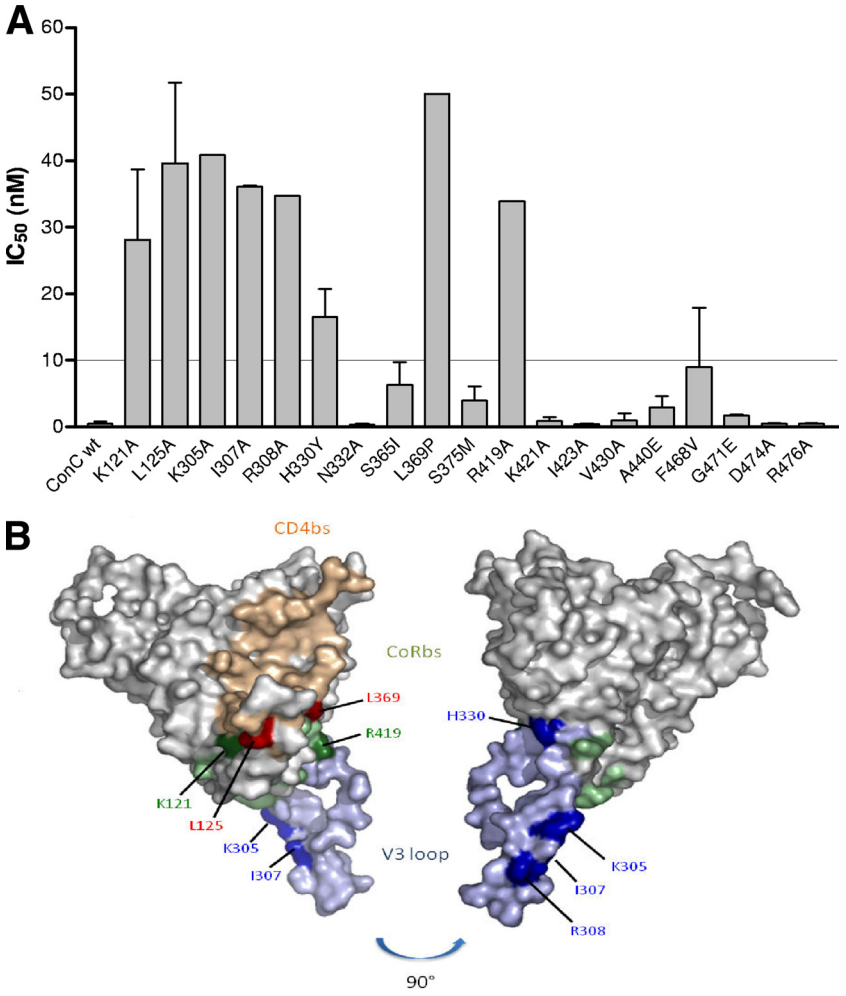

FIG 4 (A) Neutralization of ConC gp120 single-point mutants with UCLA1. Graph depicts the IC_{50}s of the mutants with those above the dotted line conferring resistance (≥10 nM). wt, wild type. (B) Structural representation of the amino acid residues involved in UCLA1 neutralization resistance. Blue depicts the V3 loop, green depicts the CoRbs, and tan depicts the CD4bs. Residues causing neutralization escape are marked in dark shades of the corresponding region. The picture was rotated at 90° for a clear view of the H330 and R308 residues. Coordinates were taken from the structure of the gp120JRFL core with V3 ligated with CD4 and X5 (Protein Data Bank accession no. 2B4C). The figure was generated with PyMOL (DeLano Scientific LLC, South San Francisco, CA [http://www.pymol.org]).

viruses (CAP84 and Du123) could not be deduced from the amino acid alignment.

A similar approach was applied to sequences from primary isolates tested for neutralization with UCLA1 in PBMCs. SW7, which was resistant in the PBMC assay, had mutations K305R, H330Y, and L369I (see Fig. S4B in the supplemental material). Since the SW7 pseudovirus contained the same changes but was sensitive in the TZM-bl assay, these residues were unlikely to be resistance conferring in the PBMC assay. Similarly, an I307V change was observed in both Du156 and Du422, which differed in their sensitivities to UCLA1 in PBMCs (see Fig. S4B). Therefore, the presence of resistance-associated mutations in some sensitive viruses in both the TZM-bl cells (see Fig. S4A) and PBMCs (see Fig. S4B) attests to the complex nature of resistance and brings into question the value of these types of analyses.

Synergy of UCLA1 with other entry inhibitors. Both T20 and b12 have been previously shown to act synergistically with other HIV-1 entry inhibitors (2, 37, 46, 58). Thus, we next evaluated any possible synergistic effects of UCLA1 with T20 or b12. Synergism

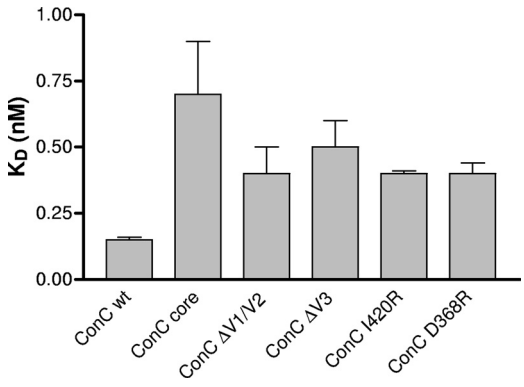

FIG 5 Bar chart representation of the K_D values of UCLA1 from the core, ΔV1/V2 and ΔV3 truncated HIV-1 ConC gp120, and from I420R (CoRbs) and D368R (CD4bs) mutated HIV-1 ConC gp120. The truncated and mutated ConC glycoproteins were compared with the K_D of the wild-type (wt) ConC gp120.

Downloaded from http://jvi.asm.org/ on April 10, 2012 by guest

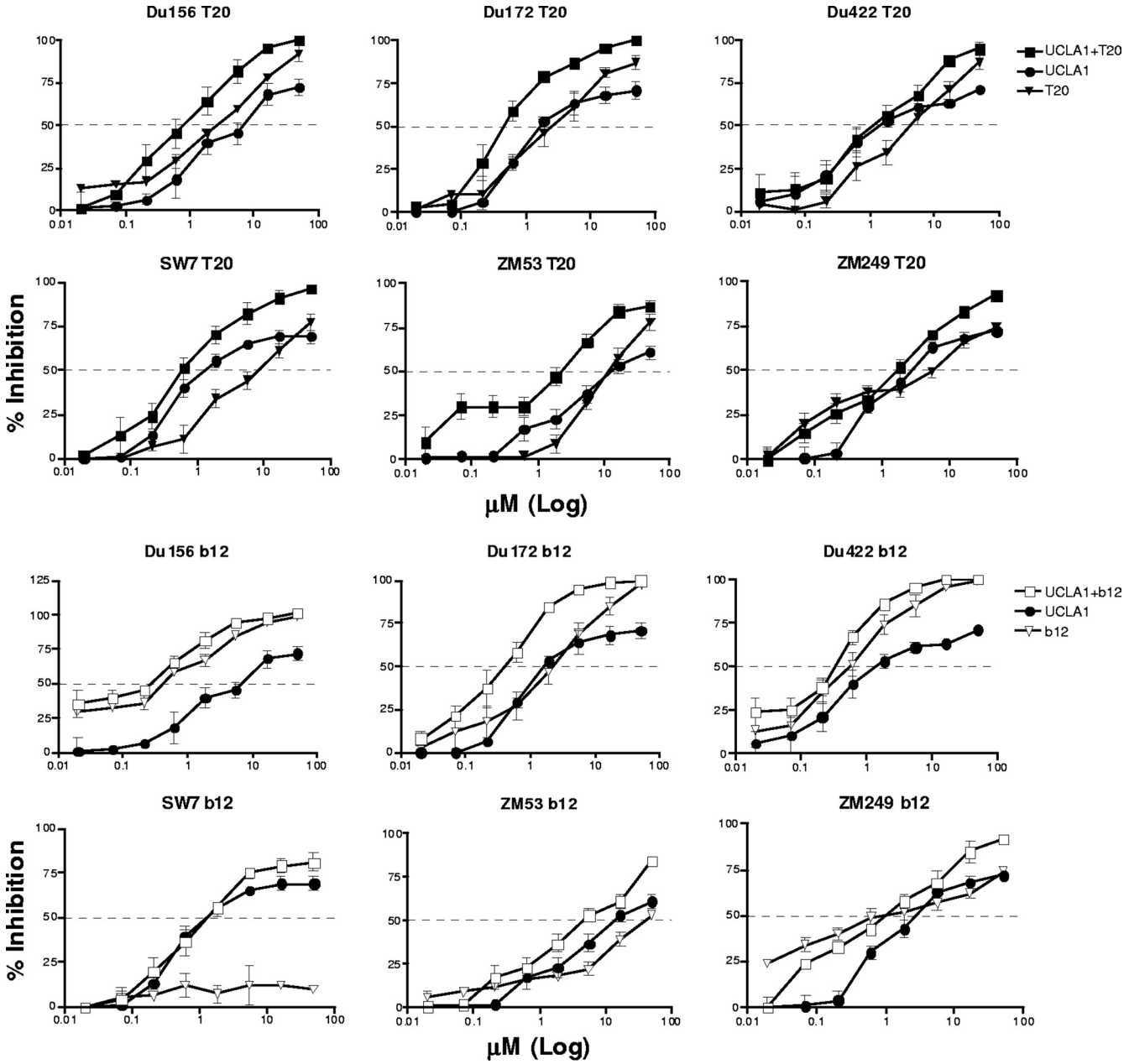

FIG 6 Dose-dependent neutralization graphs of HIV-1 subtype C Env-pseudotyped viruses showing synergism between UCLA1 and T20 or UCLA1 and b12. The aptamer was used at a maximum starting concentration of 50 nM when used alone or in combination. b12 and T20 were used at a maximum initial concentration of 50 μg/ml each and in combination with UCLA1. The 50-μg/ml concentration used for b12 and T20 is equivalent to 312 μM and 1,1131 μM, respectively.

was examined using the single-cycle neutralization assay with Env-pseudotyped viruses. The aptamer showed synergism with T20 for 5 of 6 (83%) viruses tested (Fig. 6), with CI values ranging from 0.13 to 0.46 (Table 3). Slight synergism was observed for ZM249 with UCLA1-T20, with a CI value of 0.84. There was also synergism between the aptamer and b12 MAb for 4 of 6 (67%) viruses tested (Fig. 6), with CI values ranging from 0.5 to 0.7 (Table 3). The combination of UCLA1 and b12 resulted in an additive effect (CI = 0.93) for the neutralization of Du156. Although b12 neutralization of ZM53 was relatively moderate (IC_{50} = 46.14 nM), the antibody combination with UCLA1 resulted in a 2-fold decrease of the IC_{50} (6.22 to 2.8 nM) (Table 3). There was no synergism between UCLA1 and b12 for the neutralization of SW7. This is probably due to the fact that this virus is resistant to b12 (E. Gray, unpublished data). The dose reduction indices for T20, b12, and UCLA1 were determined to be in the range of 3.7 to 27.0, 1.5 to 16.4, and 1.8 to 11.2, respectively, clearly indicating that lower concentrations of these compounds were required to neutralize the viruses, when used in combination. Thus, on average, 11-fold less T20, 5-fold less b12, and 5-fold less UCLA1 were required to neutralize virus infection when in combination.

Downloaded from http://jvi.asm.org/ on April 10, 2012 by guest

TABLE 3 Combination therapy using the UCLA1 aptamer, T20, and b12 against subtype C Env pseudotype viruses

Virus	CI[a]	Concn of UCLA1	Concn of UCLA1 + T20 or b12	Dose reduction index[c]	Concn of T20 or b12	Concn of T20 or b12 + UCLA1	Dose reduction index[c]
		UCLA1 (nM)[b]	UCLA1 + T20 (μM)		T20 (μg/ml)[d]	T20 + UCLA1 (μM)	
Du156.12	**0.37**	1.20	0.31	3.9	2.87	0.31	9.3
Du172.17	**0.43**	1.83	0.34	5.4	1.39	0.34	4.1
Du422.1	**0.13**	3.69	0.33	11.2	8.90	0.33	27.0
SW7.14	**0.43**	0.74	0.27	2.7	3.98	0.27	14.7
ZM53 M.PB12	**0.46**	6.22	1.73	3.6	9.72	1.73	5.6
ZM249 M.PL1	0.84	2.80	1.60	1.8	5.85	1.60	3.7
		UCLA1 (nM)[b]	UCLA1 + b12 (μM)		b12 (μg/ml)[d]	b12 + UCLA1 (μM)	
Du156.12	0.93	1.20	0.30	4.0	0.44	0.30	1.5
Du172.17	**0.56**	1.83	0.22	8.3	0.50	0.22	2.3
Du422.1	**0.65**	3.69	0.53	7.0	1.04	0.53	2.0
SW7.14	1.62	0.74	1.19	0.6	50.00	1.19	42.0
ZM53 M.PB12	**0.5**	6.22	2.82	2.2	46.14	2.82	16.4
ZM249 M.PL1	**0.7**	2.80	0.87	3.2	2.26	0.87	2.6

[a] The combination index (CI) was calculated using the Chou and Talalay equation (7). CI values of 0.3 to 0.7, 0.7 to 0.85, 0.85 to 0.9, 0.9 to 1.1, and >1.1 represent synergism, moderate synergism, slight synergism, additive effect, and antagonism, respectively. CI values representing synergism are in bold.
[b] The UCLA1 aptamer was used at an initial concentration of 50 nM alone and in combination with T20 or b12.
[c] Dose reduction index is calculated as the ratio of drug concentration required for inhibition when the drug is used alone or in combination.
[d] T20 and b12 were used at an initial concentration of 50 μg/ml (equivalent to 312 μM and 11,131 μM, respectively) alone or in combination with UCLA1.

DISCUSSION

In this study, the UCLA1 RNA aptamer was examined for its antiviral activity against HIV-1 subtype C viruses. Its efficacy was demonstrated by the high binding affinity for HIV-1 ConC gp120 and broad neutralization of primary isolates and Env-pseudotyped viruses. The lack of toxicity in both TZM-bl cells and PBMCs confirmed that its action was due to its efficacy and not cell toxicity. Mapping of the aptamer binding sites revealed 8 residues that modulated neutralization resistance to the aptamer. Most of the residues were localized within the CoRbs at the base of the V3 and the bridging sheet within the conserved V1/V2 stem-loop of gp120 that makes up the CD4bs. The aptamer exhibited synergism with T20 fusion inhibitor and b12 MAb, with dose reduction indices indicating that lower concentrations of T20 and b12 can be used to inhibit HIV-1 when combined with the aptamer.

The modified UCLA1 exhibited higher affinity for its ligand compared to the parental B40 aptamer and the truncated version, B40t77 (13). The low K_D value of UCLA1 contributed to a stable association and better binding energy. This was also demonstrated by another study that showed increased binding of modified aptamers and higher potency, albeit on a limited number of viruses (10). Whether the breadth and potency of neutralization seen in our study can be attributed to UCLA1's increased affinity for gp120 requires a head-to-head comparison with other aptamers. In addition to its improved binding and its broad neutralizing activity, UCLA1 has been shown to be stable in biological fluids in a study conducted with another derivative, named UCLA005 (36). A further chemical modification (UCLA005v11) resulted in a 4-fold increase in aptamer stability with a half-life of 242 min (36), therefore confirming that modified aptamers are highly stable compounds.

UCLA1 neutralized infection of a large panel of subtype C viruses isolated from both acute and chronically infected adult and pediatric patients. There was no neutralization preference noted between viruses isolated from acute and chronic infections or between isolates from adult and pediatric patients in both the TZM-bl cells and PBMC assays. The aptamer was not strain or tropism restricted since it neutralized R5 and X4 viruses, although more X4-tropic strains need to be tested. These neutralization data concur with other studies that have utilized similar aptamers for inhibition of HIV-1 subtype B R5-tropic viruses (10, 14, 25, 36). It was noted that UCLA1 showed higher efficiency against Env-pseudotyped viruses compared to primary isolates, which has been noted by others (1, 5, 16, 30). Overall, its breadth and potency of neutralization were comparable to those of other HIV-1 entry inhibitors (1, 5, 45, 48, 49, 51). The reasons why UCLA1 was less potent in the PBMC assay are unknown but may be related to the presence of viral quasispecies, longer culture periods, nonspecific uptake by other cells, or inactivation of the aptamer in the culture. Nevertheless, high concentrations of aptamer were not cytotoxic in PBMCs. Indeed, we previously showed that the parental B40 aptamer was not toxic to PBMCs and human cardiomyocytes even at a 2 μM concentration of the aptamer (33).

Mutagenesis was performed to define the residues on gp120 influencing UCLA1 reactivity. Eight mutated residues were found to confer UCLA1 neutralization resistance. Six of these were involved in CCR5 binding and were localized at the base of the V3 loop (K305A, I307A, R308A, and H330Y), the bridging sheet within the conserved V1/V2 stem-loop that makes up the CD4-induced epitope (K121A) and the C4 domain (R419A) (28, 43, 57). Two residues in the CD4bs, K125A in the bridging sheet region and the L369P residue in the C3 domain adjacent to the Phe43 cavity (28, 40, 42), were also implicated. Residues K121, H330, L369, and R419 have been previously shown to modulate binding of other HIV-1 inhibitors within the conserved core residues (11, 40, 42, 43), including aptamers 299.5 (10) and B40t77 (23). Overall, 4 of the 8 residues were located within the V3 loop and 2 within the V1/V2 bridging sheet, confirming the SPR data using V-loop-deleted gp120 proteins, which was also shown by others (10, 14, 23, 25). Differences in the K_D values between wild-type and V-loop-deleted proteins were more subtle than the effect

Downloaded from http://jvi.asm.org/ on April 10, 2012 by guest

of single point mutations in gp120 on neutralization. The effect of 1420R and D368R in reducing binding is likely due to their close proximity to identified residues rather than a direct effect, although this could not be tested. UCLA1 neutralization resistance could not be fully explained from the amino acid sequence alignments, probably because other residues within gp120 modulate aptamer neutralization efficacy. In addition there might be distal conformational changes that reduce UCLA1 binding affinity to gp120, as previously shown with the B40t77 aptamer against HIV-1_{BaL} gp120 (23).

Studies done by others have also shown aptamer epitopes that overlap the base of the α1 helix, the CD4-induced binding sites in the bridging sheet (β21 and β20), and the variable loops (F and V3) for 299.5 and B40t77 aptamers (10, 23). This is not surprising given that UCLA1, B40t77, and 299.5 are modified derivatives, possessing the same core structure, which is suggested to be their binding core (10, 13). We previously reported competition between B40t77 and various MAbs (23) which confirmed these mapping data. Thus, competition between B40t77 and b12 or b6 suggested shared binding sites, possibly including L369 and R419 identified in this study. Competition between B40t77 and 17b or CD4 (22) confirmed the L125 and L369 UCLA1 sites within the CD4 complex. Inhibition enhancement was observed when B40t77 was used together with the anti-V3 MAb, 19b, suggesting that the aptamer and the MAb have nonoverlapping binding sites within the V3 loop (23). This also confirms that the identified V3 loop residues are indeed UCLA1 binding sites.

UCLA1 exhibited synergism with the gp41 fusion inhibitor, T20, likely because these compounds target different regions of the viral envelope. Synergism was also noted with b12, although the effect was more modest. Since the b12 epitope includes the L369 and R419 residues, which were both shown in this study to affect UCLA1 neutralization; it was interesting to discover synergism between these two agents. This finding suggests that L369 and R419 might not be direct-contact residues for UCLA1 but peripheral sites that modulate the aptamers' reactivity accounting for the lack of competition when used in combination with b12. Alternatively, these agents might be causing an allosteric effect on the neighboring protomers, thus increasing binding affinity or site accessibility. The b12 MAb was previously shown to effectively neutralize most of the currently tested viruses (31); however, ZM53 required a higher concentration, while SW7 was resistant to this MAb (E. Gray, unpublished data). Thus, synergism between b12 and UCLA1 for ZM53 neutralization suggests that UCLA1 can increase the sensitivity of viruses that are partially resistant to the MAb. On the other hand, the lack of synergism for SW7 implies that this increase in sensitivity cannot be achieved if the virus is completely resistant to the antibody.

Taken together, the results indicate that the UCLA1 RNA aptamer has broad-spectrum potency against several subtype C viruses at low nanomolar concentrations. The noncytotoxic nature, high therapeutic index, neutralization potency, and synergistic effect of the aptamer suggest that UCLA1 can be further developed and tested in preclinical and clinical studies as a potential new entry inhibitor drug, especially against HIV-1 subtype C viruses.

ACKNOWLEDGMENTS

This work was supported by the South African Department of Science and Technology (DST) and a Council for Scientific and Industrial Research (CSIR) Parliamentary Grant. Hazel Mufhandu was funded by The Young Researcher Establishment Fund (YREF 2007 029), the Poliomyelitis Research Foundation (08/37), the Wits Medical Faculty Research Endowment Fund (001 410 MUFH011 TS), and a CSIR Ph.D. studentship. The authors acknowledge the generous donation of aptamer UCLA1 by Ian McGowan, William James, and Brian Sproat under the NIH Aptamer Microbicide Program, grant 5U01AI066734-03.

We thank Mary Phoswa (NICD), Sarah Cohen (NICD), and Lia Rotherham (CSIR) for technical assistance.

REFERENCES

1. **Alexandre KB, et al.** 2010. Mannose-rich glycosylation patterns on HIV-1 subtype C gp120 and sensitivity to the lectins, griffithsin, cyanovirin-N and scytovirin. Virology **402**:187–196.
2. **Alexandre KB, et al.** 2011. Binding of the mannose-specific lectin, griffithsin, to HIV-1 gp120 exposes the CD4-binding site. J. Virol. **85**:9039–9050.
3. **Alkhatib G, et al.** 1996. CC CKR5: a RANTES, MIP-1alpha, MIP-1beta receptor as a fusion cofactor for macrophage-tropic HIV-1. Science **272**:1955–1958.
4. **Atchison RE, et al.** 1996. Multiple extracellular elements of CCR5 and HIV-1 entry: dissociation from response to chemokines. Science **274**:1924–1926.
5. **Binley JM, et al.** 2004. Comprehensive cross-clade neutralization analysis of a panel of anti-human immunodeficiency virus type 1 monoclonal antibodies. J. Virol. **78**:13232–13252.
6. **Bures R, et al.** 2000. Immunization with recombinant canarypox vectors expressing membrane-anchored glycoprotein 120 followed by glycoprotein 160 boosting fails to generate antibodies that neutralize R5 primary isolates of human immunodeficiency virus type 1. AIDS Res. Hum. Retroviruses **16**:2019–2035.
7. **Castanotto D, Rossi JJ.** 2009. The promises and pitfalls of RNA-interference-based therapeutics. Nature **457**:426–433.
8. **Chou TC, Talalay P.** 1984. Quantitative analysis of dose-effect relationships: the combined effects of multiple drugs or enzyme inhibitors. Adv. Enzyme Regul. **22**:27–55.
9. **Cilliers T, et al.** 2003. The CCR5 and CXCR4 coreceptors are both used by human immunodeficiency virus type 1 primary isolates from subtype C. J. Virol. **77**:4449–4456.
10. **Cohen C, et al.** 2008. An aptamer that neutralizes R5 strains of HIV-1 binds to core residues of gp120 in the CCR5 binding site. Virology **381**:46–54.
11. **Cormier EG, Tran DN, Yukhayeva L, Olson WC, Dragic T.** 2001. Mapping the determinants of the CCR5 amino-terminal sulfopeptide interaction with soluble human immunodeficiency virus type 1 gp120-CD4 complexes. J. Virol. **75**:5541–5549.
12. **Decker JM, et al.** 2005. Antigenic conservation and immunogenicity of the HIV coreceptor binding site. J. Exp. Med. **201**:1407–1419.
13. **Dey AK, Griffiths C, Lea SM, James W.** 2005. Structural characterization of an anti-gp120 RNA aptamer that neutralizes R5 strains of HIV-1. RNA **11**:873–884.
14. **Dey AK, et al.** 2005. An aptamer that neutralizes R5 strains of human immunodeficiency virus type 1 blocks gp120-CCR5 interaction. J. Virol. **79**:13806–13810.
15. **Ellington AD, Szostak JW.** 1990. In vitro selection of RNA molecules that bind specific ligands. Nature **346**:818–822.
16. **Fenyo EM, et al.** 2009. International network for comparison of HIV neutralization assays: the NeutNet report. PLoS One **4**:e4505.
17. **Gray ES, Meyers T, Gray G, Montefiori DC, Morris L.** 2006. Insensitivity of paediatric HIV-1 subtype C viruses to broadly neutralising monoclonal antibodies raised against subtype B. PLoS Med. **3**:e255.
18. **Gray ES, et al.** 2007. Neutralizing antibody responses in acute human immunodeficiency virus type 1 subtype C infection. J. Virol. **81**:6187–6196.
19. **Gray ES, Moore PL, Pantophlet RA, Morris L.** 2007. N-linked glycan modifications in gp120 of human immunodeficiency virus type 1 subtype C render partial sensitivity to 2G12 antibody neutralization. J. Virol. **81**:10769–10776.
20. **Gray ES, et al.** 2009. Antibody specificities associated with neutralization breadth in plasma from human immunodeficiency virus type 1 subtype C-infected blood donors. J. Virol. **83**:8925–8937.
21. **Honnen WJ, et al.** 2007. Type-specific epitopes targeted by monoclonal antibodies with exceptionally potent neutralizing activities for selected

Downloaded from http://jvi.asm.org/ on April 10, 2012 by guest

strains of human immunodeficiency virus type 1 map to a common region of the V2 domain of gp120 and differ only at single positions from the clade B consensus sequence. J. Virol. **81**:1424–1432.
22. **Jacobson JM, et al.** 2000. Single-dose safety, pharmacology, and antiviral activity of the human immunodeficiency virus (HIV) type 1 entry inhibitor PRO 542 in HIV-infected adults. J. Infect. Dis. **182**:326–329.
23. **Joubert MK, et al.** 2010. A modeled structure of an aptamer-gp120 complex provides insight into the mechanism of HIV-1 neutralization. Biochemistry **49**:5880–5890.
24. **Keefe AD, Pai S, Ellington A.** 2010. Aptamers as therapeutics. Nat. Rev. Drug Discov. **9**:537–550.
25. **Khati M, et al.** 2003. Neutralization of infectivity of diverse R5 clinical isolates of human immunodeficiency virus type 1 by gp120-binding 2′F-RNA aptamers. J. Virol. **77**:12692–12698.
26. **Kothe DL, et al.** 2006. Ancestral and consensus envelope immunogens for HIV-1 subtype C. Virology **352**:438–449.
27. **Kwong PD, et al.** 2002. HIV-1 evades antibody-mediated neutralization through conformational masking of receptor-binding sites. Nature **420**: 678–682.
28. **Kwong PD, et al.** 1998. Structure of an HIV gp120 envelope glycoprotein in complex with the CD4 receptor and a neutralizing human antibody. Nature **393**:648–659.
29. **Lalezari JP, et al.** 2003. Enfuvirtide, an HIV-1 fusion inhibitor, for drug-resistant HIV infection in North and South America. N. Engl. J. Med. **348**:2175–2185.
30. **Li M, et al.** 2005. Human immunodeficiency virus type 1 env clones from acute and early subtype B infections for standardized assessments of vaccine-elicited neutralizing antibodies. J. Virol. **79**:10108–10125.
31. **Li M, et al.** 2006. Genetic and neutralization properties of subtype C human immunodeficiency virus type 1 molecular env clones from acute and early heterosexually acquired infections in Southern Africa. J. Virol. **80**:11776–11790.
32. **Li Y, et al.** 2007. Broad HIV-1 neutralization mediated by CD4-binding site antibodies. Nat. Med. **13**:1032–1034.
33. **Lopes de Campos WR, Coopusamy D, Morris L, Mayosi BM, Khati M.** 2009. Cytotoxicological analysis of a gp120 binding aptamer with cross-clade human immunodeficiency virus type 1 entry inhibition properties: comparison to conventional antiretrovirals. Antimicrob. Agents Chemother. **53**:3056–3064.
34. **Montefiori DC.** 2004. Evaluating neutralizing antibodies against HIV, SIV and SHIV in luciferase reporter gene assay, **vol 12. John Wiley**, Hoboken, NJ.
35. **Moore JP, Doms RW.** 2003. The entry of entry inhibitors: a fusion of science and medicine. Proc. Natl. Acad. Sci. U. S. A. **100**:10598–10602.
36. **Moore MD, et al.** 2011. Protection of HIV neutralizing aptamers against rectal and vaginal nucleases: implications for RNA-based therapeutics. J. Biol. Chem. **286**:2526–2535.
37. **Nagashima KA, et al.** 2001. Human immunodeficiency virus type 1 entry inhibitors PRO 542 and T-20 are potently synergistic in blocking virus-cell and cell-cell fusion. J. Infect. Dis. **183**:1121–1125.
38. **O'Sullivan CK.** 2002. Aptasensors—the future of biosensing? Anal. Bioanal Chem. **372**:44–48.
39. **Osztie E, et al.** 2001. Combined intraarterial carboplatin, intraarterial etoposide phosphate, and IV cytoxan chemotherapy for progressive optic-hypothalamic gliomas in young children. AJNR Am. J. Neuroradiol. **22**: 818–823.
40. **Pantophlet R, et al.** 2003. Fine mapping of the interaction of neutralizing and nonneutralizing monoclonal antibodies with the CD4 binding site of human immunodeficiency virus type 1 gp120. J. Virol. **77**:642–658.
41. **Pinter A, et al.** 2005. The C108g epitope in the V2 domain of gp120 functions as a potent neutralization target when introduced into envelope proteins derived from human immunodeficiency virus type 1 primary isolates. J. Virol. **79**:6909–6917.
42. **Rizzuto C, Sodroski J.** 2000. Fine definition of a conserved CCR5-binding region on the human immunodeficiency virus type 1 glycoprotein 120. AIDS Res. Hum. Retroviruses **16**:741–749.
43. **Rizzuto CD, et al.** 1998. A conserved HIV gp120 glycoprotein structure involved in chemokine receptor binding. Science **280**:1949–1953.
44. **Sayer N, Ibrahim J, Turner K, Tahiri-Alaoui A, James W.** 2002. Structural characterization of a 2′F-RNA aptamer that binds a HIV-1 SU glycoprotein, gp120. Biochem. Biophys. Res. Commun. **293**:924–931.
45. **Schols D.** 2006. HIV co-receptor inhibitors as novel class of anti-HIV drugs. Antiviral Res. **71**:216–226.
46. **Tremblay CL, Kollmann C, Giguel F, Chou TC, Hirsch MS.** 2000. Strong in vitro synergy between the fusion inhibitor T-20 and the CXCR4 blocker AMD-3100. J. Acquir. Immune Defic. Syndr. **25**:99–102.
47. **Van Harmelen JH, et al.** 1999. A predominantly HIV type 1 subtype C-restricted epidemic in South African urban populations. AIDS Res. Hum. Retroviruses **15**:395–398.
48. **Walker LM, et al.** 2011. Broad neutralization coverage of HIV by multiple highly potent antibodies. Nature **477**:466–470.
49. **Walker LM, et al.** 2009. Broad and potent neutralizing antibodies from an African donor reveal a new HIV-1 vaccine target. Science **326**:285–289.
50. **Wang W, Jia L-Y.** 2009. Progress in aptamer screening methods. Chin. J. Anal. Chem. **37**:454–460.
51. **Wu X, et al.** 2010. Rational design of envelope identifies broadly neutralizing human monoclonal antibodies to HIV-1. Science **329**:856–861.
52. **Wyatt R, et al.** 1998. The antigenic structure of the HIV gp120 envelope glycoprotein. Nature **393**:705–711.
53. **Zhou J, Li H, Li S, Zaia J, Rossi JJ.** 2008. Novel dual inhibitory function aptamer-siRNA delivery system for HIV-1 therapy. Mol. Ther. **16**:1481–1489.
54. **Zhou J, Rossi JJ.** 2010. Cell-specific aptamer-mediated targeted drug delivery. Oligonucleotides **21**:1–10.
55. **Zhou J, Shu Y, Guo P, Smith DD, Rossi JJ.** 2011. Dual functional RNA nanoparticles containing phi29 motor pRNA and anti-gp120 aptamer for cell-type specific delivery and HIV-1 inhibition. Methods **54**:284–294.
56. **Zhou J, et al.** 2009. Selection, characterization and application of new RNA HIV gp 120 aptamers for facile delivery of Dicer substrate siRNAs into HIV infected cells. Nucleic Acids Res. **37**:3094–3109.
57. **Zhou T, et al.** 2007. Structural definition of a conserved neutralization epitope on HIV-1 gp120. Nature **445**:732–737.
58. **Zwick MB, et al.** 2005. Anti-human immunodeficiency virus type 1 (HIV-1) antibodies 2F5 and 4E10 require surprisingly few crucial residues in the membrane-proximal external region of glycoprotein gp41 to neutralize HIV-1. J. Virol. **79**:1252–1261.
59. **Zwick MB, et al.** 2001. Neutralization synergy of human immunodeficiency virus type 1 primary isolates by cocktails of broadly neutralizing antibodies. J. Virol. **75**:12198–12208.

Downloaded from http://jvi.asm.org/ on April 10, 2012 by guest

SUPPLEMENTARY FIGURE LEGENDS

Figure S1: Representative dose-dependent neutralization graphs of HIV-1 subtype C Env-pseudotyped viruses and a subtype B HxB2 reference strain with the UCLA1 aptamer using the TZM-bl cell line. The aptamer was used at a starting concentration of 50 nM. The IC_{50} of UCLA1 is indicated with the dotted line. Nine viruses sensitive to UCLA1 and three viruses resistant to UCLA1 neutralization are shown.

Figure S2: BIAcore® sensorgrams to detect the dissociation constant (K_D) of UCLA1 aptamer from the core, ΔV1/V2 and ΔV3 truncated HIV-1 Con-C gp120, and from I420R (CoRbs) and D368R (CD4bs) mutated HIV-1 Con-C gp120. The truncated and mutated ConC glycoproteins were compared with the wildtype ConC gp120. The UCLA1 aptamer was simultaneously injected over the immobilized gp120 at 2-fold dilutions (500 nM to 8 nM).

Figure S3: The binding profile of ½ log dilutions (500 nM to 1.0 nM) of the UCLA1 aptamer over the immobilized HIV-1 Du151 gp120. The binding kinetics was performed in triplicate.

Figure S4: [A] Amino acid sequence alignment of HIV-1 gp120 of the Env-pseudotyped viruses that were tested for neutralization with UCLA1 aptamer in the TZM-bl assay. The resistant viruses, listed below the horizontal line in the alignment, were compared with viruses that were sensitive to UCLA1 neutralization including the ConC virus that was used to map the UCLA1 binding sites. The amino acid residues that were changed by site-directed mutagenesis of the ConC gp120 are numbered and their respective regions exhibited within the *env* genome. The numbering is according to the sequence of the

HxB2 (IIIB) gp120. The amino acid residues that were shown to modulate binding of UCLA1 aptamer are bolded and highlighted in grey colour. **[B]** Amino acid sequence alignment of HIV-1 gp120 of primary isolates that were tested for neutralization with UCLA1 aptamer in the PBMC assay. The viruses that were not neutralized by the aptamer are listed below the horizontal line in the sequence alignment. The amino acid residues that were changed by site-directed mutagenesis of ConC gp120 are numbered and their respective regions exhibited within the env genome. The numbering is according to the sequence of the HxB2 (IIIB) gp120. The amino acid residues that were shown to modulate binding of UCLA1 aptamer are bolded and highlighted in grey colour.

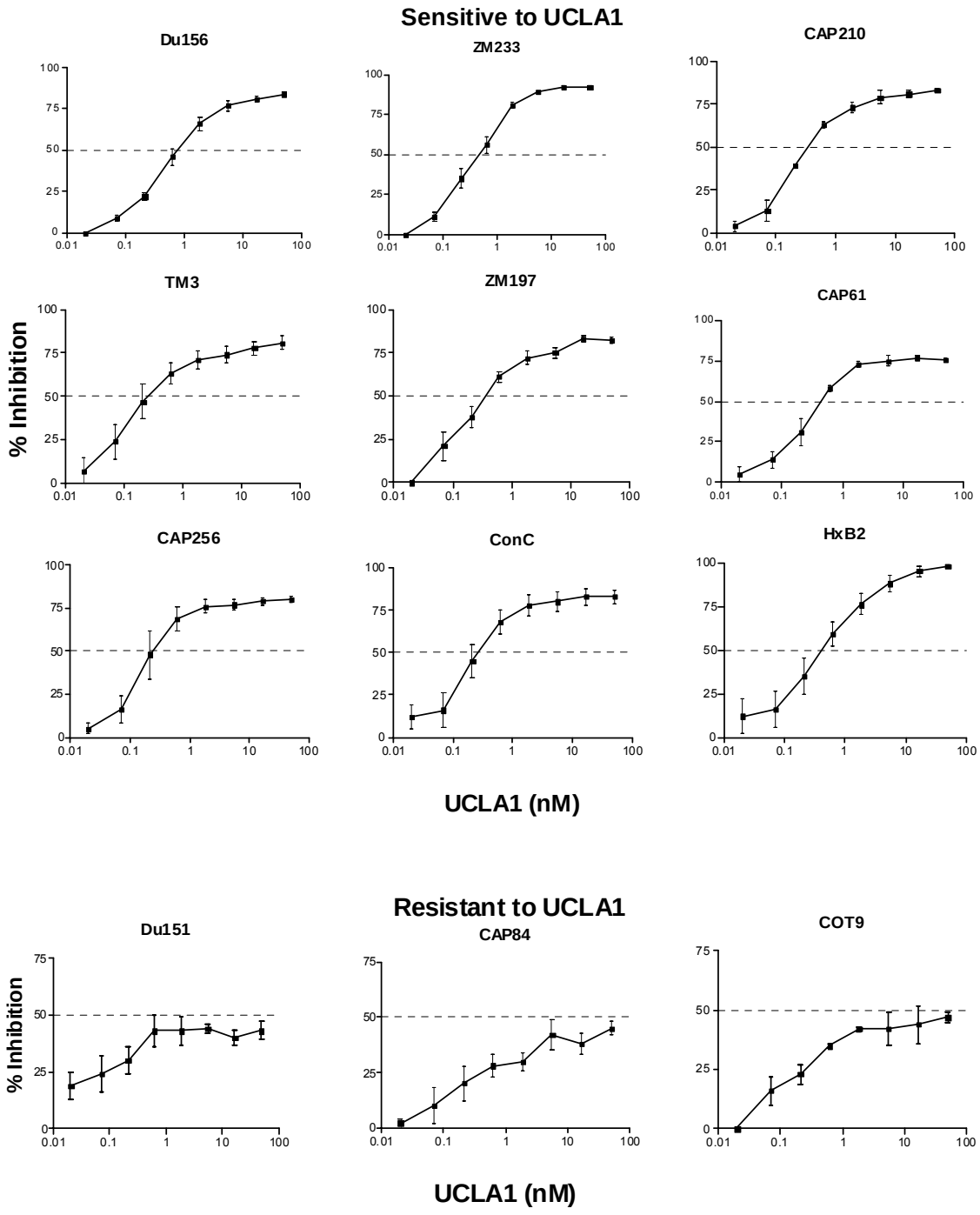

1

2 **Supplementary Figure 1.**

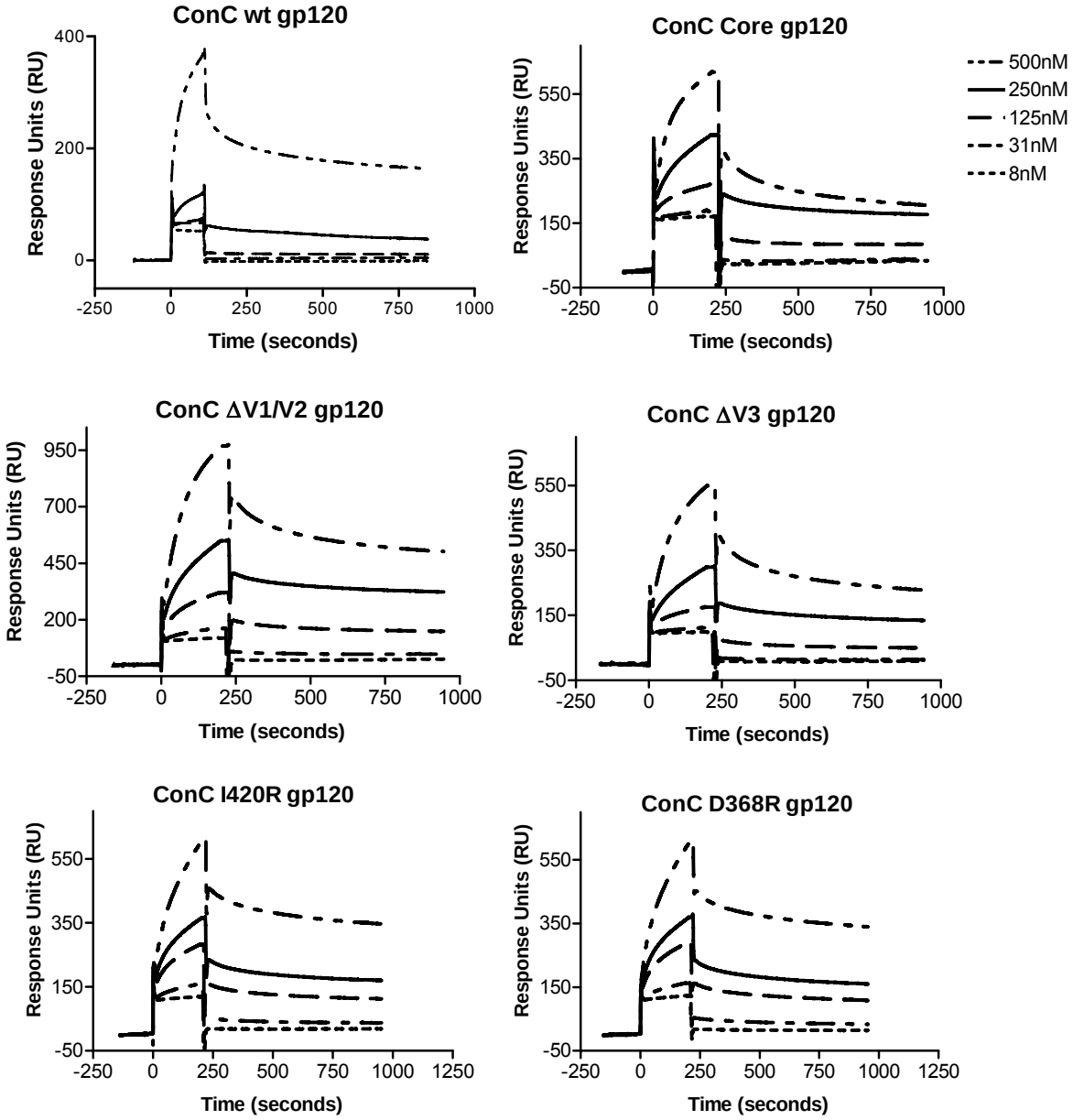

Supplementary Figure 2.

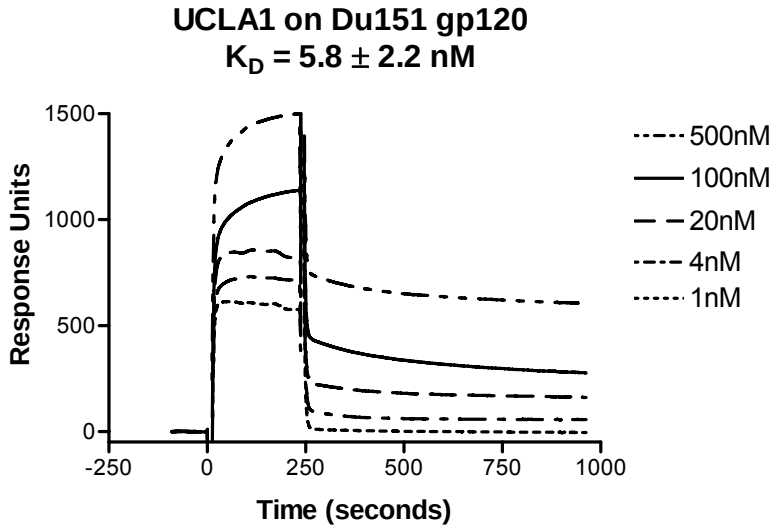

Supplementary Figure 3.

A

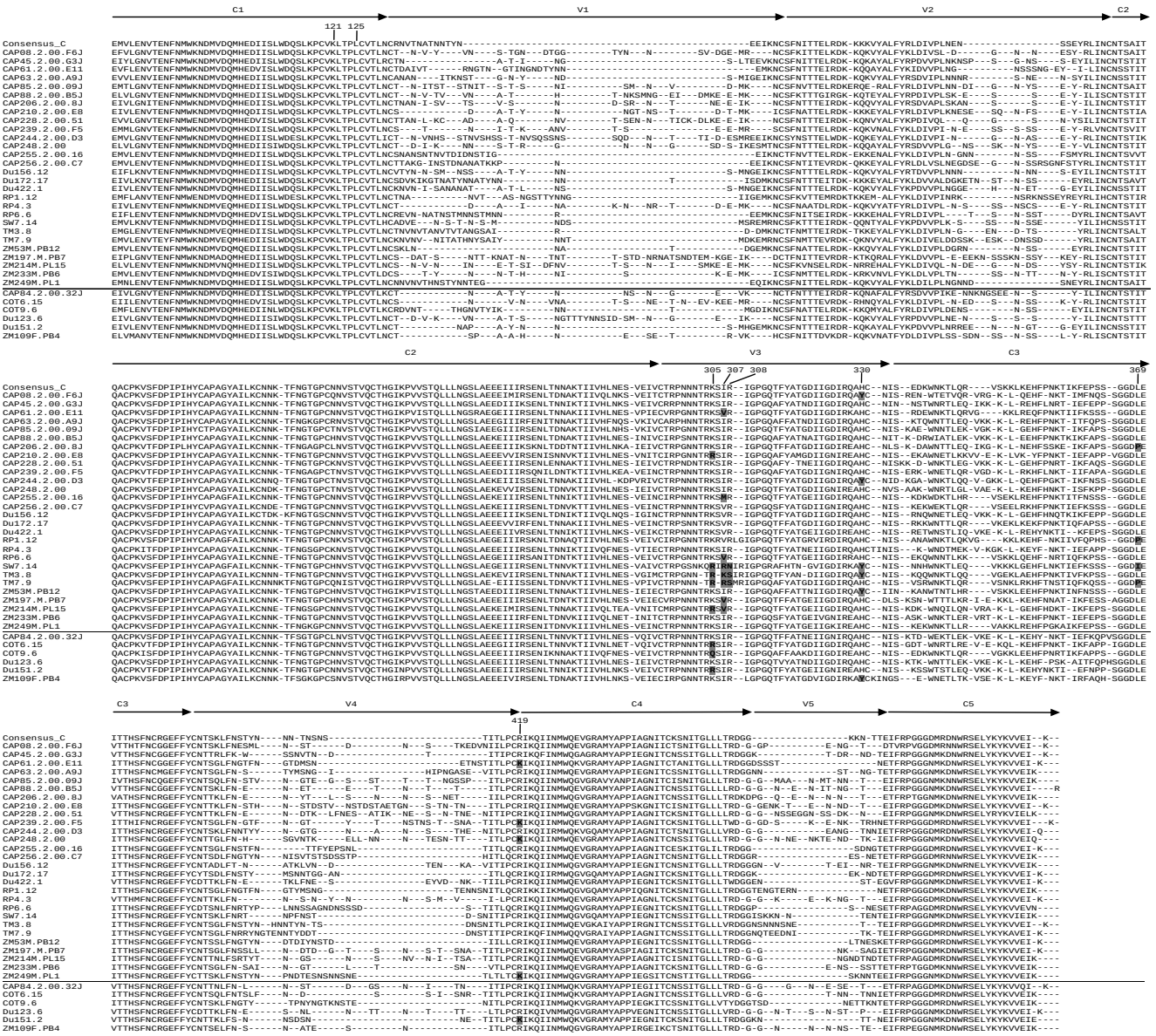

B

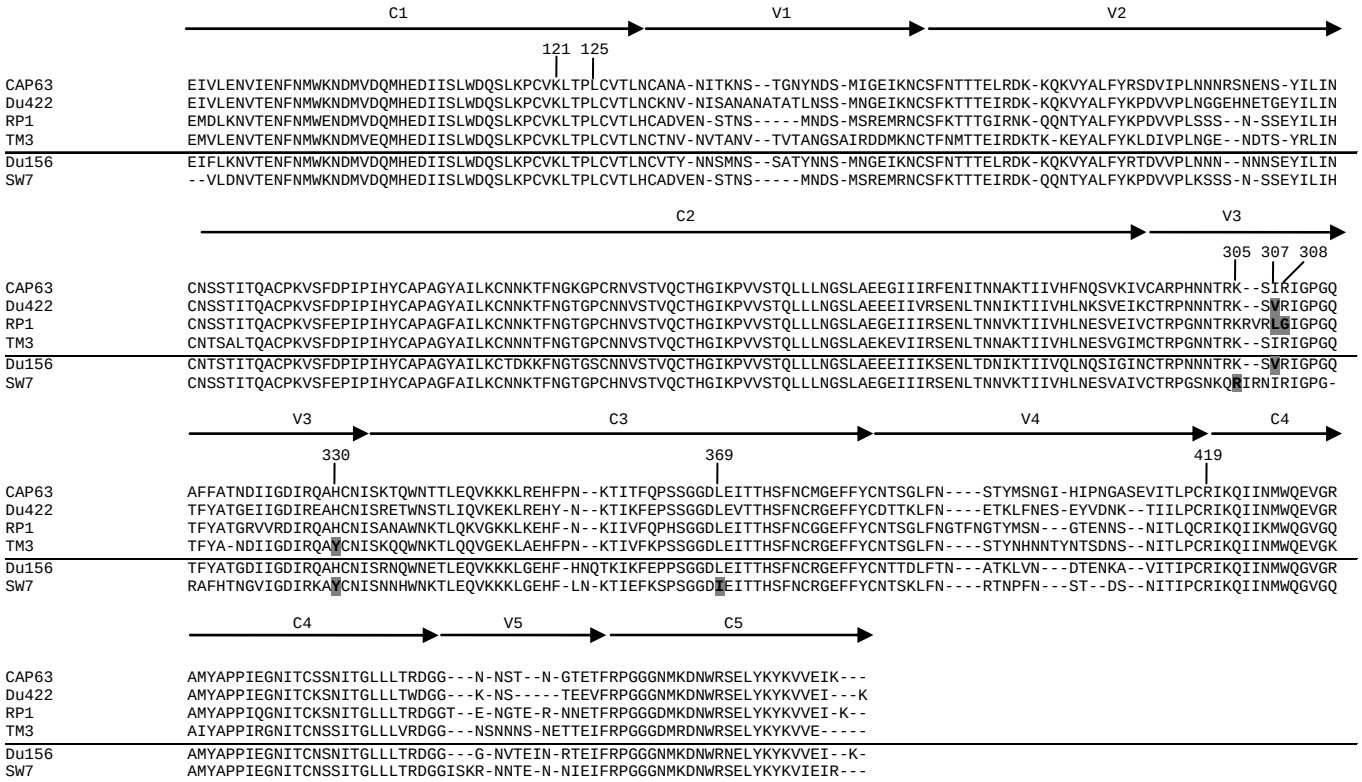

Supplementary Figure 4.

REFERENCES

Abdool Karim, S. S., Churchyard, G. J., Abdool Karim, Q. & Lawn, S. D. (2009). HIV infection and tuberculosis in South Africa: an urgent need to escalate the public health response. *Lancet* **374**, 921-33.

Akiyama, H., Kachi, S., Silva, R. L., Umeda, N., Hackett, S. F., McCauley, D., McCauley, T., Zoltoski, A., Epstein, D. M. & Campochiaro, P. A. (2006). Intraocular injection of an aptamer that binds PDGF-B: a potential treatment for proliferative retinopathies. *J Cell Physiol* **207**, 407-12.

Alexandre, K. B., Gray, E. S., Lambson, B. E., Moore, P. L., Choge, I. A., Mlisana, K., Karim, S. S., McMahon, J., O'Keefe, B., Chikwamba, R. & Morris, L. (2010). Mannose-rich glycosylation patterns on HIV-1 subtype C gp120 and sensitivity to the lectins, Griffithsin, Cyanovirin-N and Scytovirin. *Virology* **402**, 187-96.

Alexandre, K. B., Gray, E. S., Pantophlet, R., Moore, P. L., McMahon, J. B., Chakauya, E., O'Keefe, B. R., Chikwamba, R. & Morris, L. (2011). Binding of the mannose-specific lectin, griffithsin, to HIV-1 gp120 exposes the CD4-binding site. *J Virol* **85**, 9039-50.

Alkhatib, G., Combadiere, C., Broder, C. C., Feng, Y., Kennedy, P. E., Murphy, P. M. & Berger, E. A. (1996). CC CKR5: a RANTES, MIP-1alpha, MIP-1beta receptor as a fusion cofactor for macrophage-tropic HIV-1. *Science* **272**, 1955-8.

An, P., Martin, M. P., Nelson, G. W., Carrington, M., Smith, M. W., Gong, K., Vlahov, D., O'Brien, S. J. & Winkler, C. A. (2000). Influence of CCR5 promoter haplotypes on AIDS progression in African-Americans. *Aids* **14**, 2117-22.

Aquaro, S., Calio, R., Balzarini, J., Bellocchi, M. C., Garaci, E. & Perno, C. F. (2002). Macrophages and HIV infection: therapeutical approaches toward this strategic virus reservoir. *Antiviral Res* **55**, 209-25.

Aquaro, S., Panti, S., Caroleo, M. C., Balestra, E., Cenci, A., Forbici, F., Ippolito, G., Mastino, A., Testi, R., Mollace, V., Calio, R. & Perno, C. F. (2000). Primary macrophages infected by human immunodeficiency virus trigger CD95-mediated apoptosis of uninfected astrocytes. *J Leukoc Biol* **68**, 429-35.

Arien, K. K., Vanham, G. & Arts, E. J. (2007). Is HIV-1 evolving to a less virulent form in humans? *Nat Rev Microbiol* **5**, 141-51.

Atchison, R. E., Gosling, J., Monteclaro, F. S., Franci, C., Digilio, L., Charo, I. F. & Goldsmith, M. A. (1996). Multiple extracellular elements of CCR5 and HIV-1 entry: dissociation from response to chemokines. *Science* **274**, 1924-6.

Bates, P. J., Laber, D. A., Miller, D. M., Thomas, S. D. & Trent, J. O. (2009). Discovery and development of the G-rich oligonucleotide AS1411 as a novel treatment for cancer. *Exp Mol Pathol* **86**, 151-64.

Beausejour, Y. & Tremblay, M. J. (2004). Envelope glycoproteins are not required for insertion of host ICAM-1 into human immunodeficiency virus type 1 and ICAM-1-bearing viruses are still infectious despite a suboptimal level of trimeric envelope proteins. *Virology* **324**, 165-72.

Berger, E. A., Doms, R. W., Fenyo, E. M., Korber, B. T., Littman, D. R., Moore, J. P., Sattentau, Q. J., Schuitemaker, H., Sodroski, J. & Weiss, R. A. (1998). A new classification for HIV-1. *Nature* **391**, 240.

Berger, E. A., Murphy, P. M. & Farber, J. M. (1999). Chemokine receptors as HIV-1 coreceptors: roles in viral entry, tropism, and disease. *Annu Rev Immunol* **17**, 657-700.

Binley, J. M., Wrin, T., Korber, B., Zwick, M. B., Wang, M., Chappey, C., Stiegler, G., Kunert, R., Zolla-Pazner, S., Katinger, H., Petropoulos, C. J. & Burton, D. R. (2004). Comprehensive cross-clade neutralization analysis of a panel of anti-human immunodeficiency virus type 1 monoclonal antibodies. *J Virol* **78**, 13232-52.

Bredell, H., Williamson, C., Sonnenberg, P., Martin, D. J. & Morris, L. (1998). Genetic characterization of HIV type 1 from migrant workers in three South African gold mines. *AIDS Res Hum Retroviruses* **14**, 677-84.

Bridger, G. J., Skerlj, R. T., Padmanabhan, S., Martellucci, S. A., Henson, G. W., Struyf, S., Witvrouw, M., Schols, D. & De Clercq, E. (1999). Synthesis and structure-activity relationships of phenylenebis(methylene)-linked bis-azamacrocycles that inhibit HIV-1 and HIV-2 replication by antagonism of the chemokine receptor CXCR4. *J Med Chem* **42**, 3971-81.

Brodie, S. J. (2000). Nonlymphoid reservoirs of HIV replication in children with chronic-progressive disease. *J Leukoc Biol* **68**, 351-9.

Brown, B. K., Karasavvas, N., Beck, Z., Matyas, G. R., Birx, D. L., Polonis, V. R. & Alving, C. R. (2007). Monoclonal antibodies to phosphatidylinositol phosphate neutralize human immunodeficiency virus type 1: role of phosphate-binding subsites. *J Virol* **81**, 2087-91.

Brown, R. J., Peters, P. J., Caron, C., Gonzalez-Perez, M. P., Stones, L., Ankghuambom, C., Pondei, K., McClure, C. P., Alemnji, G., Taylor, S., Sharp, P. M., Clapham, P. R. & Ball, J. K. (2011). Intercompartmental recombination of HIV-1 contributes to env intrahost diversity and modulates viral tropism and sensitivity to entry inhibitors. *J Virol* **85**, 6024-37.

Bunka, D. H. & Stockley, P. G. (2006). Aptamers come of age - at last. *Nat Rev Microbiol* **4**, 588-96.

Bures, R., Gaitan, A., Zhu, T., Graziosi, C., McGrath, K. M., Tartaglia, J., Caudrelier, P., El Habib, R., Klein, M., Lazzarin, A., Stablein, D. M., Deers, M., Corey, L., Greenberg, M. L., Schwartz, D. H. & Montefiori, D. C. (2000). Immunization with recombinant canarypox vectors expressing membrane-anchored glycoprotein 120 followed by glycoprotein 160 boosting fails to generate antibodies that neutralize R5 primary isolates of human immunodeficiency virus type 1. *AIDS Res Hum Retroviruses* **16**, 2019-35.

Bures, R., Morris, L., Williamson, C., Ramjee, G., Deers, M., Fiscus, S. A., Abdool-Karim, S. & Montefiori, D. C. (2002). Regional clustering of shared neutralization determinants on primary isolates of clade C human immunodeficiency virus type 1 from South Africa. *J Virol* **76**, 2233-44.

Burton, D. R., Barbas, C. F., 3rd, Persson, M. A., Koenig, S., Chanock, R. M. & Lerner, R. A. (1991). A large array of human monoclonal antibodies to type 1 human immunodeficiency virus from combinatorial libraries of asymptomatic seropositive individuals. *Proc Natl Acad Sci U S A* **88**, 10134-7.

Cameron, P. U., Dawkins, R. L., Armstrong, J. A. & Bonifacio, E. (1987). Western blot profiles, lymph node ultrastructure and viral expression in HIV-infected patients: a correlative study. *Clin Exp Immunol* **68**, 465-78.

Cerchia, L., Duconge, F., Pestourie, C., Boulay, J., Aissouni, Y., Gombert, K., Tavitian, B., de Franciscis, V. & Libri, D. (2005). Neutralizing aptamers from whole-cell SELEX inhibit the RET receptor tyrosine kinase. *PLoS Biol* **3**, e123.

Chan, D. C., Chutkowski, C. T. & Kim, P. S. (1998). Evidence that a prominent cavity in the coiled coil of HIV type 1 gp41 is an attractive drug target. *Proc Natl Acad Sci U S A* **95**, 15613-7.

Chan, D. C., Fass, D., Berger, J. M. & Kim, P. S. (1997). Core structure of gp41 from the HIV envelope glycoprotein. *Cell* **89**, 263-73.

Chen, B., Vogan, E. M., Gong, H., Skehel, J. J., Wiley, D. C. & Harrison, S. C. (2005a). Structure of an unliganded simian immunodeficiency virus gp120 core. *Nature* **433**, 834-41.

Chen, C. H., Matthews, T. J., McDanal, C. B., Bolognesi, D. P. & Greenberg, M. L. (1995). A molecular clasp in the human immunodeficiency virus (HIV) type 1 TM protein determines the anti-HIV activity of gp41 derivatives: implication for viral fusion. *J Virol* **69**, 3771-7.

Chen, F., Zhou, J., Luo, F., Mohammed, A. B. & Zhang, X. L. (2007). Aptamer from whole-bacterium SELEX as new therapeutic reagent against virulent Mycobacterium tuberculosis. *Biochem Biophys Res Commun* **357**, 743-8.

Chen, H., Xu, X., Bishop, A. & Jones, I. M. (2005b). Reintroduction of the 2G12 epitope in an HIV-1 clade C gp120. *Aids* **19**, 833-5.

Choge, I., Cilliers, T., Walker, P., Taylor, N., Phoswa, M., Meyers, T., Viljoen, J., Violari, A., Gray, G., Moore, P. L., Papathanosopoulos, M. & Morris, L. (2006). Genotypic and phenotypic characterization of viral isolates from HIV-1 subtype C-infected children with slow and rapid disease progression. *AIDS Res Hum Retroviruses* **22**, 458-65.

Chou, T. C. & Talalay, P. (1984). Quantitative analysis of dose-effect relationships: the combined effects of multiple drugs or enzyme inhibitors. *Adv Enzyme Regul* **22**, 27-55.

Choudhry, V., Zhang, M. Y., Harris, I., Sidorov, I. A., Vu, B., Dimitrov, A. S., Fouts, T. & Dimitrov, D. S. (2006). Increased efficacy of HIV-1 neutralization by antibodies at low CCR5 surface concentration. *Biochem Biophys Res Commun* **348**, 1107-15.

Choudhry, V., Zhang, M. Y., Sidorov, I. A., Louis, J. M., Harris, I., Dimitrov, A. S., Bouma, P., Cham, F., Choudhary, A., Rybak, S. M., Fouts, T., Montefiori, D. C., Broder, C. C., Quinnan, G. V., Jr. & Dimitrov, D. S. (2007). Cross-reactive HIV-1 neutralizing monoclonal antibodies selected by screening of an immune human phage library against an envelope glycoprotein (gp140) isolated from a patient (R2) with broadly HIV-1 neutralizing antibodies. *Virology* **363**, 79-90.

Chushak, Y. & Stone, M. O. (2009). In silico selection of RNA aptamers. *Nucleic Acids Res* **37**, e87.

Cilliers, T., Nhlapo, J., Coetzer, M., Orlovic, D., Ketas, T., Olson, W. C., Moore, J. P., Trkola, A. & Morris, L. (2003). The CCR5 and CXCR4 coreceptors are both used by human immunodeficiency virus type 1 primary isolates from subtype C. *J Virol* **77**, 4449-56.

Cocchi, F., DeVico, A. L., Garzino-Demo, A., Cara, A., Gallo, R. C. & Lusso, P. (1996). The V3 domain of the HIV-1 gp120 envelope glycoprotein is critical for chemokine-mediated blockade of infection. *Nat Med* **2**, 1244-7.

Cohen, C., Forzan, M., Sproat, B., Pantophlet, R., McGowan, I., Burton, D. & James, W. (2008). An aptamer that neutralizes R5 strains of HIV-1 binds to core residues of gp120 in the CCR5 binding site. *Virology* **381**, 46-54.

Coiras, M., Lopez-Huertas, M. R., Perez-Olmeda, M. & Alcami, J. (2009). Understanding HIV-1 latency provides clues for the eradication of long-term reservoirs. *Nat Rev Microbiol* **7**, 798-812.

Collett, J. R., Cho, E. J. & Ellington, A. D. (2005). Production and processing of aptamer microarrays. *Methods* **37**, 4-15.

Collin, M., James, W. & Gordon, S. (1991). Development of techniques to analyse the formation of HIV provirus in primary human macrophages. *Res Virol* **142**, 105-12.

Cormier, E. G., Tran, D. N., Yukhayeva, L., Olson, W. C. & Dragic, T. (2001). Mapping the determinants of the CCR5 amino-terminal sulfopeptide interaction with soluble human immunodeficiency virus type 1 gp120-CD4 complexes. *J Virol* **75**, 5541-9.

Cox, J. C. & Ellington, A. D. (2001). Automated selection of anti-protein aptamers. *Bioorg Med Chem* **9**, 2525-31.

Crowe, S., Maslin, C., Ellery, P., and Kedzierska, K. (2004). Current Protocols in Immunology. Eds: Coligen., J.E., Bierer, B.E., Margulies, D.H. et al., National Institute of Health. John Wiley & Sons, Inc. **3**, pp 12.4.4-12.4.13.

Crowe, S., Zhu, T. & Muller, W. A. (2003). The contribution of monocyte infection and trafficking to viral persistence, and maintenance of the viral reservoir in HIV infection. *J Leukoc Biol* **74**, 635-41.

Crowe, S. M. & Sonza, S. (2000). HIV-1 can be recovered from a variety of cells including peripheral blood monocytes of patients receiving highly active antiretroviral therapy: a further obstacle to eradication. *J Leukoc Biol* **68**, 345-50.

Dalgleish, A. G., Beverley, P. C., Clapham, P. R., Crawford, D. H., Greaves, M. F. & Weiss, R. A. (1984). The CD4 (T4) antigen is an essential component of the receptor for the AIDS retrovirus. *Nature* **312**, 763-7.

Dang, C. & Jayasena, S. D. (1996). Oligonucleotide inhibitors of Taq DNA polymerase facilitate detection of low copy number targets by PCR. *J Mol Biol* **264**, 268-78.

Daniels, D. A., Chen, H., Hicke, B. J., Swiderek, K. M. & Gold, L. (2003). A tenascin-C aptamer identified by tumor cell SELEX: systematic evolution of ligands by exponential enrichment. *Proc Natl Acad Sci U S A* **100**, 15416-21.

Davis, K. A., Lin, Y., Abrams, B. & Jayasena, S. D. (1998). Staining of cell surface human CD4 with 2'-F-pyrimidine-containing RNA aptamers for flow cytometry. *Nucleic Acids Res* **26**, 3915-24.

de la Vega, M., Marin, M., Kondo, N., Miyauchi, K., Kim, Y., Epand, R. F., Epand, R. M. & Melikyan, G. B. Inhibition of HIV-1 endocytosis allows lipid mixing at the plasma membrane, but not complete fusion. *Retrovirology* **8**, 99.

de Oliveira, T., Pillay, D. & Gifford, R. J. (2010). The HIV-1 subtype C epidemic in South America is linked to the United Kingdom. *PLoS One* **5**, e9311.

Dean, M., Carrington, M., Winkler, C., Huttley, G. A., Smith, M. W., Allikmets, R., Goedert, J. J., Buchbinder, S. P., Vittinghoff, E., Gomperts, E., Donfield, S., Vlahov, D., Kaslow, R., Saah, A., Rinaldo, C., Detels, R. & O'Brien, S. J. (1996). Genetic restriction of HIV-1 infection and progression to AIDS by a

deletion allele of the CKR5 structural gene. Hemophilia Growth and Development Study, Multicenter AIDS Cohort Study, Multicenter Hemophilia Cohort Study, San Francisco City Cohort, ALIVE Study. *Science* **273**, 1856-62.

Decker, J. M., Bibollet-Ruche, F., Wei, X., Wang, S., Levy, D. N., Wang, W., Delaporte, E., Peeters, M., Derdeyn, C. A., Allen, S., Hunter, E., Saag, M. S., Hoxie, J. A., Hahn, B. H., Kwong, P. D., Robinson, J. E. & Shaw, G. M. (2005). Antigenic conservation and immunogenicity of the HIV coreceptor binding site. *J Exp Med* **201**, 1407-19.

Dey, A. K., Griffiths, C., Lea, S. M. & James, W. (2005a). Structural characterization of an anti-gp120 RNA aptamer that neutralizes R5 strains of HIV-1. *Rna* **11**, 873-84.

Dey, A. K., Khati, M., Tang, M., Wyatt, R., Lea, S. M. & James, W. (2005b). An aptamer that neutralizes R5 strains of human immunodeficiency virus type 1 blocks gp120-CCR5 interaction. *J Virol* **79**, 13806-10.

Dhar, S., Gu, F. X., Langer, R., Farokhzad, O. C. & Lippard, S. J. (2008). Targeted delivery of cisplatin to prostate cancer cells by aptamer functionalized Pt(IV) prodrug-PLGA-PEG nanoparticles. *Proc Natl Acad Sci U S A* **105**, 17356-61.

Doms, R. W. & Moore, J. P. (2000). HIV-1 membrane fusion: targets of opportunity. *J Cell Biol* **151**, F9-14.

Donzella, G. A., Schols, D., Lin, S. W., Este, J. A., Nagashima, K. A., Maddon, P. J., Allaway, G. P., Sakmar, T. P., Henson, G., De Clercq, E. & Moore, J. P. (1998). AMD3100, a small molecule inhibitor of HIV-1 entry via the CXCR4 co-receptor. *Nat Med* **4**, 72-7.

Dorr, P., Westby, M., Dobbs, S., Griffin, P., Irvine, B., Macartney, M., Mori, J., Rickett, G., Smith-Burchnell, C., Napier, C., Webster, R., Armour, D., Price, D., Stammen, B., Wood, A. & Perros, M. (2005). Maraviroc (UK-427,857), a potent, orally bioavailable, and selective small-molecule inhibitor of chemokine receptor CCR5 with broad-spectrum anti-human immunodeficiency virus type 1 activity. *Antimicrob Agents Chemother* **49**, 4721-32.

Drolet, D. W., Moon-McDermott, L. & Romig, T. S. (1996). An enzyme-linked oligonucleotide assay. *Nat Biotechnol* **14**, 1021-5.

Dube, M., Bego, M. G., Paquay, C. & Cohen, E. A. (2010). Modulation of HIV-1-host interaction: role of the Vpu accessory protein. *Retrovirology* **7**, 114.

Duenas-Decamp, M. J., Peters, P. J., Burton, D. & Clapham, P. R. (2009). Determinants flanking the CD4 binding loop modulate macrophage tropism of human immunodeficiency virus type 1 R5 envelopes. *J Virol* **83**, 2575-83.

Duncan, C. J. & Sattentau, Q. J. (2011). Viral determinants of HIV-1 macrophage tropism. *Viruses* **3**, 2255-79.

Dunfee, R. L., Thomas, E. R. & Gabuzda, D. (2009). Enhanced macrophage tropism of HIV in brain and lymphoid tissues is associated with sensitivity to the broadly neutralizing CD4 binding site antibody b12. *Retrovirology* **6**, 69.

Ellington, A. D. & Szostak, J. W. (1990). In vitro selection of RNA molecules that bind specific ligands. *Nature* **346**, 818-22.

Engelbrecht, S., Smith, T. L., Kasper, P., Faatz, E., Zeier, M., Moodley, D., Clay, C. G. & van Rensburg, E. J. (1999). HIV type 1 V3 domain serotyping and

genotyping in Gauteng, Mpumalanga, KwaZulu-Natal, and Western Cape Provinces of South Africa. *AIDS Res Hum Retroviruses* **15**, 325-8.

Essex, M. (1999). Human immunodeficiency viruses in the developing world. *Adv Virus Res* **53**, 71-88.

Eulberg, D., Buchner, K., Maasch, C. & Klussmann, S. (2005). Development of an automated in vitro selection protocol to obtain RNA-based aptamers: identification of a biostable substance P antagonist. *Nucleic Acids Res* **33**, e45.

Eyetech (2002). Preclinical and phase 1A clinical evaluation of an anti-VEGF pegylated aptamer (EYE001) for the treatment of exudative age-related macular degeneration. *Retina* **22**, 143-152.

Eyetech (2003). Anti-vascular endothelial growth factor therapy for subfoveal choroidal neovascularization secondary to age-related macular degeneration: phase II study results. *Opthalmology* **110**, 979-986.

Falkowska, E., Ramos, A., Feng, Y., Zhou, T., Moquin, S., Walker, L. M., Wu, X., Seaman, M. S., Wrin, T., Kwong, P. D., Wyatt, R. T., Mascola, J. R., Poignard, P. & Burton, D. R. (2012). PG V04, an HIV-1 gp120 CD4 binding site antibody, is broad and potent in neutralization but does not induce conformational changes characteristic of CD4. *J Virol*.

Farokhzad, O. C., Cheng, J., Teply, B. A., Sherifi, I., Jon, S., Kantoff, P. W., Richie, J. P. & Langer, R. (2006). Targeted nanoparticle-aptamer bioconjugates for cancer chemotherapy in vivo. *Proc Natl Acad Sci U S A* **103**, 6315-20.

Fauci, S. A., and Desrosiers, R.C. (1997). Pathogenesis of HIV and SIV. *Retroviruses*, Eds: Coffin, J.M., Hughes, S.H., Varmus, H.E. Cold Spring Harbor, NY.

Fenyo, E. M., Heath, A., Dispinseri, S., Holmes, H., Lusso, P., Zolla-Pazner, S., Donners, H., Heyndrickx, L., Alcami, J., Bongertz, V., Jassoy, C., Malnati, M., Montefiori, D., Moog, C., Morris, L., Osmanov, S., Polonis, V., Sattentau, Q., Schuitemaker, H., Sutthent, R., Wrin, T. & Scarlatti, G. (2009). International network for comparison of HIV neutralization assays: the NeutNet report. *PLoS One* **4**, e4505.

Fenyo, E. M., Morfeldt-Manson, L., Chiodi, F., Lind, B., von Gegerfelt, A., Albert, J., Olausson, E. & Asjo, B. (1988). Distinct replicative and cytopathic characteristics of human immunodeficiency virus isolates. *J Virol* **62**, 4414-9.

Fukuda, K., Toyokawa, Y., Kikuchi, K., Konno, K., Ishihara, R., Fukazawa, C., Nishikawa, S. & Hasegawa, T. (2008). Isolation of RNA aptamers specific for the 3' X tail of HCV. *Nucleic Acids Symp Ser (Oxf)*, 205-6.

Gao, F., Morrison, S. G., Robertson, D. L., Thornton, C. L., Craig, S., Karlsson, G., Sodroski, J., Morgado, M., Galvao-Castro, B., von Briesen, H., Beddows, S., Weber, J., Sharp, P. M., Shaw, G. M. & Hahn, B. H. (1996). Molecular cloning and analysis of functional envelope genes from human immunodeficiency virus type 1 sequence subtypes A through G. The WHO and NIAID Networks for HIV Isolation and Characterization. *J Virol* **70**, 1651-67.

Gartner, S., Markovits, P., Markovitz, D. M., Kaplan, M. H., Gallo, R. C. & Popovic, M. (1986). The role of mononuclear phagocytes in HTLV-III/LAV infection. *Science* **233**, 215-9.

Ge, Q., Dallas, A., Ilves, H., Shorenstein, J., Behlke, M. A. & Johnston, B. H. (2010). Effects of chemical modification on the potency, serum stability, and immunostimulatory properties of short shRNAs. *Rna* **16**, 118-30.

Geiger, A., Burgstaller, P., von der Eltz, H., Roeder, A. & Famulok, M. (1996). RNA aptamers that bind L-arginine with sub-micromolar dissociation constants and high enantioselectivity. *Nucleic Acids Res* **24**, 1029-36.

Gendelman, H. E., Narayan, O., Molineaux, S., Clements, J. E. & Ghotbi, Z. (1985). Slow, persistent replication of lentiviruses: role of tissue macrophages and macrophage precursors in bone marrow. *Proc Natl Acad Sci U S A* **82**, 7086-90.

Gendelman, H. E., Orenstein, J. M., Baca, L. M., Weiser, B., Burger, H., Kalter, D. C. & Meltzer, M. S. (1989). The macrophage in the persistence and pathogenesis of HIV infection. *Aids* **3**, 475-95.

German, I., Buchanan, D. D. & Kennedy, R. T. (1998). Aptamers as ligands in affinity probe capillary electrophoresis. *Anal Chem* **70**, 4540-5.

Gilbert, M. T., Rambaut, A., Wlasiuk, G., Spira, T. J., Pitchenik, A. E. & Worobey, M. (2007). The emergence of HIV/AIDS in the Americas and beyond. *Proc Natl Acad Sci U S A* **104**, 18566-70.

Gobeil, L. A., Lodge, R. & Tremblay, M. J. (2012). Differential HIV-1 endocytosis and susceptibility to virus infection in human macrophages correlate with cell activation status. *J Virol* **86**, 10399-407.

Gold, L., Ayers, D., Bertino, J., Bock, C., Bock, A., Brody, E. N., Carter, J., Dalby, A. B., Eaton, B. E., Fitzwater, T., Flather, D., Forbes, A., Foreman, T., Fowler, C., Gawande, B., Goss, M., Gunn, M., Gupta, S., Halladay, D., Heil, J., Heilig, J., Hicke, B., Husar, G., Janjic, N., Jarvis, T., Jennings, S., Katilius, E., Keeney, T. R., Kim, N., Koch, T. H., Kraemer, S., Kroiss, L., Le, N., Levine, D., Lindsey, W., Lollo, B., Mayfield, W., Mehan, M., Mehler, R., Nelson, S. K., Nelson, M., Nieuwlandt, D., Nikrad, M., Ochsner, U., Ostroff, R. M., Otis, M., Parker, T., Pietrasiewicz, S., Resnicow, D. I., Rohloff, J., Sanders, G., Sattin, S., Schneider, D., Singer, B., Stanton, M., Sterkel, A., Stewart, A., Stratford, S., Vaught, J. D., Vrkljan, M., Walker, J. J., Watrobka, M., Waugh, S., Weiss, A., Wilcox, S. K., Wolfson, A., Wolk, S. K., Zhang, C. & Zichi, D. (2010). Aptamer-based multiplexed proteomic technology for biomarker discovery. *PLoS One* **5**, e15004.

Gold, L., Polisky, B., Uhlenbeck, O. & Yarus, M. (1995). Diversity of oligonucleotide functions. *Annu Rev Biochem* **64**, 763-97.

Gopinath, S. C. (2007). Antiviral aptamers. *Arch Virol* **152**, 2137-57.

Gordon, S. & Martinez, F. O. (2010). Alternative activation of macrophages: mechanism and functions. *Immunity* **32**, 593-604.

Gorny, M. K., Xu, J. Y., Karwowska, S., Buchbinder, A. & Zolla-Pazner, S. (1993). Repertoire of neutralizing human monoclonal antibodies specific for the V3 domain of HIV-1 gp120. *J Immunol* **150**, 635-43.

Gottlieb, M. S., Groopman, J. E., Weinstein, W. M., Fahey, J. L. & Detels, R. (1983). The acquired immunodeficiency syndrome. *Ann Intern Med* **99**, 208-20.

Gourlain, T., Sidorov, A., Mignet, N., Thorpe, S. J., Lee, S. E., Grasby, J. A. & Williams, D. M. (2001). Enhancing the catalytic repertoire of nucleic acids. II. Simultaneous incorporation of amino and imidazolyl functionalities by two modified triphosphates during PCR. *Nucleic Acids Res* **29**, 1898-905.

Gousset, K., Ablan, S. D., Coren, L. V., Ono, A., Soheilian, F., Nagashima, K., Ott, D. E. & Freed, E. O. (2008). Real-time visualization of HIV-1 GAG trafficking in infected macrophages. *PLoS Pathog* **4**, e1000015.

Graham, F. L., Smiley, J., Russell, W. C. & Nairn, R. (1977). Characteristics of a human cell line transformed by DNA from human adenovirus type 5. *J Gen Virol* **36**, 59-74.

Gras, G. & Kaul, M. (2010). Molecular mechanisms of neuroinvasion by monocytes-macrophages in HIV-1 infection. *Retrovirology* **7**, 30.

Gray, E. S., Meyers, T., Gray, G., Montefiori, D. C. & Morris, L. (2006). Insensitivity of paediatric HIV-1 subtype C viruses to broadly neutralising monoclonal antibodies raised against subtype B. *PLoS Med* **3**, e255.

Gray, E. S., Moore, P. L., Bibollet-Ruche, F., Li, H., Decker, J. M., Meyers, T., Shaw, G. M. & Morris, L. (2008). 4E10-resistant variants in a human immunodeficiency virus type 1 subtype C-infected individual with an anti-membrane-proximal external region-neutralizing antibody response. *J Virol* **82**, 2367-75.

Gray, E. S., Moore, P. L., Choge, I. A., Decker, J. M., Bibollet-Ruche, F., Li, H., Leseka, N., Treurnicht, F., Mlisana, K., Shaw, G. M., Karim, S. S., Williamson, C. & Morris, L. (2007a). Neutralizing antibody responses in acute human immunodeficiency virus type 1 subtype C infection. *J Virol* **81**, 6187-96.

Gray, E. S., Moore, P. L., Pantophlet, R. A. & Morris, L. (2007b). N-linked glycan modifications in gp120 of human immunodeficiency virus type 1 subtype C render partial sensitivity to 2G12 antibody neutralization. *J Virol* **81**, 10769-76.

Gray, E. S., Taylor, N., Wycuff, D., Moore, P. L., Tomaras, G. D., Wibmer, C. K., Puren, A., DeCamp, A., Gilbert, P. B., Wood, B., Montefiori, D. C., Binley, J. M., Shaw, G. M., Haynes, B. F., Mascola, J. R. & Morris, L. (2009). Antibody specificities associated with neutralization breadth in plasma from human immunodeficiency virus type 1 subtype C-infected blood donors. *J Virol* **83**, 8925-37.

Gray, L., Sterjovski, J., Churchill, M., Ellery, P., Nasr, N., Lewin, S. R., Crowe, S. M., Wesselingh, S. L., Cunningham, A. L. & Gorry, P. R. (2005). Uncoupling coreceptor usage of human immunodeficiency virus type 1 (HIV-1) from macrophage tropism reveals biological properties of CCR5-restricted HIV-1 isolates from patients with acquired immunodeficiency syndrome. *Virology* **337**, 384-98.

Groot, F., Welsch, S. & Sattentau, Q. J. (2008). Efficient HIV-1 transmission from macrophages to T cells across transient virological synapses. *Blood* **111**, 4660-3.

Guo, K. T., Ziemer, G., Paul, A. & Wendel, H. P. (2008). CELL-SELEX: Novel perspectives of aptamer-based therapeutics. *Int J Mol Sci* **9**, 668-78.

Hartley, O., Klasse, P. J., Sattentau, Q. J. & Moore, J. P. (2005). V3: HIV's switch-hitter. *AIDS Res Hum Retroviruses* **21**, 171-89.

Healy, J. M., Lewis, S. D., Kurz, M., Boomer, R. M., Thompson, K. M., Wilson, C. & McCauley, T. G. (2004). Pharmacokinetics and biodistribution of novel aptamer compositions. *Pharm Res* **21**, 2234-46.

Held, D. M., Kissel, J. D., Patterson, J. T., Nickens, D. G. & Burke, D. H. (2006). HIV-1 inactivation by nucleic acid aptamers. *Front Biosci* **11**, 89-112.

Hemelaar, J., Gouws, E., Ghys, P. D. & Osmanov, S. (2006). Global and regional distribution of HIV-1 genetic subtypes and recombinants in 2004. *Aids* **20**, W13-23.

Hesselberth, J., Robertson, M. P., Jhaveri, S. & Ellington, A. D. (2000). In vitro selection of nucleic acids for diagnostic applications. *J Biotechnol* **74**, 15-25.

Hioe, C. E., Wrin, T., Seaman, M. S., Yu, X., Wood, B., Self, S., Williams, C., Gorny, M. K. & Zolla-Pazner, S. (2010). Anti-V3 monoclonal antibodies display broad neutralizing activities against multiple HIV-1 subtypes. *PLoS One* **5**, e10254.

Ho, H. T., Fan, L., Nowicka-Sans, B., McAuliffe, B., Li, C. B., Yamanaka, G., Zhou, N., Fang, H., Dicker, I., Dalterio, R., Gong, Y. F., Wang, T., Yin, Z., Ueda, Y., Matiskella, J., Kadow, J., Clapham, P., Robinson, J., Colonno, R. & Lin, P. F. (2006). Envelope conformational changes induced by human immunodeficiency virus type 1 attachment inhibitors prevent CD4 binding and downstream entry events. *J Virol* **80**, 4017-25.

Honnen, W. J., Krachmarov, C., Kayman, S. C., Gorny, M. K., Zolla-Pazner, S. & Pinter, A. (2007). Type-specific epitopes targeted by monoclonal antibodies with exceptionally potent neutralizing activities for selected strains of human immunodeficiency virus type 1 map to a common region of the V2 domain of gp120 and differ only at single positions from the clade B consensus sequence. *J Virol* **81**, 1424-32.

Hout, D. R., Mulcahy, E. R., Pacyniak, E., Gomez, L. M., Gomez, M. L. & Stephens, E. B. (2004). Vpu: a multifunctional protein that enhances the pathogenesis of human immunodeficiency virus type 1. *Curr HIV Res* **2**, 255-70.

Huang, C. C., Lam, S. N., Acharya, P., Tang, M., Xiang, S. H., Hussan, S. S., Stanfield, R. L., Robinson, J., Sodroski, J., Wilson, I. A., Wyatt, R., Bewley, C. A. & Kwong, P. D. (2007). Structures of the CCR5 N terminus and of a tyrosine-sulfated antibody with HIV-1 gp120 and CD4. *Science* **317**, 1930-4.

Huang, C. C., Tang, M., Zhang, M. Y., Majeed, S., Montabana, E., Stanfield, R. L., Dimitrov, D. S., Korber, B., Sodroski, J., Wilson, I. A., Wyatt, R. & Kwong, P. D. (2005). Structure of a V3-containing HIV-1 gp120 core. *Science* **310**, 1025-8.

Jacobson, J. M., Lowy, I., Fletcher, C. V., O'Neill, T. J., Tran, D. N., Ketas, T. J., Trkola, A., Klotman, M. E., Maddon, P. J., Olson, W. C. & Israel, R. J. (2000). Single-dose safety, pharmacology, and antiviral activity of the human immunodeficiency virus (HIV) type 1 entry inhibitor PRO 542 in HIV-infected adults. *J Infect Dis* **182**, 326-9.

James, W. (2001). Nucleic acid and polypeptide aptamers: a powerful approach to ligand discovery. *Curr Opin Pharmacol* **1**, 540-6.

Jayasena, S. D. (1999). Aptamers: an emerging class of molecules that rival antibodies in diagnostics. *Clin Chem* **45**, 1628-50.

Jennes, W., Kyongo, J. K., Vanhommerig, E., Camara, M., Coppens, S., Seydi, M., Mboup, S., Heyndrickx, L. & Kestens, L. Molecular epidemiology of HIV-1 transmission in a cohort of HIV-1 concordant heterosexual couples from Dakar, Senegal. *PLoS One* **7**, e37402.

Jere, A., Fujita, M., Adachi, A. & Nomaguchi, M. (2010). Role of HIV-1 Nef protein for virus replication in vitro. *Microbes Infect* **12**, 65-70.

Johnson, V. A., and R.E. Byington. (1990). Infectivity assay (viral yield assay). In: Techniques in HIV Research (Aldovani, A., and Walker, B.D., eds). pp. 71-76. New York, N.Y., pp71-76: Stockton Press.

Joubert, M. K., Kinsley, N., Capovilla, A., Sewell, B. T., Jaffer, M. A. & Khati, M. (2010). A modeled structure of an aptamer-gp120 complex provides insight into the mechanism of HIV-1 neutralization. *Biochemistry* **49**, 5880-90.

Kawano, Y., Tanaka, Y., Misawa, N., Tanaka, R., Kira, J. I., Kimura, T., Fukushi, M., Sano, K., Goto, T., Nakai, M., Kobayashi, T., Yamamoto, N. & Koyanagi, Y. (1997). Mutational analysis of human immunodeficiency virus type 1 (HIV-1) accessory genes: requirement of a site in the nef gene for HIV-1 replication in activated CD4+ T cells in vitro and in vivo. *J Virol* **71**, 8456-66.

Keefe, A. D., Pai, S. & Ellington, A. (2010). Aptamers as therapeutics. *Nat Rev Drug Discov* **9**, 537-50.

Kessler, J. A., 2nd, McKenna, P. M., Emini, E. A., Chan, C. P., Patel, M. D., Gupta, S. K., Mark, G. E., 3rd, Barbas, C. F., 3rd, Burton, D. R. & Conley, A. J. (1997). Recombinant human monoclonal antibody IgG1b12 neutralizes diverse human immunodeficiency virus type 1 primary isolates. *AIDS Res Hum Retroviruses* **13**, 575-82.

Khati, M. (2010). The future of aptamers in medicine. *J Clin Pathol* **63**, 480-7.

Khati, M., James, W. & Gordon, S. (2001). HIV-macrophage interactions at the cellular and molecular level. *Arch Immunol Ther Exp (Warsz)* **49**, 367-78.

Khati, M., Schuman, M., Ibrahim, J., Sattentau, Q., Gordon, S. & James, W. (2003). Neutralization of infectivity of diverse R5 clinical isolates of human immunodeficiency virus type 1 by gp120-binding 2'F-RNA aptamers. *J Virol* **77**, 12692-8.

Kilby, J. M., Hopkins, S., Venetta, T. M., DiMassimo, B., Cloud, G. A., Lee, J. Y., Alldredge, L., Hunter, E., Lambert, D., Bolognesi, D., Matthews, T., Johnson, M. R., Nowak, M. A., Shaw, G. M. & Saag, M. S. (1998). Potent suppression of HIV-1 replication in humans by T-20, a peptide inhibitor of gp41-mediated virus entry. *Nat Med* **4**, 1302-7.

Kilby, J. M., Lalezari, J. P., Eron, J. J., Carlson, M., Cohen, C., Arduino, R. C., Goodgame, J. C., Gallant, J. E., Volberding, P., Murphy, R. L., Valentine, F., Saag, M. S., Nelson, E. L., Sista, P. R. & Dusek, A. (2002). The safety, plasma pharmacokinetics, and antiviral activity of subcutaneous enfuvirtide (T-20), a peptide inhibitor of gp41-mediated virus fusion, in HIV-infected adults. *AIDS Res Hum Retroviruses* **18**, 685-93.

Klopper, J. M. (1985). AIDS--report of an epidemiological seminar. *S Afr Med J* **68**, 617-8.

Knudsen, S. M., Robertson, M. P. & Ellington, A. D. (2002). In vitro selection using modified or unnatural nucleotides. *Curr Protoc Nucleic Acid Chem* **Chapter 9**, Unit 9 6.

Kolchinsky, P., Kiprilov, E., Bartley, P., Rubinstein, R. & Sodroski, J. (2001). Loss of a single N-linked glycan allows CD4-independent human immunodeficiency virus type 1 infection by altering the position of the gp120 V1/V2 variable loops. *J Virol* **75**, 3435-43.

Kothe, D. L., Li, Y., Decker, J. M., Bibollet-Ruche, F., Zammit, K. P., Salazar, M. G., Chen, Y., Weng, Z., Weaver, E. A., Gao, F., Haynes, B. F., Shaw, G. M.,

Korber, B. T. & Hahn, B. H. (2006). Ancestral and consensus envelope immunogens for HIV-1 subtype C. *Virology* **352**, 438-49.

Kubik, M. F., Bell, C., Fitzwater, T., Watson, S. R. & Tasset, D. M. (1997). Isolation and characterization of 2'-fluoro-, 2'-amino-, and 2'-fluoro-/amino-modified RNA ligands to human IFN-gamma that inhibit receptor binding. *J Immunol* **159**, 259-67.

Kuhmann, S. E., Pugach, P., Kunstman, K. J., Taylor, J., Stanfield, R. L., Snyder, A., Strizki, J. M., Riley, J., Baroudy, B. M., Wilson, I. A., Korber, B. T., Wolinsky, S. M. & Moore, J. P. (2004). Genetic and phenotypic analyses of human immunodeficiency virus type 1 escape from a small-molecule CCR5 inhibitor. *J Virol* **78**, 2790-807.

Kwong, P. D., Doyle, M. L., Casper, D. J., Cicala, C., Leavitt, S. A., Majeed, S., Steenbeke, T. D., Venturi, M., Chaiken, I., Fung, M., Katinger, H., Parren, P. W., Robinson, J., Van Ryk, D., Wang, L., Burton, D. R., Freire, E., Wyatt, R., Sodroski, J., Hendrickson, W. A. & Arthos, J. (2002). HIV-1 evades antibody-mediated neutralization through conformational masking of receptor-binding sites. *Nature* **420**, 678-82.

Kwong, P. D., Wyatt, R., Robinson, J., Sweet, R. W., Sodroski, J. & Hendrickson, W. A. (1998). Structure of an HIV gp120 envelope glycoprotein in complex with the CD4 receptor and a neutralizing human antibody. *Nature* **393**, 648-59.

Lalezari, J. P., Henry, K., O'Hearn, M., Montaner, J. S., Piliero, P. J., Trottier, B., Walmsley, S., Cohen, C., Kuritzkes, D. R., Eron, J. J., Jr., Chung, J., DeMasi, R., Donatacci, L., Drobnes, C., Delehanty, J. & Salgo, M. (2003). Enfuvirtide, an HIV-1 fusion inhibitor, for drug-resistant HIV infection in North and South America. *N Engl J Med* **348**, 2175-85.

Lebruska, L. L. & Maher, L. J., 3rd (1999). Selection and characterization of an RNA decoy for transcription factor NF-kappa B. *Biochemistry* **38**, 3168-74.

Lee, H. S., Kim, K. S., Kim, C. J., Hahn, S. K. & Jo, M. H. (2009). Electrical detection of VEGFs for cancer diagnoses using anti-vascular endotherial growth factor aptamer-modified Si nanowire FETs. *Biosens Bioelectron* **24**, 1801-5.

Levy, J. A. (2007). HIV and the Pathogenesis of AIDS. 3rd Edition, pp 1-8. ASM Press, Washington DC, USA.

Li, M., Gao, F., Mascola, J. R., Stamatatos, L., Polonis, V. R., Koutsoukos, M., Voss, G., Goepfert, P., Gilbert, P., Greene, K. M., Bilska, M., Kothe, D. L., Salazar-Gonzalez, J. F., Wei, X., Decker, J. M., Hahn, B. H. & Montefiori, D. C. (2005). Human immunodeficiency virus type 1 env clones from acute and early subtype B infections for standardized assessments of vaccine-elicited neutralizing antibodies. *J Virol* **79**, 10108-25.

Li, M., Salazar-Gonzalez, J. F., Derdeyn, C. A., Morris, L., Williamson, C., Robinson, J. E., Decker, J. M., Li, Y., Salazar, M. G., Polonis, V. R., Mlisana, K., Karim, S. A., Hong, K., Greene, K. M., Bilska, M., Zhou, J., Allen, S., Chomba, E., Mulenga, J., Vwalika, C., Gao, F., Zhang, M., Korber, B. T., Hunter, E., Hahn, B. H. & Montefiori, D. C. (2006). Genetic and neutralization properties of subtype C human immunodeficiency virus type 1 molecular env clones from acute and early heterosexually acquired infections in Southern Africa. *J Virol* **80**, 11776-90.

Li, N., Wang, Y., Pothukuchy, A., Syrett, A., Husain, N., Gopalakrisha, S., Kosaraju, P. & Ellington, A. D. (2008). Aptamers that recognize drug-resistant HIV-1 reverse transcriptase. *Nucleic Acids Res* **36**, 6739-51.

Li, Y., Migueles, S. A., Welcher, B., Svehla, K., Phogat, A., Louder, M. K., Wu, X., Shaw, G. M., Connors, M., Wyatt, R. T. & Mascola, J. R. (2007). Broad HIV-1 neutralization mediated by CD4-binding site antibodies. *Nat Med* **13**, 1032-4.

Li, Y., O'Dell, S., Walker, L. M., Wu, X., Guenaga, J., Feng, Y., Schmidt, S. D., McKee, K., Louder, M. K., Ledgerwood, J. E., Graham, B. S., Haynes, B. F., Burton, D. R., Wyatt, R. T. & Mascola, J. R. (2011). Mechanism of neutralization by the broadly neutralizing HIV-1 monoclonal antibody VRC01. *J Virol* **85**, 8954-67.

Lin, P. F., Blair, W., Wang, T., Spicer, T., Guo, Q., Zhou, N., Gong, Y. F., Wang, H. G., Rose, R., Yamanaka, G., Robinson, B., Li, C. B., Fridell, R., Deminie, C., Demers, G., Yang, Z., Zadjura, L., Meanwell, N. & Colonno, R. (2003). A small molecule HIV-1 inhibitor that targets the HIV-1 envelope and inhibits CD4 receptor binding. *Proc Natl Acad Sci U S A* **100**, 11013-8.

Liu, J., Bartesaghi, A., Borgnia, M. J., Sapiro, G. & Subramaniam, S. (2008). Molecular architecture of native HIV-1 gp120 trimers. *Nature* **455**, 109-13.

Liu, J., Mazumdar, D. & Lu, Y. (2006). A simple and sensitive "dipstick" test in serum based on lateral flow separation of aptamer-linked nanostructures. *Angew Chem Int Ed Engl* **45**, 7955-9.

Liu, R., Paxton, W. A., Choe, S., Ceradini, D., Martin, S. R., Horuk, R., MacDonald, M. E., Stuhlmann, H., Koup, R. A. & Landau, N. R. (1996). Homozygous defect in HIV-1 coreceptor accounts for resistance of some multiply-exposed individuals to HIV-1 infection. *Cell* **86**, 367-77.

Liu, Y., Kuan, C. T., Mi, J., Zhang, X., Clary, B. M., Bigner, D. D. & Sullenger, B. A. (2009). Aptamers selected against the unglycosylated EGFRvIII ectodomain and delivered intracellularly reduce membrane-bound EGFRvIII and induce apoptosis. *Biol Chem* **390**, 137-44.

Lobritz, M. A., Ratcliff, A. N. & Arts, E. J. (2010). HIV-1 Entry, Inhibitors, and Resistance. *Viruses* **2**, 1069-105.

Lochrie, M. A., Waugh, S., Pratt, D. G., Jr., Clever, J., Parslow, T. G. & Polisky, B. (1997). In vitro selection of RNAs that bind to the human immunodeficiency virus type-1 gag polyprotein. *Nucleic Acids Res* **25**, 2902-10.

Lopes de Campos, W. R., Coopusamy, D., Morris, L., Mayosi, B. M. & Khati, M. (2009). Cytotoxicological analysis of a gp120 binding aptamer with cross-clade human immunodeficiency virus type 1 entry inhibition properties: comparison to conventional antiretrovirals. *Antimicrob Agents Chemother* **53**, 3056-64.

Louder, M. K., Sambor, A., Chertova, E., Hunte, T., Barrett, S., Ojong, F., Sanders-Buell, E., Zolla-Pazner, S., McCutchan, F. E., Roser, J. D., Gabuzda, D., Lifson, J. D. & Mascola, J. R. (2005). HIV-1 envelope pseudotyped viral vectors and infectious molecular clones expressing the same envelope glycoprotein have a similar neutralization phenotype, but culture in peripheral blood mononuclear cells is associated with decreased neutralization sensitivity. *Virology* **339**, 226-38.

Lupold, S. E., Hicke, B. J., Lin, Y. & Coffey, D. S. (2002). Identification and characterization of nuclease-stabilized RNA molecules that bind human

prostate cancer cells via the prostate-specific membrane antigen. *Cancer Res* **62**, 4029-33.

Mann, A. M., Rusert, P., Berlinger, L., Kuster, H., Gunthard, H. F. & Trkola, A. (2009). HIV sensitivity to neutralization is determined by target and virus producer cell properties. *Aids* **23**, 1659-67.

Mannironi, C., Di Nardo, A., Fruscoloni, P. & Tocchini-Valentini, G. P. (1997). In vitro selection of dopamine RNA ligands. *Biochemistry* **36**, 9726-34.

Mao, Y., Wang, L., Gu, C., Herschhorn, A., Xiang, S. H., Haim, H., Yang, X. & Sodroski, J. (2012). Subunit organization of the membrane-bound HIV-1 envelope glycoprotein trimer. *Nat Struct Mol Biol*.

Marozsan, A. J., Kuhmann, S. E., Morgan, T., Herrera, C., Rivera-Troche, E., Xu, S., Baroudy, B. M., Strizki, J. & Moore, J. P. (2005). Generation and properties of a human immunodeficiency virus type 1 isolate resistant to the small molecule CCR5 inhibitor, SCH-417690 (SCH-D). *Virology* **338**, 182-99.

Martin, M. P., Dean, M., Smith, M. W., Winkler, C., Gerrard, B., Michael, N. L., Lee, B., Doms, R. W., Margolick, J., Buchbinder, S., Goedert, J. J., O'Brien, T. R., Hilgartner, M. W., Vlahov, D., O'Brien, S. J. & Carrington, M. (1998). Genetic acceleration of AIDS progression by a promoter variant of CCR5. *Science* **282**, 1907-11.

Mascola, J. R., D'Souza, P., Gilbert, P., Hahn, B. H., Haigwood, N. L., Morris, L., Petropoulos, C. J., Polonis, V. R., Sarzotti, M. & Montefiori, D. C. (2005). Recommendations for the design and use of standard virus panels to assess neutralizing antibody responses elicited by candidate human immunodeficiency virus type 1 vaccines. *J Virol* **79**, 10103-7.

Mayer, G. (2009). The chemical biology of aptamers. *Angew Chem Int Ed Engl* **48**, 2672-89.

McCaffrey, R. A., Saunders, C., Hensel, M. & Stamatatos, L. (2004). N-linked glycosylation of the V3 loop and the immunologically silent face of gp120 protects human immunodeficiency virus type 1 SF162 from neutralization by anti-gp120 and anti-gp41 antibodies. *J Virol* **78**, 3279-95.

McCutchan, F. E. (2006). Global epidemiology of HIV. *J Med Virol* **78 Suppl 1**, S7-S12.

McInerney, T. L., McLain, L., Armstrong, S. J. & Dimmock, N. J. (1997). A human IgG1 (b12) specific for the CD4 binding site of HIV-1 neutralizes by inhibiting the virus fusion entry process, but b12 Fab neutralizes by inhibiting a postfusion event. *Virology* **233**, 313-26.

McKeating, J. A., McKnight, A. & Moore, J. P. (1991). Differential loss of envelope glycoprotein gp120 from virions of human immunodeficiency virus type 1 isolates: effects on infectivity and neutralization. *J Virol* **65**, 852-60.

McNamara, J. O., 2nd, Andrechek, E. R., Wang, Y., Viles, K. D., Rempel, R. E., Gilboa, E., Sullenger, B. A. & Giangrande, P. H. (2006). Cell type-specific delivery of siRNAs with aptamer-siRNA chimeras. *Nat Biotechnol* **24**, 1005-15.

Melikyan, G. B., Markosyan, R. M., Hemmati, H., Delmedico, M. K., Lambert, D. M. & Cohen, F. S. (2000). Evidence that the transition of HIV-1 gp41 into a six-helix bundle, not the bundle configuration, induces membrane fusion. *J Cell Biol* **151**, 413-23.

Meltzer, M. S., Skillman, D. R., Gomatos, P. J., Kalter, D. C. & Gendelman, H. E. (1990). Role of mononuclear phagocytes in the pathogenesis of human immunodeficiency virus infection. *Annu Rev Immunol* **8**, 169-94.

Metifiot, M., Leon, O., Tarrago-Litvak, L., Litvak, S. & Andreola, M. L. (2005). Targeting HIV-1 integrase with aptamers selected against the purified RNase H domain of HIV-1 RT. *Biochimie* **87**, 911-9.

Meyaard, L., Schuitemaker, H. & Miedema, F. (1993). T-cell dysfunction in HIV infection: anergy due to defective antigen-presenting cell function? *Immunol Today* **14**, 161-4.

Michael, N. L. (1999). Host genetic influences on HIV-1 pathogenesis. *Curr Opin Immunol* **11**, 466-74.

Miyauchi, K., Kim, Y., Latinovic, O., Morozov, V. & Melikyan, G. B. (2009a). HIV enters cells via endocytosis and dynamin-dependent fusion with endosomes. *Cell* **137**, 433-44.

Miyauchi, K., Kozlov, M. M. & Melikyan, G. B. (2009b). Early steps of HIV-1 fusion define the sensitivity to inhibitory peptides that block 6-helix bundle formation. *PLoS Pathog* **5**, e1000585.

Montefiori, D. C. (2004). Evaluating neutralizing antibodies against HIV, SIV and SHIV in luciferase reporter gene assay. In *Current Protocols in Immunology*, pp. 1-15. Edited by K. A. M. In: Coligan J. E., Margulies D. H., Shevach E. M., Strober W., et al., editors: Hoboken: John Wiley.

Montefiori, D. C. (2009). Measuring HIV neutralization in a luciferase reporter gene assay. *Methods Mol Biol* **485**, 395-405.

Montefiori, D. C. & Mascola, J. R. (2009). Neutralizing antibodies against HIV-1: can we elicit them with vaccines and how much do we need? *Curr Opin HIV AIDS* **4**, 347-51.

Moore, J. P. & Doms, R. W. (2003). The entry of entry inhibitors: a fusion of science and medicine. *Proc Natl Acad Sci U S A* **100**, 10598-602.

Moore, J. P., McKeating, J. A., Weiss, R. A. & Sattentau, Q. J. (1990). Dissociation of gp120 from HIV-1 virions induced by soluble CD4. *Science* **250**, 1139-42.

Moore, M. D., Cookson, J., Coventry, V. K., Sproat, B., Rabe, L., Cranston, R. D., McGowan, I. & James, W. (2011). Protection of HIV neutralizing aptamers against rectal and vaginal nucleases: implications for RNA-based therapeutics. *J Biol Chem* **286**, 2526-35.

Morris, L., M. Coetzer, E. S. Gray, T. Cilliers, K. B. Alexandre, P. L. Moore, and J. M. Binley. (2007). Entry inhibition of HIV-1 subtype C isolates. In *Entry Inhibitors in HIV Therapy*, 1 edn. Edited by J. D. Reeves, Derdeyn, C. A.: Springer.

Mosier, D. & Sieburg, H. (1994). Macrophage-tropic HIV: critical for AIDS pathogenesis? *Immunol Today* **15**, 332-9.

Muesing, M. A., Smith, D. H., Cabradilla, C. D., Benton, C. V., Lasky, L. A. & Capon, D. J. (1985). Nucleic acid structure and expression of the human AIDS/lymphadenopathy retrovirus. *Nature* **313**, 450-8.

Mufhandu, H. T., Gray, E. S., Madiga, M. C., Tumba, N., Alexandre, K. B., Khoza, T., Wibmer, C. K., Moore, P. L., Morris, L. & Khati, M. (2012). UCLA1, a Synthetic Derivative of a gp120 RNA Aptamer, Inhibits Entry of Human Immunodeficiency Virus Type 1 Subtype C. *J Virol* **86**, 4989-99.

Murray, P. J. & Wynn, T. A. (2011). Protective and pathogenic functions of macrophage subsets. *Nat Rev Immunol* **11**, 723-37.

Musich, T., Peters, P. J., Duenas-Decamp, M. J., Gonzalez-Perez, M. P., Robinson, J., Zolla-Pazner, S., Ball, J. K., Luzuriaga, K. & Clapham, P. R. (2011). A conserved determinant in the V1 loop of HIV-1 modulates the V3 loop to prime low CD4 use and macrophage infection. *J Virol* **85**, 2397-405.

Nagashima, K. A., Thompson, D. A., Rosenfield, S. I., Maddon, P. J., Dragic, T. & Olson, W. C. (2001). Human immunodeficiency virus type 1 entry inhibitors PRO 542 and T-20 are potently synergistic in blocking virus-cell and cell-cell fusion. *J Infect Dis* **183**, 1121-5.

Neff, C. P., Zhou, J., Remling, L., Kuruvilla, J., Zhang, J., Li, H., Smith, D. D., Swiderski, P., Rossi, J. J. & Akkina, R. (2011). An aptamer-siRNA chimera suppresses HIV-1 viral loads and protects from helper CD4(+) T cell decline in humanized mice. *Sci Transl Med* **3**, 66ra6.

Nieuwlandt, D., Wecker, M. & Gold, L. (1995). In vitro selection of RNA ligands to substance P. *Biochemistry* **34**, 5651-9.

Nimjee, S. M., Rusconi, C. P. & Sullenger, B. A. (2005). Aptamers: an emerging class of therapeutics. *Annu Rev Med* **56**, 555-83.

Ogert, R. A., Wojcik, L., Buontempo, C., Ba, L., Buontempo, P., Ralston, R., Strizki, J. & Howe, J. A. (2008). Mapping resistance to the CCR5 co-receptor antagonist vicriviroc using heterologous chimeric HIV-1 envelope genes reveals key determinants in the C2-V5 domain of gp120. *Virology* **373**, 387-99.

Ometto, L., Bertorelle, R., Mainardi, M., Zanchetta, M., Tognazzo, S., Rampon, O., Ruga, E., Chieco-Bianchi, L. & De Rossi, A. (2001). Polymorphisms in the CCR5 promoter region influence disease progression in perinatally human immunodeficiency virus type 1-infected children. *J Infect Dis* **183**, 814-8.

Ostroff, R. M., Bigbee, W. L., Franklin, W., Gold, L., Mehan, M., Miller, Y. E., Pass, H. I., Rom, W. N., Siegfried, J. M., Stewart, A., Walker, J. J., Weissfeld, J. L., Williams, S., Zichi, D. & Brody, E. N. (2010). Unlocking biomarker discovery: large scale application of aptamer proteomic technology for early detection of lung cancer. *PLoS One* **5**, e15003.

Osztie, E., Varallyay, P., Doolittle, N. D., Lacy, C., Jones, G., Nickolson, H. S. & Neuwelt, E. A. (2001). Combined intraarterial carboplatin, intraarterial etoposide phosphate, and IV Cytoxan chemotherapy for progressive optic-hypothalamic gliomas in young children. *AJNR Am J Neuroradiol* **22**, 818-23.

Pancera, M., McLellan, J. S., Wu, X., Zhu, J., Changela, A., Schmidt, S. D., Yang, Y., Zhou, T., Phogat, S., Mascola, J. R. & Kwong, P. D. (2010). Crystal structure of PG16 and chimeric dissection with somatically related PG9: structure-function analysis of two quaternary-specific antibodies that effectively neutralize HIV-1. *J Virol* **84**, 8098-110.

Pandit, A. & Sinha, S. (2010). Using genomic signatures for HIV-1 sub-typing. *BMC Bioinformatics* **11 Suppl 1**, S26.

Pantophlet, R., Ollmann Saphire, E., Poignard, P., Parren, P. W., Wilson, I. A. & Burton, D. R. (2003). Fine mapping of the interaction of neutralizing and nonneutralizing monoclonal antibodies with the CD4 binding site of human immunodeficiency virus type 1 gp120. *J Virol* **77**, 642-58.

Park, S. Y., Kim, S., Yoon, H., Kim, K. B., Kalme, S. S., Oh, S., Song, C. S. & Kim, D. E. Selection of an antiviral RNA aptamer against hemagglutinin of the subtype H5 avian influenza virus. *Nucleic Acid Ther* **21**, 395-402.

Parren, P. W., Fisicaro, P., Labrijn, A. F., Binley, J. M., Yang, W. P., Ditzel, H. J., Barbas, C. F., 3rd & Burton, D. R. (1996). In vitro antigen challenge of human antibody libraries for vaccine evaluation: the human immunodeficiency virus type 1 envelope. *J Virol* **70**, 9046-50.

Patience, C., Moore, J.P., Boyd, M. (1991). Methods in Molecular biology Vol 8 in Practical Molecular Virology. The Humana Press Inc., Clifton, NJ., pp 131-140.

Pegu, A., Yang, Z., Chen, X., Todd, J., McKee, K., Rao, S., Mascola, J. & Nabel, G. (2011). VRC01 provides sterilizing protection to non human primates from mucosal SHIV challenges. *The Journal of Immunology. Meeting Abstract.* **155.11**.

Perelson, A. S., Essunger, P., Cao, Y., Vesanen, M., Hurley, A., Saksela, K., Markowitz, M. & Ho, D. D. (1997). Decay characteristics of HIV-1-infected compartments during combination therapy. *Nature* **387**, 188-91.

Perno, C. F., Newcomb, F. M., Davis, D. A., Aquaro, S., Humphrey, R. W., Calio, R. & Yarchoan, R. (1998). Relative potency of protease inhibitors in monocytes/macrophages acutely and chronically infected with human immunodeficiency virus. *J Infect Dis* **178**, 413-22.

Peters, P. J., Duenas-Decamp, M. J., Sullivan, W. M., Brown, R., Ankghuambom, C., Luzuriaga, K., Robinson, J., Burton, D. R., Bell, J., Simmonds, P., Ball, J. & Clapham, P. R. (2008). Variation in HIV-1 R5 macrophage-tropism correlates with sensitivity to reagents that block envelope: CD4 interactions but not with sensitivity to other entry inhibitors. *Retrovirology* **5**, 5.

Phillips, D. M., Tan, X., Perotti, M. E. & Zacharopoulos, V. R. (1998). Mechanism of monocyte-macrophage-mediated transmission of HIV. *AIDS Res Hum Retroviruses* **14 Suppl 1**, S67-70.

Pietzsch, J., Scheid, J. F., Mouquet, H., Klein, F., Seaman, M. S., Jankovic, M., Corti, D., Lanzavecchia, A. & Nussenzweig, M. C. (2010). Human anti-HIV-neutralizing antibodies frequently target a conserved epitope essential for viral fitness. *J Exp Med* **207**, 1995-2002.

Pinter, A., Honnen, W. J., D'Agostino, P., Gorny, M. K., Zolla-Pazner, S. & Kayman, S. C. (2005). The C108g epitope in the V2 domain of gp120 functions as a potent neutralization target when introduced into envelope proteins derived from human immunodeficiency virus type 1 primary isolates. *J Virol* **79**, 6909-17.

Pizzato, M., Popova, E. & Gottlinger, H. G. (2008). Nef can enhance the infectivity of receptor-pseudotyped human immunodeficiency virus type 1 particles. *J Virol* **82**, 10811-9.

Platt, E. J., Wehrly, K., Kuhmann, S. E., Chesebro, B. & Kabat, D. (1998). Effects of CCR5 and CD4 cell surface concentrations on infections by macrophagetropic isolates of human immunodeficiency virus type 1. *J Virol* **72**, 2855-64.

Polonis, V. R., Brown, B. K., Rosa Borges, A., Zolla-Pazner, S., Dimitrov, D. S., Zhang, M. Y., Barnett, S. W., Ruprecht, R. M., Scarlatti, G., Fenyo, E. M., Montefiori, D. C., McCutchan, F. E. & Michael, N. L. (2008). Recent advances in the characterization of HIV-1 neutralization assays for standardized evaluation of the antibody response to infection and vaccination. *Virology* **375**, 315-20.

Potyrailo, R. A., Conrad, R. C., Ellington, A. D. & Hieftje, G. M. (1998). Adapting selected nucleic acid ligands (aptamers) to biosensors. *Anal Chem* **70**, 3419-25.

Proske, D., Blank, M., Buhmann, R. & Resch, A. (2005). Aptamers--basic research, drug development, and clinical applications. *Appl Microbiol Biotechnol* **69**, 367-74.

Puren, A. J. (2002). The HIV-1 epidemic in South Africa. *Oral Dis* **8 Suppl 2**, 27-31.

Purschke, W. G., Radtke, F., Kleinjung, F. & Klussmann, S. (2003). A DNA Spiegelmer to staphylococcal enterotoxin B. *Nucleic Acids Res* **31**, 3027-32.

Ras, G. J., Simson, I. W., Anderson, R., Prozesky, O. W. & Hamersma, T. (1983). Acquired immunodeficiency syndrome. A report of 2 South African cases. *S Afr Med J* **64**, 140-2.

Reeves, J. D., Gallo, S. A., Ahmad, N., Miamidian, J. L., Harvey, P. E., Sharron, M., Pohlmann, S., Sfakianos, J. N., Derdeyn, C. A., Blumenthal, R., Hunter, E. & Doms, R. W. (2002). Sensitivity of HIV-1 to entry inhibitors correlates with envelope/coreceptor affinity, receptor density, and fusion kinetics. *Proc Natl Acad Sci U S A* **99**, 16249-54.

Rizzuto, C. & Sodroski, J. (2000). Fine definition of a conserved CCR5-binding region on the human immunodeficiency virus type 1 glycoprotein 120. *AIDS Res Hum Retroviruses* **16**, 741-9.

Rizzuto, C. D. & Sodroski, J. G. (1997). Contribution of virion ICAM-1 to human immunodeficiency virus infectivity and sensitivity to neutralization. *J Virol* **71**, 4847-51.

Rizzuto, C. D., Wyatt, R., Hernandez-Ramos, N., Sun, Y., Kwong, P. D., Hendrickson, W. A. & Sodroski, J. (1998). A conserved HIV gp120 glycoprotein structure involved in chemokine receptor binding. *Science* **280**, 1949-53.

Rockey, W. M., Hernandez, F. J., Huang, S. Y., Cao, S., Howell, C. A., Thomas, G. S., Liu, X. Y., Lapteva, N., Spencer, D. M., McNamara, J. O., Zou, X., Chen, S. J. & Giangrande, P. H. (2011). Rational truncation of an RNA aptamer to prostate-specific membrane antigen using computational structural modeling. *Nucleic Acid Ther* **21**, 299-314.

Rotherham, L. S., Maserumule, C., Dheda, K., Theron, J. & Khati, M. (2012). Selection and application of ssDNA aptamers to detect active TB from sputum samples. *PLoS One* **7**, e46862.

Ryan, C. E., Gare, J., Crowe, S. M., Wilson, K., Reeder, J. C. & Oelrichs, R. B. (2007). The heterosexual HIV type 1 epidemic in Papua New Guinea is dominated by subtype C. *AIDS Res Hum Retroviruses* **23**, 941-4.

Salazar-Gonzalez, J. F., Bailes, E., Pham, K. T., Salazar, M. G., Guffey, M. B., Keele, B. F., Derdeyn, C. A., Farmer, P., Hunter, E., Allen, S., Manigart, O., Mulenga, J., Anderson, J. A., Swanstrom, R., Haynes, B. F., Athreya, G. S., Korber, B. T., Sharp, P. M., Shaw, G. M. & Hahn, B. H. (2008). Deciphering human immunodeficiency virus type 1 transmission and early envelope diversification by single-genome amplification and sequencing. *J Virol* **82**, 3952-70.

Salminen, M. O., Johansson, B., Sonnerborg, A., Ayehunie, S., Gotte, D., Leinikki, P., Burke, D. S. & McCutchan, F. E. (1996). Full-length sequence of an

ethiopian human immunodeficiency virus type 1 (HIV-1) isolate of genetic subtype C. *AIDS Res Hum Retroviruses* **12**, 1329-39.

Samson, M., Libert, F., Doranz, B. J., Rucker, J., Liesnard, C., Farber, C. M., Saragosti, S., Lapoumeroulie, C., Cognaux, J., Forceille, C., Muyldermans, G., Verhofstede, C., Burtonboy, G., Georges, M., Imai, T., Rana, S., Yi, Y., Smyth, R. J., Collman, R. G., Doms, R. W., Vassart, G. & Parmentier, M. (1996). Resistance to HIV-1 infection in caucasian individuals bearing mutant alleles of the CCR-5 chemokine receptor gene. *Nature* **382**, 722-5.

Santulli-Marotto, S., Nair, S. K., Rusconi, C., Sullenger, B. & Gilboa, E. (2003). Multivalent RNA aptamers that inhibit CTLA-4 and enhance tumor immunity. *Cancer Res* **63**, 7483-9.

Sayer, N., Ibrahim, J., Turner, K., Tahiri-Alaoui, A. & James, W. (2002). Structural characterization of a 2'F-RNA aptamer that binds a HIV-1 SU glycoprotein, gp120. *Biochem Biophys Res Commun* **293**, 924-31.

Schaeffer, E., Geleziunas, R. & Greene, W. C. (2001). Human immunodeficiency virus type 1 Nef functions at the level of virus entry by enhancing cytoplasmic delivery of virions. *J Virol* **75**, 2993-3000.

Scheid, J. F., Mouquet, H., Feldhahn, N., Seaman, M. S., Velinzon, K., Pietzsch, J., Ott, R. G., Anthony, R. M., Zebroski, H., Hurley, A., Phogat, A., Chakrabarti, B., Li, Y., Connors, M., Pereyra, F., Walker, B. D., Wardemann, H., Ho, D., Wyatt, R. T., Mascola, J. R., Ravetch, J. V. & Nussenzweig, M. C. (2009). Broad diversity of neutralizing antibodies isolated from memory B cells in HIV-infected individuals. *Nature* **458**, 636-40.

Schols, D. (2006). HIV co-receptor inhibitors as novel class of anti-HIV drugs. *Antiviral Res*.

Schols, D., Proost, P., Struyf, S., Wuyts, A., De Meester, I., Scharpe, S., Van Damme, J. & De Clercq, E. (1998). CD26-processed RANTES(3-68), but not intact RANTES, has potent anti-HIV-1 activity. *Antiviral Res* **39**, 175-87.

Schols, D., Struyf, S., Van Damme, J., Este, J. A., Henson, G. & De Clercq, E. (1997). Inhibition of T-tropic HIV strains by selective antagonization of the chemokine receptor CXCR4. *J Exp Med* **186**, 1383-8.

Schuitemaker, H., Koot, M., Kootstra, N. A., Dercksen, M. W., de Goede, R. E., van Steenwijk, R. P., Lange, J. M., Schattenkerk, J. K., Miedema, F. & Tersmette, M. (1992). Biological phenotype of human immunodeficiency virus type 1 clones at different stages of infection: progression of disease is associated with a shift from monocytotropic to T-cell-tropic virus population. *J Virol* **66**, 1354-60.

Shafer, R. W. & Schapiro, J. M. (2008). HIV-1 drug resistance mutations: an updated framework for the second decade of HAART. *AIDS Rev* **10**, 67-84.

Shangguan, D., Li, Y., Tang, Z., Cao, Z. C., Chen, H. W., Mallikaratchy, P., Sefah, K., Yang, C. J. & Tan, W. (2006). Aptamers evolved from live cells as effective molecular probes for cancer study. *Proc Natl Acad Sci U S A* **103**, 11838-43.

Sharp, P. M., Bailes, E., Chaudhuri, R. R., Rodenburg, C. M., Santiago, M. O. & Hahn, B. H. (2001). The origins of acquired immune deficiency syndrome viruses: where and when? *Philos Trans R Soc Lond B Biol Sci* **356**, 867-76.

Sher, R. (1989). HIV infection in South Africa, 1982-1988--a review. *S Afr Med J* **76**, 314-8.

Smith, D., Collins, B. D., Heil, J. & Koch, T. H. (2003). Sensitivity and specificity of photoaptamer probes. *Mol Cell Proteomics* **2**, 11-8.

Sokal, D. C., Karim, Q. A., Sibeko, S., Yende-Zuma, N., Mansoor, L. E., Baxter, C., Grobler, A., Frolich, J., Kharsany, A. B., Omar, Z., Miya, N., Mlisana, K., Maarshalk, S. & Karim, S. S. (2012). Safety of tenofovir gel, a vaginal microbicide, in South African women: results of the CAPRISA 004 Trial. *Antivir Ther*.

Sousa, J. D., Alvarez, C., Vandamme, A. M. & Muller, V. (2012). Enhanced Heterosexual Transmission Hypothesis for the Origin of Pandemic HIV-1. *Viruses* **4**, 1950-83.

Sterjovski, J., Roche, M., Churchill, M. J., Ellett, A., Farrugia, W., Gray, L. R., Cowley, D., Poumbourios, P., Lee, B., Wesselingh, S. L., Cunningham, A. L., Ramsland, P. A. & Gorry, P. R. (2010). An altered and more efficient mechanism of CCR5 engagement contributes to macrophage tropism of CCR5-using HIV-1 envelopes. *Virology* **404**, 269-78.

Stojanovic, M. N. & Kolpashchikov, D. M. (2004). Modular aptameric sensors. *J Am Chem Soc* **126**, 9266-70.

Stoltenburg, R., Reinemann, C. & Strehlitz, B. (2007). SELEX--a (r)evolutionary method to generate high-affinity nucleic acid ligands. *Biomol Eng* **24**, 381-403.

Swetnam, J., Shmelkov, E., Zolla-Pazner, S. & Cardozo, T. (2010). Comparative magnitude of cross-strain conservation of HIV variable loop neutralization epitopes. *PLoS One* **5**, e15994.

Symensma, T. L., Giver, L., Zapp, M., Takle, G. B. & Ellington, A. D. (1996). RNA aptamers selected to bind human immunodeficiency virus type 1 Rev in vitro are Rev responsive in vivo. *J Virol* **70**, 179-87.

Takashima, K., Miyake, H., Kanzaki, N., Tagawa, Y., Wang, X., Sugihara, Y., Iizawa, Y. & Baba, M. (2005). Highly potent inhibition of human immunodeficiency virus type 1 replication by TAK-220, an orally bioavailable small-molecule CCR5 antagonist. *Antimicrob Agents Chemother* **49**, 3474-82.

Takebe, Y., Uenishi, R. & Li, X. (2008). Global molecular epidemiology of HIV: understanding the genesis of AIDS pandemic. *Adv Pharmacol* **56**, 1-25.

Tebit, D. M., Nankya, I., Arts, E. J. & Gao, Y. (2007). HIV diversity, recombination and disease progression: how does fitness "fit" into the puzzle? *AIDS Rev* **9**, 75-87.

Thomson, M. M. & Fernandez-Garcia, A. (2011). Phylogenetic structure in African HIV-1 subtype C revealed by selective sequential pruning. *Virology* **415**, 30-8.

Thomson, M. M. & Najera, R. (2005). Molecular epidemiology of HIV-1 variants in the global AIDS pandemic: an update. *AIDS Rev* **7**, 210-24.

Townson, J. R., Graham, G. J., Landau, N. R., Rasala, B. & Nibbs, R. J. (2000). Aminooxypentane addition to the chemokine macrophage inflammatory protein-1alpha P increases receptor affinities and HIV inhibition. *J Biol Chem* **275**, 39254-61.

Tremblay, C. L., Kollmann, C., Giguel, F., Chou, T. C. & Hirsch, M. S. (2000). Strong in vitro synergy between the fusion inhibitor T-20 and the CXCR4 blocker AMD-3100. *J Acquir Immune Defic Syndr* **25**, 99-102.

Trkola, A., Kuster, H., Rusert, P., Joos, B., Fischer, M., Leemann, C., Manrique, A., Huber, M., Rehr, M., Oxenius, A., Weber, R., Stiegler, G., Vcelar, B., Katinger, H., Aceto, L. & Gunthard, H. F. (2005). Delay of HIV-1 rebound after cessation

of antiretroviral therapy through passive transfer of human neutralizing antibodies. *Nat Med* **11**, 615-22.

Trkola, A., Paxton, W. A., Monard, S. P., Hoxie, J. A., Siani, M. A., Thompson, D. A., Wu, L., Mackay, C. R., Horuk, R. & Moore, J. P. (1998). Genetic subtype-independent inhibition of human immunodeficiency virus type 1 replication by CC and CXC chemokines. *J Virol* **72**, 396-404.

Trkola, A., Purtscher, M., Muster, T., Ballaun, C., Buchacher, A., Sullivan, N., Srinivasan, K., Sodroski, J., Moore, J. P. & Katinger, H. (1996). Human monoclonal antibody 2G12 defines a distinctive neutralization epitope on the gp120 glycoprotein of human immunodeficiency virus type 1. *J Virol* **70**, 1100-8.

Tsibris, A. M., Sagar, M., Gulick, R. M., Su, Z., Hughes, M., Greaves, W., Subramanian, M., Flexner, C., Giguel, F., Leopold, K. E., Coakley, E. & Kuritzkes, D. R. (2008). In vivo emergence of vicriviroc resistance in a human immunodeficiency virus type 1 subtype C-infected subject. *J Virol* **82**, 8210-4.

Tuerk, C. & Gold, L. (1990). Systematic evolution of ligands by exponential enrichment: RNA ligands to bacteriophage T4 DNA polymerase. *Science* **249**, 505-10.

UNAIDS (2010). UNAIDS report on the global AIDS epidemic.

Van Damme, L., Chandeying, V., Ramjee, G., Rees, H., Sirivongrangson, P., Laga, M. & Perriens, J. (2000). Safety of multiple daily applications of COL-1492, a nonoxynol-9 vaginal gel, among female sex workers. COL-1492 Phase II Study Group. *Aids* **14**, 85-8.

Van Harmelen, J. H., Van der Ryst, E., Loubser, A. S., York, D., Madurai, S., Lyons, S., Wood, R. & Williamson, C. (1999). A predominantly HIV type 1 subtype C-restricted epidemic in South African urban populations. *AIDS Res Hum Retroviruses* **15**, 395-8.

Van Heuverswyn, F., Li, Y., Neel, C., Bailes, E., Keele, B. F., Liu, W., Loul, S., Butel, C., Liegeois, F., Bienvenue, Y., Ngolle, E. M., Sharp, P. M., Shaw, G. M., Delaporte, E., Hahn, B. H. & Peeters, M. (2006). Human immunodeficiency viruses: SIV infection in wild gorillas. *Nature* **444**, 164.

van Loggerenberg, F., Mlisana, K., Williamson, C., Auld, S. C., Morris, L., Gray, C. M., Abdool Karim, Q., Grobler, A., Barnabas, N., Iriogbe, I. & Abdool Karim, S. S. (2008). Establishing a cohort at high risk of HIV infection in South Africa: challenges and experiences of the CAPRISA 002 acute infection study. *PLoS One* **3**, e1954.

Vinores, S. A. (2003). Technology evaluation: pegaptanib, Eyetech/Pfizer. *Curr Opin Mol Ther* **5**, 673-9.

von Kockritz-Blickwede, M., Chow, O. A. & Nizet, V. (2009). Fetal calf serum contains heat-stable nucleases that degrade neutrophil extracellular traps. *Blood* **114**, 5245-6.

Waki, K. & Freed, E. O. (2010). Macrophages and Cell-Cell Spread of HIV-1. *Viruses* **2**, 1603-1620.

Walker, L. M., Huber, M., Doores, K. J., Falkowska, E., Pejchal, R., Julien, J. P., Wang, S. K., Ramos, A., Chan-Hui, P. Y., Moyle, M., Mitcham, J. L., Hammond, P. W., Olsen, O. A., Phung, P., Fling, S., Wong, C. H., Phogat, S., Wrin, T., Simek, M. D., Principal Investigators, P. G., Koff, W. C., Wilson, I. A.,

Burton, D. R. & Poignard, P. (2011). Broad neutralization coverage of HIV by multiple highly potent antibodies. *Nature* **477**, 466-470.

Walker, L. M., Phogat, S. K., Chan-Hui, P. Y., Wagner, D., Phung, P., Goss, J. L., Wrin, T., Simek, M. D., Fling, S., Mitcham, J. L., Lehrman, J. K., Priddy, F. H., Olsen, O. A., Frey, S. M., Hammond, P. W., Kaminsky, S., Zamb, T., Moyle, M., Koff, W. C., Poignard, P. & Burton, D. R. (2009). Broad and potent neutralizing antibodies from an African donor reveal a new HIV-1 vaccine target. *Science* **326**, 285-9.

Walker, P. R., Pybus, O. G., Rambaut, A. & Holmes, E. C. (2005). Comparative population dynamics of HIV-1 subtypes B and C: subtype-specific differences in patterns of epidemic growth. *Infect Genet Evol* **5**, 199-208.

Wei, X., Decker, J. M., Liu, H., Zhang, Z., Arani, R. B., Kilby, J. M., Saag, M. S., Wu, X., Shaw, G. M. & Kappes, J. C. (2002). Emergence of resistant human immunodeficiency virus type 1 in patients receiving fusion inhibitor (T-20) monotherapy. *Antimicrob Agents Chemother* **46**, 1896-905.

Wheeler, L. A., Trifonova, R., Vrbanac, V., Basar, E., McKernan, S., Xu, Z., Seung, E., Deruaz, M., Dudek, T., Einarsson, J. I., Yang, L., Allen, T. M., Luster, A. D., Tager, A. M., Dykxhoorn, D. M. & Lieberman, J. (2011). Inhibition of HIV transmission in human cervicovaginal explants and humanized mice using CD4 aptamer-siRNA chimeras. *J Clin Invest* **121**, 2401-12.

White, R., Rusconi, C., Scardino, E., Wolberg, A., Lawson, J., Hoffman, M. & Sullenger, B. (2001). Generation of species cross-reactive aptamers using "toggle" SELEX. *Mol Ther* **4**, 567-73.

WHO-UNAIDS (2002). Guidelines for standard HIV Isolation and Characterization procedures. **Second Edition**, pp54-64.

WHO/UNAIDS (2011). Global HIV/AIDS response. Epidemic update and health sector progress towards universal access. Progress report 2011.

Wild, C., Greenwell, T. & Matthews, T. (1993). A synthetic peptide from HIV-1 gp41 is a potent inhibitor of virus-mediated cell-cell fusion. *AIDS Res Hum Retroviruses* **9**, 1051-3.

Wolkowicz, R. & Nolan, G. P. (2005). Gene therapy progress and prospects: novel gene therapy approaches for AIDS. *Gene Ther* **12**, 467-76.

Wu, X., Yang, Z. Y., Li, Y., Hogerkorp, C. M., Schief, W. R., Seaman, M. S., Zhou, T., Schmidt, S. D., Wu, L., Xu, L., Longo, N. S., McKee, K., O'Dell, S., Louder, M. K., Wycuff, D. L., Feng, Y., Nason, M., Doria-Rose, N., Connors, M., Kwong, P. D., Roederer, M., Wyatt, R. T., Nabel, G. J. & Mascola, J. R. (2010). Rational design of envelope identifies broadly neutralizing human monoclonal antibodies to HIV-1. *Science* **329**, 856-61.

www.fda.gov/newsevents/newsroom/pressannouncements/2004/ucm108385.htm.

Wyatt, R., Kwong, P. D., Desjardins, E., Sweet, R. W., Robinson, J., Hendrickson, W. A. & Sodroski, J. G. (1998). The antigenic structure of the HIV gp120 envelope glycoprotein. *Nature* **393**, 705-11.

Xiang, S. H., Finzi, A., Pacheco, B., Alexander, K., Yuan, W., Rizzuto, C., Huang, C. C., Kwong, P. D. & Sodroski, J. (2010). A V3 loop-dependent gp120 element disrupted by CD4 binding stabilizes the human immunodeficiency virus envelope glycoprotein trimer. *J Virol* **84**, 3147-61.

Yoshida, W., Mochizuki, E., Takase, M., Hasegawa, H., Morita, Y., Yamazaki, H., Sode, K. & Ikebukuro, K. (2009). Selection of DNA aptamers against insulin

and construction of an aptameric enzyme subunit for insulin sensing. *Biosens Bioelectron* **24**, 1116-20.

Zanetti, G., Briggs, J. A., Grunewald, K., Sattentau, Q. J. & Fuller, S. D. (2006). Cryo-electron tomographic structure of an immunodeficiency virus envelope complex in situ. *PLoS Pathog* **2**, e83.

Zhang, P. F., Bouma, P., Park, E. J., Margolick, J. B., Robinson, J. E., Zolla-Pazner, S., Flora, M. N. & Quinnan, G. V., Jr. (2002). A variable region 3 (V3) mutation determines a global neutralization phenotype and CD4-independent infectivity of a human immunodeficiency virus type 1 envelope associated with a broadly cross-reactive, primary virus-neutralizing antibody response. *J Virol* **76**, 644-55.

Zhang, Z., Blank, M. & Schluesener, H. J. (2004). Nucleic acid aptamers in human viral disease. *Arch Immunol Ther Exp (Warsz)* **52**, 307-15.

Zhou, J., Li, H., Li, S., Zaia, J. & Rossi, J. J. (2008). Novel dual inhibitory function aptamer-siRNA delivery system for HIV-1 therapy. *Mol Ther* **16**, 1481-9.

Zhou, J. & Rossi, J. J. (2010). Cell-specific aptamer-mediated targeted drug delivery. *Oligonucleotides* **21**, 1-10.

Zhou, J., Shu, Y., Guo, P., Smith, D. D. & Rossi, J. J. (2011). Dual functional RNA nanoparticles containing phi29 motor pRNA and anti-gp120 aptamer for cell-type specific delivery and HIV-1 inhibition. *Methods* **54**, 284-94.

Zhou, J., Swiderski, P., Li, H., Zhang, J., Neff, C. P., Akkina, R. & Rossi, J. J. (2009). Selection, characterization and application of new RNA HIV gp 120 aptamers for facile delivery of Dicer substrate siRNAs into HIV infected cells. *Nucleic Acids Res* **37**, 3094-109.

Zhou, J. Y. & Montefiori, D. C. (1997). Antibody-mediated neutralization of primary isolates of human immunodeficiency virus type 1 in peripheral blood mononuclear cells is not affected by the initial activation state of the cells. *J Virol* **71**, 2512-7.

Zhou, T., Georgiev, I., Wu, X., Yang, Z. Y., Dai, K., Finzi, A., Kwon, Y. D., Scheid, J. F., Shi, W., Xu, L., Yang, Y., Zhu, J., Nussenzweig, M. C., Sodroski, J., Shapiro, L., Nabel, G. J., Mascola, J. R. & Kwong, P. D. (2010). Structural basis for broad and potent neutralization of HIV-1 by antibody VRC01. *Science* **329**, 811-7.

Zhou, T., Xu, L., Dey, B., Hessell, A. J., Van Ryk, D., Xiang, S. H., Yang, X., Zhang, M. Y., Zwick, M. B., Arthos, J., Burton, D. R., Dimitrov, D. S., Sodroski, J., Wyatt, R., Nabel, G. J. & Kwong, P. D. (2007). Structural definition of a conserved neutralization epitope on HIV-1 gp120. *Nature* **445**, 732-7.

Zhu, P., Winkler, H., Chertova, E., Taylor, K. A. & Roux, K. H. (2008). Cryoelectron tomography of HIV-1 envelope spikes: further evidence for tripod-like legs. *PLoS Pathog* **4**, e1000203.

Zhu, T. (2000). HIV-1 genotypes in peripheral blood monocytes. *J Leukoc Biol* **68**, 338-44.

Zuker, M. (1989). Computer prediction of RNA structure. *Methods Enzymol* **180**, 262-88.

Zwick, M. B., Jensen, R., Church, S., Wang, M., Stiegler, G., Kunert, R., Katinger, H. & Burton, D. R. (2005). Anti-human immunodeficiency virus type 1 (HIV-1) antibodies 2F5 and 4E10 require surprisingly few crucial residues in the

membrane-proximal external region of glycoprotein gp41 to neutralize HIV-1. *J Virol* **79**, 1252-61.

Zwick, M. B., Wang, M., Poignard, P., Stiegler, G., Katinger, H., Burton, D. R. & Parren, P. W. (2001). Neutralization synergy of human immunodeficiency virus type 1 primary isolates by cocktails of broadly neutralizing antibodies. *J Virol* **75**, 12198-208.